

University of Groningen

## Manganese catalysed oxidations with hydrogen peroxide

Saisaha, Pattama

**IMPORTANT NOTE:** You are advised to consult the publisher's version (publisher's PDF) if you wish to cite from it. Please check the document version below.

*Document Version*

Publisher's PDF, also known as Version of record

*Publication date:*

2012

[Link to publication in University of Groningen/UMCG research database](#)

*Citation for published version (APA):*

Saisaha, P. (2012). *Manganese catalysed oxidations with hydrogen peroxide: applications and mechanistic insights*. s.n.

### Copyright

Other than for strictly personal use, it is not permitted to download or to forward/distribute the text or part of it without the consent of the author(s) and/or copyright holder(s), unless the work is under an open content license (like Creative Commons).

The publication may also be distributed here under the terms of Article 25fa of the Dutch Copyright Act, indicated by the "Taverne" license. More information can be found on the University of Groningen website: <https://www.rug.nl/library/open-access/self-archiving-pure/taverne-amendment>.

### Take-down policy

If you believe that this document breaches copyright please contact us providing details, and we will remove access to the work immediately and investigate your claim.

Downloaded from the University of Groningen/UMCG research database (Pure): <http://www.rug.nl/research/portal>. For technical reasons the number of authors shown on this cover page is limited to 10 maximum.

# **Manganese Catalysed Oxidations with Hydrogen Peroxide**

Applications and Mechanistic Insights

Pattama Saisaha



The work described in this thesis was carried out at the Stratingh Institute for Chemistry, University of Groningen, The Netherlands.

Ubbo Emmius Scholarship is acknowledged for financial support.

Printed by: Ipskamp Drukkers, Enschede, The Netherlands

Cover design

Photographer: Thitikorn Angsusingha

Artwork: Umaporn Pupphachai

**RIJKSUNIVERSITEIT GRONINGEN**

**Manganese Catalysed Oxidations with Hydrogen Peroxide**

Applications and Mechanistic Insights

**Proefschrift**

ter verkrijging van het doctoraat in de  
Wiskunde en Natuurwetenschappen  
aan de Rijksuniversiteit Groningen  
op gezag van de  
Rector Magnificus, dr. E. Sterken,  
in het openbaar te verdedigen op  
vrijdag 7 december 2012  
om 12.45 uur

door

**Pattama Saisaha**

geboren op 17 juni 1981  
te Lop Buri, Thailand

Promotor: Prof. dr. B.L. Feringa

Copromotor: Dr. W.R. Browne

Beoordelingscommissie: Prof. dr. M. Costas  
Prof. dr. R.J.M. Klein Gebbink  
Prof. dr. J.G. Roelfes

ISBN: 978-90-367-5880-2 (print)  
978-90-367-5881-9 (digital)



# Table of Contents

<b>Chapter 1 Mechanisms in manganese catalysed oxidation of alkenes with H<sub>2</sub>O<sub>2</sub></b>	<b>1</b>
1.1 Introduction	2
1.2 Studying mechanism in manganese catalysed oxidation chemistry: tools of the trade	2
1.3 Oxidations catalysed by 'ligand free' Mn systems	3
1.4 Quinoline based ligands for manganese catalysed oxidation	7
1.5 Polypyridyl amine based ligands for manganese catalysed oxidation	8
1.6 Trimethyl-triazacyclononane based ligands for manganese catalysed oxidation	12
1.7 Tetraazamacrocyclic based ligands for manganese catalysed oxidation	21
1.8 Conclusions	23
1.9 Overview of the thesis	23
1.10 References and notes	24
 <b>Chapter 2 Selective catalytic oxidation of alcohols, aldehydes, alkanes and alkenes employing manganese catalysts and H<sub>2</sub>O<sub>2</sub></b>	 <b>29</b>
2.1 Introduction	30
2.2 Results and discussion	31
2.2.1 Oxidation of secondary alcohols to ketones	31
2.2.2 Oxidation of primary and benzyl alcohols to carboxylic acids	34
2.2.3 Oxidation of aldehydes to carboxylic acids	36
2.2.4 Oxidation of alkenes	38
2.2.5 C-H activation	41
2.2.6 Oxidation of bifunctional substrates	43
2.2.7 Protecting group tolerance	48
2.3 Summary and conclusions	50
2.4 Experimental section	51
2.5 References and notes	66
 <b>Chapter 3 The unexpected role of pyridine-2-carboxylic acid in manganese based oxidation catalysis with pyridin-2-yl based ligands</b>	 <b>69</b>
3.1 Introduction	70
3.2 Results	73
3.2.1 Catalytic activity of Mn <sup>II</sup> with TPTN, 2 and 3	73
3.2.2 Stability of ligands 2 and 3 in the presence of iron salts and under acid and basic conditions	74
3.2.3 Catalytic activity of Mn <sup>II</sup> /ligand in relation to ligand structure	77
3.2.4 Ligand stability under reaction conditions	79

3.2.5 Oxidation catalysis with pyridine-2-carboxylic acid/Mn <sup>II</sup>	80
3.2.6 C-H activation and alcohol oxidation with pyridine-2-carboxylic acid/Mn <sup>II</sup> /NaOAc	82
3.3 Summary and conclusions	82
3.4 Experimental section	83
3.5 References and notes	95

## **Chapter 4 Manganese catalysed *cis*-dihydroxylation of electron deficient alkenes with H<sub>2</sub>O<sub>2</sub>**

**99**

4.1 Introduction	100
4.2 Results and discussion	101
4.2.1 <i>cis</i> -Dihydroxylation of electron deficient alkenes	101
4.2.2 <i>cis</i> -Dihydroxylation and epoxidation of electron rich alkenes	106
4.2.3 Catalyst composition	107
4.2.4 Solvent dependence	110
4.3 Mechanistic considerations	111
4.4 Summary and conclusions	112
4.5 Experimental section	113
4.6 References and notes	120

## **Chapter 5 Mechanistic study of an *in situ* prepared Mn<sup>II</sup>/pyridine-2-carboxylic acid catalytic system**

**123**

5.1 Introduction	124
5.2 Mechanistic considerations	125
5.2.1 Information from substrate scope	125
5.2.2 Kinetic analysis: order of reaction with respect to various components and the rate determining step	126
5.2.3 Role(s) of ketone in the catalytic reaction	131
5.2.4 Effect of acetic acid on the catalytic oxidation of alkenes	138
5.2.5 Effect of other acids on catalysis with butanedione	141
5.2.6 <sup>18</sup> O-labelling studies	147
5.3 Proposed mechanism	149
5.4 Summary and conclusions	151
5.5 Experimental section	152
5.6 References and notes	153

## **Chapter 6 General discussion and future perspectives**

**155**

6.1 References	158
----------------	-----

## **Summary**

**159**

## **Samenvatting**

**165**

## **Acknowledgements**

**171**





## Chapter 1

# Mechanisms in manganese catalysed oxidation of alkenes with H<sub>2</sub>O<sub>2</sub>

*The development of new catalytic systems for cis-dihydroxylation and epoxidation of alkenes, based on atom economic and environmentally friendly concepts, is a major contemporary challenge. In recent years, several systems based on manganese catalysts using H<sub>2</sub>O<sub>2</sub> as terminal oxidant have been developed. In this chapter, selected homogeneous manganese catalytic systems, including 'ligand free' and pyridylamine ligand based systems, that have been applied to alkene oxidation will be discussed with a strong focus on mechanistic studies*

## 1.1 Introduction

A central challenge in modern chemical synthesis is the development of replacement methods for economically and environmentally unsustainable and energy demanding methods. The continued reliance of contemporary synthetic methods on predominantly stoichiometric atom inefficient and often toxic oxidants, such as peracids, chromates, permanganates and  $\text{OsO}_4$ , reflects in large part the challenge that is faced. In addition to the evident environmental benefits, catalyst development is also driven by the increased scarcity of metals such as ruthenium and osmium. Indeed, it is this latter aspect that moves 1<sup>st</sup> row transition metal catalysed oxidation<sup>1</sup> with  $\text{O}_2$  and  $\text{H}_2\text{O}_2$  to centre stage,<sup>2,3,4</sup> in particular systems based on titanium, copper,<sup>5</sup> iron and manganese.<sup>6,7,8,9</sup>

Manganese, together with iron,<sup>10,11</sup> has proven to be one of the more promising metals on which to base new catalytic oxidation systems. This is in large part due to the remarkably versatile redox chemistry of manganese with the formal oxidation states II-V and VII being readily accessible. Initial interest regarding manganese coordination chemistry focused on developing structural and functional mimics for manganese catalases and the oxygen evolving complexes of photosystem II.<sup>12,13</sup> However, over the last two decades the focus has shifted towards applying such systems in oxidation catalysis.

In this chapter, the focus will be placed on a select group of manganese based homogeneous catalyst systems for alkene oxidation that have received attention with regard to the mechanism by which the catalysts work and their potential active intermediates. Manganese porphyrin, Schiff base and salen<sup>14,15,16</sup> based systems have been discussed in depth elsewhere, and will not be discussed here.<sup>17</sup> In addition, the substrate scope of individual systems will only be discussed where relevant with regard to mechanistic considerations. Finally, because of the increased importance placed on sustainability in chemical processes, the scope of this chapter will be limited to systems that employ  $\text{H}_2\text{O}_2$  to effect alkene oxidation and, in some cases for comparison, peracetic acid as terminal oxidant.

The goal of this chapter is to survey the various approaches that have been taken to understand how these catalysts actually work and in particular understanding the role of additives in controlling reactivity.

## 1.2 Studying mechanism in manganese catalysed oxidation chemistry: tools of the trade<sup>18</sup>

One of the major challenges in studying manganese based catalytic systems is that  $\text{Mn}^{\text{II}}$  ions and complexes are essentially spectroscopically white (high spin  $d^5$ ) and highly labile, making detection difficult, often even by EPR spectroscopy and mass spectrometry. In the case of EPR spectroscopy<sup>19</sup> the range of oxidation and spin states that can be obtained with manganese is unusually broad and hence this technique is one of the few available to probe metal oxidation states and environments *in situ*.

Mononuclear high spin  $Mn^{II}$  complexes are characterised by a strong 6-line ( $s = 5/2$ ) signal at *ca.*  $g = 2$ . For di- and multinuclear complexes the EPR spectra are generally more informative, but signals may be weaker than those for  $Mn^{II}$ , and can be quite complex in terms of  $g$  values and hyperfine coupling.

$Mn^{III}$  and  $Mn^{IV}$  mono- and multi-nuclear complexes are kinetically much more stable with regard to ligand exchange and exhibit, generally, quite intense UV absorption bands, assigned to ligand to metal charge transfer transitions, and moderately intense visible and near-infrared absorption bands, the latter bands generally being assigned to metal centred transitions. Mononuclear (HS)  $Mn^{III}$  and  $Mn^{IV}$  complexes show 6-line EPR spectra typically at  $g = 2$  and 4, respectively, however, they are often difficult to observe due to line broadening and are dependent on the crystal field strength of the complex.

In general both  $Mn^{IV,IV}_2$  and  $Mn^{III,III}_2$  dinuclear complexes are EPR silent, however, their diamagnetic and paramagnetic (*i.e.* over the 100 to -100 ppm range) can be informative and in some cases detailed assignments have been made using deuterium isotope labelling.<sup>20</sup> By contrast, the mixed valent  $Mn^{II,III}_2$  and  $Mn^{III,IV}_2$  complexes show quite rich EPR spectra that are characteristic of each redox state. For example  $Mn^{III,IV}_2$  dimers exhibit a 16-line spectrum at *ca.*  $g = 2$ .

Conveniently the complexes in oxidation states higher than  $Mn^{II}$  have sufficient stability towards ligand exchange, which allows for mass spectral studies to be of use. Although even for these systems care should be taken in making assignments as ligand exchange and change in redox state can occur under the conditions of electro-spray measurements.<sup>21</sup>

Perhaps two of the most powerful tools for studying mechanisms in manganese oxidation catalysis, and catalysis in general, are kinetics and isotopic labelling.<sup>22</sup> They can be used both for kinetic isotope effect determination and, more importantly, for atom tracking of oxygen, *i.e.* whether the oxygen(s) incorporated into the products originate from the oxidant ( $H_2O_2$ ), oxygen ( $O_2$ ), solvent and/or  $H_2O$ . A key challenge with regard to kinetics is that sufficient data are necessary in order to achieve reliable fits. Furthermore, it should not be forgotten that kinetic studies generally provide information only up to and including the rate determining step. This point can easily be overlooked and is made more challenging by the fact that in many systems the rate determining step, and indeed the mechanism itself, can change as conditions are varied.

Finally, the role of computational chemistry in mechanistic research continues to increase, despite the challenge presented by manganese systems, especially  $Mn^{II}$ , and has already made important contributions to the field (*vide infra*).

### 1.3 Oxidations catalysed by ‘ligand free’ Mn systems

Perhaps the simplest manganese based catalyst system, at least from the point of view of catalyst composition, is to use  $Mn^{II}$  salts with  $H_2O_2$  in aqueous solvents. The oxidation of alkenes with  $Mn^{II}$  salts and  $H_2O_2$  in carbonate buffer was reported by Hage and coworkers in the 1990s.<sup>23</sup> Richardson *et al.* subsequently reported that the epoxidation of

alkenes could be achieved with  $\text{NaHCO}_3/\text{H}_2\text{O}_2$  alone (*i.e.* without deliberate addition of metal ions).<sup>24</sup>

Burgess and coworkers placed  $\text{Mn}^{\text{II}}$  salts as catalysts on a synthetically applicable level, in what is a remarkably simple and effective ‘ligand free’ Mn-based epoxidation system.<sup>25,26</sup> Under their typical conditions, 0.1-1.0 mol%  $\text{MnSO}_4$  and 30% aqueous  $\text{H}_2\text{O}_2$  (10 equiv.) as oxidant in bicarbonate buffer (Figure 1), a substantial increase in both the yield and the rate of reaction was achieved compared with the metal free system reported by Richardson *et al.*<sup>24</sup>

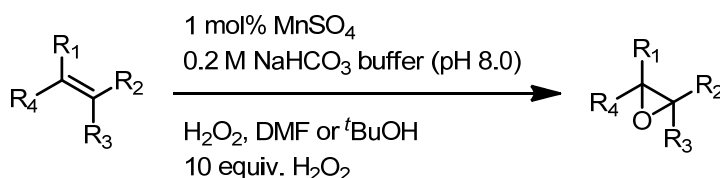


**Figure 1** Typical reaction conditions employed by Burgess and coworkers for the manganese catalysed epoxidation of alkenes with bicarbonate/hydrogen peroxide.<sup>25</sup>

Limitations due to substrate solubility demanded the use of organic co-solvents such as  $t\text{BuOH}$  or DMF. The system allowed for conversion of cyclic, aryl- and trialkyl-substituted alkenes to their corresponding epoxides in high yields, however, terminal alkenes were unreactive.<sup>25</sup> Although the system is ‘ligand free’, Burgess and coworkers investigated the use of additives to enhance activity towards epoxidation and, more importantly, to suppress wasteful decomposition of  $\text{H}_2\text{O}_2$ .<sup>26</sup> This latter issue has also driven the use of additives in other manganese based catalytic systems as will be discussed below. The optimum conditions for epoxidation with respect to product yield, decreased reaction times and  $\text{H}_2\text{O}_2$  consumption (2.8-5 equiv.) were found to be sodium acetate (6 mol%) in  $t\text{BuOH}$  or salicylic acid (4 mol%) in DMF.

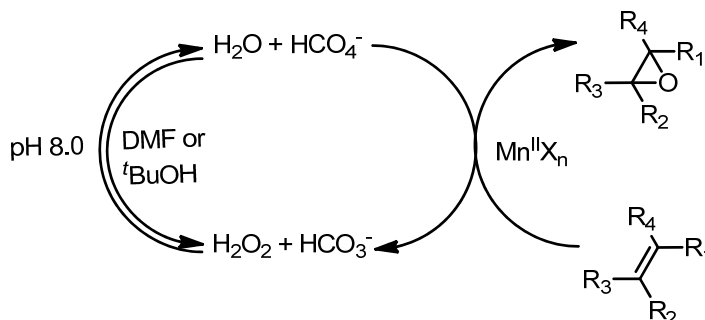
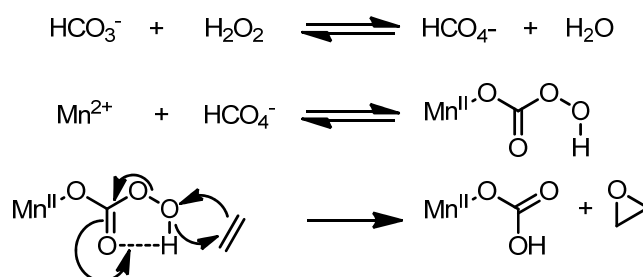


**Figure 2** Proposed catalytic cycle for manganese catalysed epoxidation with bicarbonate/hydrogen peroxide, where  $\text{X}_n$  is an undefined ligand.<sup>25,26</sup>

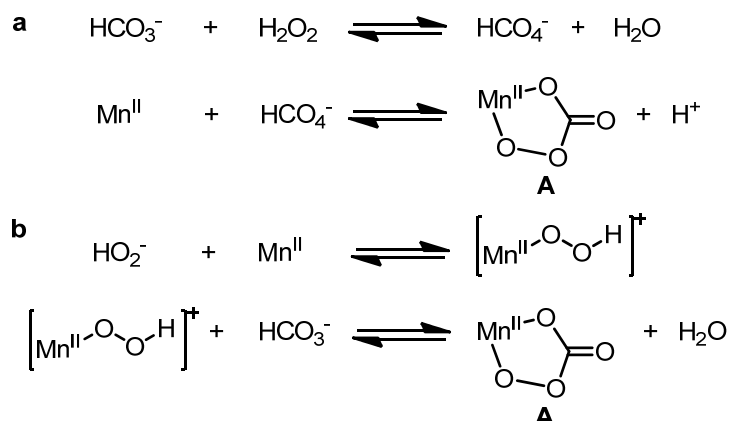
From a mechanistic perspective, a key feature of the system is the necessity for bicarbonate to be present (*i.e.* as buffer). In addition to acting as a buffer, it is believed that bicarbonate generates the peroxydicarbonate ion ( $\text{HCO}_4^-$ ) *in situ* (Figure 2), based on  $^{13}\text{C}$  NMR spectroscopic data. Upon mixing of  $\text{NaH}^{13}\text{CO}_3$  (at  $\delta$  160.4 ppm) with  $\text{H}_2\text{O}_2$

in <sup>t</sup>BuOH, a <sup>13</sup>C signal appeared at  $\delta$  158.5 ppm that corresponds to the chemical shift of peroxymonocarbonate.<sup>26</sup> Also, saturation transfer NMR spectroscopy indicated that on equilibrium between peroxymonocarbonate and bicarbonate is established rapidly.<sup>25</sup> EPR spectroscopy of the reaction mixture before the reaction showed the characteristic 6-line spectrum of mononuclear Mn<sup>II</sup> centred at *ca.*  $g = 2$ . The signal decreased in intensity upon addition of H<sub>2</sub>O<sub>2</sub> and disappeared completely within several minutes. The 6-line signal was replaced by a broad signal at  $g = 4$ , characteristic of high-spin mononuclear Mn<sup>IV</sup>. As the reaction reached completion the 6-line signal of mononuclear Mn<sup>II</sup> recovered. These data suggest that the resting state for the manganese ion under reaction conditions is not a Mn<sup>II</sup> but rather a Mn<sup>IV</sup> species. When the H<sub>2</sub>O<sub>2</sub> concentration decreases below a certain level, reoxidation of the Mn<sup>II</sup> ions becomes the rate limiting step in the catalytic cycle. The authors<sup>26</sup> surmised that the Mn<sup>II</sup> ions activate HCO<sub>4</sub><sup>-</sup> by acting as a Lewis acid (Scheme 1). The EPR data and the fact that most other metal salts screened were unreactive, despite the fact that many of them have comparable Lewis acidities to MnSO<sub>4</sub> suggests that the actual mechanism may be more complicated.



**Scheme 1** Epoxidation mechanism relying on Mn<sup>II</sup> acting as a Lewis acid.

The other pathway proposed involved a manganese  $\eta^2$ -peroxymonocarbonate ([Mn<sup>II</sup>- $\eta^2$ -HCO<sub>4</sub>]<sup>+</sup>) (A) species (Scheme 2).<sup>26</sup> This species can be generated either from peroxymonocarbonate (HCO<sub>4</sub><sup>-</sup>) coordinated directly with Mn<sup>II</sup> or HO<sub>2</sub><sup>-</sup> coordination to Mn<sup>II</sup> followed by coordination of bicarbonate (Scheme 2). Pathway **b** would be facilitated by an increase in pH and *vice versa*. The decreased levels of epoxidation observed at higher pH and the relatively high  $pK_a$  of H<sub>2</sub>O<sub>2</sub> suggests that it is the peroxymonocarbonate that coordinates to the manganese (pathway **a** in Scheme 2).



**Scheme 2** Formation of peroxymonocarbonate complex **A** (a) by direct reaction of peroxymonocarbonate and (b) by reaction of peroxy complex with bicarbonate.

With regard to oxygen transfer to the alkene, it remains unclear whether intermediate **A** epoxidises the alkene directly or via a  $\text{Mn}^{\text{IV}}=\text{O}$  species. Of particular note is the observed lack of stereoretention in the oxidation of *cis*- and *trans*-acyclic disubstituted alkenes, which indicates a stepwise oxygen atom transfer process. However, as yet there is insufficient evidence to fully elucidate whether oxygen transfer to the alkene occurs via the peroxy species or the  $\text{Mn}^{\text{IV}}=\text{O}$  species.

Although, not ‘free manganese ion’ based, the system reported recently by Kwong *et al.*<sup>27</sup> demonstrated the activity of a relatively simple  $\text{Mn}^{\text{IV}}$  complex,  $[\text{Mn}^{\text{IV}}(\text{N})(\text{CN})_4]$ , originally reported by Wieghardt and coworkers.<sup>28</sup> The system shows remarkable efficiency in the epoxidation of alkenes with, as for the system of Burgess and coworkers above, lower reactivity being observed for terminal alkenes. In addition, efficient oxidation of primary and secondary alcohols was reported. From a mechanistic point of view, the retention of configuration observed for *cis*-stilbene is important and suggests an essentially concerted oxygen transfer process. Moreover, the mechanistic probe, 2-methyl-1-phenyl-2-propyl hydroperoxide, indicated that heterolysis of the O-O bond rather than homolysis occurred.<sup>29</sup>

The effect of additives, a recurring theme in manganese catalysed oxidation with  $\text{H}_2\text{O}_2$ , was studied also.<sup>27</sup> Acetic acid was found to have a moderate positive effect on the yields and a considerable effect on reaction rates. It could be argued that this may indicate the formation of peracetic acid *in situ*, however, as noted in other studies (*vide infra*), this can be discounted under the conditions employed.

Instead, DFT calculations indicate that the manganese centre acts as a Lewis acid to activate the O-O bond of H<sub>2</sub>O<sub>2</sub> towards heterolytic cleavage rather than the formation of a high valent manganese-oxo species. Based on calculated intermediates, it is proposed that the role of acetic acid is to further weaken the O-O bond through hydrogen bonding interactions and facilitate proton transfer.

## 1.4 Quinoline based ligands for manganese catalysed oxidation

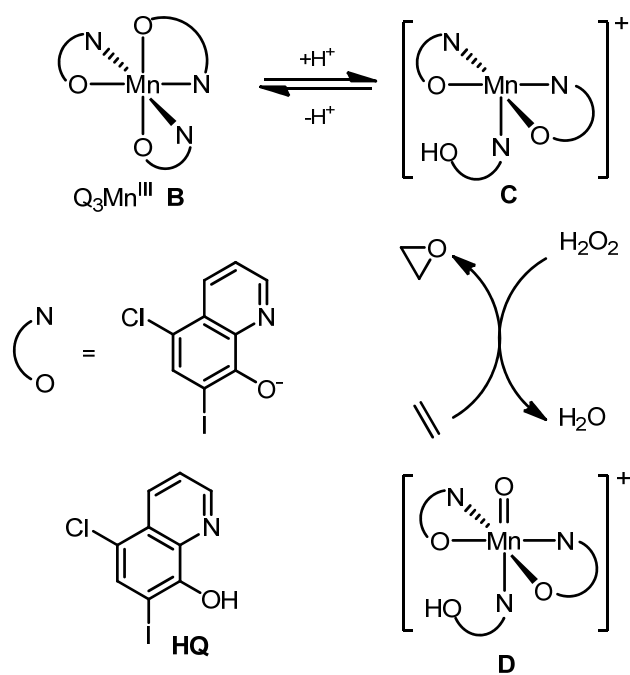
It is arguable whether or not it is appropriate to use the term ‘ligand free’ in catalyst systems based on manganese salts, since in principle the additives used to promote activity, can play a role in forming defined complexes. In the case of pyridine based additives, it is generally assumed that they promote activity by acting as ligands, with the catalysts being formed *in situ*. Perhaps one of the most simple pyridine based ligands applied to manganese based oxidation catalysis, with  $H_2O_2$ , is the 8-hydroxyquinolines.

Recently, Zhong and coworkers reported a manganese catalyst based on 6-chloro-8-hydroxy-7-iodo-quinoline (**HQ**) (Scheme 3).<sup>30</sup> The authors demonstrated that the system is highly efficient in the epoxidation of a broad range of alkenes with  $H_2O_2$  in acetone/water. The tris-complex  $Q_3Mn^{III}$  can be prepared *in situ* by mixing **HQ** with  $Mn^{II}$  salts or can be prepared in advance.

The coordination mode of the complex was found to be pH dependent, which allowed for the activity to be ‘switched’ on and off. Notably, the preformed complexes ( $Q_3Mn^{III}$ ) provided only low substrate conversion. As with the system of Burgess and coworkers described above,<sup>25,26</sup> weakly acidic additives, *e.g.*  $NH_4Cl$  or  $NH_4OAc$ - $AcOH$ , increased conversion, whereas basic additives, except  $NaHCO_3$ , resulted in a decrease in conversion. The fact that the addition of  $NaHCO_3$  increased activity is possibly due to formation of the peroxymonocarbonate ion ( $HCO_4^-$ ) as noted by Burgess and coworkers.<sup>25</sup> This highlights a common difficulty in the field in which tuning of reaction conditions can sometimes lead to convergence of conditions between systems that are, at first sight, quite different.

Notwithstanding this, the **HQ** based system of Zhong *et al.*<sup>30</sup> allows for epoxidation of both aliphatic and aromatic alkenes where acid-sensitive epoxides are formed. This suggests that the ligand decreases the Lewis acidity of the  $Mn^{III}$  ion and hence the propensity for the catalyst to engage in catalytic epoxide ring opening. Although the spectroscopic data available is limited, the authors proposed that a pendant OH group in species **C** (Scheme 3) is important in the reaction and plays two roles; firstly it acts as a labile ligand that inhibits the formation of potentially inactive  $\mu$ -oxo-manganese dimers and, secondly, it facilitates O-O bond cleavage through hydrogen bonding interactions. This mechanism rationalises the low substrate conversion observed in the presence of basic additives, such as imidazole, which would shift the equilibrium in favour of species **B**.





**Scheme 3** Epoxidation of alkenes using Mn-quinoline complex and  $\text{H}_2\text{O}_2$ .<sup>30</sup>

## 1.5 Polypyridyl amine based ligands for manganese catalysed oxidation

While the development of ‘ligand free’ catalyst systems is highly desirable in terms of alkene epoxidation and *cis*-dihydroxylation where stereochemistry is not a consideration, the paradigm for achieving stereocontrol over oxidation reactions is to employ well defined complexes in which the chiral environment is provided by a ligand. This concept has driven the design and synthesis of ligands for manganese based catalysts over recent decades, with the ultimate goal of achieving the same level of control achieved with, *e.g.* osmium based catalysts.<sup>31</sup> Perhaps the most successful ligand systems to date are those based on porphyrins<sup>17</sup> and salens<sup>14</sup> using oxidants such as oxone and  $\text{NaClO}$ . However, with notable exceptions, enantioselectivities and especially turnover numbers are limited when  $\text{H}_2\text{O}_2$  is employed as terminal oxidant.<sup>32</sup>

A key challenge faced by the field has been to design ligand systems which can be tuned easily and can be based on readily available chiral reagents, such as 1,2-diaminocyclohexane.

Dinuclear manganese complexes based on TPTN/TPEN type ligands (Figure 4) (where TPTN = *N,N,N',N'*-tetrakis(2-pyridylmethyl)-1,3-propanediamine and TPEN = *N,N,N',N'*-tetrakis(2-pyridylmethyl)-1,2-ethylenediamine) have been investigated by Brinksmas *et al.* in the epoxidation of alkenes<sup>33</sup> as well as oxidation of alcohols to their corresponding ketones or aldehydes.<sup>34</sup> An attractive feature of this type of ligand is that the route used in their synthesis allows for facile introduction of various groups either on the central diamine unit or by replacing one or more of the pyridyl rings. However, a key drawback of these catalysts in the oxidation of alkenes was that excess oxidant was

required (8-16 equiv. of  $\text{H}_2\text{O}_2$ ) to compensate for the extensive decomposition of  $\text{H}_2\text{O}_2$  that occurred in the initial stage of the reaction. Furthermore, the solvent used, acetone, is potentially hazardous in the presence of  $\text{H}_2\text{O}_2$ .<sup>35,36,37</sup>

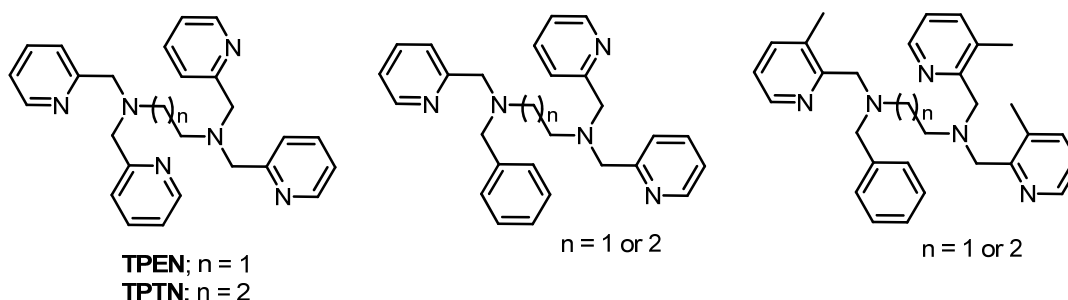


**Figure 4** Structure of TPEN/TPTN ligands and their derivatives.<sup>33,34</sup>

A remarkable observation was that although the complex  $[(\text{Mn}^{\text{III,III}}_2\text{O}(\text{OAc})_2\text{TPTN})]^{2+}$  was able to catalyse the oxidation of a broad scope of alkenes including styrene, cyclohexene and *trans*-2-octene to the corresponding epoxides in good yields and turnovers (up to 870), its analogue  $[(\text{Mn}^{\text{III,III}}_2\text{O}(\text{OAc})_2\text{TPEN})]^{2+}$ , featuring a two-carbon spacer between the two *N*-donor sets in the ligand, was unreactive both in the epoxidation of alkenes and in the oxidation of alcohols.<sup>34</sup>

A lack of retention of configuration was reported, *i.e.* a mixture of *cis*- and *trans*-epoxide products were formed upon epoxidation of *cis*- $\beta$ -methyl-styrene, and the observation of benzaldehyde in the oxidation of styrene and cinnamyl alcohol<sup>38</sup> indicated that radical intermediates are formed in the reaction mixture.

Although pre-prepared complexes were used in initial studies, *in situ* catalyst preparation was also investigated in the oxidation of alcohols.<sup>34</sup> Depending on the ligand used, a lag period of between 30 min and 3 h was observed. An (X-band) EPR spectroscopic and ESI-MS study of the reaction mixture with *in situ* prepared catalysts was described.<sup>34</sup> Initially, the reaction mixture was EPR silent at 77 K, however, 15-90 min (depending on the ligand used) after addition of substrate and  $\text{H}_2\text{O}_2$  a 16-line signal ( $A = 78$  G), characteristic of a  $\text{Mn}^{\text{III,IV}}_2$  complex was observed. ESI-MS measurements were less informative as only the mononuclear  $\text{Mn}^{\text{II}}$  complexes of the ligands were observed (*vide supra*).<sup>21</sup>

Although it will be shown in Chapter 3 of this thesis that ligand degradation to pyridine-2-carboxylic acid was responsible for the conversion observed (under slightly basic conditions in the presence of ketones), this, *a priori*, does not mean that the use of polypyridyl amines as ligands for manganese is unpromising in oxidation catalysis when  $\text{H}_2\text{O}_2$  is used as terminal oxidant.

On the contrary, following on from the excellent results reported by Stack and coworkers, using peracetic acid (PAA) as terminal oxidant,<sup>39</sup> Costas and coworkers demonstrated that this class of ligand can show exceptional efficiency (turn over frequency of  $30 \text{ s}^{-1}$ , 0.1 mol% catalyst, 1.1 equiv.  $\text{H}_2\text{O}_2$  w.r.t. substrate) in the oxidation

of alkenes with  $\text{H}_2\text{O}_2$ , when used in the presence of a moderate excess of acetic acid (14 equiv. w.r.t. substrate).<sup>40</sup> While  $[\text{Mn}^{\text{II}}(\text{OTf})_2(\text{H},\text{MePyTACN})]$  showed the best performance, the synthetically more accessible complex  $[\text{Mn}^{\text{II}}(\text{OTf})_2(\text{BPMCN})]$  also demonstrated conversions and yields of epoxides within acceptable ranges (Figure 5). The substrate scope was as broad as that obtained with PAA and a key advantage of the combination of acetic acid and  $\text{H}_2\text{O}_2$ , over the use of PAA, was shown with acid sensitive products obtained from substrates such as 1-phenyl-cyclohex-1-ene and stilbene. The  $[\text{Mn}^{\text{II}}(\text{OTf})_2(\text{BPMCN})]$  system showed limited activity, especially with respect to electron-poor and aromatic substrates. For the related complex  $[\text{Mn}^{\text{II}}(\text{OTf})_2(\text{BPMEN})]$  a substantial decrease in conversion and yield was observed demonstrating the sensitivity of the activity observed to structural variation in these systems.

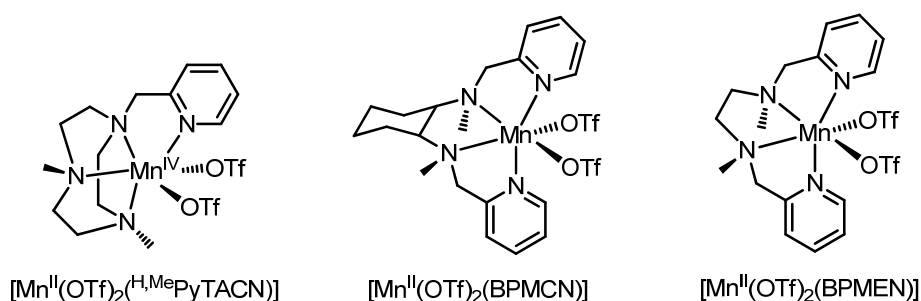


**Figure 5** Structures of Mn complexes with polypyridyl amine based ligands.

A central question, however, is the role of acetic acid. Indeed, given that PAA contains significant amounts of  $\text{H}_2\text{O}_2$ , it could be argued that the primary difference is that by using acetic acid and  $\text{H}_2\text{O}_2$ , traces of strong acids present in PAA are avoided. It should be noted, as demonstrated in Chapter 3, that degradation of pyridyl amine based ligands was not observed under acidic conditions with  $\text{H}_2\text{O}_2$  (*i.e.* in the presence of acetic acid) and hence it could be speculated that one role played by the acetic acid is to inhibit ligand oxidation. Furthermore, it is apparent from the report of Garcia *et al.*<sup>40</sup> and Dong *et al.*<sup>41</sup> (*vide supra*) that the *in situ* formation of PAA does not occur, as has been reported earlier by Que and coworkers.<sup>42</sup>

Overall, though several mechanistic differences between the acetic acid/ $\text{H}_2\text{O}_2$  and the PAA systems demonstrate that the mechanisms involved in each case are likely to be different. The rate of oxidation of *trans*-stilbene is six times that of *cis*-stilbene, in contrast to the PAA system, where it is only twice the rate.<sup>40</sup> Furthermore, the difference in the Hammett sensitivity parameter between the acetic acid/ $\text{H}_2\text{O}_2$  ( $\rho = -1.2$ ) and PAA ( $\rho = -0.67$ ) systems suggests that, although the mechanisms could be analogous (*i.e.* both active species are electrophilic), the active oxidant in each case is different. Regarding the mechanism, epoxidation was found to be highly stereospecific, even for stilbene, indicating a concerted oxygen transfer to the alkene. These data taken together with the incorporation of  $^{18}\text{O}$  solely from  $\text{H}_2\text{O}_2$  indicate a Lewis acid activation towards heterolysis of the O-O bond, which is assisted by the acetic acid.

### 1.5.1 Enantioselective epoxidation with pyridyl amine based manganese catalysts

The synthetic accessibility of complexes such as [Mn<sup>II</sup>(OTf)<sub>2</sub>(BPMCN)], together with the remarkable activity with acetic acid/H<sub>2</sub>O<sub>2</sub> demonstrated by Garcia *et al.*,<sup>40</sup> prompted Sun and coworkers<sup>43,44</sup> and later Lyakin *et al.*,<sup>45</sup> to develop enantioselective epoxidation catalysts based on this class of ligand. In these series of reports, the enantioselectivities achieved for a wide range of substrates are good to excellent, which holds considerable promise for the future.

### 1.5.2 Mechanistic considerations with pyridyl amine based manganese catalysts

From a mechanistic perspective, the evidence available to date is still limited, although on the basis of analogy with FeII complexes of the same ligands Lyakin *et al.*<sup>45</sup> have proposed that the manganese systems involve a [L(RCOO)MnV=O] species in alkene epoxidation. However, direct evidence of such manganese species is unavailable, except for the <sup>18</sup>O labelling studies reported by Garcia *et al.*,<sup>40</sup> which support a peroxy species as the oxygen transfer agent (*vide supra*). Indirect evidence available in the reports of Sun and coworkers,<sup>44</sup> in which <sup>18</sup>O from water is incorporated to a minor degree in the epoxide products, favour the postulation of a Mn=O species as an intermediate.

The complex [Mn<sup>II</sup>(OTf)<sub>2</sub>(<sup>H,Me</sup>PyTACN)] warrants further discussion in regard to possible active intermediates in oxidation catalysis. As will be discussed below with Me<sub>2</sub>EBC systems, the ability to generate isolable high valent (Mn<sup>IV</sup> and Mn<sup>V</sup>) oxo and peroxy complexes presents the opportunity of testing the kinetic competence of such species. In the case of [Mn<sup>II</sup>(OTf)<sub>2</sub>(<sup>H,Me</sup>PyTACN)], Costas and coworkers have isolated the Mn<sup>IV</sup> dihydroxy bound mononuclear complex [Mn<sup>IV</sup>(OH)<sub>2</sub>(<sup>H,Me</sup>PyTACN)]<sup>2+</sup> by oxidation of [Mn<sup>II</sup>(OTf)<sub>2</sub>(<sup>H,Me</sup>PyTACN)] with H<sub>2</sub>O<sub>2</sub> (10 equiv.) at 0 °C.<sup>46</sup> The Mn<sup>IV</sup> complex can be deprotonated reversibly to form a Mn<sup>IV</sup> oxo species [Mn<sup>IV</sup>(=O)(OH)(<sup>H,Me</sup>PyTACN)]<sup>+</sup> (Figure 6).

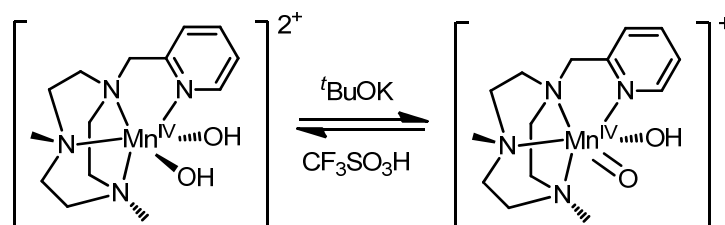


**Figure 6** Acid base chemistry of [Mn<sup>IV</sup>(OH)<sub>2</sub>(<sup>H,Me</sup>PyTACN)]<sup>2+</sup>.<sup>46</sup>

The Mn-O bands in the Raman spectrum (632 cm<sup>-1</sup> for [Mn<sup>IV</sup>(OH)<sub>2</sub>(<sup>H,Me</sup>PyTACN)]<sup>2+</sup> and 712 cm<sup>-1</sup> for [Mn<sup>IV</sup>(O)(OH)(<sup>H,Me</sup>PyTACN)]<sup>+</sup>) underwent the expected isotopic shifts (-30 cm<sup>-1</sup> based on the two atom oscillator approximation) in the presence of H<sub>2</sub><sup>18</sup>O. The increased Raman shift of [Mn<sup>IV</sup>(O)(OH)(<sup>H,Me</sup>PyTACN)]<sup>+</sup> at 712 cm<sup>-1</sup> is consistent with deprotonation to form a Mn=O bond. The complexes were characterised by ESI-MS and notably, despite the relatively high oxidation state, exchange of both Mn-OH and Mn=O

with  $\text{H}_2^{18}\text{O}$  was observed. Although these species have demonstrated activity in C-H abstraction, it is important to note that they are completely inactive in the epoxidation of alkenes, and hence cannot be viewed as ‘active intermediates’ in a catalytic cycle.<sup>47</sup> This point is considered below in regard to cyclam based systems.

It can be expected that the range of compounds within the BPMEN class will expand in the near future providing ligands with high enantio- and regio-selectivity, which will see application with more non-standard substrates, such as in the selective epoxidation of a precursor to epoxomicin demonstrated by Sun and coworkers<sup>44</sup> and the selective oxidation of the *cis*-alkene in *trans,cis*-2,6-nonadienyl demonstrated by Costas and coworkers.<sup>40</sup> A key challenge, however, in light of results reported in Chapter 3, is that ligand oxidation can occur and the involvement of pyridine-2-carboxylic acid should not be neglected.

In this aspect the recent report by Song *et al.*,<sup>48</sup> albeit not using  $\text{H}_2\text{O}_2$ , in which a more oxidatively stable pyridyl amide based ligand design is of note (Figure 7). The system showed good activity in oxidation catalysis with *m*CPBA (*meta*-chloroperbenzoic acid) and PAA. Mechanistic studies indicated that multiple pathways were involved, the relative importance of each depending on the exact conditions employed. In light of the systems described above it would be of interest for these systems to be studied with acetic acid/ $\text{H}_2\text{O}_2$  also.

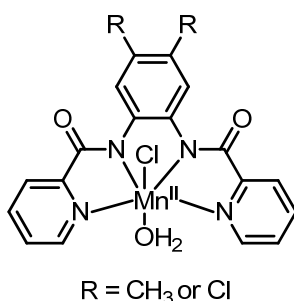


**Figure 7** Structure of amide based catalyst reported by Song *et al.*<sup>48</sup>

## 1.6 Trimethyl-triazacyclononane based ligands for manganese catalysed oxidation

Manganese complexes of the ligand *N,N',N''*-trimethyl-1,4,7-triazacyclononane (TMTACN), which were originally developed by Wieghardt and coworkers<sup>49</sup> as models for the oxygen evolving complex of photosystem II and to mimic dinuclear manganese catalases, have attracted the attention of several research groups towards oxidation catalysis over the last two decades.<sup>50</sup> This interest was prompted by researchers at Unilever in 1994, whom reported that the complex  $[\text{Mn}^{\text{IV,IV}}_2(\mu\text{-O})_3(\text{TMTACN})_2]^{2+}$  was a potent catalyst for low temperature stain bleaching with  $\text{H}_2\text{O}_2$  and for epoxidation of alkenes, specifically 4-vinylbenzoic acid and styrylacetic acid in carbonate buffer (with 100 equiv. of  $\text{H}_2\text{O}_2$  w.r.t. substrate).<sup>23,51</sup>

Due to its application in laundry and dye bleaching, initial mechanistic studies focused on oxidations and speciation analysis in aqueous media. An important finding by Hage and coworkers with respect to later studies, was the identification of the formation of carboxylic acid bridged dinuclear manganese complexes (*i.e.*  $[Mn^{III,III}_2(\mu-O)(\mu-RCO_2)_2(TMTACN)_2]^{2+}$ ) upon reduction of  $[Mn^{IV,IV}_2(\mu-O)_3(TMTACN)_2](PF_6)_2$  in aqueous media.

With regard to potential active species, Lindsay-Smith and coworkers reported a UV/Vis absorption and EPR spectroscopic and ESI-MS study of the oxidation of cinnamates in buffered aqueous acetonitrile.<sup>52,53,54,55</sup> ESI-MS experiments identified a mononuclear  $Mn^V=O$  species,<sup>55</sup> that could also be generated in oxidation reactions using a mononuclear  $Mn^{IV}$ -complex and from an *in situ* prepared  $Mn^{II}$ -complex using  $MnSO_4$  and the TMTACN ligand.<sup>55</sup> A central question, however, relates to the actual relevance of such species in the oxidation of alkenes as will be discussed in the last section.

Shortly after the initial reports of the activity of  $[Mn^{IV,IV}_2(\mu-O)_3(TMTACN)_2]^{2+}$  by Hage and coworkers efforts were directed to oxidation reactions in organic solvents. However, although several manganese complexes based on TMTACN derivatives showed activity in organic solvents, a key challenge faced in applying Mn-TMTACN was in overcoming wasteful disproportionation of  $H_2O_2$ .

A breakthrough came when De Vos and Bein reported that, in acetone, only 2 equiv. of  $H_2O_2$  were required to achieve good conversion (up to 80%) of alkenes to their corresponding epoxide products.<sup>56</sup> The dramatically increased efficiency in  $H_2O_2$ , achieved by carrying out reactions in acetone, could be assigned to the ‘buffering’ of the system by forming acetone- $H_2O_2$  adducts. However, the potential oxidation of acetone itself, which competes with oxidation of organic substrates, may be an alternate explanation for the effects observed. This is especially the case in light of the later discovery by De Vos *et al.*, where efficient epoxidation of a range of alkenes was achieved with suppression of the  $H_2O_2$  decomposition (using 1.5 equiv. of  $H_2O_2$ ) when carboxylic acids (such as fumaric acid) and especially oxalate-buffered aqueous acetonitrile were used.<sup>57</sup>

It is interesting to note, in light of later studies (*vide supra*), that in the report of De Vos *et al.* acetic acid was not found to be effective in promoting the epoxidation activity of  $[Mn^{IV,IV}_2(\mu-O)_3(TMTACN)_2]^{2+}$  whereas dicarboxylic acids and 1,3-diones were. Indeed, only 3 equiv. of acetic acid (w.r.t. catalyst) were employed. This, together with the generally poor enhancement seen with electron-rich carboxylic acids,<sup>64</sup> would not be sufficient to form an active system. In contrast, electron-poor dicarboxylic acids have an effective concentration of carboxylic acid groups, twice that of their molar concentration, and would be expected to be able to form catalytically active *bis*-carboxylato bridged complexes. Lindsay-Smith, Schul’pin and coworkers subsequently demonstrated that with excess acetic acid (w.r.t. substrate) activity was observed in the oxidation of alkanes and alkenes.<sup>58</sup>

Subsequent to the reports of De Vos and coworkers,<sup>56,57</sup> Berkessel and Sklorz reported that addition of L-ascorbic acid and sodium ascorbate was equally effective in

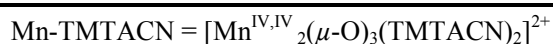
suppressing  $\text{H}_2\text{O}_2$  decomposition with this catalyst (prepared *in situ* from the ligand TMTACN and a  $\text{Mn}^{\text{II}}$  salt) and enabled both the epoxidation of alkenes and oxidation of alcohols with 2 equiv. of  $\text{H}_2\text{O}_2$ .<sup>59</sup>

Although the primary focus initially was on alkene epoxidation, a key observation in terms of reactivity was made by De Vos and coworkers in the first example of a heterogenised version of the catalyst system.<sup>60</sup> In addition to obtaining the expected epoxide product upon oxidation of alkenes with  $\text{H}_2\text{O}_2$ , De Vos *et al.* also observed the *cis*-dihydroxylation product. Although low selectivity is not normally a positive result in catalysis, the observation of *cis*-dihydroxylation with a manganese catalyst and  $\text{H}_2\text{O}_2$  was remarkable. Subsequent efforts to identify additives for the Mn-TMTACN system identified glyoxylic acid methylester methyl hemiacetal (GMHA) as an additive to promote the activity of the catalyst, suppress  $\text{H}_2\text{O}_2$  disproportionation and provide moderate selectivity towards *cis*-dihydroxylation.<sup>61</sup>

A notable feature of the additive GMHA is that, although it suppressed  $\text{H}_2\text{O}_2$  disproportionation completely, a significant lag period (1 h) was observed. Indeed a lag period is a common feature of the Mn-TMTACN system, except where L-ascorbic or oxalic acid is employed (*vide infra*). The lag phase indicates that the  $[\text{Mn}^{\text{IV,IV}}_2(\mu\text{-O})_3(\text{TMTACN})_2]^{2+}$  complex must first undergo conversion to a catalytically active species. Indeed, Zondervan *et al.*<sup>62</sup> noted, earlier, a significant increase in the activity of the  $[\text{Mn}^{\text{IV,IV}}_2(\mu\text{-O})_3(\text{TMTACN})_2]^{2+}$  in acetone when pre-treated with excess  $\text{H}_2\text{O}_2$  prior to addition of the substrate (in the case of benzyl alcohol oxidation).<sup>62</sup>

**Table 1** Comparison of efficiency in  $\text{H}_2\text{O}_2$ , conversion and selectivity for selected conditions covering a range of additives for Mn-TMTACN catalyst.

catalyst	additive (mol%)	equiv. of H <sub>2</sub> O <sub>2</sub>	conv. (%)	T.O.N.		ref.
				epoxide	cis-diol	
<i>1-hexene</i>						
Mn <sup>II</sup> + TMTACN	oxalic acid (0.2)/ Na oxalate (0.2)	1.5	>99	666	0	57
<i>1-octene</i>						
Mn-TMTACN	oxalic acid (1)	1.3	86	724	0	65
Mn <sup>II</sup> + TMTACN	L-ascobic acid (0.04)/ NaL-ascorbate (0.16)	2.6	<i>n.d.</i>	1110	0	59
Mn-TMTACN	L-ascorbic acid (1)	1.3	89	672	36	65
Mn-TMTACN	salicylic acid (1)	1.3	75	590	30	63
Mn-TMTACN	trichloroacetic acid (1)	1.3	66	200	115	63
Mn-TMTACN	2,6-dichlobenzoic acid (1)	1.3	71	295	125	63



More recently, attention has focused on elucidating both the mechanism by which the catalysts work and understanding the specific role(s) played by various additives in

enhancing the efficiency and selectivity of the reaction.<sup>63</sup> Initial studies focusing on catalytic properties had shown that addition of aldehydes (25 mol%) suppressed H<sub>2</sub>O<sub>2</sub> decomposition and increased conversion. Furthermore, the selectivity between epoxide and (*cis*)-diol products was affected considerably by the nature of the aldehyde used. However, the origin of this effect became apparent during mechanistic studies where it was shown that the corresponding carboxylic acids, present as impurities, were in fact responsible for the effects observed.<sup>63</sup> Reaction monitoring by UV/Vis spectroscopy, together with comparison with data reported earlier by Wieghardt,<sup>49</sup> Hage<sup>20</sup> and co-workers and independent synthesis of the complexes involved,<sup>63</sup> demonstrated the formation of *bis*-carboxylato bridged dinuclear manganese complexes, *i.e.* [Mn<sup>III,III</sup><sub>2</sub>(μ-O)(μ-RCO<sub>2</sub>)<sub>2</sub>(TMTACN)<sub>2</sub>]<sup>2+</sup>, was central to achieving reactivity (over 5000 turnovers) and selectivity (up to 7 : 1 *cis*-diol:epoxide product) with only 1.5 equiv. of H<sub>2</sub>O<sub>2</sub> w.r.t. the substrate.<sup>63</sup>

In addition, de Boer *et al.*<sup>64</sup> highlighted that individual components in a reaction mixture can have more than a single role. In the case of the carboxylic acids, the first role is to protonate [Mn<sup>IV,IV</sup><sub>2</sub>(μ-O)<sub>3</sub>(TMTACN)<sub>2</sub>]<sup>2+</sup> thereby moving its reduction potential to more positive potentials. The change in reduction potential allows H<sub>2</sub>O<sub>2</sub> to act as a two electron reductant (it should be noted that H<sub>2</sub>O<sub>2</sub> is isoelectronic with, albeit a much weaker reductant than, H<sub>2</sub>NNH<sub>2</sub>), and reduce the complex to a {Mn<sup>III,III</sup><sub>2</sub>} and then a {Mn<sup>II,II</sup><sub>2</sub>} redox state. This is followed by rapid ligand exchange and ultimately the formation of the catalytically important [Mn<sup>III,III</sup><sub>2</sub>(μ-O)(μ-RCO<sub>2</sub>)<sub>2</sub>(TMTACN)<sub>2</sub>]<sup>2+</sup> complex. This process is autocatalytic, *i.e.* the complex [Mn<sup>III,III</sup><sub>2</sub>(μ-O)(μ-RCO<sub>2</sub>)<sub>2</sub>(TMTACN)<sub>2</sub>]<sup>2+</sup> served to catalyse the reduction of [Mn<sup>IV,IV</sup><sub>2</sub>(μ-O)<sub>3</sub>(TMTACN)<sub>2</sub>]<sup>2+</sup> and it is this phenomenon that was demonstrated to cause the lag-time observed, after which a sudden onset of the reaction occurred (Figure 8).

The second role played by the carboxylic acids is of course to act as a bridging ligand and it is this role that allows the (epoxide vs. *cis*-diol) selectivity and activity of the catalyst to be tuned. It should be noted that whereas electron withdrawing groups increase activity (presumably by facilitating the opening of the μ-oxo bridge of the complex and allowing for H<sub>2</sub>O<sub>2</sub> to coordinate to one of the Mn<sup>III</sup> ions), it is the steric effects that dictate selectivity.<sup>64</sup> A third, but no less important role for the carboxylic acids, is to stabilise the [Mn<sup>III,III</sup><sub>2</sub>(μ-O)(μ-RCO<sub>2</sub>)<sub>2</sub>(TMTACN)<sub>2</sub>]<sup>2+</sup> complex; in the absence of several equivalents of the carboxylic acid (w.r.t. to the catalyst) the decomposition of the catalyst occurs. A final point with regard to mechanism is that at high carboxylic acid concentrations the selectivity shifts towards the epoxide product; the origin of this shift was found to be due to changes in solvent properties (specifically the ‘wetness’ of the solvent) and not to changes in the catalyst *per se*.



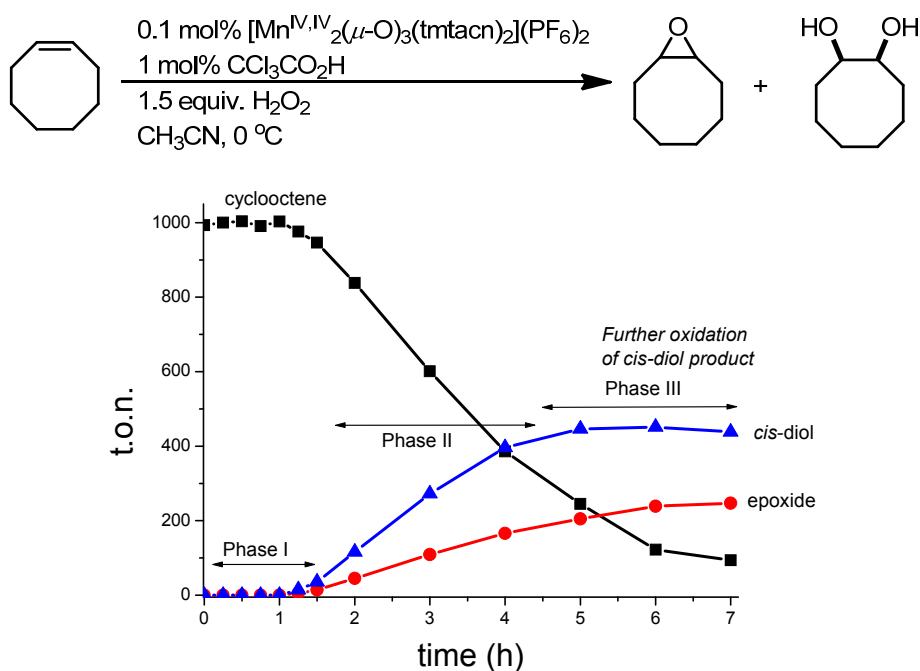


**Figure 8** Time dependence of consumption of cyclooctene and formation of its *cis*-diol and epoxide products catalysed by  $[\text{Mn}^{\text{IV,IV}}_2(\mu\text{-O})_3(\text{TMTACN})_2]^{2+}$ . At the end of the lag phase (I),  $[\text{Mn}^{\text{IV,IV}}_2(\mu\text{-O})_3(\text{TMTACN})_2]^{2+}$  converts to  $[\text{Mn}^{\text{III,III}}_2(\mu\text{-O})(\mu\text{-RCO}_2)_2(\text{TMTACN})_2]^{2+}$ , determined by UV/Vis absorption spectroscopy, which is concomitant to the start of conversion of cyclooctene (phase II). Reproduced with permission from ref. 64. Copyright ACS (2007).

Mechanistic studies demonstrated the interdependence of solvent, initial catalyst oxidation state, water and carboxylic acid concentration, and the nature of the carboxylic acid employed on both the activity and the selectivity of the catalysis.<sup>64</sup> With regard to the mechanism for the actual activation of  $\text{H}_2\text{O}_2$  and oxidation of the alkene, an understanding of the coordination chemistry of the  $[\text{Mn}^{\text{III,III}}_2(\mu\text{-O})(\mu\text{-RCO}_2)_2(\text{TMTACN})_2]^{2+}$  is necessary.

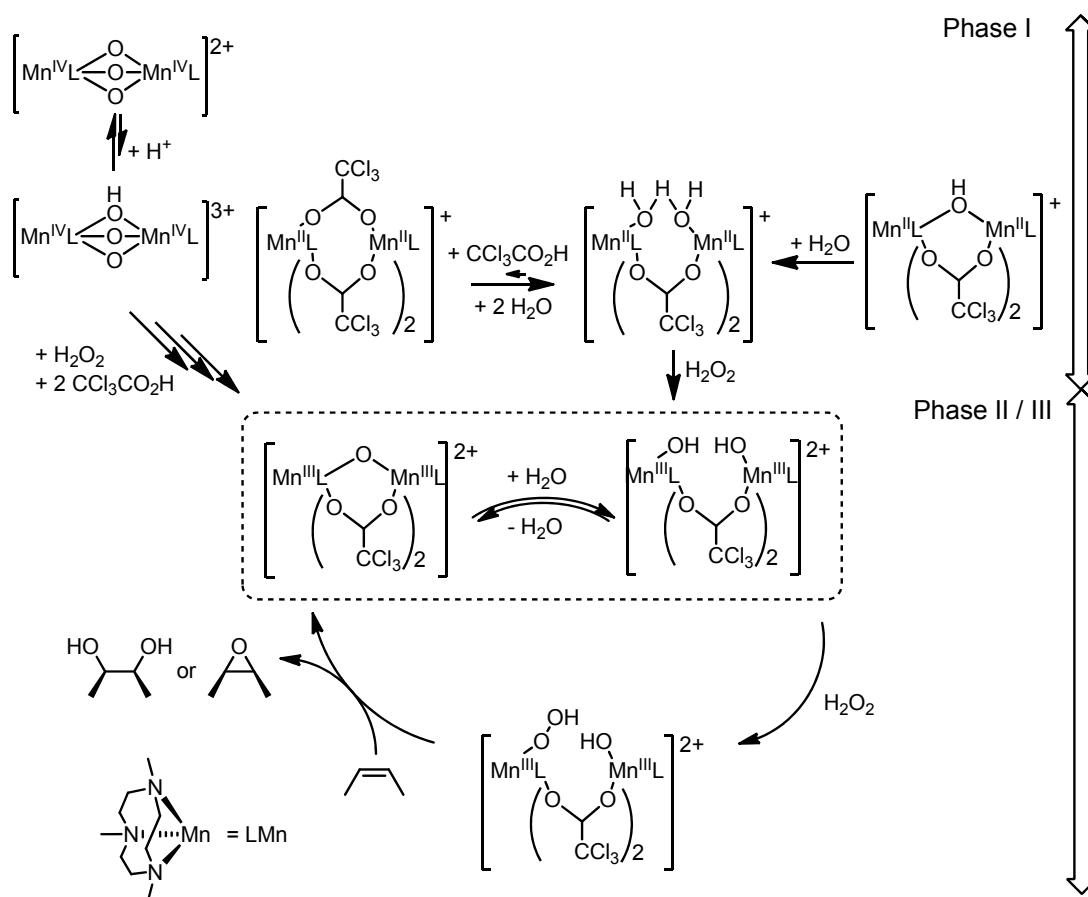
$[\text{Mn}^{\text{III,III}}_2(\mu\text{-O})(\mu\text{-RCO}_2)_2(\text{TMTACN})_2]^{2+}$  was shown to be stable in solution in the presence of substrate and, notably, in the presence of  $\text{H}_2\text{O}_2$ . Complexes of the type  $[\text{Mn}^{\text{III,III}}_2(\mu\text{-O})(\mu\text{-RCO}_2)_2(\text{TMTACN})_2]^{2+}$  also show a wide range of redox and solvent dependent coordination chemistry, in particular with regard to the bridging  $\mu$ -oxo moiety. Indeed, ESI-MS studies using  $\text{H}_2^{18}\text{O}$  and  $\text{CD}_3\text{CO}_2\text{H}$ , demonstrated that the  $\mu$ -oxo bridge ‘opens’ and ‘closes’ by reversible addition of water at a rate considerably faster than the exchange of the carboxylato ligands.<sup>64</sup>

No evidence for redox changes or a change in their dinuclear structure throughout the catalytic cycle has been found to date (Scheme 4). Absence of evidence, of course, does not preclude transient formation of a high-valent mononuclear species in the catalytic cycle, as proposed by several other groups.<sup>50</sup> However, it does imply that a mechanism in which the catalyst acts as a Lewis acid, together with a proximal -O-H ligand, should be

considered also. Indeed the role of proximal hydrogen bond donors (*e.g.* acetic acid), together with Lewis acidic metal centres, in facilitating heterolytic cleavage of the O-O bond of  $\text{H}_2\text{O}_2$  has been inferred in several systems (*vide infra*).

Although direct observation of the active species may not be possible, a key mechanistic tool in oxidation chemistry with  $\text{H}_2\text{O}_2$  is atom tracking with  $^{18}\text{O}$  labelling. de Boer *et al.* found, rather surprisingly, that only one of the oxygen atoms incorporated into the *cis*-diol product originates from  $\text{H}_2\text{O}_2$  with the other oxygen atom being provided by  $\text{H}_2\text{O}$ , regardless of the type of carboxylic acid used as co-catalyst.<sup>64</sup>

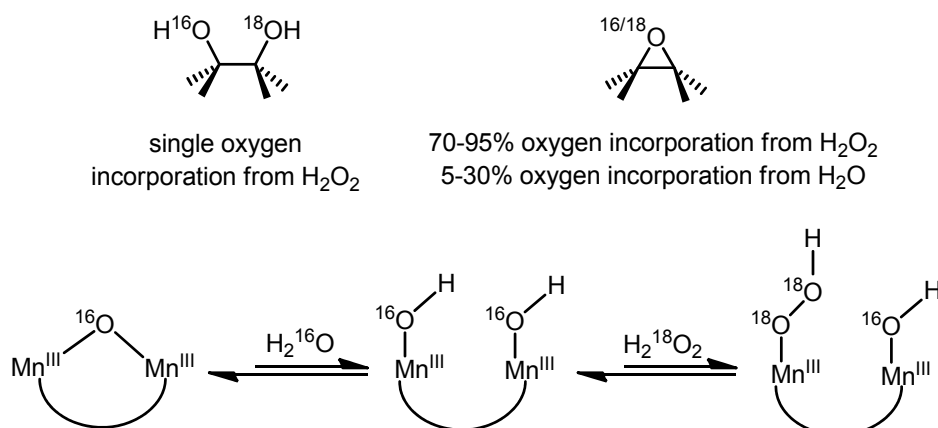
Concerning the origin of the oxygen atom in the epoxide product, the situation is less straightforward with both  $\text{H}_2\text{O}_2$  and  $\text{H}_2\text{O}$  providing oxygen atoms, the extent of which depends on the particular carboxylic acid employed. A correlation between the selectivity of the catalyst/carboxylic acid system towards the *cis*-diol/epoxide ratio and the incorporation of oxygen into the epoxide from  $\text{H}_2\text{O}$  was observed. The incorporation of oxygen from  $\text{H}_2\text{O}$  into the epoxide product ranged from 18% for the 2,6-dichlorobenzoate complex (*cis*-diol/epoxide ratio 7) to 13.4% for the 2,4-dichlorobenzoic acid complex (*cis*-diol/epoxide ratio 2.7), to 3.4% for the salicylic acid (*cis*-diol/epoxide ratio 0.7).



**Scheme 4** *cis*-Dihydroxylation and epoxidation of alkenes by  $[\text{Mn}^{\text{IV,IV}}(\mu\text{-O})_3(\text{TMTACN})_2]^{2+}$ .<sup>64</sup>

It was concluded that the more electrophilic the Mn-OH group of the proposed  $\{\text{Mn}^{\text{III}}(\text{OOH})\text{-Mn}^{\text{III}}(\text{OH})\}$  active species, the higher the *cis*-diol:epoxide product ratio would be. It should be noted that with the more electron withdrawing  $\text{CCl}_3\text{CO}_2\text{H}$ , an unprecedented 33% incorporation of oxygen from  $\text{H}_2\text{O}$  into the epoxide product was observed.

A final point worth noting with regard to mechanistic studies is that in the absence of carboxylic acid, *i.e.* using the catalyst  $[\text{Mn}^{\text{III,III}}_2(\mu\text{-O})(\mu\text{-CCl}_3\text{CO}_2)_2(\text{TMTACN})_2]^{2+}$ , more oxygen from  $\text{H}_2\text{O}_2$  was incorporated into both the *cis*-diol and epoxide products, and a significant amount of *cis*-diol showed both oxygen atoms originating from  $\text{H}_2\text{O}_2$ . This observation can be rationalized by considering that the rate of exchange of Mn-O-Mn with  $\text{H}_2\text{O}$  is slower in the absence of an excess of carboxylic acid and, hence, after the first dihydroxylation with  $\text{H}_2^{18}\text{O}_2$ ,  $[\text{Mn}^{\text{III,III}}_2(\mu\text{-}^{18}\text{O})(\mu\text{-RCO}_2)_2(\text{TMTACN})_2]^{2+}$  would be regenerated and this would then form  $[\text{Mn}^{\text{III,III}}_2(^{18}\text{O})(^{18}\text{O}^{18}\text{OH})(\mu\text{-RCO}_2)_2(\text{TMTACN})_2]^{2+}$  (Scheme 5) on the next cycle. This also highlights the importance of considering the rates of ligand exchange when interpreting  $^{18}\text{O}$  labelling data.



**Scheme 5** Possible  $\text{H}_2\text{O}_2$  activated species and observed oxygen incorporation from  $\text{H}_2\text{O}_2$  and  $\text{H}_2\text{O}$  in *cis*-diol and epoxide products for the oxidation of alkenes by  $[\text{Mn}^{\text{III,III}}_2(\mu\text{-O})(\mu\text{-RCO}_2)_2(\text{TMTACN})_2]^{2+}$ .<sup>64</sup>

Overall, however, the data reported by de Boer *et al.*<sup>63,64</sup> supports a mechanism in which a dinuclear manganese complex acts both as a Lewis acid, to activate the O-O bond of  $\text{H}_2\text{O}_2$  towards heterolytic cleavage and to present a proximal Mn-O-H unit to facilitate epoxidation, and to provide the 2<sup>nd</sup> oxygen in *cis*-dihydroxylation (Scheme 5). The increased reaction rates observed with more electron-poor carboxylic acids, and the preference for electron-rich alkenes, are manifestations of the electrophilic character of the active species also.

Although it may be tempting to expect that the mechanism by which the Mn-TMTACN catalysts operate is only ‘tweaked’ by variation in the additive used, *i.e.* complexes of the type  $[\text{Mn}^{\text{III,III}}_2(\mu\text{-O})(\mu\text{-RCO}_2)_2(\text{TMTACN})_2]^{2+}$  forming *in situ*, this is in fact not necessarily the case. Following on from the study of the effect of alkyl and aryl

carboxylic acid additives, de Boer *et al.*<sup>65</sup> examined the systems of De Vos<sup>57</sup> and Berkessel,<sup>59</sup> whom first employed the use of additives with the Mn-TMTACN catalysts, *i.e.* reactions catalysed by  $[Mn^{IV,IV}_2(\mu-O)_3(TMTACN)_2]^{2+}$  with oxalic acid and L-ascorbic acid. The spectroscopy and catalysis observed with  $[Mn^{IV,IV}_2(\mu-O)_3(TMTACN)_2]^{2+}$  in the presence of salicylic acid, L-ascorbic acid and oxalic acid were compared by de Boer *et al.*<sup>65</sup>

In the case of salicylic acid as additive, despite differences in UV/Vis absorption spectroscopy during catalysis (compared with, *e.g.* 3-hydroxybenzoic acid<sup>64</sup>) and the isolation of a green mononuclear complex  $[Mn^{III}(OH)(salicylate)(TMTACN)]$ , in which the salicylic acid bound to the  $Mn^{III}$  ion via the carboxylate and the phenoxide, it was found that  $[Mn^{III,III}_2(\mu-O)(\mu-RCO_2)_2(TMTACN)_2]^{2+}$  species were responsible for the catalysis observed. This example highlights the difficulties encountered in mechanistic studies in that the observation of a species does not necessarily imply its actual involvement in a catalytic cycle.

With L-ascorbic acid and oxalic acid, in contrast to the alkyl and aryl carboxylic acids, a lag period was not observed, *i.e.* conversion of substrate began immediately upon addition of  $H_2O_2$ .<sup>65</sup> Mechanistically, this difference can be understood in light of studies of the carboxylic acid promoted systems (*vide supra*, Scheme 4).<sup>64</sup> Both L-ascorbic acid and oxalic acid are reductants and hence the lag time, caused by the need for  $[Mn^{IV,IV}_2(\mu-O)_3(TMTACN)_2]^{2+}$  to be protonated and then reduced by  $H_2O_2$ , is absent.<sup>64,66</sup>

In the case of L-ascorbic acid as additive, the characteristic absorption spectrum of a  $[Mn^{III,III}_2(\mu-O)(\mu-RCO_2)_2(TMTACN)_2]^{2+}$  species was identified by UV/Vis spectroscopy.<sup>67</sup> This suggests that, except for the elimination of the lag time, mechanistically L-ascorbic acid promotes the reaction in a similar manner to the carboxylic acids. However, a caveat to such a conclusion is that electron-poor alkenes can be epoxidised with L-ascorbic acid as additive,<sup>59</sup> in contrast to the  $[Mn^{III,III}_2(\mu-O)(\mu-RCO_2)_2(TMTACN)_2]^{2+}$  catalysts, and hence in the former case a distinct mechanism may be in operation.

de Boer *et al.*<sup>65</sup> found that the oxalic acid/oxalate system developed by De Vos and coworkers<sup>57</sup> presented considerable complexity with regard to the mechanism. With the substrate, cyclooctene, initially only epoxidation was observed, however at a certain point in the reaction the *cis*-dihydroxylation product was also formed. Addition of extra oxalic acid before the change in selectivity occurred (*ca.* 3 h) results in only epoxidation occurring over the entire reaction.<sup>65</sup> These observations can be understood by considering that oxalic acid is unstable and, for example, can undergo oxidation to  $CO_2$ . Hence the switch in reactivity observed is due to the eventual loss of the oxalic acid from the reaction mixture. Carboxylic acids present (formed by further oxidation of diols) are available to form the *bis*-carboxylato mn-TMTACN catalysts.

This latter mechanistic study highlights a general challenge in elucidating mechanisms in manganese oxidation catalysis; it is not necessarily the case that only a single mechanism can be in operation in a particular system. Although the mechanism

switch observed with the oxalic acid/[Mn<sup>IV,IV</sup><sub>2</sub>(μ-O)<sub>3</sub>(TMTACN)<sub>2</sub>]<sup>2+</sup> system can be viewed as an extreme case, it is important to realise that changes in reaction conditions can switch mechanisms and that, as a reaction progresses, the changes in the reaction mixture (*e.g.* solvent polarity and composition, water content, product inhibition) can be sufficient to trigger such switches.

Although the present discussion has focused on mechanistic aspects, in particular the role of additives in promoting the activity of the Mn-TMTACN family of complexes, a brief mention regarding enantioselective alkene oxidation is pertinent as well. A review of enantioselective epoxidation including systems catalysed by manganese is provided by Watkinson and coworkers.<sup>8</sup> More recently, de Boer *et al.* demonstrated that enantioselective *cis*-dihydroxylation could be achieved with [Mn<sup>IV,IV</sup><sub>2</sub>(μ-O)<sub>3</sub>(TMTACN)<sub>2</sub>]<sup>2+</sup>.<sup>68</sup> In contrast to earlier studies by Beller,<sup>69</sup> Bolm<sup>70,71</sup> and co-worker where the chirality was introduced via derivatives of the TMTACN ligand, in the report of de Boer *et al.* a different approach was taken which built on the mechanistic studies carried out earlier that indicated that carboxylic acids acted as ligands in the catalytically active species. Hence, screening of a wide range of chiral carboxylic acids identified *N*-acetylphenylglycine (*N*-Ac-D-Phg) in particular with 55% conversion and an *ee* of 54% in the *cis*-dihydroxylation of chromene (with 1.7 equiv. of H<sub>2</sub>O<sub>2</sub>, 0.4 mol% [Mn<sup>III,III</sup><sub>2</sub>(μ-O)(μ-*N*-Ac-D-Phg)<sub>2</sub>(TMTACN)<sub>2</sub>]<sup>2+</sup> and 4 mol% *N*-Ac-D-Phg at -20 °C in CH<sub>3</sub>CN/H<sub>2</sub>O 19:1).

The recognition that carboxylic acids act as ligands stimulated renewed interest in heterogeneous Mn-TMTACN catalysts first investigated by De Vos and coworkers.<sup>72</sup> In contrast to the early studies in which the complexes were immobilised on mesoporous silica gel via a specifically modified TMTACN derivative, Notestein and coworkers<sup>73,74,75</sup> reported that immobilisation of the catalyst by *in situ* reduction of [Mn<sup>IV,IV</sup><sub>2</sub>(μ-O)<sub>3</sub>(TMTACN)<sub>2</sub>]<sup>2+</sup> in the presence of carboxylic acid coated silica particles allowed for similar levels of activity to be observed, both for epoxidation and *cis*-dihydroxylation, as found previously in homogeneous reactions by de Boer *et al.* (*vide supra*).<sup>64</sup> Although characterisation of the species formed in solution is relatively straightforward, when immobilised on surfaces/particles, the application of spectroscopic methods becomes more challenging. Nevertheless X-ray absorption spectroscopy and UV/Vis diffuse reflectance spectroscopy are particularly suited to studying the oxidation states of manganese and were applied in this case, demonstrating that [Mn<sup>IV,IV</sup><sub>2</sub>(μ-O)<sub>3</sub>(TMTACN)<sub>2</sub>]<sup>2+</sup> was grafted onto the silica surface as [Mn<sup>III,III</sup><sub>2</sub>(μ-O)(μ-RCO<sub>2</sub>)<sub>2</sub>(TMTACN)<sub>2</sub>]<sup>2+</sup> (where R = carboxy functionalised silica surface), upon addition of H<sub>2</sub>O<sub>2</sub>.<sup>75</sup> As for the homogenous systems discussed above, recycling of the heterogenised catalyst was limited which was ascribed tentatively to the effect of build-up of *cis*-diol in the reaction mixture.<sup>75</sup> Recently Bjorkman *et al.*<sup>76</sup> reported a microkinetic study of the heterogenised system with extensive use of modelling and concluded that the rate determining step was activation of the complex with H<sub>2</sub>O<sub>2</sub>. While direct extension of the conclusion of their study to the homogeneous system cannot be made, it is

nevertheless consistent with the observation that the resting state for the catalyst is the complex  $[\text{Mn}^{\text{III,III}}_2(\mu\text{-O})(\mu\text{-RCO}_2)_2(\text{TMTACN})_2]^{2+}$ .

## 1.7 Tetraazamacrocyclic based ligands for manganese catalysed oxidation

Busch and coworkers have studied the tetraazamacrobicyclic ligands in depth over the last decade with regard to activity, substrate scope and mechanism. These complexes have shown activity in the epoxidation of alkenes (employing H<sub>2</sub>O<sub>2</sub><sup>77,78,79,80</sup> as terminal oxidant and 'BuOOH<sup>81</sup> also) as well as in hydrogen abstraction.<sup>82,83,84,85</sup> In contrast to the TMTACN family of ligands, the methyl groups on the non-bridging nitrogen atoms of the Me<sub>2</sub>EBC ligand (where Me<sub>2</sub>EBC = 4,11-dimethyl-1,4,8,11-tetraazabicyclo[6.6.2]hexadecane) (Figure 9) preclude formation of di- and multi-nuclear manganese complexes. The manganese complexes of the cross-bridged Me<sub>2</sub>EBC have been characterised structurally, *i.e.*  $[\text{Mn}^{\text{II}}(\text{Me}_2\text{EBC})(\text{Cl})_2]$ ,<sup>77</sup>  $[\text{Mn}^{\text{III}}(\text{Me}_2\text{EBC})(\text{OMe})_2]^+$ ,<sup>86</sup>  $[\text{Mn}^{\text{III}}(\text{Me}_2\text{EBC})(\text{OH})(\text{OAc})]^+$ <sup>86</sup> and  $[\text{Mn}^{\text{IV}}(\text{Me}_2\text{EBC})(\text{OH})_2]^{2+}$ .<sup>79</sup>

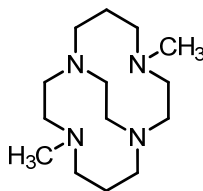


**Figure 9** Structure of Me<sub>2</sub>EBC.

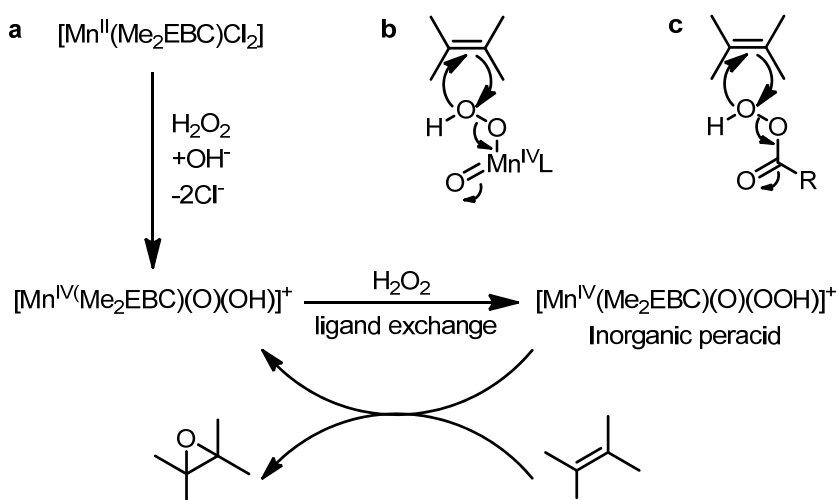
The product distribution in the epoxidation of selected alkenes catalysed by  $[\text{Mn}^{\text{II}}(\text{Me}_2\text{EBC})(\text{Cl})_2]$  in acetone/water with excess H<sub>2</sub>O<sub>2</sub> (17.7 equiv. w.r.t. substrate), together with <sup>18</sup>O-labelling studies and mass spectrometry, provided considerable mechanistic insight into this system.<sup>78</sup> Of particular note, with regard to selectivity, is the oxidation of cyclohexene which results in formation of cyclohexene oxide (18%) and cyclohexen-1-one (13%), as this indicates that the C-H abstraction ability (allylic oxidation) of the catalyst is substantial. However, the good selectivity in the oxidation of *cis*-stilbene and styrene, to their epoxide products, with minimal formation of benzaldehyde suggests that the catalyst does not generate radical species such as hydroxyl radicals.

Although catalysts based on this class of ligand have shown relatively modest activity (*i.e.* <45 turnovers in the oxidation of alkenes with excess H<sub>2</sub>O<sub>2</sub> using the catalyst  $[\text{Mn}^{\text{II}}(\text{Me}_2\text{EBC})(\text{Cl})_2]$ ),<sup>78</sup> these systems are highly amenable to mechanistic studies as a consequence of their stability in higher oxidation states which facilitates their isolation. This allows the kinetic competence of various species to be determined in stoichiometric reactions and hence, their involvement under catalytic conditions to be evaluated.

In aqueous solutions,  $[\text{Mn}^{\text{II}}(\text{Me}_2\text{EBC})(\text{Cl})_2]$  undergoes facile aquation to form  $[\text{Mn}^{\text{II}}(\text{Me}_2\text{EBC})(\text{OH})_2]$ , which can be oxidised reversibly to both the Mn<sup>III</sup> and Mn<sup>IV</sup>

oxidation states electrochemically. Indeed upon addition of  $\text{H}_2\text{O}_2$ ,  $[\text{Mn}^{\text{II}}(\text{Me}_2\text{EBC})(\text{OH})_2]$  is oxidised to  $[\text{Mn}^{\text{IV}}(\text{Me}_2\text{EBC})(\text{OH})_2]^{2+}$ , which when protonated forms a  $\text{Mn}=\text{O}$  species  $[\text{Mn}^{\text{IV}}(\text{Me}_2\text{EBC})(\text{O})(\text{OH})]^+$ . The isolated and structurally characterised complex  $[\text{Mn}^{\text{IV}}(\text{Me}_2\text{EBC})(\text{OH})_2]^{2+}$  was tested as a stoichiometric oxidant in the oxidation of norbornylene, styrene and *cis*-stilbene. For all three substrates, conversion was not observed even after standing for several days at room temperature. Generation of the  $\text{Mn}^{\text{V}}=\text{O}$  analogue (by deprotonation of  $[\text{Mn}^{\text{IV}}(\text{Me}_2\text{EBC})(\text{OH})_2]^{2+}$ ) did not result in alkene oxidation either. The absence of activity towards epoxidation excludes these species as being kinetically competent under reaction conditions with  $\text{H}_2\text{O}_2$ .<sup>79</sup>

This is supported further by  $^{18}\text{O}$  labelling studies including the use of  $^{18}\text{O}_2$ ,  $\text{H}_2^{18}\text{O}$  and  $\text{H}_2^{18}\text{O}_2$ . Ready exchange of  $[\text{Mn}^{\text{IV}}(\text{Me}_2\text{EBC})(^{16}\text{OH})_2]^{2+}$  with  $\text{H}_2^{18}\text{O}$  to form  $[\text{Mn}^{\text{IV}}(\text{Me}_2\text{EBC})(^{18}\text{O})(^{18}\text{OH})]^+$  was observed, as noted later for related systems (*vide supra*).<sup>79</sup> Hence, the absence of  $^{18}\text{O}$  incorporation into the epoxide products confirmed the lack of involvement of  $[\text{Mn}^{\text{IV}}(\text{Me}_2\text{EBC})(\text{OH})_2]^{2+}$ . Overall  $^{18}\text{O}$  labelling studies confirmed that, for epoxidation, the oxygen atom originates from the  $\text{H}_2\text{O}_2$ . It should be noted, however, that, although these species do not engage in alkene epoxidation,  $[\text{Mn}^{\text{IV}}(\text{Me}_2\text{EBC})(\text{OH})_2]^{2+}$  can engage in stoichiometric C-H abstraction.<sup>83</sup>



**Scheme 5** (a) Proposed Lewis acid activation mechanism for epoxidation of alkenes using  $[\text{Mn}^{\text{II}}(\text{Me}_2\text{EBC})\text{Cl}_2]$  and  $\text{H}_2\text{O}_2$  (b) Oxygen transfer by an inorganic peracid and (c) by an organic peracid.<sup>78</sup>

Busch and coworkers have proposed<sup>78</sup> a Lewis acid pathway rather than a manganese oxo pathway; that is that  $[\text{Mn}^{\text{IV}}(\text{Me}_2\text{EBC})(\text{O})(\text{OH})]^+$  reacts with  $\text{H}_2\text{O}_2$  to form  $[\text{Mn}^{\text{IV}}(\text{Me}_2\text{EBC})(\text{O})(\text{OOH})]^+$ , which acts as an inorganic peracid and transfers an oxygen atom directly to alkenes, similar to the mechanism with organic peracids (Scheme 5). This hypothesis is further supported by the detection of signals assignable to  $[\text{Mn}^{\text{IV}}(\text{Me}_2\text{EBC})(\text{O})(\text{OOH})]^+$  by ESI-MS under catalytic conditions<sup>79</sup> and by recent DFT studies by Haras and Ziegler which indicate that the mode of action of these complexes is via a  $\text{Mn}^{\text{IV}}\text{-OOH}$  species.<sup>87</sup>

## 1.8 Conclusions

In this chapter, several approaches to manganese based catalyst systems for the oxidation of alkenes with  $H_2O_2$  are discussed. At the simplest level, ‘ligand free’ or, more correctly, *in situ* prepared catalysts, offer considerable promise towards low cost catalyst systems not only for epoxidation of alkenes but also for *cis*-dihydroxylation. However, such systems do present drawbacks, especially with regard to substrate scope, and the generally limited opportunities to tune selectivity and activity and also in regard to enantioselective oxidations. The near stoichiometric efficiency with respect to terminal oxidant ( $H_2O_2$ ) that has been achieved in several systems recently means that such systems are now suitable for application, even in large scale processes. From a mechanistic perspective it is apparent that, although such systems are simple to use, they are far from simple in regard to both the manganese itself and the roles played by other species in the reaction mixture.

With regard to enantioselective oxidation of alkenes, the use of chiral ligands has shown some success. Indeed pyridyl amine based ligands offer perhaps the best prospects to date for epoxidation. By contrast, the synthetic challenges faced in preparing chiral Mn-TMTACN based catalysts have proven to be a serious impediment to progress in enantioselective oxidations. Here, the benefit of a mechanistic understanding is exemplified in the modest success achieved by use of chiral carboxylic acids as ligands.

From a mechanistic perspective, the ligand based systems discussed above indicate that, in the case of C-H abstraction, Mn=O species are likely to be involved whereas such species are less likely to be involved in alkene oxidations. In contrast to porphyrin and salen based manganese catalysts, mechanistic data available for the systems discussed in this chapter generally point towards involvement of Lewis acid activation of  $H_2O_2$  towards heterolytic cleavage of the O-O bond rather than a high valent manganese oxo species being responsible for oxygen transfer to alkenes.

Finally, perhaps the most important take home message with regard to the mechanistic studies on these systems is that one should always remain open to the possibility that, even in the simplest systems, more than one mechanism may be in operation and that minor changes in conditions can lead to a switch between distinct mechanisms. This increases the difficulties encountered in mechanistic studies, of course, but on the positive side it also makes such studies much more fascinating.

## 1.9 Overview of the thesis

The research described in this thesis is concerned with the development of new methods for oxidative transformations of organic substrates, in particular, the *cis*-dihydroxylation and epoxidation of alkenes as well as the oxidation of alcohols and aldehydes and C-H activation. These methods are based on manganese catalysts and  $H_2O_2$ . A key aspect that is focussed on, is to achieve a mechanistic understanding of systems developed.

In Chapter 2, the application of Mn-TMTACN (*N,N,N'*-trimethyl-1,4,7-triazacyclononane) based catalysts for selective oxidation of organic substrates with



multiple oxidation sensitive functional groups including alcohols, aldehydes, alkenes and alkanes is described. The goal of this study is to build on the recent identification of carboxylato bridge complexes as the catalytically important species.<sup>64</sup>

Chapter 3 describes the discovery that many polypyridyl amine based ligands decompose *in situ* to pyridine-2-carboxylic acid and its derivatives, in the presence of  $\text{Mn}^{\text{II}}$ ,  $\text{H}_2\text{O}_2$  and a base in ketone containing solvents. This phenomenon is demonstrated by  $^1\text{H}$  NMR spectroscopy. The activity and selectivity of the catalytic system, discovered through this study, was found to be identical to that observed with polypyridyl amine based catalysts for the oxidation of alkenes described previously.

In Chapter 4, a new practical method is reported for selective *cis*-dihydroxylation of electron deficient alkenes and epoxidation of electron rich alkenes based on the Mn-pyridine-2-carboxylic acid catalytic system, the discovery of which is described in Chapter 3. The key role played by Raman spectroscopy for lead identification and reaction optimisation is also discussed.

Chapter 5 describes mechanistic insights into the catalytic system described in Chapter 4 consisting of pyridine-2-carboxylic acid/ $\text{Mn}^{\text{II}}$ /base/ketone additive and  $\text{H}_2\text{O}_2$ . The study focusses on the role(s) of butanedione (the ketone additive) and its by-product (acetic acid) formed by the decomposition of butanedione by  $\text{H}_2\text{O}_2$ . A range of physical techniques including NMR, UV/Vis, Raman spectroscopy and mass spectroscopy was employed to follow the reaction both online and offline. The complex interplay of reaction components is discussed in depth.

In Chapter 6 the results presented in this thesis are discussed in term of the advantages and drawbacks of the systems as well as placed in perspective with regard to solutions and possibilities for future development.

## 1.10 References and notes

- 
- 1 S. Caron, R. W. Dugger, S. G. Ruggeri, J. A. Ragan and D. H. B. Ripin, *Chem. Rev.*, 2006, **106**, 2943.
  - 2 (a) *Industrial Organic Chemistry*, K. Weissmehl and H. J. Arpe (eds.), Wiley-VCH Weinheim, 1993; (b) *Transition Metals for Organic Synthesis, Vol 2*, M. Beller and C. Bolm (eds.), Wiley-VCH, Weinheim, 2004.
  - 3 T. Punniyamurthy, S. Velusamy and J. Iqbal, *Chem. Rev.*, 2005, **105**, 2329.
  - 4 M. Beller, *Adv. Synth. Catal.*, 2004, **346**, 107.
  - 5 M. Costas, *Chem. Cat. Chem.*, 2012, **4**, 175.
  - 6 *Modern Oxidation Methods*, 2nd Ed. J.-E. Bäckvall (ed.), Wiley-VCH, Weinheim, 2010.
  - 7 R. Hage, J. W. de Boer, F. Gaulard and K. Maaijen, *Adv. Inorg. Chem.*, 2012, **65**, in press.
  - 8 G. De Faveri, G. Ilyashenko and M. Watkinson, *Chem. Soc. Rev.*, 2011, **40**, 1722.
  - 9 C. J. R. Bataille and T. J. Donohoe, *Chem. Soc. Rev.*, 2011, **40**, 114.

- 10 K. Chen, M. Costas, J. H. Kim, A. K. Tipton and L. Que, Jr., *J. Am. Chem. Soc.*, 2002, **124**, 3026.
- 11 K. Suzuki, P. D. Oldenburg and L. Que, Jr., *Angew. Chem. Int. Ed.*, 2008, **47**, 1887.
- 12 J. W. de Boer, W. R. Browne, B. L. Feringa and R. Hage, *C. R. Chim.*, 2007, **10**, 341.
- 13 S. Signorella and C. Hureau, *Coord. Chem. Rev.*, 2012, **256**, 1229.
- 14 K. Srinivasan, P. Michaud and J. K. Kochi, *J. Am. Chem. Soc.*, 1986, **108**, 2309.
- 15 W. Zhang, J. L. Loebach, S. R. Wilson and E. N. Jacobsen, *J. Am. Chem. Soc.*, 1990, **112**, 2801.
- 16 R. Irie, K. Noda, Y. Ito, N. Matsumoto and T. Katsuki, *Tetrahedron Lett.*, 1990, **31**, 7345.
- 17 B. Meunier, *Chem. Rev.*, 1992, **92**, 1411.
- 18 The interested reader is directed to *Physical Methods in Bioinorganic Chemistry*, ed. L. Que, Jr., University Science Books, Sausalito, 2000.
- 19 *Electron Spin Resonance, analysis and interpretation*, P. H. Rieger, RSC Publishing, Cambridge, 2007.
- 20 R. Hage, E. A. Gunnewegh, J. Niel, F. S. B. Tjan, T. Weyhermuller and K. Wieghardt, *Inorg. Chim. Acta*, 1998, **268**, 43.
- 21 For a review of the application of mass spectrometry in inorganic oxidation chemistry see O. Bortolini and V. Conte, *Mass Spect. Rev.*, 2006, **25**, 724. See also reference 64 for examples of artefacts that can arise in ESI-MS studies of manganese complexes.
- 22 (a) M. Costas, K. Chen and L. Que, Jr., *Coord. Chem. Rev.*, 2000, **200-202**, 517; (b) E. M. Simmons and J. F. Hartwig, *Angew. Chem. Int. Ed.*, 2012, **51**, 3066.
- 23 R. Hage, J. E. Iburg, J. Kerschner, J. H. Koek, E. L. M. Lempers, R. J. Martens, U. S. Racherla, S. W. Russell, T. Swarthoff, M. R. P. van Vliet, J. B. Warnaar, L. van der Wolf and B. Krijnen, *Nature*, 1994, **369**, 637.
- 24 (a) D. E. Richardson, H. Yao, K. M. Frank and D. A. Bennett, *J. Am. Chem. Soc.*, 2000, **122**, 1729; (b) H. Yao and D. E. Richardson, *J. Am. Chem. Soc.*, 2000, **122**, 3220.
- 25 B. S. Lane and K. Burgess, *J. Am. Chem. Soc.*, 2001, **123**, 2933.
- 26 B. S. Lane, M. Vogt, V. J. De Rose and K. Burgess, *J. Am. Chem. Soc.*, 2002, **124**, 11946.
- 27 H. K. Kwong, P.-K. Lo, K.-C. Lau and T.-C. Lau, *Chem. Commun.*, 2011, **47**, 4273.
- 28 J. Bendix, K. Meyer, T. Weyhermuller, E. Bill, N. Metzler-Nolte and K. Wieghardt, *Inorg. Chem.*, 1998, **37**, 1767.
- 29 It should be noted however that this conclusion is based on the assumption that the O-O bond strength and stability of products are similar between H<sub>2</sub>O<sub>2</sub> and 2-methyl-1-phenyl-2-propyl hydroperoxide.
- 30 S. Zhong, Z. Fu, Y. Tan, Q. Xie, F. Xie, X. Zhou, Z. Ye, G. Peng and D. Yina, *Adv. Synth. Catal.*, 2008, **350**, 802.
- 31 D. W. Nelson, A. Gypser, P. T. Ho, H. C. Kolb, T. Kondo, H.-L. Kwong, D. V. McGrath, A. E. Rubin, P.-O. Norrby, K. P. Gable and K. B. Sharpless, *J. Am. Chem. Soc.*, 1997, **119**, 1840.
- 32 (a) K. Matsumoto, Y. Sawada and T. Katsuki, *Pure & Appl. Chem.*, 2008, **80**, 1071; (b) Y. Sawada, K. Matsumoto and T. Katsuki, *Angew. Chem. Int. Ed.*, 2007, **46**, 4559; (c) Y. Sawada, K.

- Matsumoto, S. Kondo, H. Watanabe, T. Ozawa, K. Suzuki and B. Saito, T. Katsuki, *Angew. Chem. Int. Ed.* 2006, **45**, 3478.
- 33 J. Brinksma, R. Hage, J. Kerschner and B. L. Feringa, *Chem. Commun.*, 2000, 537.
- 34 J. Brinksma, M. T. Rispens, R. Hage and B. L. Feringa, *Inorg. Chim. Acta*, 2002, **337**, 75.
- 35 F. Dubnikova, R. Kosloff, J. Almog, Y. Zeiri, R. Boese, H. Itzhaky, A. Alt and E. Keinan, *J. Am. Chem. Soc.*, 2005, **127**, 1146.
- 36 R. Schulte-Ladbeck, P. Kolla and U. Karst, *Anal. Chem.*, 2003, **75**, 731.
- 37 H. Jiang, G. Chu, H. Gong and Q. Qiao, *J. Chem. Res.(S)*, 1999, 288.
- 38 W. Zhang, N. H. Lee and E. N. Jacobsen, *J. Am. Chem. Soc.*, 1994, **116**, 425.
- 39 A. Murphy, G. Dubois and T. D. P. Stack, *J. Am. Chem. Soc.*, 2003, **125**, 5250; A. Murphy, A. Pace and T. D. P. Stack, *Org. Lett.*, 2004, **6**, 3119.
- 40 I. Garcia-Bosch, X. Ribas and M. Costas, *Adv. Synth. Catal.*, 2009, **351**, 348.
- 41 J. Dong, P. Saisaha, T. G. Meinds, P. L. Alsters, E. G. Ijpeij, R. P. van Summeren, B. Mao, M. Fañanás-Mastral, J. W. de Boer, R. Hage, B. L. Feringa and W. R. Browne, *ACS Catal.*, 2012, **2**, 1087.
- 42 M. Fujita and L. Que, Jr., *Adv. Synth. Catal.*, 2004, **346**, 190. It should be noted that the authors proposed *in situ* formation of PAA from acetic acid and H<sub>2</sub>O<sub>2</sub>, but only in the presence of certain iron catalysts.
- 43 M. Wu, B. Wang, S. Wang, C. Xia and W. Sun, *Org. Lett.*, 2009, **11**, 3622.
- 44 B. Wang, C. Miao, S. Wang, C. Xia and W. Sun, *Chem. Eur. J.*, 2012, **18**, 6750.
- 45 (a) O. Y. Lyakin, R. V. Ottenbacher, K. P. Bryliakov and E. P. Talsi, *ACS Catal.*, 2012, **2**, 1196; (b) R. V. Ottenbacher, K. P. Bryliakov and E. P. Talsi, *Adv. Synth. Catal.* 2011, **353**, 885.
- 46 I. Garcia-Bosch, A. Company, C. W. Cady, S. Styring, W. R. Browne, X. Ribas and M. Costas, *Angew. Chem. Int. Ed.* 2011, **50**, 5648.
- 47 Private communication Prof. M. Costas, University of Girona, Spain.
- 48 Y. J. Song, S. H. Lee, H. M. Park, S. H. Kim, H. G. Goo, G. H. Eom, J. H. Lee, M. S. Lah, Y. Kim, S.-J. Kim, J. E. Lee, H.-I. Lee and C. Kim, *Chem Eur J.*, 2011, **17**, 7336.
- 49 K. Wieghardt, U. Bossek, B. Nuber, J. Weiss, J. Bonvoisin, M. Corbella, S. E. Vitols and J. J. Girerd, *J. Am. Chem. Soc.*, 1988, **110**, 7398.
- 50 K. F. Sibbons, K. Shastri and M. Watkinson, *Dalton Trans.*, 2006, 645.
- 51 V. C. QueeSmith, L. DelPizzo, S. H. Jureller, J. L. Kerschner and R. Hage, *Inorg. Chem.* 1996, **35**, 6461.
- 52 B. C. Gilbert, N. W. J. Kamp, J. R. L. Smith and J. Oakes, *J. Chem. Soc., Perkin Trans. 2*, 1997, 216.
- 53 B. C. Gilbert, N. W. J. Kamp, J. R. L. Smith and J. Oakes, *J. Chem. Soc., Perkin Trans. 2*, 1998, 1841.
- 54 B. C. Gilbert, J. R. L. Smith, M. S. Newton, J. Oakes and R. P. I. Prats, *Org. Biomol. Chem.*, 2003, **1**, 1568.
- 55 J. R. L. Smith, B. C. Gilbert, A. M. I. Payeras, J. Murray, T. R. Lowdon, J. Oakes, R. P. I. Prats and P. H. Walton, *J. Mol. Cat. A – Chem.*, 2006, **251**, 114.

- 56 D. E. De Vos and T. Bein, *J. Organometallic Chem.*, 1996, **520**, 195.
- 57 D. E. De Vos, B. F. Sels, M. Reynaers, Y. V. S. Rao and P. A. Jacobs, *Tetrahedron Lett.*, 1998, **39**, 3221.
- 58 (a) G. B. Shul'pin, G. Suss-Fink and J. R. Lindsay Smith, *Tetrahedron*, 1999, **55**, 5345; (b) G. B. Shul'pin, G. Suss-Fink and L. S. Shul'pina, *J. Mol. Cat. A – Chem.*, 2001, **170**, 17.
- 59 A. Berkessel and C. A. Sklorz, *Tetrahedron Lett.*, 1999, **40**, 7965.
- 60 D. E. De Vos, S. de Wildeman, B. F. Sels, P. J. Grobet and P. A. Jacobs, *Angew. Chem., Int. Ed.*, 1999, **38**, 980.
- 61 J. Brinksma, L. Schmieder, G. van Vliet, R. Boaron, R. Hage, D. E. De Vos, P. L. Alsters and B. L. Feringa, *Tetrahedron Lett.*, 2002, **43**, 2619.
- 62 C. Zondervan, R. Hage and B. L. Feringa, *Chem. Commun.*, 1997, 419.
- 63 J. W. de Boer, J. Brinksma, W. R. Browne, A. Meetsma, P. L. Alsters, R. Hage and B. L. Feringa, *J. Am. Chem. Soc.*, 2005, **127**, 7990.
- 64 J. W. de Boer, W. R. Browne, J. Brinksma, A. Meetsma, P. L. Alsters, R. Hage and B. L. Feringa, *Inorg. Chem.*, 2007, **46**, 6353.
- 65 J. W. de Boer, P. L. Alsters, A. Meetsma, R. Hage, W. R. Browne and B. L. Feringa, *Dalton*, **2008**, **44**, 6283.
- 66 Indeed L-ascorbic acid can be used in the synthesis of [Mn<sup>III,III</sup><sub>2</sub>(μ-O)(μ-RCO<sub>2</sub>)<sub>2</sub>(TMTACN)<sub>2</sub>](PF<sub>6</sub>)<sub>2</sub> complexes by reduction of [Mn<sup>IV,IV</sup><sub>2</sub>(μ-O)<sub>3</sub>(TMTACN)<sub>2</sub>]<sup>2+</sup>.
- 67 It should be noted that Mn<sup>III,IV</sup><sub>2</sub> dinuclear species were observed by EPR spectroscopy during catalysis also; the intensity of its EPR signal increased upon each addition of H<sub>2</sub>O<sub>2</sub>, and then decreased as the H<sub>2</sub>O<sub>2</sub> was consumed. However, observing such species does not in itself imply their involvement catalytically. Indeed with other carboxylic acids such species were observed by de Boer *et al.*<sup>63</sup> when the catalyst concentration was increased to 5 mM instead of the more typical catalytic reaction conditions (*i.e.* 1 mM catalyst concentration).
- 68 J. W. de Boer, W. R. Browne, S. R. Harutyunyan, L. Bini, T. D. Tiemersma-Wegman, P. L. Alsters, R. Hage and B. L. Feringa, *Chem. Commun.*, 2008, 3747.
- 69 (a) M. Beller, A. Tafesh, R. W. Fischer and B. Schabert, Patent, DE 195 23 890, C1; 30.06.95; (b) M. Beller, A. Tafesh, R. W. Fischer and B. Schabert, Patent, DE 195 23 891 C1; 30.06.95.
- 70 C. Bolm, D. Kadereit and M. Valacchi, *Synlett.*, 1997, 687.
- 71 C. Bolm, N. Meyer, G. Raabe, T. Weyhermüller and E. Bothe, *Chem. Commun.*, 2000, 2435.
- 72 D. E. De Vos, B. F. Sels and P. A. Jacobs, *Adv. Synth. Catal.*, 2003, **345**, 457.
- 73 N. J. Schoenfeldt and A. W. Korinda and J. M. Notestein, *Chem. Commun.*, 2010, **46**, 1640.
- 74 N. J. Schoenfeldt and J. M. Notestein, *ACS Catal.*, 2011, **1**, 1691.
- 75 N. J. Schoenfeldt, Z. Ni, A. W. Korinda, R. J. Meyer and J. M. Notestein, *J. Am. Chem. Soc.*, 2011, **133**, 18684.
- 76 K. R. Bjorkman, N. J. Schoenfeldt, J. M. Notestein and L. J. Broadbelt, *J. Catal.*, 2012, **291**, 17.

- 
- 77 T. J. Hubin, J. M. McCormick, S. R. Collinson, M. Buchalova, C. M. Perkins, N. W. Alcock, P. K. Kahol, A. Raghunathan and D. H. Busch, *J. Am. Chem. Soc.*, 2000, **122**, 2512.
- 78 G. Yin, M. Buchalova, A. M. Danby, C. M. Perkins, D. Kitko, J. D. Carter, W. M. Scheper and D. H. Busch, *J. Am. Chem. Soc.*, 2005, **127**, 17170.
- 79 G. Yin, M. Buchalova, A. M. Danby, C. M. Perkins, D. Kitko, J. D. Carter, W. M. Scheper and D. H. Busch, *Inorg. Chem.*, 2006, **45**, 3467.
- 80 G. Yin, A. M. Danby, D. Kitko, J. D. Carter, W. M. Scheper and D. H. Busch, *Inorg. Chem.*, 2007, **46**, 2173.
- 81 D. H. Busch, G. Yin and H. Lee in *Chapter 3, S. T. Oyama, (ed.) Mechanisms in Homogeneous and Heterogeneous Epoxidation Catalysis*, 2008, Elsevier Science, 119.
- 82 S. Chattopadhyay, R. A. Geiger, G. Yin, D. H. Busch and T. A. Jackson, *Inorg. Chem.*, 2010, **49**, 7530.
- 83 G. Yin, A. M. Danby, D. Kitko, J. D. Carter, W. M. Scheper and D. H. Busch, *J. Am. Chem. Soc.*, 2007, **129**, 1512.
- 84 G. Yin, A. M. Danby, D. Kitko, J. D. Carter, W. M. Scheper and D. H. Busch, *J. Am. Chem. Soc.*, 2008, **130**, 16245.
- 85 S. Shi, Y. Wang, A. Xu, H. Wang, D. Zhu, S. B. Roy, T. A. Jackson, D. H. Busch and G. Yin, *Angew. Chem. Int. Ed.*, 2011, **50**, 7321.
- 86 T. J. Hubbin, J. M. McCormick, N. W. Alcock and D. H. Busch, *Inorg. Chem.*, 2001, **40**, 435.
- 87 A. Haras and T. Ziegler, *Can. J. Chem.*, 2009, **87**, 3.

## Chapter 2

# Selective catalytic oxidation of alcohols, aldehydes, alkanes and alkenes employing manganese catalysts and H<sub>2</sub>O<sub>2</sub>

*A catalytic system employing a combination of  $[\text{Mn}^{\text{IV,IV}}_2\text{O}_3(\text{TMTACN})_2]^{2+}$  and carboxylic acids for the oxidation of organic substrates containing oxidatively sensitive functional groups, using H<sub>2</sub>O<sub>2</sub> as terminal oxidant, is examined in this chapter. The focus is on tuning the reactivity and selectivity of the reaction by varying the carboxylic acid employed. Raman spectroscopy was used for both offline and online analysis providing useful kinetic information for controlling the selectivity of the reaction.*

P. Saisaha, M. van der Meer, L. Buettner, J. W. de Boer, R. Hage and W. R. Browne, manuscript in preparation.

## 2.1 Introduction

Oxidative transformations, in particular the oxidation of alkenes to their corresponding diols or epoxides,<sup>1,2</sup> alcohols to aldehydes, ketones or carboxylic acids and selective C-H bond activation are central processes in biology, synthetic organic chemistry and industrial chemistry.<sup>3</sup> In recent years, the development of atom-efficient and environmentally friendly catalytic systems has been a major challenge.<sup>4</sup> A primary goal is to develop systems that show high atom efficiency and minimal formation of by-products, with molecular oxygen (O<sub>2</sub>) and hydrogen peroxide (H<sub>2</sub>O<sub>2</sub>) being the most atom economic as water is the sole by-product.<sup>5</sup>

As discussed in Chapter 1, over the last two decades several groups have focused on the use of manganese catalysts based on the *N,N',N''*-trimethyl-1,4,7-triazacyclononane (TMTACN) ligand originally developed by Wieghardt and coworkers in the late 1980s as model systems for the water splitting component of photosystem II (PS II) and dinuclear manganese-based catalase enzymes.<sup>6,7,8,9</sup> The first report on the use of [Mn<sup>IV,IV</sup><sub>2</sub>O<sub>3</sub>(TMTACN)<sub>2</sub>]<sup>2+</sup> (**1**) (Figure 1) as a catalyst was by Hage *et al.* in 1994, where it was employed in an aqueous carbonate buffer (pH 8-9) with H<sub>2</sub>O<sub>2</sub> as terminal oxidant for clean and efficient low-temperature bleaching as well as the epoxidation of alkenes.<sup>10</sup> Since then, several research groups have focused on applying this catalyst in oxidative transformations with initial efforts focusing on the use of additives to suppress the wasteful catalase-type activity of **1** and to enhance its activity towards the oxidation of alkenes.<sup>11,12,13</sup> De Vos *et al.* reported the efficient epoxidation of a range of alkenes using this catalyst in oxalate-buffered aqueous acetonitrile. Under these conditions the catalase-type activity was effectively suppressed.<sup>14</sup> Subsequently, Berkessel and coworkers showed that the use of a mixture of L-ascorbic acid and sodium ascorbate in combination with TMTACN and Mn<sup>II</sup> could effect the epoxidation of alkenes and the oxidation of alcohols, albeit with excess H<sub>2</sub>O<sub>2</sub>.<sup>15</sup> Since then, the range of substrate classes that have been examined with **1** includes alkanes, alkenes, primary and secondary alcohols and allylic alcohols.<sup>13,16</sup> However, later reports showed that in the presence of a large excess of acid, *e.g.* acetic acid,<sup>17</sup> or aldehydes such as choral,<sup>18</sup> the catalytic activity of the Mn-TMTACN system towards C-H bond activation of alkanes and epoxidation of alkenes could be enhanced dramatically. Importantly, in the latter case and in the earlier example by De Vos with a heterogeneous version of this catalyst, manganese-catalysed *cis*-dihydroxylation was observed also.<sup>19</sup> Consequently, it was shown that carboxylic acids were key to the activity of **1** by de Boer *et al.*<sup>20,21</sup> (see Chapter 1 for details).

The recognition of the role of certain acids and other additives in controlling the reactivity of catalyst **1** in the oxidation of alkenes, as discussed in Chapter 1, raises the question as to how conversion of other substrate classes can be controlled and, importantly, how primary and secondary oxidation products can affect the reactivity of the active species formed from **1**, in particular the *bis*-carboxylato bridged complexes such as **2** (Figure 1). In this chapter the focus is on the catalytic system employing Mn-TMTACN, carboxylic acids as co-catalyst and H<sub>2</sub>O<sub>2</sub> as terminal oxidant for the selective

oxidation of organic substrates, especially those bearing multiple oxidation sensitive functional groups. The substrate classes examined in detail are secondary and primary aliphatic and aromatic alcohols, aldehydes, alkenes and also the activation of C-H bonds. In all cases, the conditions used for alkene oxidation in the earlier reports<sup>20</sup> are initially applied followed by optimisation. The goal, however, is not primarily to identify optimum conditions for each individual substrate but to understand the various factors that affect the reactivity of the catalytic system in each case. Additionally, more complex molecules with multiple functional groups will be examined with a view to understanding to what extent selectivity can be achieved. Finally, the tolerance of the protecting groups to the present system will be examined.

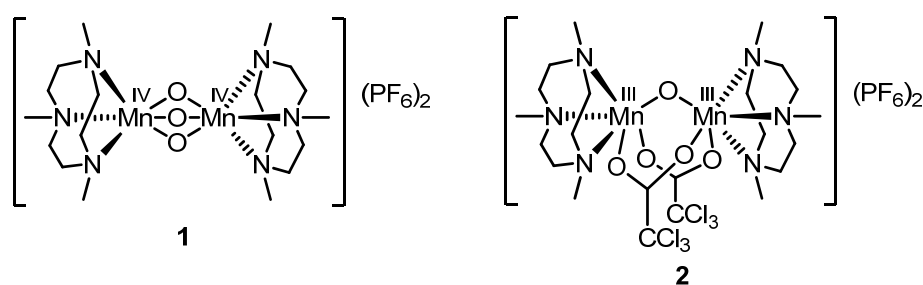


**Figure 1** Complexes  $[\text{Mn}^{\text{IV,IV}}_2\text{O}_3(\text{TMTACN})](\text{PF}_6)_2$  **1** and  $[\text{Mn}^{\text{III,III}}_2\text{O}(\text{CCl}_3\text{CO}_2)_2(\text{TMTACN})_2](\text{PF}_6)_2$  **2**.

## 2.2 Results and discussion<sup>i</sup>

### 2.2.1 Oxidation of secondary alcohols to ketones

Treatment of aromatic secondary alcohols (Table 1, entries 1-3) by a slow addition of 1.45 equiv. of H<sub>2</sub>O<sub>2</sub> in the presence of 0.1 mol% **1** and 1 mol% trichloroacetic acid in acetonitrile afforded the corresponding ketones in excellent conversions and moderate to good isolated yields. Side reactions or side products were not observed. Aliphatic secondary alcohols (entries 4-9) also provided equally good yields and importantly cyclohexanol and cyclooctanol (entries 4 and 5) can be oxidised selectively to cyclohexanone and cyclooctanone, respectively, without formation of Baeyer-Villiger type oxidation products. This was confirmed by performing the reaction (entry 4) in acetonitrile-*d*<sub>3</sub> followed by direct analysis by <sup>1</sup>H-NMR spectroscopy. The isolated yield of cyclohexanone (entry 4) is low, however, this is due to its relatively high volatility and not the poor performance of the catalyst. For longer linear aliphatic alcohols, *e.g.* 2-octanol (entry 6) and bicyclic alcohols, *e.g.* isborneol (entry 8), high conversions and isolated yields were obtained.

<sup>i</sup> Unless stated otherwise, the catalyst was pre-treated before use by mixing **1** with carboxylic acid and H<sub>2</sub>O<sub>2</sub> prior to addition of substrate to generate, *e.g.* **2** *in situ* (see the experimental section for details).

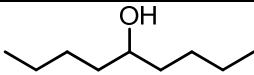
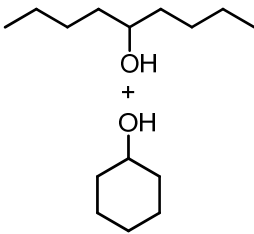
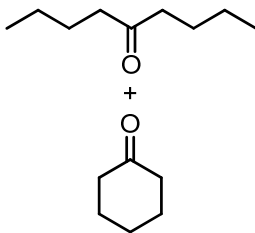
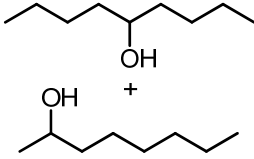
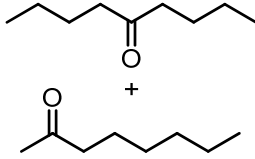
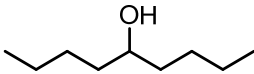
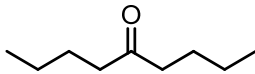
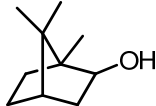
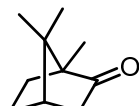
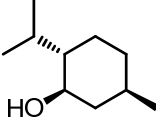
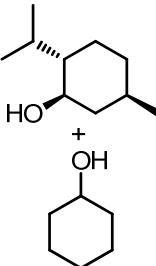
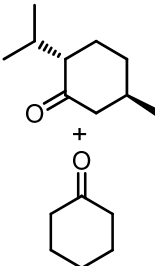
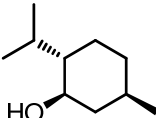


Oxidation of several aliphatic secondary alcohols such as 5-nonanol and 1-menthol (entries 7a and 9a, respectively) was found not to proceed under standard reaction conditions (*i.e.* in acetonitrile). Remarkably, >90% conversion of 5-nonanol to 5-nonanone was obtained when 1 : 1 mole ratio mixture of 5-nonanol : cyclohexanol (Table 1, entry 7b) or 5-nonanol : 2-octanol (Table 1, entry 7c) was employed. This observation indicates that 5-nonanol is not intrinsically unreactive with respect to the catalyst system but instead microscopic phase separation of substrate may be of substantial importance in limiting the reactivity. Indeed in *tert*-butanol/H<sub>2</sub>O (2/1 v/v), 5-nonanol could be converted to 5-nonanone with greater than 95% conversion (entry 7d).

The effect of steric hindrance was inferred in the case of reaction with L-menthol and cyclohexanol, which differ by the presence of an isopropyl group adjacent to the hydroxyl moiety. In contrast to the case with 5-nonanol, full conversion of cyclohexanol to cyclohexanone was obtained, however, only 10% conversion of L-menthol to menthone when a 1 : 1 mixture of cyclohexanol : L-menthol was used (Table 1, entry 9a). Furthermore, in contrast to 5-nonanol, conversion of L-menthol was not observed with *tert*-butanol/H<sub>2</sub>O (2/1 v/v) as solvent (Table 1, entry 9c). These data highlight the potential influence of steric effects on the activity of catalysts based on **1**/ carboxylic acid.

**Table 1** Oxidation of secondary alcohols to ketones using H<sub>2</sub>O<sub>2</sub> catalysed by **1**<sup>a</sup>

entry	substrate	conversion (%) <sup>c</sup>	product	isolated yield (%)
1		full		77
2		full		63
3		full		93
4		>90		31
5		>95		86
6		full		92

7a		<20	-	-
7b		>90 (for both)		<i>n.d.</i>
7c		>90 (for both)		<i>n.d.</i>
7d <sup>b</sup>		>95		<i>n.d.</i>
8		full		99
9a		<20	-	-
9b		12 (for menthol) + full (for cyclohexanol)		<i>n.d.</i>
9c <sup>b</sup>		<20	-	-

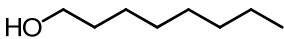
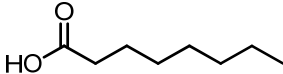
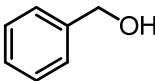
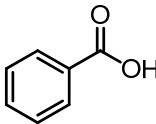
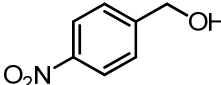
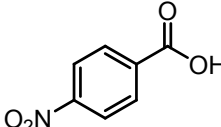
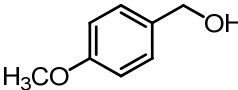
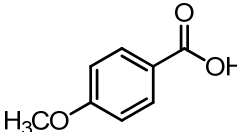
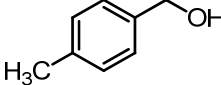
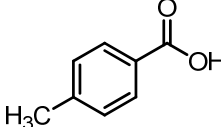
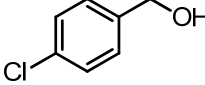
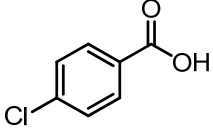
<sup>a</sup> Reaction conditions: 0.1 mol% **1**, 1.0 mol% Cl<sub>3</sub>CCO<sub>2</sub>H, 1.45 equiv. H<sub>2</sub>O<sub>2</sub>, CH<sub>3</sub>CN ([SM] = 0.5 M), r.t. <sup>b</sup> 0.5 mol% **1**, 5.0 mol% Cl<sub>3</sub>CCO<sub>2</sub>H, 1.45 equiv. H<sub>2</sub>O<sub>2</sub>, <sup>t</sup>BuOH/ H<sub>2</sub>O (2/1 v/v) ([SM] = 0.5 M), r.t. <sup>c</sup> Conversion was determined by <sup>1</sup>H NMR spectroscopy.

### 2.2.2 Oxidation of primary and benzyl alcohols to carboxylic acids

In earlier studies, Mn-TMTACN based catalysts were found to be active in the oxidation of benzyl alcohols to their corresponding aldehydes employing either H<sub>2</sub>O<sub>2</sub> or TBHP and to carboxylic acids when excess H<sub>2</sub>O<sub>2</sub> (80 equiv. w.r.t. substrate) was used.<sup>22</sup> Although acid co-catalysts were not added deliberately in these cases, it is nevertheless probable that the activity observed was due to the *in situ* formation of carboxylic acids from the substrates themselves or from decomposition of acetone by H<sub>2</sub>O<sub>2</sub> to form acetic acid (see Chapter 5 for details).<sup>23</sup> In the present study this aspect is examined further. Primary aliphatic alcohols, e.g. 1-octanol (Table 2, entry 1), were converted to a mixture of the corresponding aldehyde and carboxylic acid with low to moderate conversion using a range of reaction conditions. This is in agreement with reports that aliphatic alcohols are less reactive than benzylic substrates and the aliphatic aldehyde products are also more susceptible to overoxidation to the carboxylic acids.<sup>24</sup> Using 0.3 mol% instead of 0.1 mol% of **1** did not lead to improved conversion. The reason for such low activity was suspected to be due to the displacement of the carboxylato ligands by the 1-octanoic acid formed. In general complexes of the type [Mn<sup>III</sup><sub>2</sub>O(RCO<sub>2</sub>)<sub>2</sub>(TMTACN)<sub>2</sub>]<sup>2+</sup> where R is a linear alkyl group (such as a methyl group) showed low activity.<sup>25</sup> Furthermore, the catalyst loses activity over time due to its reduction to the Mn<sup>II</sup> oxidation state followed by ligand dissociation, and hence increasing of the initial catalyst loading does not result in a significant increase in conversion. However, adding the catalyst in small portions over time (see the experimental section) improved the conversion of 1-octanol to 54% with a 37% yield of the corresponding carboxylic acid.

The same reaction conditions (0.1 mol% of **1**/1.0 mol% trichloroacetic acid and 3 equiv. H<sub>2</sub>O<sub>2</sub>) were applied in the oxidation of benzyl alcohol. However only 60% conversion of benzyl alcohol to a mixture of benzaldehyde and benzoic acid (1 : 2 ratio) was achieved initially (data not shown). Salicylic acid, 2,6-dichlorobenzoic acid and benzoic acid itself were then used as co-catalyst and all provided full conversion of benzyl alcohol to benzoic acid in excellent isolated yields (96-98%). These results are in contrast to the previous report by Zondervan and coworkers in which benzaldehyde was the sole product obtained.<sup>22</sup> To investigate this difference further, online monitoring of the oxidation of benzyl alcohol catalysed by **1** and salicylic acid was performed using Raman spectroscopy (Figure 2). Formation of benzaldehyde and benzoic acid as well as the presence of H<sub>2</sub>O<sub>2</sub> in the reaction are plotted against time. Over the first hour, the rate of benzaldehyde formation is higher than that of benzoic acid, however, after that period both rates are comparable. The highest yield of benzaldehyde is obtained at 3 h and full conversion to benzoic acid occurs afterwards. This confirms the observation of oxidation of benzyl alcohol to benzoic acid after 16 h under the present conditions and that selective aldehyde formation was not observed. If the aldehyde is the desired product, performing the reaction with shorter reaction times (such as stopping the reaction within 2 h), followed by separation of the product and recycling of starting material is necessary to provide better yields of benzaldehyde.

**Table 2** Mn-TMTACN catalysed oxidation of primary alcohols to carboxylic acids using H<sub>2</sub>O<sub>2</sub><sup>a</sup>

entry	substrate	conversion (%) <sup>b</sup>	product	isolated yield (%)
1		54		37
2		full		>95
3		91		81
4		<50		22
5		full		94
6		full		95

<sup>a</sup> Reaction conditions are varied; see details in the experimental section. <sup>b</sup> Conversion was determined by <sup>1</sup>H NMR spectroscopy.

This system is also efficient in the oxidation of benzyl alcohol derivatives, *i.e.* 4-methylbenzyl alcohol and 4-chlorobenzyl alcohol (entries 5 and 6, respectively) were converted to their corresponding carboxylic acid in excellent conversions and isolated yields using only 0.1 mol% of **1** and 1.0 mol% salicylic acid as co-catalyst.

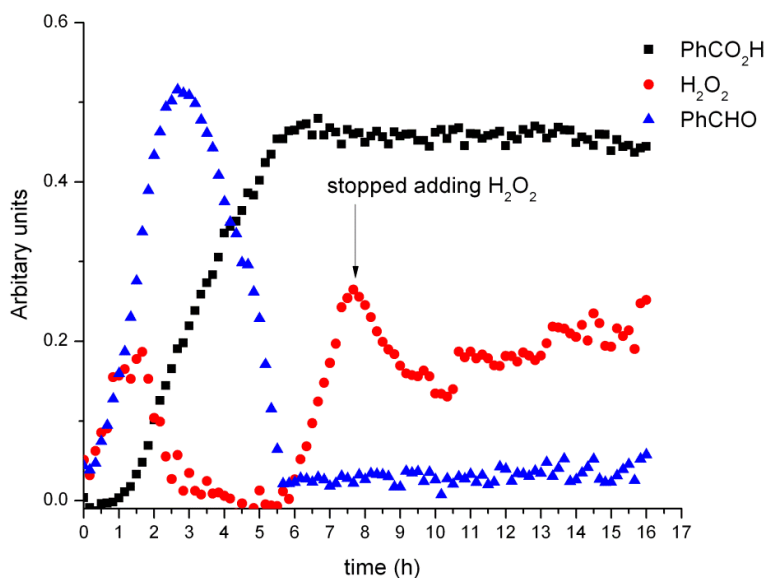


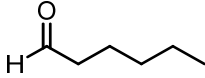
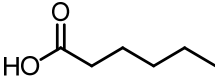
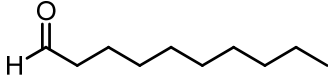
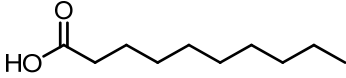
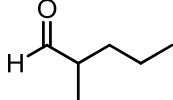
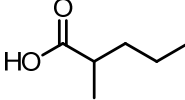
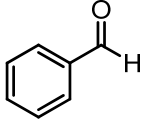
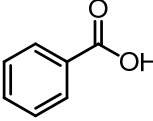
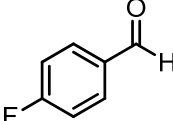
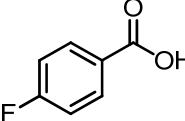
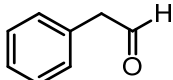
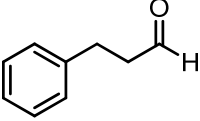
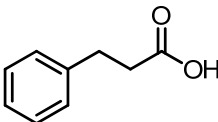
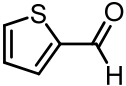
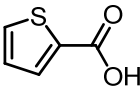
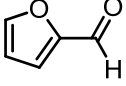
**Figure 2** Online monitoring of oxidation of benzyl alcohol (with 3 equiv. of H<sub>2</sub>O<sub>2</sub>) in CH<sub>3</sub>CN catalysed by **1** (0.1 mol%) with salicylic acid (1.0 mol%) monitored by Raman spectroscopy ( $\lambda_{\text{exc}}$  785 nm).

For certain substituted benzyl alcohols a higher catalyst loading was required, *i.e.* 4-nitrobenzyl alcohol gave 91% conversion and 81% isolated yield of carboxylic acid after applying 0.4 mol% of catalyst in total with stepwise addition (entry 3). Several substituted benzyl alcohols did not show high conversion under these conditions. However, 4-methoxy benzyl alcohol (entry 4), in particular, gave less than 50% conversion even with higher catalyst loadings. In this case it should be noted that the reaction mixture turned black, which indicates oxidation of the substrate to a redox active quinone type species that may interfere with the catalyst leading to catalyst decomposition.

### 2.2.3 Oxidation of aldehydes to carboxylic acids

As expected (*vide infra*) aliphatic aldehydes (Table 3, entries 1-3) were found to be oxidised to give the corresponding carboxylic acids in high conversions and good isolated yields. The aromatic aldehydes, benzaldehyde and 4-fluorobenzaldehyde (entries 4 and 5) were converted fully to their corresponding carboxylic acids in 89% and 97% isolated yield, respectively. By contrast, phenylacetaldehyde (entry 6) showed very low conversion and the formation of cleavage products (benzaldehyde and benzoic acid) was observed. Interestingly, the heteroaromatic aldehyde, thiophene-2-carbaldehyde (entry 8), was oxidised to thiophene-2-carboxylic acid as the sole product selectively, with further oxidation to the corresponding sulfoxide or sulfone not observed. However, oxidation of furan-2-carbaldehyde did not reach completion even with 0.5 mol% of **1**, with mainly substrate being recovered and only trace amounts of furan-2-carboxylic acid being obtained (entry 9).

**Table 3** Oxidation of aldehydes to carboxylic acids with H<sub>2</sub>O<sub>2</sub> catalysed by **1**<sup>a</sup>

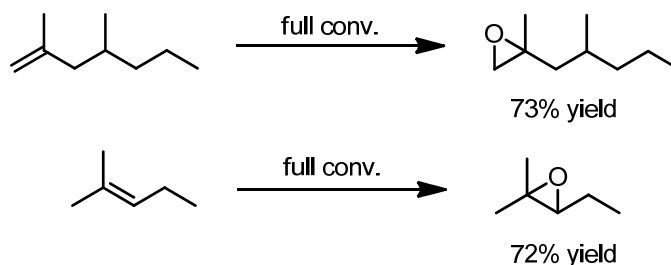
entry	substrate	conversion (%) <sup>b</sup>	product	isolated yield (%)
1		93		61
2		79		56
3		full		66
4		full		97
5		full		89
6		<i>n.d.</i>	recovered SM + PhCHO+PhCO <sub>2</sub> H	<i>n.d.</i>
7		67		56
8		92		77
9		<i>n.d.</i>	recovered SM (mainly)	<i>n.d.</i>

<sup>a</sup> Reaction conditions: 0.1 mol% **1**, 1.0 mol% Cl<sub>3</sub>CCO<sub>2</sub>H, 1.45 equiv. H<sub>2</sub>O<sub>2</sub>, CH<sub>3</sub>CN ([SM] = 0.5 M), r.t. <sup>b</sup> Conversion was determined by <sup>1</sup>H NMR spectroscopy.

### 2.2.4 Oxidation of alkenes

Previously, the carboxylic acid-promoted *cis*-dihydroxylation and epoxidation of alkenes catalysed by  $[\text{Mn}^{\text{III,III}}_2\text{O}(\text{RCO}_2)_2(\text{TMTACN})_2]^{2+}$  employing  $\text{H}_2\text{O}_2$  as oxidant was reported by de Boer *et al.*<sup>20</sup> This system shows highest activity for electron rich alkenes, *i.e.* cyclooctene, cyclohexene, *cis*- and *trans*-heptene, and shows relatively little activity with electron deficient alkenes such as dimethyl fumarate and dimethyl maleate. The general trend that the ligand 2,6-dichlorobenzoic acid leads to higher selectivity towards the *cis*-dihydroxylation products and that salicylic acid leads to higher selectivity for the epoxide products holds for these substrates (Table 4).

To expand the scope of alkene substrates, *gem*-disubstituted and trisubstituted alkenes were examined. For 2,4-dimethyl-1-heptene and 2-methyl-2-pentene, full conversion and ~72-73% yield of epoxide were obtained employing salicylic acid as co-catalyst (Scheme 1).



**conditions:** 0.1 mol% **1**, 1.0 mol% salicylic acid, 1.1 equiv.  $\text{H}_2\text{O}_2$ ,  
0.5 equiv. DCB,  $\text{CD}_3\text{CN}$ , 0 °C to r.t.

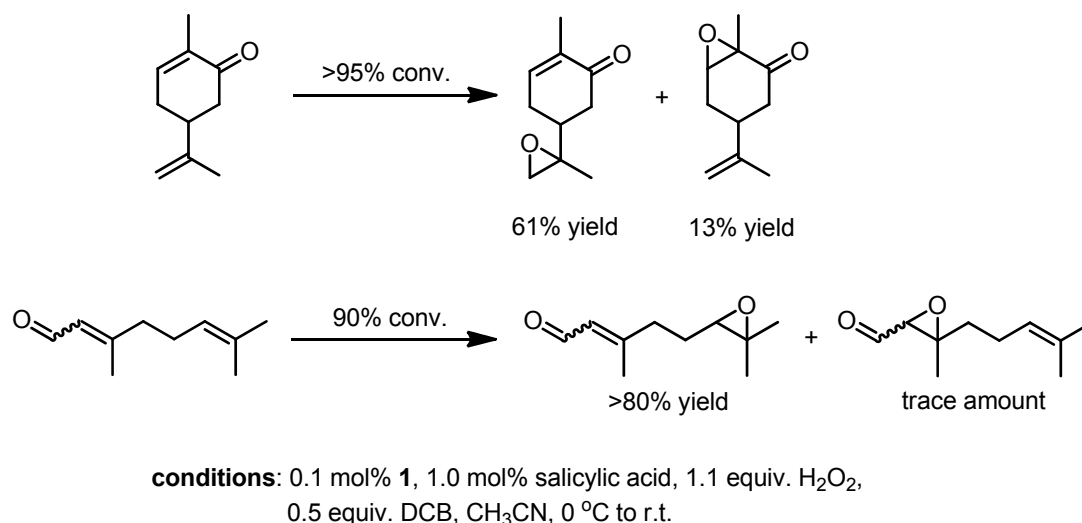
**Scheme 1** Oxidation of *gem*-disubstituted and trisubstituted alkenes.

Oxidation of substrates containing progressively dissimilar double bonds, *i.e.* substrates containing an electron rich alkene and an electron deficient alkene in the same molecule, was investigated. When salicylic acid was used as co-catalyst, selectivity for epoxidation of the electron rich alkene was observed for both carvone and citral (Scheme 2). This is in agreement with previous results that the present system is more reactive to electron rich alkenes over electron deficient alkenes (see Table 4), *i.e.* the catalyst is electrophilic. For carvone, 74% yield of both epoxide isomers was obtained with side products such as the diepoxide. Similar selectivity was obtained for citral as well. Interestingly oxidation of the potentially reactive aldehyde was not observed under these conditions.

**Table 4** Mn-TMTACN catalysed oxidation of alkenes using H<sub>2</sub>O<sub>2</sub><sup>20</sup>

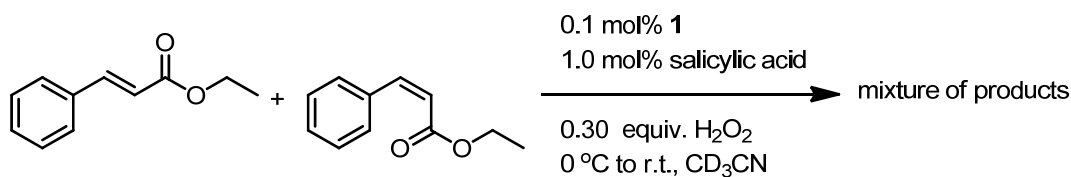
	2,6-dichloro- benzoic acid	CCl <sub>3</sub> CO <sub>2</sub> H	salicylic acid
Substrate Product (s)	( <i>conv.</i> ) t.o.n.	( <i>conv.</i> ) t.o.n.	( <i>conv.</i> ) t.o.n.
<b>cyclooctene</b>	(67%)	(82%)	(82%)
<i>cis</i> -diol	525	445	60
epoxide	75	225	695
<b><i>cis</i>-2-heptene</b>	(86%)	(94%)	(82%)
<i>erythro</i> -/ <i>threo</i> -diol	440 / 10	295 / 5	145 / 5
<i>cis</i> -/ <i>trans</i> -epoxide	125 / 5	330 / 10	485 / 15
<b><i>trans</i>-2-heptene</b>	(64%)	(79%)	(72%)
<i>erythro</i> -/ <i>threo</i> -diol	0 / 85	0 / 240	0 / 90
<i>cis</i> -/ <i>trans</i> -epoxide	10 / 90	25 / 85	15 / 285
<b>cyclohexene</b>	(92%)	(94%)	( <i>full</i> )
<i>cis</i> -diol	110	70	0
epoxide	400	570	735
2-cyclohexen-1-ol	25	30	0
2-cyclohexen-2-one	135	35	60
<b>cyclopentene</b>	( <i>n.d.</i> )	( <i>n.d.</i> )	( <i>n.d.</i> )
<i>cis</i> -diol	305	190	120
epoxide	360	460	505
2-cyclopenten-2-one	85	35	60
<b>1-octene</b>	(71%)	(66%)	(75%)
diol	125	115	30
epoxide	295	200	590
<b>styrene</b>	(97%)	(74%)	( <i>full</i> )
diol	0	35	0
epoxide	770	615	815
<b>dimethylmaleate</b>	(< 1%)	(< 1%)	(6%)
<i>meso</i> - / <i>D,L</i> -diol	0 / 0	0 / 0	0 / 0
<i>cis</i> -/ <i>trans</i> -epoxide	0 / 0	0 / 0	0 / 20
<b>dimethylfumarate</b>	(5%)	(21%)	(32%)
<i>meso</i> - / <i>D,L</i> -diol	0 / 15	0 / 105	0 / 105
<i>cis</i> -/ <i>trans</i> -epoxide	0 / 0	0 / 0	0 / 40





**Scheme 2** Oxidation of dienes.

A key question regarding the control of selectivity through the use of various carboxylic acid co-catalysts in the oxidation of less electron rich alkenes was investigated with ethyl cinnamate, in which the alkene is polarised. A notable difference in selectivity is observed in its oxidation with salicylic acid compare to 2,6-dichlorobenzoic acid. However, significant further oxidation of the *cis*-diol product to the corresponding  $\alpha$ -hydroxy ketone was also observed (Table 5).



**Scheme 3** Oxidation of *cis*- and *trans*-ethyl cinnamate.

Furthermore, in earlier studies *cis*-2-heptene was found to show higher conversion than *trans*-2-heptene under the same reaction conditions.<sup>20</sup> In the present study a competition reaction between *cis*- and *trans*-ethyl cinnamate was carried out (Scheme 3). Oxidation of a mixture of *cis*- and *trans*-ethyl cinnamate (ratio 9 : 10) using salicylic acid as co-catalyst under limiting oxidant conditions ( $\text{H}_2\text{O}_2$  0.3 equiv. w.r.t. substrate) in acetonitrile- $d_3$  allowed for direct analysis by  $^1\text{H}$ -NMR spectroscopy. After 6 h and 22 h, the ratios of *cis*- and *trans*-ethyl cinnamate were 7 : 10 and 5 : 10, respectively. This observation indicates that although both *cis*- and *trans*-ethyl cinnamate undergo conversion the rate of oxidation of *cis*-ethyl cinnamate is higher than that of *trans*-ethyl cinnamate.

**Table 5** Oxidation of ethyl cinnamate with catalyst **1** and various carboxylic acids

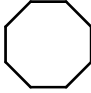
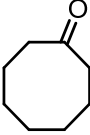
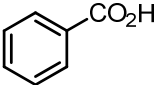
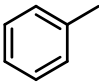
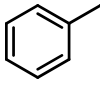
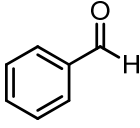
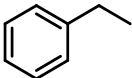
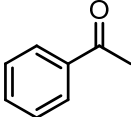
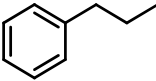
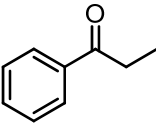
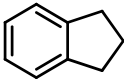
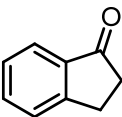
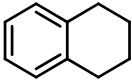
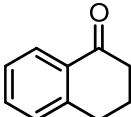
<div style="display: flex; align-items: center; justify-content: center;"> <div style="text-align: center;"> </div> <div style="margin-left: 20px;"> <p>0.1 mol% <b>1</b> 1.0 mol% co-acid</p> <p>1.50 equiv. H<sub>2</sub>O<sub>2</sub> 0 °C to r.t., CH<sub>3</sub>CN, 16 h</p> </div> <div style="margin-left: 20px;"> <p><b>A</b></p> <p><b>B</b></p> <p><b>C</b></p> </div> </div>			
entry	co-acid	conversion (%)	product ratio A : C : B
1	salicylic acid	full	1 : 1.6 : 1.1
2	2,6-dichlorobenzoic acid	60	2 : 1 : 2

### 2.2.5 C-H activation

Although the primary focus of the present study is on oxidative transformations of functional groups, the activity of **1** towards C-H activation in alkanes has been noted previously.<sup>17a,20</sup> The good to excellent selectivity towards the oxidation of alkenes, alcohols and aldehydes indicates the C-H activation is not the preferred mode of action for this catalyst system, however, in the absence of such functional groups some activity is expected. Here the activity of **1** with trichloroacetic acid in the selective C-H oxidation of alkanes is examined.

Remarkably, aliphatic cyclic alkenes, such as cyclooctane (Table 6, entry 1), can be converted with good selectivity to the corresponding mono-ketone products. This is attributed to the fact that the system is more effective in oxidation of the initially formed alcohol to the corresponding ketone (*vide supra*), than towards C-H activation.

**Table 6** C-H activation<sup>a</sup>

entry	substrate	conversion (%) <sup>c</sup>	product	isolated yield (%)
1 <sup>b</sup>		80	 	61 <sup>d</sup>
2		60	 + 	11(CO <sub>2</sub> H)
3		70		37
4		30-40		30
5		70		40
6		70		69

<sup>a</sup> Reaction conditions: 0.1 mol% **1**, 1.0 mol% Cl<sub>3</sub>CCO<sub>2</sub>H, 1.45 equiv. H<sub>2</sub>O<sub>2</sub>, CH<sub>3</sub>CN ([SM] = 0.5 M), 0 °C to r.t. <sup>b</sup> Normal reaction conditions but with 4.5 equiv. H<sub>2</sub>O<sub>2</sub>. <sup>c</sup> Conversion of the substrate was determined by Raman spectroscopy ( $\lambda_{\text{exc}}$  785 nm) using 1,2-dichlorobenzene as internal standard. <sup>d</sup> Yield determined by <sup>1</sup>H NMR spectroscopy.

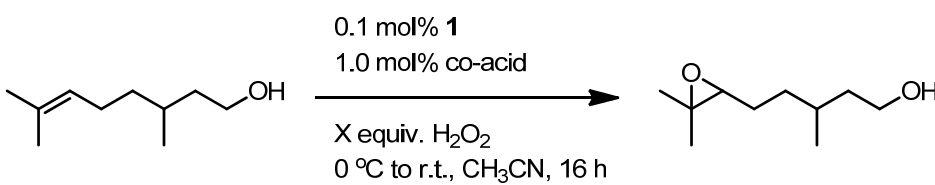
As would be expected for aromatic alkanes, the benzylic protons are the most sensitive to oxidation and indeed good conversion and yield of the mono-ketone products can be achieved for several substrates. In the case of ethylbenzene (entry 3), however, the sensitivity of the product to subsequent aldol reactions may have had a substantial impact on the yield achieved. Propylbenzene (entry 4) seems unreactive under the reaction conditions used (trichloroacetic acid as co-catalyst) even increasing the catalyst loading

and adjusting the rate of H<sub>2</sub>O<sub>2</sub> addition did not improve on the conversion. Although, using another co-catalyst such as benzoic acid and salicylic acid or changing the solvent system might improve its conversion. This system has high selectivity and efficiency for oxidation at the benzylic position over the  $\beta$ -position, *i.e.* in case of indane and tetraline (entries 5 and 6, respectively). Moreover, by controlling the amount of H<sub>2</sub>O<sub>2</sub> (1.5 equiv.) added,  $\alpha$ -tetralone (mono-ketone product) can be obtained in high yield (entry 6).

### 2.2.6 Oxidation of bifunctional substrates

A key challenge in modern oxidation catalysis is the selective oxidative transformation of one functional group in the presence of a second oxidation sensitive functional group as seen above for citral. As previously discussed, the selectivity of the catalyst, with respect to product formed upon oxidation of an alkene, can be controlled to a significant extent by varying the nature of the carboxylic acid co-catalyst. Therefore, in a study of functional group selectivity, it is interesting to investigate if the co-catalyst employed exerts similar levels of control.

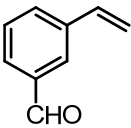
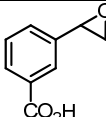
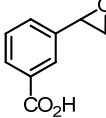
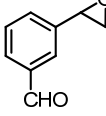
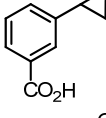
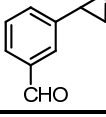
**Table 7** Oxidation of citronellol under various reaction conditions

<div style="text-align: center;">  </div>				
entry	co-acid	equiv. of H <sub>2</sub> O <sub>2</sub>	conversion (%)	isolated yield (%)
1	2,6-dichlorobenzoic acid	1.05	50	<i>n.d.</i>
2	salicylic acid	1.05	65-80	30
3	salicylic acid	1.15	>95	62

The bifunctional substrate, citronellol, which contains a trisubstituted electron-rich alkene and a primary alcohol, was oxidised with 1.05 equiv. of H<sub>2</sub>O<sub>2</sub> catalysed by **1** together with either 2,6-dichlorobenzoic acid or salicylic acid (Table 7). Good conversion of citronellol (50-80%) to the corresponding epoxy-alcohol as the major product was obtained in each case with salicylic acid providing better conversion. The corresponding diol-, epoxide-, and alkene-aldehyde were also obtained as by-products. With 1.15 equiv. of H<sub>2</sub>O<sub>2</sub>, >95% conversion of citronellol was achieved and despite the instability of the

product during purification (silica gel as stationary phase for column chromatography), the epoxy-alcohol could be isolated in 62% yield.

**Table 8** Oxidation of 3-vinyl benzaldehyde under various reaction conditions

<div style="display: flex; align-items: center; justify-content: center;"> <div style="text-align: center; margin-right: 10px;">  </div> <div style="text-align: center; margin-right: 10px;"> <math>\xrightarrow[\text{5 } ^\circ\text{C, CH}_3\text{CN, 16 h}]{\begin{array}{l} 0.1 \text{ mol\% } \mathbf{1} \\ 1.0 \text{ mol\% co-acid} \\ \text{X equiv. H}_2\text{O}_2 \end{array}}</math> </div> <div>product(s)</div> </div>			
entry	co-acid	equiv. of H <sub>2</sub> O <sub>2</sub>	product
1	salicylic acid	1.50	
2	salicylic acid	0.80	
3 <sup>a</sup>	salicylic acid	0.80	
4	CCl <sub>3</sub> CO <sub>2</sub> H	1.50	
5 <sup>a</sup>	CCl <sub>3</sub> CO <sub>2</sub> H	0.80	

<sup>a</sup> Reaction was performed under N<sub>2</sub> in CD<sub>3</sub>CN to enable direct analysis by <sup>1</sup>H NMR spectroscopy.

In the case of 3-vinyl benzaldehyde, where the highly oxidation sensitive aldehyde group is present, the catalysed oxidation was examined with salicylic acid and trichloroacetic acid as co-catalyst (Table 8). Conversion and product distribution were confirmed by <sup>1</sup>H NMR spectroscopic analysis after reaction work up. For both co-catalysts only the epoxide product was obtained with no diol product detected by <sup>1</sup>H NMR spectroscopy. However, almost full conversion of substrate to product bearing both oxidised functional groups (epoxide and carboxylic acid) was obtained even when less than 1 equiv. of H<sub>2</sub>O<sub>2</sub> was used (Table 8, entry 2). It was postulated that the oxidation of the aldehyde to the carboxylic acid could occur due to air oxidation during the reaction or work up and not from the catalytic system itself. To study this in more detail, reactions were performed

under a nitrogen atmosphere in acetonitrile-*d*<sub>3</sub> (degassed) to allow for direct analysis by <sup>1</sup>H NMR spectroscopy (entries 3 and 5, example of analysis is shown in Figure 3). Online monitoring by Raman spectroscopy was also used to follow the conversion of each functional group in real time (for entry 3, see Figures 4 and 5).

Direct <sup>1</sup>H and <sup>13</sup>C NMR analysis showed that both reactions from Table 8, entries 3 and 5 provided only epoxy benzaldehyde as the product. No epoxy-benzoic acid and only trace amounts of diol-benzaldehyde were observed in either case (see example of <sup>1</sup>H NMR analysis in Figure 3). This means that the alkene moiety of this compound is more reactive than the aldehyde as high selectivity of alkene oxidation was observed with the present system.

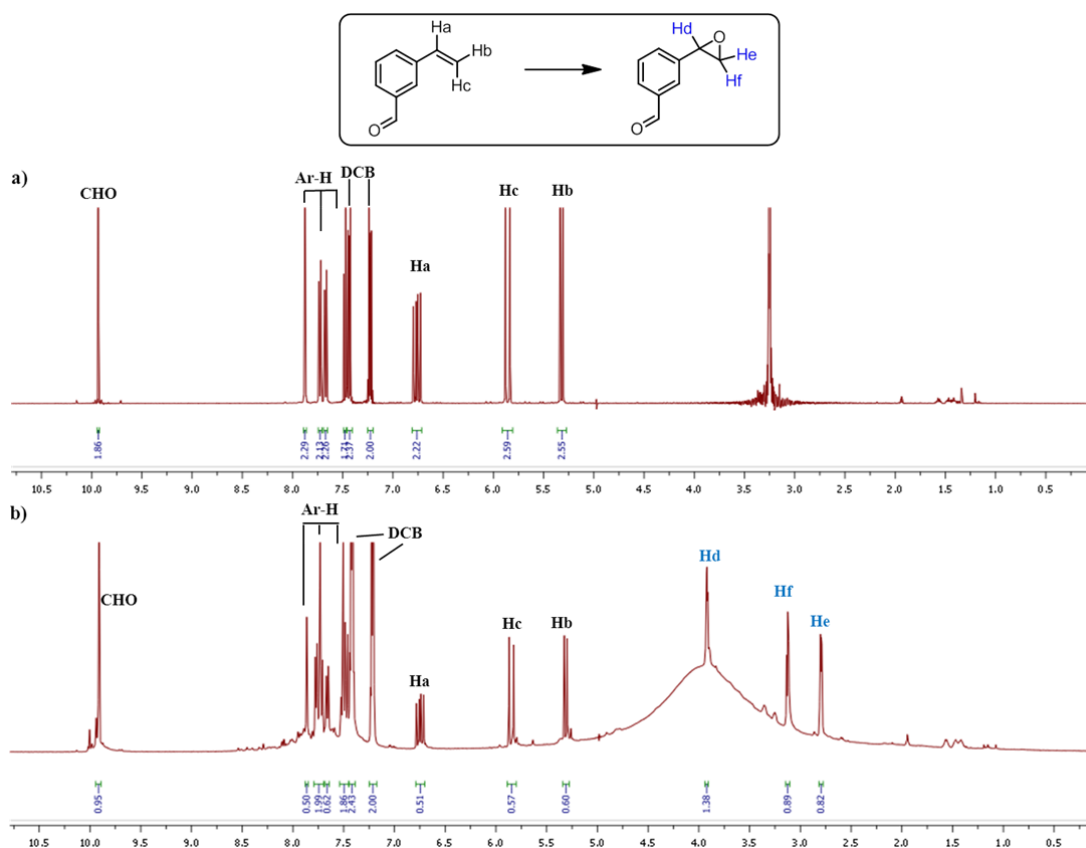


**Figure 3** Direct <sup>1</sup>H NMR analysis of oxidation of 3-vinyl benzaldehyde a) at  $t_0$  b) after 7 h in CD<sub>3</sub>CN (from Table 8, entry 3).

To confirm this observation, Raman spectroscopy was used to monitor the reaction (Table 8, entry 3) in real time by following the intensity of the band at 1630 cm<sup>-1</sup> (C=C stretching mode) and 1705 cm<sup>-1</sup> (C=O stretching mode) (Figure 4). Plotting the intensity of each band against time shows a lag time lasting the first hour. After that period the intensity of the band due to the alkene moiety decreased rapidly, while the intensity of the band due to the aldehyde did not change substantially (Figure 5). The minor changes in the band of the aldehyde was due to the steady increase in water content (from H<sub>2</sub>O<sub>2</sub>) that

changed the shape of the peak (peak became broader as can be seen in Figure 4). The changes are not due to transformation to the carboxylic acid. These data support the results from  $^1\text{H}$  and  $^{13}\text{C}$  NMR spectroscopic analysis.

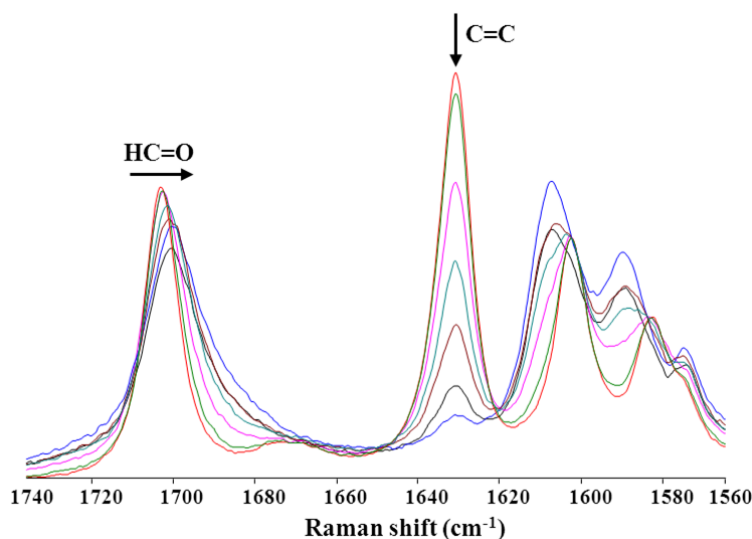


**Figure 4** Online reaction monitoring of 3-vinyl benzaldehyde with catalyst **1**, salicylic acid and  $\text{H}_2\text{O}_2$  using Raman spectroscopy ( $\lambda_{\text{exc}}$  532 nm).

A lag time was observed over the first hour when the reaction was performed using acetonitrile as solvent (Figure 5). Based on the previous reports it was surmised that the lag time in the present system was due to the equilibrium between  $\{\text{Mn}^{\text{III,III}}_2\text{O}(\text{RCO}_2)_2\}$  and  $\{\text{Mn}^{\text{III,III}}_2(\text{OH})(\text{RCO}_2)_2\}$  species and this equilibrium was controlled by the amount of  $\text{H}_2\text{O}$  present in the reaction media.<sup>21</sup> It was suspected that the latter species are needed for the reaction with  $\text{H}_2\text{O}_2$  to form the  $\text{H}_2\text{O}_2$ -activated complex that acts as the oxidant for the reaction. So the more of the latter species that is present in the reaction mixture, the sooner the reaction starts. To confirm this, acetonitrile/  $\text{H}_2\text{O}$  (90/10 v/v) was used as the solvent instead. Online reaction monitoring with Raman spectroscopy shows that the decrease in the intensity of the band due to the alkene moiety started immediately after addition of  $\text{H}_2\text{O}_2$  as expected (Figure 6).

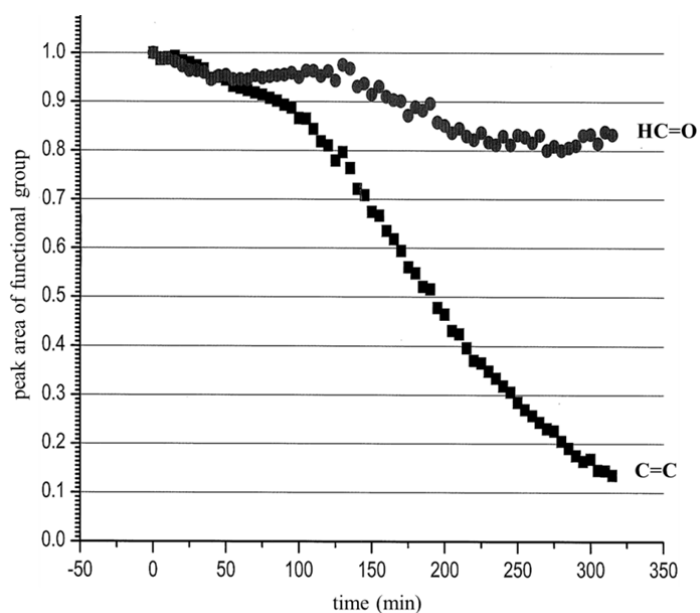


**Figure 5** Plot of remaining amount of alkene and aldehyde against time from online monitoring of oxidation of 3-vinyl benzaldehyde with catalyst **1**, salicylic acid and  $H_2O_2$  in  $CD_3CN$  under  $N_2$  using Raman spectroscopy ( $\lambda_{exc}$  532 nm).

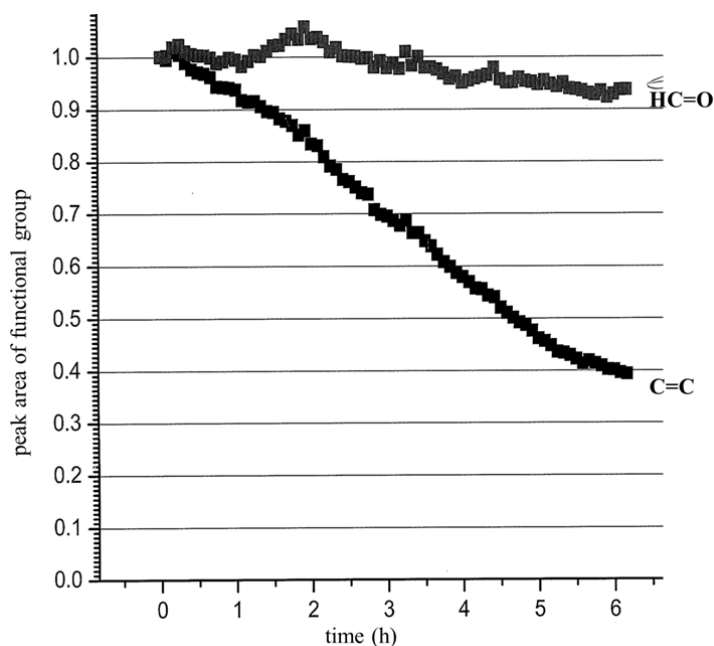
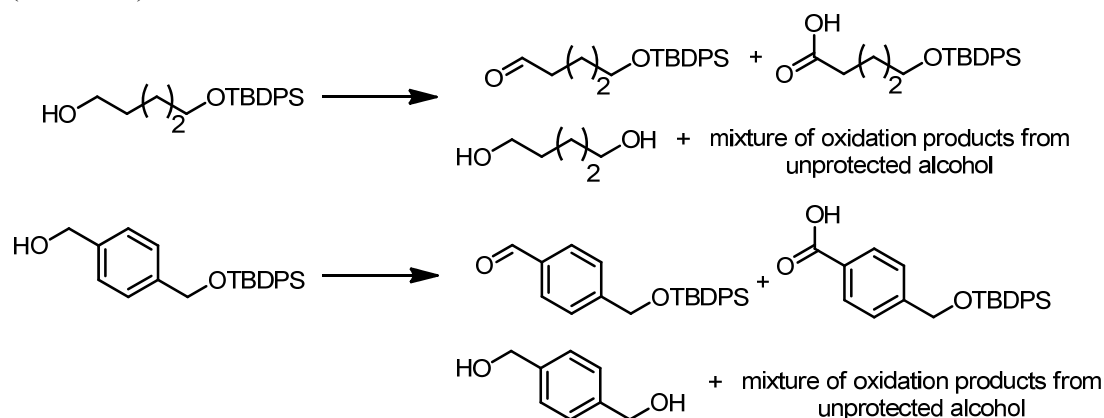


**Figure 6** Plot of remaining amount of alkene and aldehyde against time from online monitoring of oxidation of 3-vinyl benzaldehyde with catalyst **1**, salicylic acid and  $H_2O_2$  in  $CD_3CN/H_2O$  (90/10 v/v) using Raman spectroscopy ( $\lambda_{exc}$  532 nm).



### 2.2.7 Protecting group tolerance

Tolerance of protecting groups is a further characteristic of the present system. In the present study silyl based protecting groups, *e.g.* *tert*-butyldiphenylsilyl (TBDPS), as expected, were found to be unstable under reaction conditions due to the sensitivity of TBDPS groups to  $\text{H}_2\text{O}_2$ . TBDPS protected primary aliphatic alcohol and benzyl alcohol were converted to their corresponding aldehyde and carboxylic acid in low yield, and many by-products from the oxidation of unprotected alcohol were obtained instead (Scheme 4).



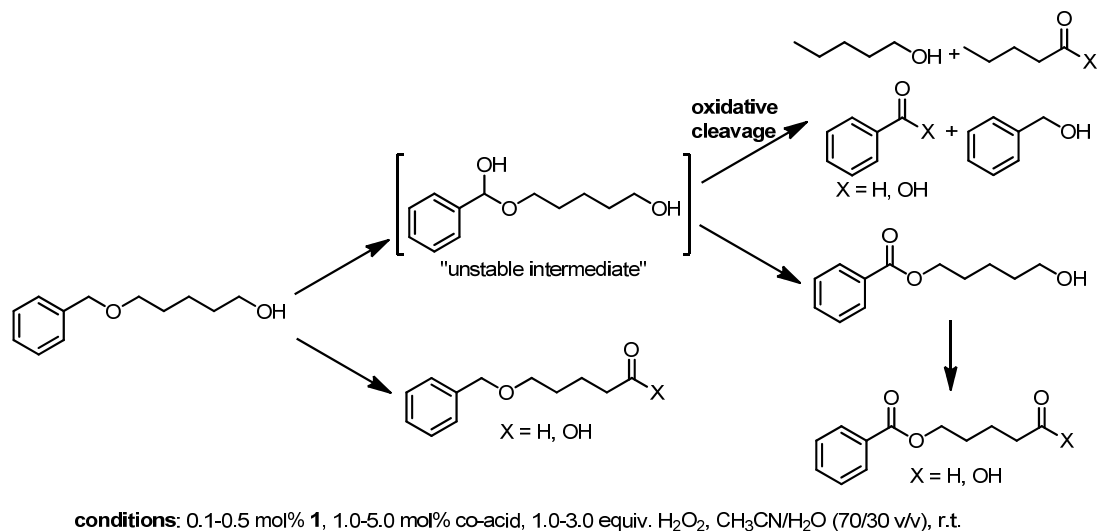
**conditions:** 0.1-0.5 mol% **1**, 1.0-5.0 mol%  $\text{Cl}_3\text{CCO}_2\text{H}$ , 1.0 or 3.0 equiv.  $\text{H}_2\text{O}_2$ ,  $\text{CH}_3\text{CN}/\text{H}_2\text{O}$  (100/0 or 70/30 v/v), vary temp. (0 °C, 30 °C or 60 °C)

**Scheme 4** Oxidation of TBDPS protected alcohols.

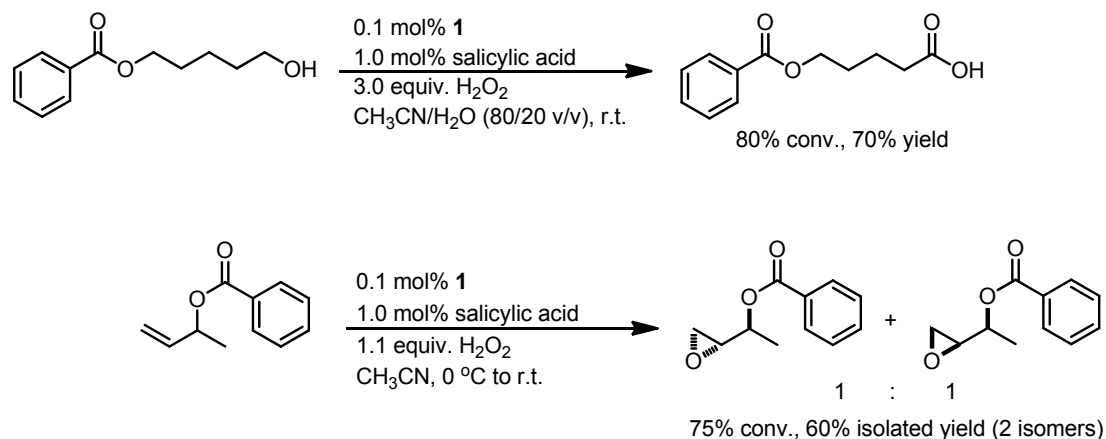
Other Si-free ether protecting groups were therefore preferable with this system, in particular the benzyl ether group (Bn). Oxidation of benzyl protected alcohol employing various reaction conditions, *i.e.* varying the co-acids (trichloroacetic acid, salicylic acid and oxalic acid) and equivalents of  $\text{H}_2\text{O}_2$  (1.0-3.0 equiv.), gave similar results (by  $^1\text{H}$  NMR spectroscopy) with differences in products ratios.  $^1\text{H}$  NMR spectroscopic data demonstrated that not only was the primary alcohol group oxidised to the corresponding aldehyde and carboxylic acid, but also the methylene unit ( $\text{CH}_2$ ) of the benzyl ether group was oxidised through an acetal intermediate pathway; the acetal is unstable under the reaction conditions used. Some intermediates were oxidized further to obtain a benzoyl group and some underwent cleavage to afford many undesired products such as pentanol, pentanal, pentanoic acid, benzyl alcohol, benzaldehyde and benzoic acid (Scheme 5). Their formation was confirmed by GC-MS analysis.

To avoid the cleavage of the protecting group under the reaction conditions used, the benzoyl group (Bz) was used for protecting the alcohol moiety instead (Scheme 6). The combination of **1** and 1.0 mol% salicylic acid with 3 equiv.  $\text{H}_2\text{O}_2$  gave 80% conversion of 5-hydroxypentyl benzoate to the corresponding carboxylic acid in 70% ( $^1\text{H}$  NMR) yield. Epoxide products (two diastereomers in a ratio 1 : 1) of protected allylic alcohol were

obtained in 60% isolated yield (75% conversion). Moreover, deprotected substrate or products were detected by <sup>1</sup>H NMR spectroscopy in both cases.

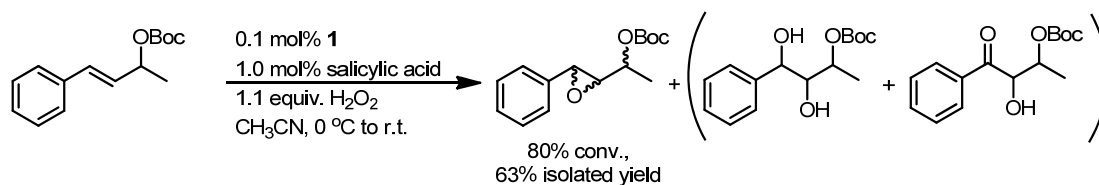


**Scheme 5** Oxidation of benzyl protected alcohol and proposed pathway for cleavage of the benzyl group.



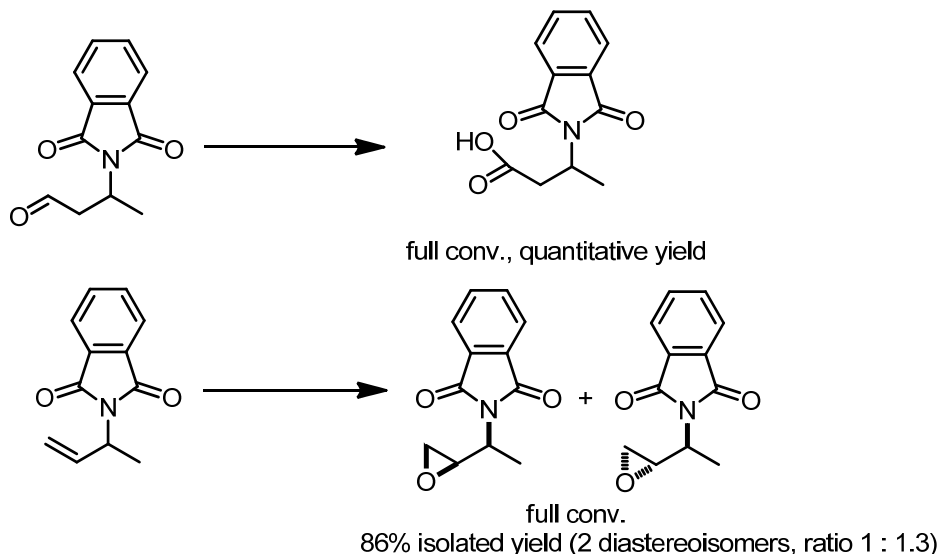
**Scheme 6** Oxidation of benzoyl protected alcohols.

*tert*-Butoxycarbonyl (Boc) protected alcohols were found to be stable under reaction conditions as well. The epoxide product of a Boc-protected allylic alcohol was achieved as the major product (80% conversion, 63% isolated yield) and minor products were diol and its overoxidation product,  $\alpha$ -hydroxy ketone (Scheme 7).



**Scheme 7** Oxidation of *tert*-butoxycarbonyl (Boc) protected alcohol.

Phthalimide (Phth) is also an alternative protecting group that was found to be suitable with the present system. Phthalimide protected allylic aldehyde and alkene were converted to their corresponding carboxylic acid and epoxide, respectively, in high conversion and isolated yield (Scheme 8). Deprotected species were not observed in either case.



**conditions:** 0.1 mol% **1**, 1.0 mol% salicylic acid, 1.1 equiv. H<sub>2</sub>O<sub>2</sub>, CH<sub>3</sub>CN, 0 °C to r.t.

**Scheme 8** Oxidation of phthalimide protected amines.

## 2.3 Summary and conclusions

Transformation of secondary alcohols and aldehydes to their corresponding ketones and carboxylic acids, respectively, is straightforward under the present system. High conversions and isolated yields were generally obtained except in some cases, *i.e.* L-menthol, where steric effects appear to be important to the activity of the catalyst. In addition, phase separation of the substrate is of substantial importance in limiting the reactivity of the system as in the case of 5-nonanol, however, this was overcome by using a different solvent.

The system is suitable for transformation of primary aliphatic alcohols and benzylic alcohols to aldehydes or carboxylic acids as well. However, it is more challenging as

these substrates are usually less reactive than the secondary alcohols and aldehydes. An improvement in reactivity of the present system towards these transformations can be obtained by changing the carboxylic acid co-catalysts. In some cases, *e.g.* 4-nitrobenzyl alcohol, increased catalyst loading and stepwise addition of catalyst are necessary. Selective transformation of primary alcohols to aldehydes is not straightforward, however, online analysis of the reaction mixture provides the opportunity to obtain good selectivity as the reaction can be stopped at an optimum time.

Oxidation of alkenes employing the same reaction conditions has been discussed before in depth,<sup>20</sup> however, more examples such as *gem*-disubstituted and trisubstituted alkenes were provided in the present study. The electrophilic character of catalyst was demonstrated as an advantage for selective oxidation of compounds bearing dissimilar double bonds as selective oxidation of electron rich double bonds over electron deficient double bonds was observed for citral and carvone.

As discussed briefly in Chapter 1, often catalysts that are good in alkene oxidation do not perform well for C-H activation.<sup>26</sup> Interestingly, the present system exhibited good reactivity and selectivity for C-H activation as well. Indeed mono-ketone products can be obtained as the major products in most cases. This can be attributed to the fact that this system is more effective in the oxidation of the secondary alcohol formed initially over further C-H activation.

This system can be used for the oxidation of compounds containing multiple functional groups also. High selectivity and reactivity was observed for 3-vinyl benzaldehyde and citronellol for instance. In these cases, carboxylic acids play an important role to control the reactivity and selectivity of the reaction.

This system is compatible with substrates bearing a variety of effective protecting groups. Benzoyl (Bz), *tert*-butoxycarbonyl (Boc) and phthalimide (Phth) are suitable protecting groups as deprotected species were not detected under the reaction conditions used.

In conclusion, a practical catalytic system employing **1**, with carboxylic acids as co-catalyst and H<sub>2</sub>O<sub>2</sub> as terminal oxidant for the oxidation of organic substrates bearing oxidation sensitive functional groups, *i.e.* alcohol, aldehyde, alkene and alkane, is described in this chapter. These results open the way to more widespread use of this catalyst in organic oxidative transformations.

## 2.4 Experimental section

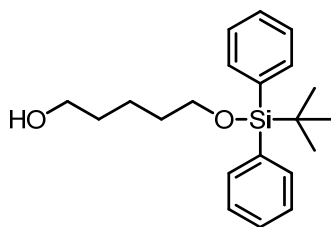
All reagents are of commercial grade and used as received unless stated otherwise. Hydrogen peroxide was used as received as a 50 wt. % solution in water; note that the grade of H<sub>2</sub>O<sub>2</sub> employed can affect the reaction when sequestrants are present as stabilizers. NMR spectra were recorded at <sup>1</sup>H NMR (400.0 or 200.0 MHz) and <sup>13</sup>C NMR (100.59 or 50.0 MHz). Chemical shifts are denoted relative to the residual solvent absorption (<sup>1</sup>H: CDCl<sub>3</sub> 7.26 ppm, CD<sub>3</sub>CN 1.94 ppm, acetone-*d*<sub>6</sub> 2.05 ppm; <sup>13</sup>C: CDCl<sub>3</sub> 77.0 ppm, CD<sub>3</sub>CN 1.4 and 118.7 ppm, acetone-*d*<sub>6</sub> 29.9 and 206.6 ppm).<sup>27</sup> Raman spectra

were recorded using a fibre optic equipped dispersive Raman spectrometer (785 nm, Perkin Elmer Raman Flex). Temperature was controlled using a cuvette holder equipped with a custom made fibre optic probe holder (Quantum Northwest). 1,2-Dichlorobenzene was employed as internal standard for Raman spectroscopy.

**Caution.** The drying or concentration of solutions that potentially contain hydrogen peroxide should be avoided. Prior to drying or concentrating, the presence of  $\text{H}_2\text{O}_2$  should be tested for, using peroxide test strips, followed by neutralisation on solid  $\text{NaHSO}_3$  or another suitable reducing agent. When working with  $\text{H}_2\text{O}_2$ , especially in acetone, suitable protective safeguards should be in place at all times.

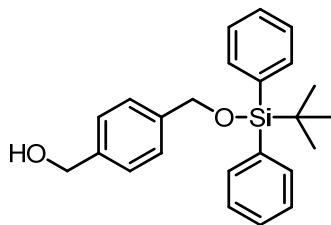
#### 2.4.1 Synthesis and characterization of substrates

##### 5-*tert*-Butyldiphenylsilyl-oxy-pentan-1-ol (Scheme 4)



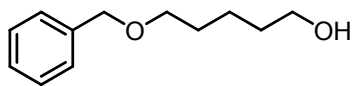
*tert*-Butylchlorodiphenylsilane (1.89 ml, 7.13 mmol) was slowly added to a solution of 1,5-pentanediol (7.6 g, 71.3 mmol) and imidazole (0.53 g, 7.84 mmol) in dry THF (70 ml) at room temperature. After stirring overnight under a nitrogen atmosphere at room temperature, the reaction mixture was diluted with water (100 ml). The aqueous layer was extracted with  $\text{Et}_2\text{O}$  (3 x 50 ml). The combined organic layers were dried over  $\text{MgSO}_4$ , filtered and concentrated *in vacuo*. The crude product was purified by column chromatography ( $\text{SiO}_2$ ,  $\text{CH}_2\text{Cl}_2$ ) to afford a colourless oil (2.05 g, 6.0 mmol, 84%).  $^1\text{H}$  NMR (400 MHz,  $\text{CDCl}_3$ )  $\delta$  7.70-7.67 (m, 4H), 7.47-7.34 (m, 6H), 3.68 (t,  $J$  = 6.4 Hz, 2H), 3.62 (t,  $J$  = 6.5 Hz, 2H), 1.65-1.51 (m, 4H), 1.45 (m, 2H), 1.07 (s, 9H);  $^{13}\text{C}$  NMR (100 MHz,  $\text{CDCl}_3$ )  $\delta$  135.5, 134.0, 129.5, 127.5, 63.7, 62.9, 32.4, 32.2, 26.9, 21.9, 19.2. HRMS (ESI+,  $m/z$ ) calc. for  $\text{C}_{21}\text{H}_{31}\text{O}_2\text{Si}$   $[\text{M}+\text{H}]^+$  343.2088, found 343.2093.

##### 4-*tert*-Butyldiphenylsilyl-oxy-methyl-phenyl-methanol (Scheme 4)



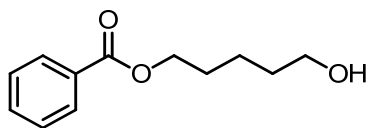
*tert*-Butylchlorodiphenylsilane (3.54 ml, 13.33 mmol) was slowly added to a solution of 1,4-benzenedimethanol (2.8 g, 20.00 mmol) and imidazole (1.0 g, 14.67 mmol) in dry THF (100 ml) at room temperature. After stirring overnight under a nitrogen atmosphere at room temperature, the reaction mixture was diluted with water (100 ml). The aqueous layer was extracted with  $\text{Et}_2\text{O}$  (3 x 50 ml). The combined organic layers were dried over  $\text{MgSO}_4$ , filtered and concentrated *in vacuo*. The crude product was purified by column chromatography ( $\text{SiO}_2$ ,  $\text{CH}_2\text{Cl}_2$ ) to afford a colourless oil (2.54 g, 6.74 mmol, 51%).  $^1\text{H}$  NMR (400 MHz,  $\text{CDCl}_3$ )  $\delta$  7.75-7.73 (m, 4H), 7.52-7.31 (m, 10H), 4.81 (s, 2H), 4.70 (s, 2H), 1.12 (s, 9H);  $^{13}\text{C}$  NMR (100 MHz,  $\text{CDCl}_3$ )  $\delta$  140.5, 139.4, 135.5, 133.4, 129.7, 127.7, 127.0, 126.2, 65.3, 65.2, 26.8, 19.3. HRMS (ESI+,  $m/z$ ) calc. for  $\text{C}_{24}\text{H}_{28}\text{O}_2\text{SiNa}$   $[\text{M}+\text{Na}]^+$  399.1756, found 399.1747.

### 5-(Benzyloxy)pentan-1-ol (Scheme 5)



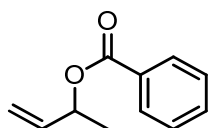
This compound was synthesised according to the literature procedure.<sup>28</sup> 1,5-Pentanediol (12.7 g, 120 mmol) was slowly added (over 1 h) to a solution of benzyl bromide (5.98 g, 35 mmol) and potassium hydroxide (8.0 g, 144 mmol) in THF (50 ml) at room temperature. After stirring at room temperature for an additional 4 h, the reaction mixture was diluted with water (50 ml). The aqueous layer was extracted with EtOAc (3 x 50 ml). The combined organic layers were dried over MgSO<sub>4</sub>, filtered and concentrated *in vacuo*. The crude product was purified by column chromatography (SiO<sub>2</sub>, EtOAc/pentane = 30/70 to 60/40) to afford a pale yellow oil (0.87 g, 4.49 mmol, 75%). <sup>1</sup>H NMR (200 MHz, CDCl<sub>3</sub>) δ 7.35-7.26 (m, 5H), 4.50 (s, 2H), 3.64 (t, *J* = 6.3 Hz, 2H), 3.49 (t, *J* = 6.3 Hz, 2H), 1.69-1.43 (m, 6H); <sup>13</sup>C NMR (50 MHz, CDCl<sub>3</sub>) δ 138.3, 128.3, 127.6, 127.5, 72.8, 70.2, 62.2, 32.0, 29.3, 21.87. HRMS (ESI+, *m/z*) calc. for C<sub>12</sub>H<sub>19</sub>O<sub>2</sub> [M+H]<sup>+</sup> 195.1385, found 195.1377 and for C<sub>12</sub>H<sub>18</sub>O<sub>2</sub>Na [M+Na]<sup>+</sup> 217.1204, found 217.1199. The spectroscopic data are in accordance with those reported in the literature.<sup>28</sup>

### 5-Hydroxypentyl benzoate (Scheme 6)



*p*-Toluenesulfonic acid (188 mg, 1.0 mmol, 5.0 mol%) was added to the solution of benzoic acid (2.44 g, 20.0 mmol) and 1,5-pentanediol (4.16 g, 40.0 mmol) in toluene (25 ml). The resulting solution was heated at reflux for 16 h with a Dean-Stark receiver to remove water. The reaction mixture was diluted with water (25 ml) after cooling to room temperature. The aqueous layer was extracted with EtOAc (3 x 25 ml). The combined organic layers were dried over MgSO<sub>4</sub>, filtered and concentrated *in vacuo*. The crude product was purified by column chromatography (SiO<sub>2</sub>, EtOAc/heptane = 17/83) to afford a colourless oil (2.53 g, 12.2 mmol, 61%). <sup>1</sup>H NMR (200 MHz, CDCl<sub>3</sub>) δ 8.08 – 7.97 (m, 2H), 7.60 – 7.50 (m, 1H), 7.50 – 7.36 (m, 2H), 4.34 (t, *J* = 6.5 Hz, 2H), 3.68 (t, *J* = 6.2 Hz, 2H), 1.81 (m, 2H), 1.70 – 1.48 (m, 4H); <sup>13</sup>C NMR (50 MHz, CDCl<sub>3</sub>) δ 132.8, 129.5, 128.3, 64.9, 62.7, 32.3, 28.5, 22.3.

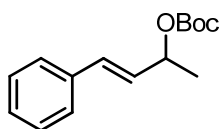
### But-3-en-2-yl benzoate (Scheme 6)



Pyridine (0.81 ml, 10 mmol) was added to the solution of 3-buten-2-ol (0.37 g, 5 mmol) in CH<sub>2</sub>Cl<sub>2</sub> (20 ml) under a nitrogen atmosphere. Benzoyl chloride (0.61 ml, 5.25 mmol) was added dropwise to the ice-water cooled mixture. The mixture was stirred overnight, allowing the temperature to rise to room temperature. The reaction mixture was added to 10% HCl (aq.) (10 ml) and CH<sub>2</sub>Cl<sub>2</sub> (20 ml). After separation of the layers, the aqueous layer was extracted with CH<sub>2</sub>Cl<sub>2</sub> (3 x 20 ml). The combined organic layers were dried on MgSO<sub>4</sub> and concentrated *in vacuo* providing the crude product. The crude product was purified by column chromatography (SiO<sub>2</sub>, EtOAc/pentane = 5/95) to afford a colourless oil (0.55 g, 3.15 mmol, 63%). <sup>1</sup>H NMR (400 MHz, CDCl<sub>3</sub>) δ 8.07 (d, *J* = 7.2 Hz, 2H), 7.57 – 7.51

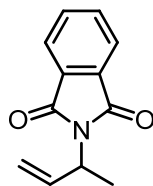
(m, 1H), 7.43 (t,  $J = 7.6$  Hz, 2H), 5.97 (ddd,  $J = 17.2$  Hz, 10.6 Hz, 5.7 Hz, 1H), 5.61 (dd,  $J = 6.4$  Hz, 5.9 Hz, 1H), 5.34 (dd,  $J = 17.3$  Hz, 1.2 Hz, 1H), 5.21 – 5.16 (m, 1H), 1.45 (d,  $J = 6.5$  Hz, 3H);  $^{13}\text{C}$  NMR (100 MHz,  $\text{CDCl}_3$ )  $\delta$  165.6, 137.6, 132.7, 130.1, 129.5, 128.2, 115.7, 71.4, 20.0. HRMS (ESI+,  $m/z$ ) calc. for  $\text{C}_{11}\text{H}_{12}\text{O}_2\text{Na}$   $[\text{M}+\text{Na}]^+$  199.0735, found 199.0730.

### (*E*)-*tert*-Butyl (4-phenylbut-3-en-2-yl) carbonate (Scheme 7)



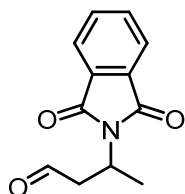
This compound was synthesised (and provided by B. Mao) according to the literature procedure.<sup>29</sup>  $^1\text{H}$  NMR (200 MHz,  $\text{CDCl}_3$ )  $\delta$  7.44 – 7.19 (m, 5H), 6.64 (d,  $J = 16.0$  Hz, 1H), 6.21 (dd,  $J = 16.0$  Hz, 6.9 Hz, 1H), 5.35 (dd,  $J = 9.6$  Hz, 3.8 Hz, 1H), 1.55 – 1.41 (m, 12H);  $^{13}\text{C}$  NMR (50 MHz,  $\text{CDCl}_3$ )  $\delta$  152.8, 136.3, 131.7, 128.5, 127.8, 126.5, 81.8, 74.0, 27.7, 20.4. HRMS (ESI+,  $m/z$ ) calc. for  $\text{C}_{15}\text{H}_{20}\text{O}_3\text{Na}$   $[\text{M}+\text{Na}]^+$  271.1310, found 271.1305. The spectroscopic data are in accordance with those reported in the literature.<sup>29</sup>

### 2-(But-3-en-2-yl)isoindoline-1,3-dione (Scheme 8)



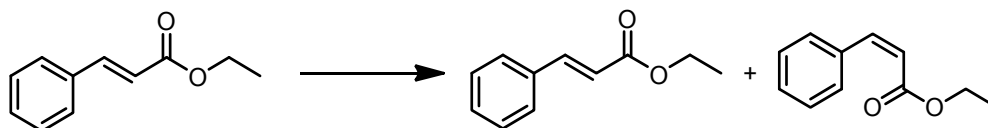
This compound was synthesised (and provided by M. Fañanás-Mastral) according to the literature procedure.<sup>30</sup>  $^1\text{H}$  NMR (200 MHz,  $\text{CDCl}_3$ )  $\delta$  7.84–7.78 (m, 2H), 7.76–7.64 (m, 2H), 6.19 (ddd,  $J = 17.0$  Hz, 10.3 Hz, 6.7 Hz, 1H), 5.22 (d,  $J = 17.5$  Hz, 1H), 5.15 (d,  $J = 10.4$  Hz, 1H), 5.00–4.84 (m, 1H), 1.58 (d,  $J = 7.1$  Hz, 3H);  $^{13}\text{C}$  NMR (50 MHz,  $\text{CDCl}_3$ )  $\delta$  167.9, 136.8, 133.9, 132.0, 123.1, 116.3, 48.9, 18.2. HRMS (ESI+,  $m/z$ ) calc. for  $\text{C}_{12}\text{H}_{12}\text{NO}_2$   $[\text{M}+\text{H}]^+$  202.0868, found 202.0862. The spectroscopic data are in accordance with those reported in the literature.<sup>30</sup>

### 2-(1,3-Dioxoisoindolin-2-yl)propanal (Scheme 8)



This compound was synthesised (and provided by J. Dong) using a method analogous to that used for related compounds.<sup>30</sup>  $^1\text{H}$  NMR (200 MHz,  $\text{CDCl}_3$ )  $\delta$  9.74 (s, 1H), 7.84 – 7.76 (m, 2H), 7.76 – 7.63 (m, 2H), 5.00 – 4.80 (m, 1H), 3.29 (ddd,  $J = 18.0$  Hz, 8.1 Hz, 1.4 Hz, 1H), 2.99 (ddd,  $J = 18.0$  Hz, 6.3 Hz, 1.1 Hz, 1H), 1.48 (d,  $J = 7.0$  Hz, 3H);  $^{13}\text{C}$  NMR (50 MHz,  $\text{CDCl}_3$ )  $\delta$  199.3, 168.0, 134.0, 131.8, 123.2, 47.3, 41.3, 18.8. HRMS (ESI+,  $m/z$ ) calc. for  $\text{C}_{12}\text{H}_{12}\text{NO}_3$   $[\text{M}+\text{H}]^+$  218.0817, found 218.0812. The spectroscopic data are in accordance with those reported in the literature.<sup>30</sup>

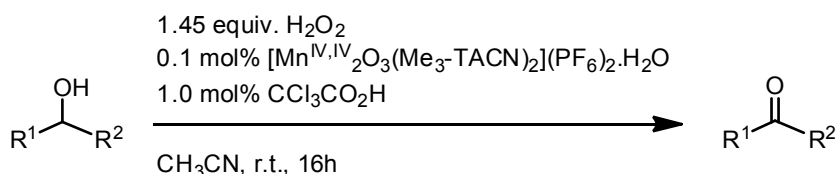
### Isomerisation from *trans*-ethyl cinnamate to *cis*-ethyl cinnamate (Scheme 3)



This isomerisation was performed according to the literature procedure.<sup>31</sup> *trans*-Ethyl cinnamate (180 mg, 1 mmol) and  $\text{BF}_3 \cdot \text{Et}_2\text{O}$  (71 mg, 0.5 mmol) were dissolved in  $\text{CH}_2\text{Cl}_2$

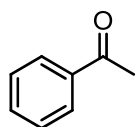
(UV spectroscopy grade 200 ml). The solution was divided equally into 10 fractions in 20 ml scintillation vials and irradiated with an UV lamp (312 nm) for 2 h at room temperature. The irradiated solution was quenched with water and the aqueous layer was discarded. The organic layer was dried over MgSO<sub>4</sub> and concentrated *in vacuo* providing a mixture of *trans*- and *cis*-ethyl cinnamate (54 : 46). <sup>1</sup>H NMR (400 MHz, CDCl<sub>3</sub>) δ *trans*-ethyl cinnamate: 7.69 (d, *J* = 16.0 Hz, 1H), 7.63 – 7.48 (m, 2H), 7.43 – 7.29 (m, 3H), 6.45 (d, *J* = 16.1 Hz, 1H), 4.27 (q, *J* = 7.1 Hz, 2H), 1.39 – 1.30 (m, 3H); *cis*-ethyl cinnamate: <sup>1</sup>H NMR (400 MHz, CDCl<sub>3</sub>) δ 7.63 – 7.48 (m, 2H), 7.43 – 7.29 (m, 3H), 6.95 (d, *J* = 12.6 Hz, 1H), 5.95 (d, *J* = 12.6 Hz, 1H), 4.18 (q, *J* = 7.1 Hz, 2H), 1.28 – 1.21 (m, 3H).

## 2.4.2 General procedure for oxidation of secondary alcohols to ketones (Table 1)



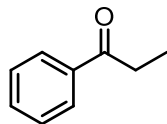
Prior to the experiment, a stock solution containing [Mn<sup>IV,IV</sup>O<sub>3</sub>(Me<sub>3</sub>-TACN)<sub>2</sub>](PF<sub>6</sub>)<sub>2</sub>·H<sub>2</sub>O (24.2 mg, 0.03 mol), trichloroacetic acid (49.0 mg, 0.30 mmol) and H<sub>2</sub>O<sub>2</sub> (50 wt. % in water, 86 μl) in CH<sub>3</sub>CN (10 ml) was prepared at room temperature. The mixture was stirred for 20 min, after which 1.0 ml of this stock solution (3.0 μmol [Mn<sup>IV,IV</sup>O<sub>3</sub>(Me<sub>3</sub>-TACN)<sub>2</sub>](PF<sub>6</sub>)<sub>2</sub>·H<sub>2</sub>O, 0.1 mol%, 30.0 μmol trichloroacetic acid, 1.0 mol%) was added to the solution of the substrate (3 mmol) in CH<sub>3</sub>CN (2 ml). H<sub>2</sub>O<sub>2</sub> (50 wt. % in water, 247 μl, 4.35 mmol, 1.45 equiv.) was added *via* syringe pump (rate 30 μl/h) and the mixture was stirred for 16 h at room temperature. After 16 h, the mixture was added to saturated aqueous NaHCO<sub>3</sub> (20 ml) and CH<sub>2</sub>Cl<sub>2</sub> (20 ml). After separation of the layers, the aqueous layer was extracted with CH<sub>2</sub>Cl<sub>2</sub> (3 x 20 ml). The combined organic layers were dried on MgSO<sub>4</sub> and concentrated *in vacuo* providing the ketone product.

### Acetophenone (entry 1)



The product was obtained as a colourless oil without purification after work up (556 mg, 4.63 mmol, 77%). <sup>1</sup>H NMR (200 MHz, CDCl<sub>3</sub>) δ 7.99 – 7.90 (m, 2H), 7.60 – 7.38 (m, 3H), 2.61 – 2.58 (m, 3H); <sup>13</sup>C NMR (50 MHz, CDCl<sub>3</sub>) δ 198.1, 137.1, 133.0, 128.5, 128.2, 26.5. HRMS (ESI+, *m/z*) calc. for C<sub>8</sub>H<sub>8</sub>O [M+H]<sup>+</sup> 121.0653, found 121.0648.

### Propiophenone (entry 2)

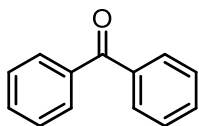


The crude material was purified by column chromatography (SiO<sub>2</sub>, CH<sub>2</sub>Cl<sub>2</sub>) to provide a colourless oil (249 mg, 1.86 mmol, 63%). <sup>1</sup>H NMR (200 MHz, CDCl<sub>3</sub>) δ 8.00 – 7.89 (m, 2H), 7.58 – 7.35 (m, 2H), 2.99 (q, *J* = 7.2 Hz, 2H), 1.21 (t, *J* = 7.2 Hz, 3H); <sup>13</sup>C NMR (50 MHz, CDCl<sub>3</sub>) δ



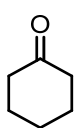
200.7, 136.8, 132.8, 128.5, 127.9, 31.7, 8.2. HRMS (ESI+,  $m/z$ ) calc. for  $C_9H_{11}O$   $[M+H]^+$  135.0810, found 135.0804.

### Benzophenone (entry 3)



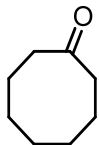
The product was obtained as a white solid without purification after work up (509 mg, 2.79 mmol, 93%).  $^1H$  NMR (200 MHz,  $CDCl_3$ )  $\delta$  7.88 – 7.74 (m, 2H), 7.64 – 7.42 (m, 3H);  $^{13}C$  NMR (50 MHz,  $CDCl_3$ )  $\delta$  196.63, 137.5, 132.3, 129.9, 128.2. HRMS (ESI+,  $m/z$ ) calc. for  $C_{13}H_{11}O$   $[M+H]^+$  183.0810, found 183.0804.

### Cyclohexanone (entry 4)



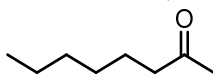
The product was obtained as a colourless oil without purification after work up (153 mg, 1.56 mmol, 31%).  $^1H$  NMR (400 MHz,  $CDCl_3$ )  $\delta$  2.23 (m, 2H), 1.76 (m, 2H), 1.67 – 1.56 (m, 1H);  $^{13}C$  NMR (100 MHz,  $CDCl_3$ )  $\delta$  211.8, 41.7, 26.8, 24.8. Elemental analysis (calc. for  $C_6H_{10}O$ ) C 72.77% (73.43%), H 10.39% (10.27%).

### Cyclooctanone (entry 5)



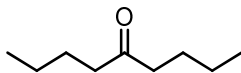
The product was obtained as a colourless oil without purification after work up (362 mg, 2.87 mmol, 86%).  $^1H$  NMR (200 MHz,  $CDCl_3$ )  $\delta$  2.30 (m, 4H), 1.77 (m, 4H), 1.45 (m, 4H), 1.26 (m, 2H);  $^{13}C$  NMR (50 MHz,  $CDCl_3$ )  $\delta$  218.4, 41.7, 26.9, 25.4, 24.5.

### 2-Octanone (entry 6)



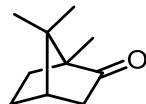
The product was obtained as a colourless oil without purification after work up (588 mg, 4.59 mmol, 92%).  $^1H$  NMR (400 MHz,  $CDCl_3$ )  $\delta$  2.38 (t,  $J$  = 7.5, 2H), 2.14 – 2.04 (m, 3H), 1.59 – 1.45 (m, 2H), 1.24 (m, 6H), 0.91 – 0.76 (m, 3H);  $^{13}C$  NMR (100 MHz,  $CDCl_3$ )  $\delta$  209.3, 43.8, 31.5, 29.8, 28.8, 23.8, 22.4, 14.0. Elemental analysis (calc. for  $C_8H_{16}O$ ) C 74.82% (74.94%), H 12.67% (12.58%).

### 5-Nonanone (entry 7d)



This reaction was carried out using 0.5 mol%  $[Mn^{IV,IV}_2O_3(Me_3TACN)_2](PF_6)_2 \cdot H_2O$  and 5.0 mol% trichloroacetic acid in  $tBuOH/H_2O$  (2/1 v/v) solvent. The product was obtained as a colourless oil without purification after work up (588 mg, 4.59 mmol, 92%).  $^1H$  NMR (400 MHz,  $CDCl_3$ )  $\delta$  2.34 (t,  $J$  = 7.3, 4H), 1.54 – 1.43 (m, 4H), 1.32 – 1.13 (m, 4H), 0.85 (t,  $J$  = 7.1, 6H).

### Camphor (entry 8)

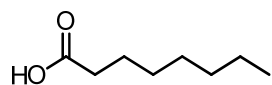


The product was obtained as a white solid without purification after work up (755 mg, 4.96 mmol, 99%). m.p. 170.2-173.2 °C.  $^1H$  NMR (400 MHz,  $CDCl_3$ )  $\delta$  2.39 – 2.30 (m, 1H), 2.08 (t,  $J$  = 4.5, 1H), 2.00 – 1.89 (m, 1H),

1.83 (d,  $J = 18.2$ , 1H), 1.72 – 1.63 (m, 1H), 1.36 (dtd,  $J = 21.5$  Hz, 9.3 Hz, 4.1 Hz, 2H), 0.95 (s, 3H), 0.90 (s, 3H), 0.83 (s, 3H); <sup>13</sup>C NMR (100 MHz, CDCl<sub>3</sub>)  $\delta$  219.7, 57.7, 46.8, 43.3, 43.0, 29.9, 27.0, 19.7, 19.1, 9.2. HRMS (ESI+,  $m/z$ ) calc. for C<sub>10</sub>H<sub>17</sub>O [M+H]<sup>+</sup> 153.1279, found 153.1281.

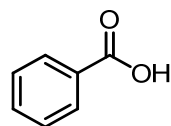
### 2.4.3 Procedure for oxidation of primary alcohols to carboxylic acids (Table 2)

#### Octanoic acid (entry 1)



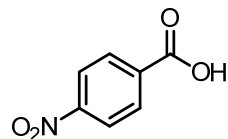
Prior to the experiment, a stock solution containing [Mn<sup>IV,IV</sup><sub>2</sub>O<sub>3</sub>(Me<sub>3</sub>-TACN)<sub>2</sub>](PF<sub>6</sub>)<sub>2</sub>·H<sub>2</sub>O (5.0 mg, 6.25  $\mu$ mol), trichloroacetic acid (10.2 mg, 0.06 mmol) and H<sub>2</sub>O<sub>2</sub> (50 wt. % in water, 35  $\mu$ l) in CH<sub>3</sub>CN (5 ml) was prepared at room temperature. The mixture was stirred for 20 min, after which 4.0 ml of this stock solution (5.0  $\mu$ mol [Mn<sup>IV,IV</sup><sub>2</sub>O<sub>3</sub>(Me<sub>3</sub>-TACN)<sub>2</sub>](PF<sub>6</sub>)<sub>2</sub>·H<sub>2</sub>O, 0.1 mol%, 50.0  $\mu$ mol trichloroacetic, 1.0 mol%) was added to the solution of 1-octanol (5.0 mmol) in CH<sub>3</sub>CN (0.5 ml) and H<sub>2</sub>O (0.5 ml). H<sub>2</sub>O<sub>2</sub> (50 wt. % in water, 850  $\mu$ l, 15 mmol, 3 equiv.) was added *via* syringe pump (rate 70  $\mu$ l/h) to the reaction mixture. Extra batches of [Mn<sup>IV,IV</sup><sub>2</sub>O<sub>3</sub>(Me<sub>3</sub>-TACN)<sub>2</sub>](PF<sub>6</sub>)<sub>2</sub>·H<sub>2</sub>O (4.1 mg, 5  $\mu$ mol, 0.1 mol% per batch) were added to the reaction mixture 3.5, 6 and 8 h after the addition of H<sub>2</sub>O<sub>2</sub> had commenced. When the addition of H<sub>2</sub>O<sub>2</sub> was completed, the mixture was stirred for an additional 1 h. Water (10 ml) and Et<sub>2</sub>O (10 ml) were added and the pH of the aqueous layer was set to pH >9 by adding saturated NaHCO<sub>3</sub> (aq.). The organic layer was separated and the aqueous layer was washed with Et<sub>2</sub>O (3 x 20 ml). The pH of the aqueous layer was subsequently set to pH <2 with 10% HCl (aq.) and was extracted with Et<sub>2</sub>O (3 x 20 ml). The combined organic layer was dried over anhydrous MgSO<sub>4</sub> and concentrated *in vacuo* providing the product as a colourless oil (282 mg, 1.96 mmol, 37%). <sup>1</sup>H NMR (400 MHz, CDCl<sub>3</sub>)  $\delta$  9.69 (s, 1H), 2.34 (t,  $J = 7.5$  Hz, 2H), 1.69 – 1.57 (m, 2H), 1.30 – 1.28 (br s, 8H), 0.87 – 0.86 (br s, 3H).

#### Benzoic acid (entry 2)



The reaction was carried out employing the general procedure for oxidation of aldehyde to carboxylic acid and 2.05 equiv. H<sub>2</sub>O<sub>2</sub> was used instead. After the work up, the product was obtained as a white solid. <sup>1</sup>H NMR (400 MHz, CDCl<sub>3</sub>)  $\delta$  8.12 (d,  $J = 7.1$  Hz, 2H), 7.63 (t,  $J = 7.4$  Hz, 1H), 7.49 (t,  $J = 7.3$  Hz, 2H); <sup>13</sup>C NMR (100 MHz, CDCl<sub>3</sub>)  $\delta$  172.1, 133.8, 130.2, 129.3, 128.5.

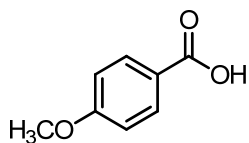
#### 4-Nitrobenzoic acid (entry 3)



Prior to the experiment, a stock solution containing [Mn<sup>IV,IV</sup><sub>2</sub>O<sub>3</sub>(Me<sub>3</sub>-TACN)<sub>2</sub>](PF<sub>6</sub>)<sub>2</sub>·H<sub>2</sub>O (10.1 mg, 12.5  $\mu$ mol), salicylic acid (17.3 mg, 0.13 mmol) and H<sub>2</sub>O<sub>2</sub> (50 wt. % in water, 35  $\mu$ l) in CH<sub>3</sub>CN (5 ml) was prepared at room temperature. The mixture was stirred for 20 min, after which 2.0 ml of this stock solution (5.0  $\mu$ mol [Mn<sup>IV,IV</sup><sub>2</sub>O<sub>3</sub>(Me<sub>3</sub>-TACN)<sub>2</sub>](PF<sub>6</sub>)<sub>2</sub>·H<sub>2</sub>O, 0.1 mol%, 50.0  $\mu$ mol salicylic acid, 1.0 mol%)

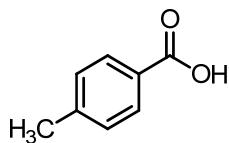
was added to the solution of 4-nitrobenzyl alcohol (5.0 mmol) in CH<sub>3</sub>CN (18 ml) and H<sub>2</sub>O (5 ml). H<sub>2</sub>O<sub>2</sub> (50 wt. % in water, 850  $\mu$ l, 15 mmol, 3 equiv.) was added *via* syringe pump (rate 70  $\mu$ l/h) to the reaction mixture. Extra batches of [Mn<sup>IV,IV</sup><sub>2</sub>O<sub>3</sub>(Me<sub>3</sub>-TACN)<sub>2</sub>](PF<sub>6</sub>)<sub>2</sub>·H<sub>2</sub>O (4.1 mg, 5  $\mu$ mol, 0.1 mol% per batch) were added to the reaction mixture 3, 6 and 9 h after the addition of H<sub>2</sub>O<sub>2</sub> had commenced. When the addition of H<sub>2</sub>O<sub>2</sub> was completed, the mixture was stirred for an additional 1 h. Water (10 ml) and Et<sub>2</sub>O (10 ml) were added and the pH of the aqueous layer was set to pH >9 by adding saturated NaHCO<sub>3</sub> (aq.). The organic layer was separated and the aqueous layer was washed with Et<sub>2</sub>O (3 x 20 ml). The pH of the aqueous layer was subsequently set to pH <2 with 10% HCl (aq.) and was extracted with Et<sub>2</sub>O (3 x 20 ml). The combined organic layer was dried over anhydrous MgSO<sub>4</sub> and concentrated *in vacuo* providing a pale yellow solid (681 mg, 4.07 mmol, 81%). <sup>1</sup>H NMR (200 MHz, acetone)  $\delta$  8.42 – 8.34 (m, 2H), 8.32 – 8.25 (m, 2H).

#### 4-Methoxybenzoic acid (entry 4)



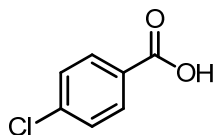
The reaction was performed using the same procedure described for 4-nitrobenzoic acid. The product was obtained as a brown solid (161 mg, 1.06 mmol, 22%). <sup>1</sup>H NMR (400 MHz, acetone)  $\delta$  8.02 – 7.96 (m, 2H), 7.04 – 6.98 (m, 2H), 3.88 (s, 3H); <sup>13</sup>C NMR (50 MHz, acetone)  $\delta$  167.8, 164.9, 132.9, 124.1, 114.9, 56.3.

#### 4-Methylbenzoic acid (entry 5)



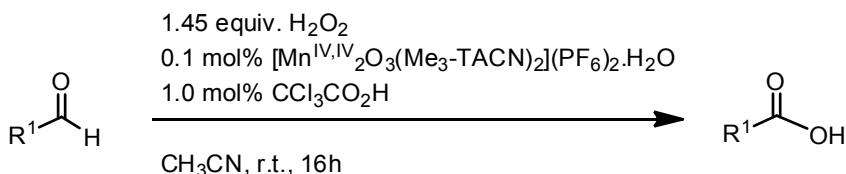
Prior to the experiment, a stock solution containing [Mn<sup>IV,IV</sup><sub>2</sub>O<sub>3</sub>(Me<sub>3</sub>-TACN)<sub>2</sub>](PF<sub>6</sub>)<sub>2</sub>·H<sub>2</sub>O (4.0 mg, 5  $\mu$ mol), salicylic acid (6.9 mg, 50  $\mu$ mol) and H<sub>2</sub>O<sub>2</sub> (50 wt. % in water, 14  $\mu$ l) in CH<sub>3</sub>CN (5 ml) was prepared at room temperature. The mixture was stirred for 20 min, after which 1.0 ml of this stock solution (1.0  $\mu$ mol [Mn<sup>IV,IV</sup><sub>2</sub>O<sub>3</sub>(Me<sub>3</sub>-TACN)<sub>2</sub>](PF<sub>6</sub>)<sub>2</sub>·H<sub>2</sub>O, 0.1 mol%, 10.0  $\mu$ mol salicylic acid, 1.0 mol%) was added to the solution of 4-methylbenzyl alcohol (1.0 mmol) in CH<sub>3</sub>CN (3 ml) and H<sub>2</sub>O (1 ml). H<sub>2</sub>O<sub>2</sub> (50 wt. % in water, 167  $\mu$ l, 2.95 mmol, 2.95 equiv.) was added *via* syringe pump (rate 17  $\mu$ l/h) to the reaction mixture. When the addition of H<sub>2</sub>O<sub>2</sub> was completed, the mixture was stirred for an additional 1 h. Water (10 ml) and Et<sub>2</sub>O (10 ml) were added and the pH of the aqueous layer was set to pH >9 by adding saturated NaHCO<sub>3</sub> (aq.). The organic layer was separated and the aqueous layer was washed with Et<sub>2</sub>O (3 x 20 ml). The pH of the aqueous layer was subsequently set to pH <2 with 10% HCl (aq.) and was extracted with Et<sub>2</sub>O (3 x 20 ml). The combined organic layer was dried over anhydrous MgSO<sub>4</sub> and concentrated *in vacuo* providing a white solid (128 mg, 0.94 mmol, 94%). <sup>1</sup>H NMR (200 MHz, acetone)  $\delta$  7.93 (d, *J* = 8.2, 2H), 7.32 (d, *J* = 7.9, 2H), 2.41 (s, 3H); <sup>13</sup>C NMR (50 MHz, acetone)  $\delta$  168.1, 144.9, 131.0, 130.5, 129.3, 22.1.

#### 4-Chlorobenzoic acid (entry 6)



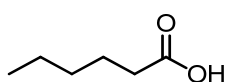
The reaction was performed using the same procedure described for 4-methylbenzoic acid. The product was obtained as a white solid (147 mg, 0.94 mmol, 95%). <sup>1</sup>H NMR (200 MHz, acetone) δ 8.13 – 7.98 (m, 2H), 7.60 – 7.51 (m, 2H); <sup>13</sup>C NMR (50 MHz, acetone) δ 167.2, 140.1, 132.7, 130.8, 130.1.

#### 2.4.4 General procedure for oxidation of aldehydes to carboxylic acid (Table 3)



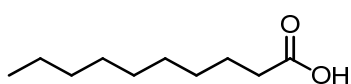
Prior to the experiment, a stock solution containing [Mn<sup>IV,IV</sup><sub>2</sub>O<sub>3</sub>(Me<sub>3</sub>-TACN)<sub>2</sub>](PF<sub>6</sub>)<sub>2</sub>·H<sub>2</sub>O (80.8 mg, 0.10 mmol), trichloroacetic acid (163.4 mg, 1.00 mmol) and H<sub>2</sub>O<sub>2</sub> (50 wt. % in water, 283 μl) in CH<sub>3</sub>CN (20 ml) was prepared at room temperature. The mixture was stirred for 20 min, after which 1.0 ml of this stock solution (5.0 μmol [Mn<sup>IV,IV</sup><sub>2</sub>O<sub>3</sub>(Me<sub>3</sub>-TACN)<sub>2</sub>](PF<sub>6</sub>)<sub>2</sub>·H<sub>2</sub>O, 0.1 mol%, 50.0 μmol trichloroacetic acid, 1.0 mol%) was added to the solution of substrate (5.0 mmol) in CH<sub>3</sub>CN (4 ml). The mixture was cooled to 0 °C and H<sub>2</sub>O<sub>2</sub> (50 wt. % in water, 410 μl, 7.25 mmol, 1.45 equiv.) was added *via* syringe pump (rate 70 μl/h). The mixture was stirred for 16 h, allowing temperature to rise to room temperature. After 16 h, the mixture was added to saturated aqueous NaHCO<sub>3</sub> (20 ml) and CH<sub>2</sub>Cl<sub>2</sub> (20 ml) to adjust the pH of the aqueous layer to pH >9. The organic layer was separated and the aqueous layer was washed with CH<sub>2</sub>Cl<sub>2</sub> (3 x 20 ml). The aqueous layer was acidified with 10% HCl (aq.) (to set to pH <2) and extracted with CH<sub>2</sub>Cl<sub>2</sub> (3 x 20 ml). The combined organic layers were dried on MgSO<sub>4</sub> and concentrated *in vacuo* providing the carboxylic acid product.

#### Hexanoic acid (entry 1)



The product was obtained as a colourless oil (354 mg, 3.05 mmol, 61%). <sup>1</sup>H NMR (400 MHz, CDCl<sub>3</sub>) δ 2.35 (t, *J* = 7.4 Hz, 2H), 1.68 – 1.58 (m, 2H), 1.39 – 1.24 (m, 4H), 0.95 – 0.85 (m, 3H); <sup>13</sup>C NMR (100 MHz, CDCl<sub>3</sub>) δ 180.7, 34.1, 31.2, 24.3, 22.3, 13.8. HRMS (ESI+, *m/z*) calc. for C<sub>6</sub>H<sub>13</sub>O<sub>2</sub> [M+H]<sup>+</sup> 117.0916, found 117.0918. Elemental analysis (calc. for C<sub>6</sub>H<sub>12</sub>O<sub>2</sub>) C 61.70% (62.04%), H 10.59% (10.41%).

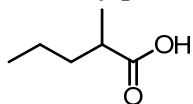
#### Decanoic acid (entry 2)



The product was obtained as a colourless solid (481 mg, 2.79 mmol, 56%). m.p. 31.0–31.1 °C. <sup>1</sup>H NMR (400 MHz, CDCl<sub>3</sub>) δ 2.35 (t, *J* = 7.5 Hz, 2H), 1.62 (m, 2H), 1.28 (br s, 12H), 0.88 (t, *J* = 6.7 Hz, 3H); <sup>13</sup>C NMR (100 MHz, CDCl<sub>3</sub>) δ 179.8, 34.0, 31.9, 29.4, 29.2, 29.1, 24.7, 22.7, 14.10. HRMS (ESI+, *m/z*) calc. for C<sub>10</sub>H<sub>21</sub>O<sub>2</sub> [M+H]<sup>+</sup> 173.1542,

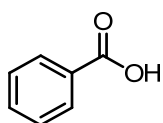
found 173.1544. Elemental analysis (calc. for  $C_{10}H_{20}O_2$ ) C 69.33% (69.72%), H 11.75% (11.70%).

### 2-Methylpentanoic acid (entry 3)



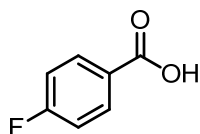
The product was obtained as a pale yellow oil (383 mg, 3.30 mmol, 66%).  $^1H$  NMR (400 MHz,  $CDCl_3$ )  $\delta$  2.53 – 2.40 (m, 1H), 1.71 – 1.60 (m, 1H), 1.46 – 1.27 (m, 3H), 1.19 – 1.10 (m, 3H), 0.94 – 0.84 (m, 3H);  $^{13}C$  NMR (100 MHz,  $CDCl_3$ )  $\delta$  183.7, 39.2, 35.6, 20.3, 16.8, 13.9. HRMS (ESI+,  $m/z$ ) calc. for  $C_6H_{13}O_2$   $[M+H]^+$  117.0916, found 117.0910. Elemental analysis (calc. for  $C_6H_{12}O_2$ ) C 61.75% (62.04%), H 10.58% (10.41%).

### Benzoic acid (entry 4)



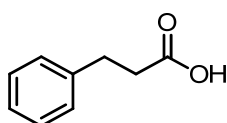
The product was obtained as a white powder (590 mg, 4.83 mmol, 97%). m.p. 122.5-123.4 °C.  $^1H$  NMR (400 MHz,  $CDCl_3$ )  $\delta$  8.13 (d,  $J$  = 7.1 Hz, 2H), 7.63 (t,  $J$  = 7.4 Hz, 1H), 7.49 (t,  $J$  = 7.7 Hz, 2H);  $^{13}C$  NMR (100 MHz,  $CDCl_3$ )  $\delta$  172.1, 133.8, 130.2, 129.3, 128.5. HRMS (ESI+,  $m/z$ ) calc. for  $C_7H_7O_2$   $[M+H]^+$  123.0446, found 123.0450. Elemental analysis (calc. for  $C_7H_6O_2$ ) C 68.78% (68.85%), H 4.91% (4.95%).

### 4-Fluorobenzoic acid (entry 5)



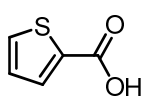
The crude product was purified by recrystallisation from EtOAc/pentane to provide a white powder (105 mg, 0.75 mmol, 89%).  $^1H$  NMR (400 MHz,  $CDCl_3$ )  $\delta$  8.14 (t,  $J$  = 8.7 Hz, 2H), 7.15 (t,  $J$  = 8.6 Hz, 2H).

### 3-Phenylpropanoic acid (entry 7)



The crude product was purified by column chromatography ( $SiO_2$ , EtOAc/pentane = 50/50) to provide a colourless solid (417 mg, 2.78 mmol, 56%). m.p. 44.0-44.5 °C.  $^1H$  NMR (400 MHz,  $CDCl_3$ )  $\delta$  7.35 – 7.11 (m, 5H), 2.97 (t,  $J$  = 7.8 Hz, 2H), 2.69 (t,  $J$  = 7.7 Hz, 2H);  $^{13}C$  NMR (100 MHz,  $CDCl_3$ )  $\delta$  179.0, 140.1, 128.5, 128.2, 126.3, 35.6, 30.5. HRMS (ESI+,  $m/z$ ) calc. for  $C_9H_{11}O_2$   $[M+H]^+$  151.0759, found 151.0768. Elemental analysis (calc. for  $C_9H_{10}O_2$ ) C 71.64% (71.95%), H 6.62% (6.71%).

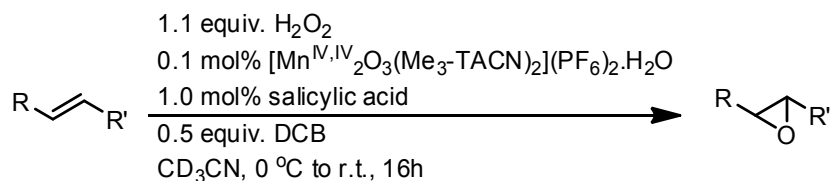
### Thiophene-2-carboxylic acid (entry 8)



This reaction was carried out using 2.0 mol%  $[Mn^{IV,IV}_2O_3(Me_3-TACN)_2](PF_6)_2 \cdot H_2O$  and 20.0 mol% trichloroacetic acid. The product was obtained as a pale yellow solid (494 mg, 3.85 mmol, 77%). m.p. 124.1-126.2 °C.  $^1H$  NMR (400 MHz,  $CDCl_3$ )  $\delta$  7.91 (ddd,  $J$  = 3.8, 1.3, 0.6, 1H), 7.66 (ddd,  $J$  = 5.0, 1.3, 0.5, 1H), 7.17 – 7.13 (m, 1H);  $^{13}C$  NMR (100 MHz,  $CDCl_3$ )  $\delta$  167.7, 135.0, 134.0, 132.8, 128.1. HRMS (ESI+,  $m/z$ ) calc. for  $C_5H_5O_2S$   $[M+H]^+$  129.0010, found

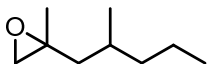
129.0018. Elemental analysis (calc. for C<sub>3</sub>H<sub>4</sub>O<sub>2</sub>S) C 46.63% (46.86%), H 3.14% (3.15%), S 25.01% (25.02%).

#### 2.4.5 General procedure for oxidation of alkenes (Scheme 1 and 2)

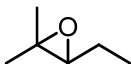


Prior to the experiment, a stock solution containing [Mn<sup>IV,IV</sup>O<sub>3</sub>(Me<sub>3</sub>-TACN)<sub>2</sub>](PF<sub>6</sub>)<sub>2</sub>·H<sub>2</sub>O (2.0 mg, 2.5 μmol), salicylic acid (3.5 mg, 25 μmol) and H<sub>2</sub>O<sub>2</sub> (50 wt. % in water, 7 μl) in CD<sub>3</sub>CN (1 ml) was prepared at room temperature. The mixture was stirred for 20 min, after which 0.4 ml of this stock solution (1.0 μmol [Mn<sup>IV,IV</sup>O<sub>3</sub>(Me<sub>3</sub>-TACN)<sub>2</sub>](PF<sub>6</sub>)<sub>2</sub>·H<sub>2</sub>O, 0.1 mol%, 10.0 μmol salicylic acid, 1.0 mol%) was added to the solution of substrate (1.0 mmol) and 1,2-dichlorobenzene (73 mg, 0.5 mmol) in CD<sub>3</sub>CN (0.6 ml). The mixture was cooled to 0 °C and H<sub>2</sub>O<sub>2</sub> (50 wt. % in water, 63 μl, 1.1 mmol, 1.1 equiv.) was added *via* syringe pump (rate 7.8 μl/h) to the reaction mixture. The mixture was stirred for 16 h, allowing temperature to rise to room temperature. After 16 h, the mixture was measured by <sup>1</sup>H NMR spectroscopy. <sup>1</sup>H NMR analysis of the solution provided product yield relative to the internal standard (1,2-dichlorobenzene) by integration and the products were identified by comparison to the <sup>1</sup>H NMR spectra of authentic samples.

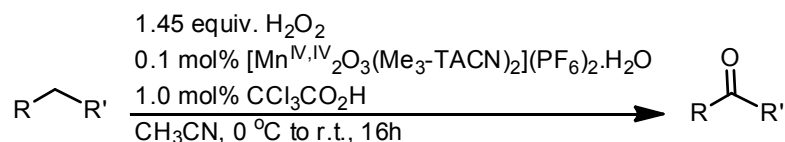
#### 2-Methyl-2-(2-methylpentyl)oxirane

 This reaction provided 73% NMR yield of epoxide. <sup>1</sup>H NMR (200 MHz, CD<sub>3</sub>CN) δ 2.53 – 2.46 (m, 2H), 1.76 – 1.52 (m, 2H), 1.31 – 1.18 (m, 7H), 1.03 – 0.95 (m, 1H), 0.91 – 0.77 (m, 6H).

#### 3-Ethyl-2,2-dimethyloxirane

 This reaction provided 72% NMR yield of epoxide. <sup>1</sup>H NMR (200 MHz, CD<sub>3</sub>CN) δ 2.67 – 2.55 (m, 2H), 1.50 – 1.34 (m, 2H), 1.21 (s, 3H), 1.18 (s, 3H), 0.94 – 0.88 (m, 3H).

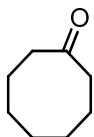
#### 2.4.6 General procedure for C-H activation (Table 6)



Prior to the experiment, a solution containing [Mn<sup>IV,IV</sup>O<sub>3</sub>(Me<sub>3</sub>-TACN)<sub>2</sub>](PF<sub>6</sub>)<sub>2</sub>·H<sub>2</sub>O (4.0 mg, 5.0 μmol), trichloroacetic acid (8.2 mg, 0.05 mmol) and H<sub>2</sub>O<sub>2</sub> (50 wt. % in water, 14 μl) in CH<sub>3</sub>CN (5 ml) was prepared at room temperature. The solution was stirred for 20 min at room temperature followed by the addition of substrate (5.0 mmol). The mixture was cooled to 0 °C and H<sub>2</sub>O<sub>2</sub> (50 wt. % in water, 410 μl, 7.25 mmol, 1.45 equiv.) was

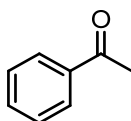
added *via* syringe pump (rate 70  $\mu\text{l/h}$ ). The mixture was stirred for 16 h, allowing temperature to rise to room temperature. After 16 h, the mixture was added to saturated aqueous  $\text{NaHCO}_3$  (20 ml) and  $\text{Et}_2\text{O}$  (20 ml). The organic layer was separated and the aqueous layer was washed with  $\text{Et}_2\text{O}$  (3 x 20 ml). The aqueous layer was acidified with 10%  $\text{HCl}$  (aq.) and extracted with  $\text{Et}_2\text{O}$  (3 x 20 ml). The combined organic layers were dried on  $\text{MgSO}_4$  and concentrated *in vacuo* providing the crude product.

#### Cyclooctanone (entry 1)



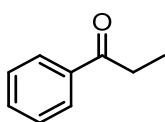
1,2-Dichloroethane (365 mg, 2.48 mmol) was added to the crude reaction mixture as an internal standard, and a sample was diluted with  $\text{CDCl}_3$  to facilitate the measurement by  $^1\text{H}$  NMR spectroscopy.  $^1\text{H}$  NMR analysis of the solution provided a product yield relative to the internal standard integration. This reaction showed 20% starting material remaining and 51% of cyclooctanone product.  $^1\text{H}$  NMR (400 MHz,  $\text{CDCl}_3$ )  $\delta$  2.34-2.27 (m, 4H), 1.79-1.75 (m, 4H), 1.45-1.43 (m, 6H);  $^{13}\text{C}$  NMR (50 MHz,  $\text{CDCl}_3$ )  $\delta$  217.9, 41.5, 26.8, 25.3, 24.4.

#### Acetophenone (entry 3)



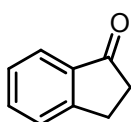
The crude product was purified by column chromatography ( $\text{SiO}_2$ ,  $\text{CH}_2\text{Cl}_2/\text{MeOH}$  = 100/0 to 98/2) to provide a yellow oil (225 mg, 1.86 mmol, 37%).  $^1\text{H}$  NMR (400 MHz,  $\text{CDCl}_3$ )  $\delta$  7.93 (d,  $J$  = 7.5 Hz, 2H), 7.61-7.27 (m, 3H), 2.58 (s, 3H).

#### Propiophenone (entry 4)



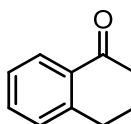
The crude product was purified by column chromatography ( $\text{SiO}_2$ ,  $\text{CH}_2\text{Cl}_2/\text{MeOH}$  = 100/0 to 98/2) to provide a yellow oil (203 mg, 1.51 mmol, 30%).  $^1\text{H}$  NMR (400 MHz,  $\text{CDCl}_3$ )  $\delta$  7.97 (m, 2H), 7.59-7.50 (m, 3H), 3.01 (q,  $J$  = 7.2 Hz, 2H), 1.23 (t,  $J$  = 7.1 Hz, 3H).

#### 2,3-Dihydro-1H-inden-1-one (entry 5)



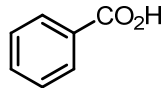
The crude product was purified by column chromatography ( $\text{SiO}_2$ ,  $\text{EtOAc}/\text{pentane}$  = 67/33) to provide a brown viscous oil (132 mg, 1.0 mmol, 40%).  $^1\text{H}$  NMR (400 MHz,  $\text{CDCl}_3$ )  $\delta$  7.75 (dd,  $J$  = 7.7 Hz, 0.7 Hz, 1H), 7.58 (dt,  $J$  = 7.5 Hz, 1.2 Hz, 1H), 7.48 (dd,  $J$  = 7.7 Hz, 0.7 Hz, 1H), 7.36 (dt,  $J$  = 7.4 Hz, 1.2 Hz, 1H), 3.14 (m, 2H), 2.69 (m, 2H).

#### 3,4-Dihydronaphthalen-1(2H)-one (entry 6)



The crude product was purified by column chromatography ( $\text{SiO}_2$ ,  $\text{EtOAc}/\text{pentane}$  = 75/25) to provide a dark brown viscous oil (454 mg, 3.4 mmol, 69%).  $^1\text{H}$  NMR (400 MHz,  $\text{CDCl}_3$ )  $\delta$  7.51-7.01 (m, 4H), 2.97 (t,  $J$  = 5.5 Hz, 1H), 2.60 (t,  $J$  = 5.7 Hz, 1H), 2.18-2.09 (m, 2H), 1.84-1.75 (m, 2H) ppm.

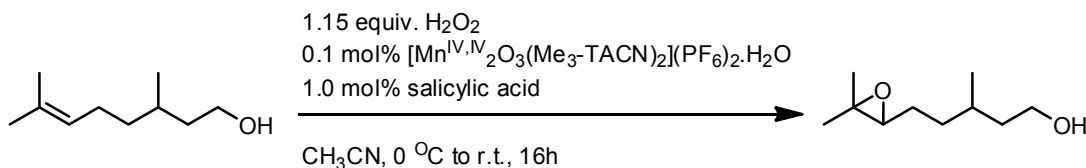
### Benzoic acid (entry 2)



Prior to the experiment, a solution containing [Mn<sup>IV,IV</sup><sub>2</sub>O<sub>3</sub>(Me<sub>3</sub>-TACN)<sub>2</sub>](PF<sub>6</sub>)<sub>2</sub>·H<sub>2</sub>O (53 mg, 65.0 μmol), trichloroacetic acid (106 mg, 0.65 mmol) and H<sub>2</sub>O<sub>2</sub> (50 wt. % in water, 92 μl) in CH<sub>3</sub>CN (66 ml) was prepared at room temperature. The solution was stirred for 20 min at room temperature followed by the addition of toluene (3.0 g, 32.6 mmol). The mixture was cooled to 0 °C and H<sub>2</sub>O<sub>2</sub> (50 wt. % in water, 8.31 ml, 146.7 mmol, 4.5 equiv.) was added *via* syringe pump (rate 1.04 ml/h). The mixture was stirred for 16 h, allowing temperature to rise to room temperature. After 16 h, the mixture was added to saturated aqueous NaHCO<sub>3</sub> (50 ml) and Et<sub>2</sub>O (50 ml). The organic layer was separated and the aqueous layer was washed with Et<sub>2</sub>O (3 x 100 ml). The aqueous layer was acidified with 10% HCl (aq.) (to pH 6) and extracted with Et<sub>2</sub>O (3 x 100 ml). The combined organic layers were dried on MgSO<sub>4</sub> and concentrated *in vacuo* providing the benzoic acid as an off-white solid (0.33 g, 3.6 mmol, 11%). <sup>1</sup>H NMR (400 MHz, CDCl<sub>3</sub>) δ 12.09 (s, 1H), 8.15 (m, 2H), 7.63-7.42 (m, 3H).

### 2.4.7 Oxidation of bifunctional substrates

#### 5-(3,3-Dimethyloxiran-2-yl)-3-methylpentan-1-ol (Table 7)



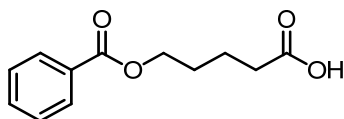
Prior to the experiment, a stock solution containing [Mn<sup>IV,IV</sup><sub>2</sub>O<sub>3</sub>(Me<sub>3</sub>-TACN)<sub>2</sub>](PF<sub>6</sub>)<sub>2</sub>·H<sub>2</sub>O (16.2 mg, 0.02 mmol), salicylic acid (27.6 mg, 0.20 mmol) and H<sub>2</sub>O<sub>2</sub> (50 wt. % in water, 56 μl) in CH<sub>3</sub>CN (10 ml) was prepared at room temperature. The mixture was stirred for 20 min, after which 1.0 ml of this stock solution (2.0 μmol [Mn<sup>IV,IV</sup><sub>2</sub>O<sub>3</sub>(Me<sub>3</sub>-TACN)<sub>2</sub>](PF<sub>6</sub>)<sub>2</sub>·H<sub>2</sub>O, 0.1 mol%, 20.0 μmol salicylic acid, 1.0 mol%) was added to the solution of citronellol (323 mg, 1.96 mmol) in CH<sub>3</sub>CN (1 ml). The mixture was cooled to 0 °C and H<sub>2</sub>O<sub>2</sub> (50 wt. % in water, 130 μl, 2.30 mmol, 1.15 equiv.) was added *via* syringe pump (rate 16 μl/h). The mixture was stirred for 16 h, allowing temperature to rise to room temperature. After 16 h, the reaction mixture was added to saturated aqueous NaHCO<sub>3</sub> (20 ml) and CH<sub>2</sub>Cl<sub>2</sub> (20 ml). After separation of the layers, the aqueous layer was extracted with CH<sub>2</sub>Cl<sub>2</sub> (3 x 20 ml). The combined organic layers were dried on MgSO<sub>4</sub> and concentrated *in vacuo* providing the crude material. Purification by column chromatography (SiO<sub>2</sub>, CH<sub>2</sub>Cl<sub>2</sub>/methanol = 100/0 to 97/3) afforded 5-(3,3-dimethyloxiran-2-yl)-3-methylpentan-1-ol product as a colourless oil (212 mg, 1.23 mmol, 63%, >95% conversion). The compound contains two diastereomers as evidenced by <sup>13</sup>C NMR. <sup>1</sup>H NMR (200 MHz, CDCl<sub>3</sub>) δ 3.74-3.57 (m, 2H), 2.69 (t, *J* = 5.9 Hz, 1H), 1.67-1.46 (m, 5H), 1.46-1.31 (m, 3H), 1.28 (s, 3H), 1.24 (s, 3H), 0.90 (d, *J* = 6.3 Hz, 3H); <sup>13</sup>C NMR (50 MHz, CDCl<sub>3</sub>) δ 64.6 and 64.6, 60.8, 58.4 and 58.3, 39.8 and 39.5, 33.7 and



33.6, 29.4 and 29.2, 26.4 and 26.2, 24.9, 19.6 and 19.4, 18.7 and 18.6. HRMS (ESI+,  $m/z$ ) calc. for  $C_{10}H_{21}O_2$   $[M+H]^+$  173.1542, found 173.1536.

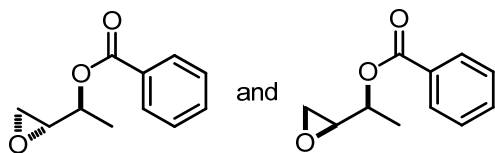
#### 2.4.8 Oxidation of protected substrates

##### 5-(Benzoyloxy)pentanoic acid (Scheme 6)



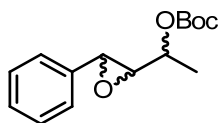
The reaction was performed using the same procedure described for 4-methylbenzoic acid. The product was obtained as a colourless oil (155 mg, 0.70 mmol, 70%).  $^1H$  NMR (200 MHz,  $CDCl_3$ )  $\delta$  8.07 – 8.01 (m, 2H), 7.60 – 7.51 (m, 1H), 7.47 – 7.39 (m, 2H), 4.39 – 4.26 (m, 2H), 2.50 – 2.36 (m, 2H), 1.90 – 1.72 (m, 4H);  $^{13}C$  NMR (50 MHz,  $CDCl_3$ )  $\delta$  179.1, 166.7, 132.9, 130.2, 129.5, 128.3, 64.4, 33.5, 28.0, 21.3.

##### (Oxiran-2-yl)ethyl benzoate (Scheme 6)



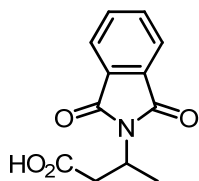
Prior to the experiment, a stock solution containing  $[Mn^{IV,IV}_2O_3(Me_3-TACN)_2](PF_6)_2 \cdot H_2O$  (4.0 mg, 5  $\mu$ mol), salicylic acid (6.9 mg, 50  $\mu$ mol) and  $H_2O_2$  (50 wt. % in water, 14  $\mu$ l) in  $CH_3CN$  (5 ml) was prepared at room temperature. The mixture was stirred for 20 min, after which 2.0 ml of this stock solution (2.0  $\mu$ mol  $[Mn^{IV,IV}_2O_3(Me_3-TACN)_2](PF_6)_2 \cdot H_2O$ , 0.1 mol%, 20.0  $\mu$ mol salicylic acid, 1.0 mol%) was added to the solution of but-3-en-2-yl benzoate (2.0 mmol) in  $CH_3CN$  (2 ml). The mixture was cooled to 0 °C and  $H_2O_2$  (50 wt. % in water, 125  $\mu$ l, 2.2 mmol, 1.1 equiv.) was added *via* syringe pump (rate 21  $\mu$ l/h) to the reaction mixture. When the addition of  $H_2O_2$  was completed, the mixture was stirred for additional 1 h. Then the mixture was added to saturated aqueous  $NaHCO_3$  (20 ml) and  $CH_2Cl_2$  (20 ml). After separation of the layers, the aqueous layer was extracted with  $CH_2Cl_2$  (3 x 20 ml). The combined organic layers were dried on  $MgSO_4$  and concentrated *in vacuo* providing the crude product. The crude product was purified by column chromatography ( $SiO_2$ , EtOAc/pentane = 10/90) to yield the product (mixture of two diastereomers) as a pale yellow oil (228 mg, 1.19 mmol, 60%).  $^1H$  NMR (200 MHz,  $CDCl_3$ )  $\delta$  mixture of two diastereomers: 8.08 – 7.99 (m, 4H), 7.56 – 7.48 (m, 2H), 7.45 – 7.38 (m, 4H), 5.18 – 5.08 (m, 1H) and 5.08 – 4.96 (m, 1H), 3.21 (ddd,  $J$  = 5.7 Hz, 4.1 Hz, 2.6 Hz, 1H) and 3.12 (ddd,  $J$  = 4.6 Hz, 3.8 Hz, 2.9 Hz, 1H), 2.83 (dd,  $J$  = 5.8 Hz, 3.2 Hz, 1H) and 2.69 (dd,  $J$  = 4.9 Hz, 2.6 Hz, 1H), 2.80 – 2.76 (m, 2H), 1.42 (d,  $J$  = 4.9 Hz, 3H) and 1.39 (d,  $J$  = 4.9 Hz, 3H);  $^{13}C$  NMR (50 MHz,  $CDCl_3$ )  $\delta$  mixture of two diastereomers: 165.6 and 165.6, 133.0 and 132.9, 130.4, 129.54 and 129.51, 128.24 and 128.22, 71.1 and 70.0, 53.6 and 53.0, 45.3 and 44.4, 16.4 and 16.0. HRMS (ESI+,  $m/z$ ) calc. for  $C_{11}H_{13}O_3$   $[M+H]^+$  193.0865, found 193.0859 and for  $C_{11}H_{12}O_3$   $(M+Na)^+$  215.0684, found 215.0678.

### ***tert*-Butyl (1-(3-phenyloxiran-2-yl)ethyl) carbonate (Scheme 7)**



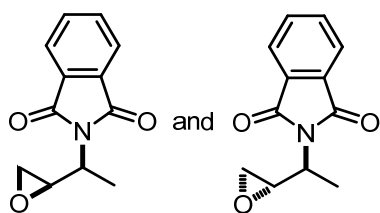
The reaction was performed using the same procedure described for 1-(oxiran-2-yl)ethyl benzoate. The crude product was purified by column chromatography (SiO<sub>2</sub>, Et<sub>3</sub>N/EtOAc/pentane = 1/2/97) to yield the product (mixture of two diastereomers) as a yellow oil (167 mg, 0.63 mmol, 63%). <sup>1</sup>H NMR (200 MHz, CDCl<sub>3</sub>) δ 7.40 – 7.21 (m, 5H), 4.82 – 4.68 (m, 1H), 3.80 (d, *J* = 2.0 Hz, 1H), 3.16 (dd, *J* = 5.9 Hz, 2.1 Hz, 1H), 1.51 (s, 9H), 1.39 (d, *J* = 6.5 Hz, 3H); <sup>13</sup>C NMR (50 MHz, CDCl<sub>3</sub>) δ 152.9, 136.4, 128.5, 128.4, 125.6, 82.5, 73.2, 63.4, 56.1, 27.8, 16.5. HRMS (ESI<sup>+</sup>, *m/z*) calc. for C<sub>15</sub>H<sub>20</sub>O<sub>4</sub>Na [M+Na]<sup>+</sup> 287.1259, found 287.1254.

### **3-(1,3-Dioxoisindolin-2-yl)butanoic acid (Scheme 8)**



The reaction was performed using the same procedure described for 1-(oxiran-2-yl)ethyl benzoate. The product was obtained as an off-white solid (116 mg, 0.50 mmol, quantitative yield). <sup>1</sup>H NMR (400 MHz, CDCl<sub>3</sub>) δ 7.82 (dt, *J* = 6.9 Hz, 3.5 Hz, 2H), 7.75 – 7.65 (m, 2H), 4.80 (dd, *J* = 15.3 Hz, 6.6 Hz, 1H), 3.23 (dd, *J* = 16.5 Hz, 8.7 Hz, 1H), 2.87 (dd, *J* = 16.6 Hz, 6.2 Hz, 1H), 1.50 (d, *J* = 6.9 Hz, 3H); <sup>13</sup>C NMR (50 MHz, CDCl<sub>3</sub>) δ 175.6, 168.1, 134.0, 131.8, 123.3, 43.2, 37.5, 18.8. HRMS (ESI<sup>+</sup>, *m/z*) calc. for C<sub>12</sub>H<sub>12</sub>NO<sub>4</sub> [M+H]<sup>+</sup> 234.0766, found 234.0760 and for C<sub>12</sub>H<sub>11</sub>NO<sub>4</sub>Na [M+Na]<sup>+</sup> 256.0586, found 256.0579. The spectroscopic data are in accordance with those reported in the literature.<sup>30</sup>

### **2-(1-(Oxiran-2-yl)ethyl)isoindoline-1,3-dione (Scheme 8)**



The reaction was performed using the same procedure described for 1-(oxiran-2-yl)ethyl benzoate. The crude product was purified by column chromatography (SiO<sub>2</sub>, CH<sub>2</sub>Cl<sub>2</sub>) to yield the product (mixture of two diastereomers) as a white solid (94 mg, 0.43 mmol, 86%). <sup>1</sup>H NMR (400 MHz, CDCl<sub>3</sub>) δ diastereomer 1: 7.86 – 7.77 (m, 2H), 7.76 – 7.62 (m, 2H), 4.09 – 4.01 (m, 1H), 3.63 – 3.56 (m, 1H), 2.91 – 2.87 (m, 1H), 2.75 – 2.71 (m, 1H), 1.50 (dd, *J* = 7.2 Hz, 1.6 Hz, 3H); diastereomer 2: 7.86 – 7.77 (m, 1.6H), 7.76 – 7.62 (m, 1.6H), 3.99 – 3.91 (m, 0.8H), 3.53 – 3.49 (m, 0.8H), 2.75 – 2.71 (m, 0.8H), 2.60 – 2.57 (m, 0.8H), 1.61 (dd, *J* = 7.1 Hz, 1.7 Hz, 2.4H); <sup>13</sup>C NMR (50 MHz, CDCl<sub>3</sub>) δ mixture of two diastereomers: 168.0 and 167.9, 134.0 and 133.9, 131.9 and 131.8, 123.2 and 123.1, 52.5 and 52.1, 49.7 and 49.6, 46.7 and 46.5, 15.8 and 14.7. HRMS (ESI<sup>+</sup>, *m/z*) calc. for C<sub>12</sub>H<sub>12</sub>NO<sub>3</sub> [M+H]<sup>+</sup> 218.0817, found 218.0811.

## 2.5 References and notes

- 1 A. K. Yudin in *Aziridines and Epoxides in Organic Synthesis*, 2006, Wiley-VCH.
- 2 H. Adolfsson in Chapter 2, J.-E. Bäckvall, (ed.) *Modern Oxidation Methods*, 2010, Wiley-VCH, 37.
- 3 See for example (a) A. J. Wu, J. E. Penner-Hahn and V. L. Pecoraro, *Chem. Rev.*, 2004, **104**, 903; (b) *Modern Oxidation Methods*, J.-E. Bäckvall, (ed.), 2010, Wiley-VCH; (c) B. S. Lane and K. Burgess, *Chem. Rev.*, 2003, **103**, 2457; (d) R. A. Sheldon and J. K. Kochi, *Metal-Catalyzed Oxidations of Organic Compounds*, 1981, Academic Press; (e) H. C. Kolb, M. S. Van Nieuwenhze and K. B. Sharpless, *Chem. Rev.*, 1994, **94**, 2483.
- 4 R. Noyori, M. Aoki and K. Sato, *Chem. Commun.*, 2003, 1977.
- 5 I. W. C. E. Arends and R. A. Sheldon in Chapter 5, J.-E. Bäckvall, (ed.) *Modern Oxidation Methods*, 2010, Wiley-VCH, 147.
- 6 K. Wieghardt, U. Bossek, B. Nuber, J. Weiss, J. Bonvoisin, M. Corbella, S. E. Vitols and J. J. Girerd, *J. Am. Chem. Soc.*, 1988, **110**, 7398.
- 7 A. Darovsky, V. Kezerashvili, P. Coppens, T. Weyhermuller, H. Hummel and K. Wieghardt, *Inorg. Chem.*, 1996, **35**, 6916.
- 8 R. Hage, B. Krijnen, J. B. Warnaar, F. Hartl, D. J. Stufkens and T. L. Snoeck, *Inorg. Chem.*, 1995, **34**, 4973.
- 9 U. Bossek, T. Weyhermuller, K. Wieghardt, B. Nuber and J. Weiss, *J. Am. Chem. Soc.*, 1990, **112**, 6387.
- 10 R. Hage, J. E. Iburg, J. Kerschner, J. H. Koek, E. L. M. Lempers, R. J. Martens, U. S. Racherla, S. W. Russell, T. Swarthoff, M. R. P. van Vliet, J. B. Warnaar, L. van der Wolf and B. Krijnen, *Nature*, 1994, **369**, 637.
- 11 R. Hage and A. Lienke, *Angew. Chem., Int. Ed.*, 2006, **45**, 206.
- 12 W. R. Browne, J. W. de Boer, D. Pijper, J. Brinksma, R. Hage and B. L. Feringa in Chapter 11, J.-E. Bäckvall, (ed.) *Modern Oxidation Methods*, 2010, Wiley-VCH, 371.
- 13 H. Kilic, W. Adam and P. L. Alsters, *J. Org. Chem.*, 2009, **74**, 1135.
- 14 D. E. De Vos and T. Bein, *J. Organomet. Chem.*, 1996, **520**, 195.
- 15 A. Berkessel and C. A. Sklorz, *Tetrahedron Lett.*, 1999, **40**, 7965.
- 16 K. F. Sibbons, K. Shastri and M. Watkinson, *Dalton Trans.*, 2006, 645.
- 17 (a) G. B. Shul'pin, G. Suss-Fink and J. R. Lindsay Smith, *Tetrahedron*, 1999, **55**, 5345; (b) G. B. Shul'pin, G. Suss-Fink and L. S. Shul'pina, *J. Mol. Cat. A – Chem.*, 2001, **170**, 17.
- 18 J. Brinksma, L. Schmieder, G. van Vliet, R. Boaron, R. Hage, D. E. De Vos, P. L. Alsters and B. L. Feringa, *Tetrahedron Lett.*, 2002, **43**, 2619.
- 19 D. E. De Vos, S. de Wildeman, B. F. Sels, P. J. Grobet and P. A. Jacobs, *Angew. Chem., Int. Ed.*, 1999, **38**, 980.
- 20 J. W. de Boer, J. Brinksma, W. R. Browne, A. Meetsma, P. L. Alsters, R. Hage and B. L. Feringa, *J. Am. Chem. Soc.*, 2005, **127**, 7990.
- 21 J. W. de Boer, W. R. Browne, J. Brinksma, A. Meetsma, P. L. Alsters, R. Hage and B. L. Feringa, *Inorg. Chem.*, 2007, **46**, 6353.
- 22 C. Zondervan, R. Hage and B. L. Feringa, *Chem. Commun.*, 1997, 419.

- 
- 23 M. C. V. Sauer and J. O. Edwards, *J. Phys. Chem.*, 1971, **75**, 3004.  
24 J. M. Hoover and S. S. Stahl, *J. Am. Chem. Soc.*, 2011, **133**, 16901.  
25 J. W. de Boer (2008). *cis-Dihydroxylation and epoxidation of alkene by manganese catalysts; selectivity, reactivity and mechanism*. Ph.D. thesis. University of Groningen: The Netherlands.  
26 I. Garcia-Bosch, A. Company, C. W. Cady, S. Styring, W. R. Browne, X. Ribas and M. Costas, *Angew. Chem. Int. Ed.*, 2011, **50**, 5648.  
27 H. E. Gottlieb, V. Kotlyar and A. Nudelman, *J. Org. Chem.*, 1997, **62**, 7512.  
28 P. M. Pihko and J. E. Aho, *Org. Lett.*, 2004, **6**, 3849.  
29 C. Li, J. Xing, J. Zhao, P. Huynh, W. Zhang, P. Jiang and Y. J. Zhang, *Org. Lett.*, 2012, **14**, 390.  
30 B. Weiner, A. Baeza, T. Jerphagnon and B. L. Feringa, *J. Am. Chem. Soc.*, 2009, **131**, 9473.  
31 F. D. Lewis, J. D. Oxman, L. L. Gibson, H. L. Hampsch and S. L. Quillen, *J. Am. Chem. Soc.*, 1986, **108**, 3005.



## Chapter 3

# The unexpected role of pyridine-2-carboxylic acid in manganese based oxidation catalysis with pyridin-2-yl based ligands

*A number of manganese-based catalysts employing ligands whose structures incorporate pyridyl groups have been reported previously to achieve both high turnover numbers and selectivity in the oxidation of alkenes and alcohols, using  $H_2O_2$  as terminal oxidant. In this chapter, the in situ decomposition of these ligands to pyridine-2-carboxylic acid and its derivatives in the presence of a manganese source,  $H_2O_2$  and a base will be demonstrated. Importantly, the decomposition occurs prior to the onset of catalysed oxidation of organic substrates. It is found that the pyridine-2-carboxylic acid formed, together with a manganese source, provides for the observed catalytic activity. The degradation of this series of pyridyl ligands to pyridine-2-carboxylic acid under reaction conditions is demonstrated by  $^1H$  NMR spectroscopy. In all cases the activity and selectivity of the manganese/pyridyl containing ligand systems are identical to that observed with the corresponding number of equivalents of pyridine-2-carboxylic acid; except that, when pyridine-2-carboxylic acid is used directly, a lag phase is not observed and the efficiency in terms of the number of equivalents of  $H_2O_2$  required decreases from 6-8 equiv. with the pyridin-2-yl based ligands to 1-1.5 equiv. with pyridine-2-carboxylic acid.*

*This chapter has been published:*

D. Pijper, P. Saisaha, J. W. de Boer, R. Hoen, C. Smit, A. Meetsma, R. Hage, R. van Summeren, P. L. Alsters, B. L. Feringa and W. R. Browne, *Dalton Trans.*, 2010, **39**, 10375.

### 3.1 Introduction

The design of new ligands for 1<sup>st</sup> row transition metal oxidation catalysts has been driven by the desire to reduce the reliance on stoichiometric oxidants (*e.g.*  $\text{MnO}_4^-$ ,  $\text{OsO}_4$ , peracids *etc.*),<sup>1</sup> and to replace 2<sup>nd</sup> and 3<sup>rd</sup> row transition metal based oxidation catalysts.<sup>2,3</sup> A key challenge this presents is to achieve high activity while at the same time avoiding oxidative degradation of ligands during catalysis. Indeed ligand stability has been a longstanding issue in transition metal oxidation catalysis, as exemplified by the design rules proposed by Collins as early as 1994.<sup>4,5</sup>

The focus on ligand stability is important since, although ligand free oxidation catalysis can be achieved with manganese as demonstrated by Burgess and co-workers,<sup>6</sup> in order to control reactivity and especially (enantio)selectivity then it is almost certainly unavoidable that ligand metal complexes are employed. Over the last decades many ligand systems have been developed that have proven their robustness with iron and manganese during oxidation catalysis, including the pyridyl based ligand families (*e.g.* TPEN,<sup>20</sup> BPMEN,<sup>7</sup> TPA<sup>8</sup> and N<sub>4</sub>Py,<sup>9</sup> Figure 1) and the paradigm TMTACN ligand (where TMTACN is *N,N',N''*-trimethyl-1,4,7-triazacyclononane, Figure 1),<sup>10</sup> which has proven one of the more effective ligands for manganese based oxidation catalysis (see also Chapter 2).<sup>11</sup> The stability of these systems have allowed for stereospecific C-H activation,<sup>12</sup> (enantioselective) epoxidation,<sup>13,14</sup> and (enantioselective) *cis*-dihydroxylation of alkenes<sup>15,16,17,18</sup> often with high turnover numbers and efficiency in terminal oxidants, *e.g.* peracetic acid and  $\text{H}_2\text{O}_2$ .

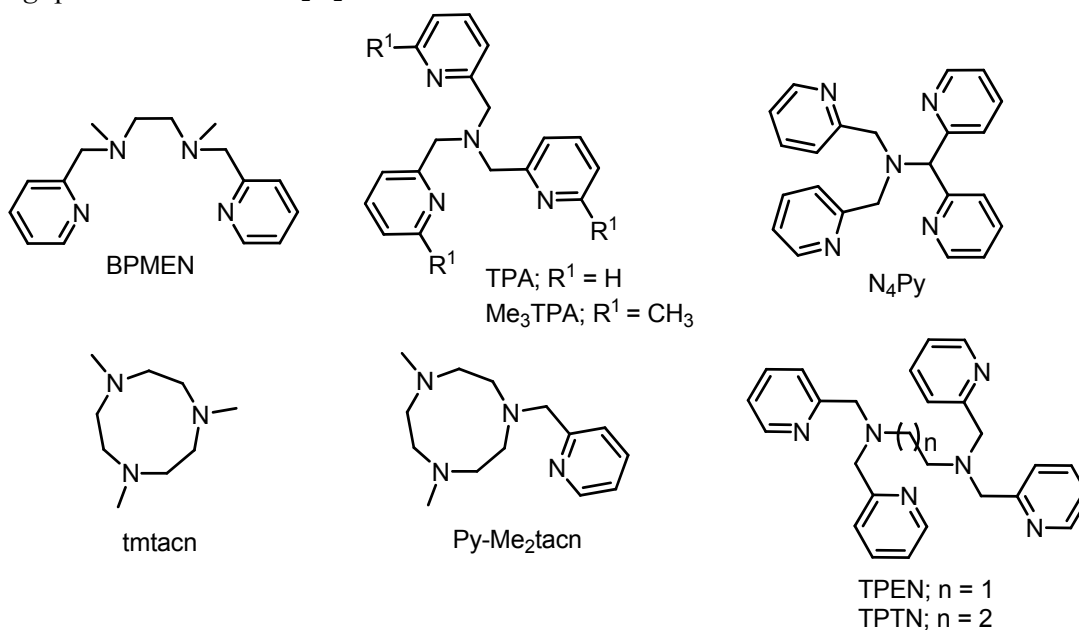


**Figure 1** Examples of pyridyl and triazacyclononane based ligands employed in Fe and Mn based oxidation catalysis

Nevertheless, many ligand systems that have been employed in oxidation catalysis to date have been limited due to their propensity to undergo oxidative degradation, as demonstrated for instance by Banse, Girerd and co-workers<sup>19</sup> for the TPEN<sup>20</sup> class of ligands (Figure 1). In 2008, Groni *et al.*,<sup>21</sup> reported a combined EPR/UV/Vis absorption spectroscopic study of the species formed by reaction of the Mn<sup>II</sup> complex of the ligand *N*-methyl-*N,N',N'*-tris(2-pyridylmethyl)-1,3-propanediamine in acetonitrile with excess H<sub>2</sub>O<sub>2</sub>. In addition to the observation of various manganese peroxy species and Mn<sup>III,IV</sup><sub>2</sub> dimers, they also isolated [Mn<sup>II</sup>(pyridine-2-carboxylate)<sub>2</sub>(H<sub>2</sub>O)<sub>2</sub>] as the ultimate degradation product of the complexes. Although the peroxy species observed would support the involvement of peroxy species in oxidation catalysis with complexes based on TPTN type ligands. Oxidative ligand degradation can be inhibited, as shown by Banse and coworkers recently,<sup>22</sup> through introduction of steric hindrance in the TPEN ligand. Degradation via C-H abstraction was reduced, an effect ascribed to inhibition of bimolecular degradation pathways. Britovsek and coworkers<sup>23</sup> have reported also that catalytic activity and catalyst stability (with respect to ligand dissociation) correlate in the non-heme iron catalyst family. This may account for the stability observed in multidentate ligands where ligand dissociation is of less importance (*vide supra*).

These observations are important as the primary tools available to tuning the catalytic activity and selectivity of transition metal complexes is to change reactions conditions, in particular solvent, co-catalysts and pH, and to vary the detailed structure of the ligands both of which can affect coordinative stability and ligand robustness in addition to catalyst performance.

This aspect is exemplified for instance by the oxidation catalyst [Mn<sup>IV,IV</sup><sub>2</sub>O<sub>3</sub>(TMTACN)<sub>2</sub>]<sup>2+</sup>. De Vos,<sup>11b,d</sup> Berkessel,<sup>11e</sup> Lindsay Smith,<sup>24</sup> Feringa<sup>15,17,18</sup> and co-workers have demonstrated that varying the solvent and co-catalyst employed has a profound effect on its activity. For example tuning selectivity from selective epoxidation to selective *cis*-dihydroxylation of alkenes.<sup>17</sup> It has been demonstrated by Feringa and co-workers that the complex reacts with the carboxylic acid co-catalysts *in situ*, to complexes of the type [Mn<sup>III,III</sup><sub>2</sub>O(RCO<sub>2</sub>)<sub>2</sub>(TMTACN)<sub>2</sub>]<sup>2+</sup> that are responsible for the activity achieved.<sup>17,18</sup> An alternative strategy taken recently by Costas and co-workers is to tune reactivity by modifying the TMTACN ligand with an additional pyridyl group (Py-Me<sub>2</sub>tacn, Figure 1). The catalysts formed by this complex with manganese<sup>25</sup> and iron<sup>26</sup> show markedly different reactivity and selectivity under acidic conditions compared with [Mn<sup>IV,IV</sup><sub>2</sub>O<sub>3</sub>(TMTACN)<sub>2</sub>]<sup>2+</sup>. In both approaches the ligand itself has proven to be robust with catalyst deactivation proceeding by ligand dissociation rather than ligand oxidation.

In general, most research effort has focused on this latter approach, *i.e.* ligand modification, with attention being directed especially towards the design of novel ligands based on pyridyl metal binding moieties.<sup>27</sup>

Over a decade ago, Feringa and co-workers took the approach in developing a family of manganese complexes, with TPEN/TPTN type of ligands (Figure 1).<sup>28,29</sup> Manganese complexes based on these pyridyl ligands were indeed found to display high oxidation activity, both in the epoxidation of alkenes<sup>28</sup> and towards alcohol oxidation.<sup>29</sup>



An attractive feature of this type of ligands is that the synthetic route allows for facile introduction of different groups both on the central diamine unit and in replacing one or more of the pyridyl rings.<sup>30</sup> Although similar levels of activity could be achieved compared with the TMTACN family of complexes, the manganese catalysts based on these pyridyl containing ligands<sup>27</sup> typically require excess of oxidant (8-16 equiv. of H<sub>2</sub>O<sub>2</sub>) to overcome the extensive catalase activity that follows addition of the H<sub>2</sub>O<sub>2</sub> at the start of the reaction.

An interesting question arises as to whether the intermediate compounds **2** and **3** in the synthetic route to the TPEN type ligands, *i.e.* intermediates containing an amination ring motif (Figure 2), are also potential ligands in their own right.

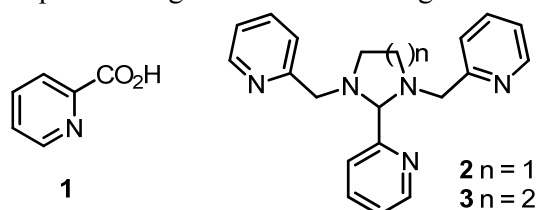


**Figure 2** Pyridine-2-carboxylic acid (**1**) and amination ligands **2** and **3**.

In this chapter the catalytic activity observed with these amination and other ligands with manganese in the oxidation of alkenes is described. With these ligands and a series of related ligands (**4-7**, **13-16**, Figure 3) essentially identical reactivity and selectivity was obtained as that observed for the TPEN based ligands reported previously.

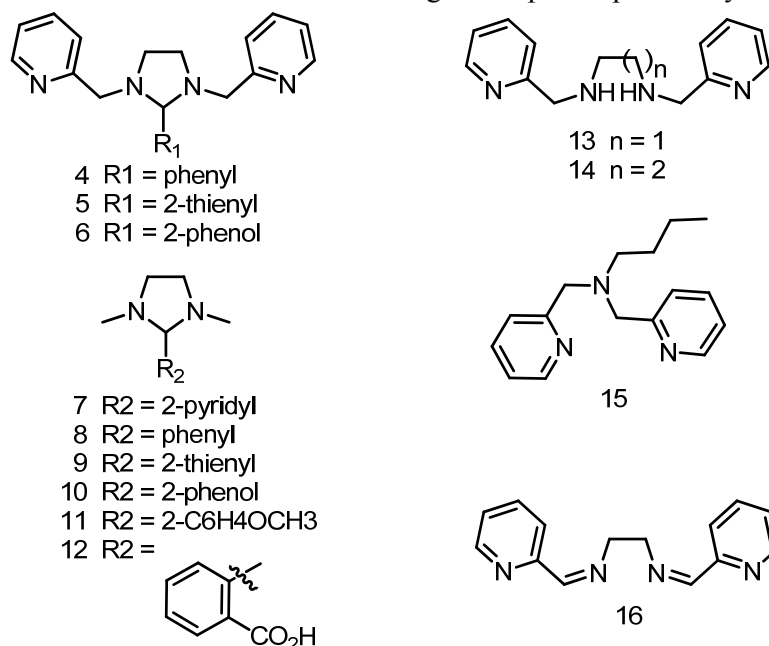
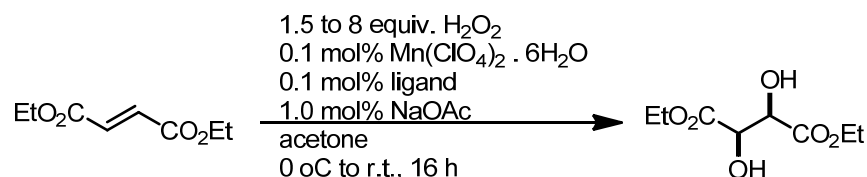


**Figure 3** Ligands employed in the present study.

The key finding is that in all cases these ligands (**2-16**) are highly unstable under the catalytic conditions employed and undergo rapid decomposition, ultimately, to pyridine-2-carboxylic acid. The catalytic activity observed for a wide range of pyridyl based ligands (**2-16**) under certain conditions is shown to be as a direct result of the pyridine-2-carboxylic acid formed *in situ*. Unexpectedly, instead of leading to reduced activity, oxidative ligand degradation allowed for the discovery of a remarkably simple yet powerful four component catalytic system for a wide range of oxidative transformations (*i.e.* pyridine-2-carboxylic acid/ $\text{Mn}^{\text{II}}$ /NaOAc/carbonyl compound, Scheme 1).<sup>30</sup>



**Scheme 1** Alkene oxidation with  $\text{H}_2\text{O}_2$ . For the electron deficient alkene diethyl fumarate full selectivity in favour of *cis*-dihydroxylation is observed with ligands TPTN, **2-7** and pyridine-2-carboxylic acid (for which 0.3 mol% and only 1.5 equiv. of  $\text{H}_2\text{O}_2$  was required for full conversion, *vide infra*).

## 3.2 Results

Ligands **2-16** (Figure 2 and 3) were prepared by standard methods based on the procedure described by Mialane et al.<sup>31</sup> and characterised by NMR spectroscopy, elemental analysis and HRMS (see the experimental section). The system of TPTN (Figure 1) was described earlier.

### 3.2.1 Catalytic activity of $\text{Mn}^{\text{II}}$ with TPTN, **2** and **3**

Previously, the activity of dinuclear  $\text{Mn}^{\text{II}}$  acetato complexes of the TPTN ligand was reported in the oxidation of alkenes<sup>28</sup> and benzyl alcohols.<sup>29</sup> In the present study we have re-examined this ligand together with the immediate synthetic precursors of TPEN and TPTN, *i.e.* **2** and **3**, respectively.

A typical example of the conditions used in the manganese catalysed oxidation reactions is shown in Scheme 1. The reaction was found to proceed with conversion in acetone and 2-butanone but not in acetonitrile or  $t\text{BuOH}/\text{H}_2\text{O}$  with TPTN, **2** and **3**. Furthermore, the addition of several equivalents of base, either with the manganese source (*e.g.*  $\text{Mn}^{\text{II}}(\text{OAc})_2$ , or  $\text{Mn}^{\text{III}}(\text{OAc})_3$ ) or as NaOAc, NaOH or  $\text{Na}_2\text{CO}_3$  (when  $\text{Mn}^{\text{II}}(\text{ClO}_4)_2$  is used) was found to be essential. With other carboxylates such as sodium trichloroacetate or benzoate the rate of reaction was substantially decreased but full conversion was nevertheless achieved.

As noted earlier,<sup>28,29</sup> the addition of at least 8 equiv. of  $\text{H}_2\text{O}_2$  is required in order to obtain reasonable conversion of the alkene substrates, due to the extensive disproportionation that is observed initially upon the addition of  $\text{H}_2\text{O}_2$ . The time dependence of product formation/substrate consumption indicates a substantial lag-time

(~20-60 min) prior to the start of substrate conversion. The addition of acid, *e.g.* acetic acid or trichloroacetic acid suppressed catalase type activity completely, however, in these cases conversion of the substrate or even consumption of the  $\text{H}_2\text{O}_2$  was not observed. For diethyl fumarate full conversion to the *cis*-diol product (*d/l*-diethyl tartrate) and for *cis*-cyclooctene full conversion to a 1 : 6 mixture of *cis*-diol and epoxide product was observed for TPTN, **2** and **3**.

The identical reactivity and selectivity observed for TPTN and ligands **2** and **3** was unexpected (*vide infra*). The observation of a significant induction period during which extensive disproportionation of  $\text{H}_2\text{O}_2$  was observed prior to onset of substrate conversion indicated that the formation of the active catalyst system was slow. Mass spectral analysis of samples from the reaction mixture using TPTN over the course of the catalysed oxidation of alkenes with  $\text{H}_2\text{O}_2$ ,  $\text{Mn}^{\text{II}}$  and TPTN, indicated that TPTN undergoes conversion to ligand **3** in this period.<sup>32</sup>

### 3.2.2 Stability of ligands **2** and **3** in the presence of iron salts and under acid and basic conditions

The stability of TPEN and TPTN in the presence of iron and manganese salts under non-oxidative conditions is evidenced by the ability to prepare iron and manganese complexes from these ligands (*vide supra*).<sup>19,20,28,29</sup> However, for the ligands containing an aminated motif, the stability is expected to be lower. The stability of ligand **2** was determined by  $^1\text{H}$  NMR spectroscopy under both acidic and basic conditions in acetone and in the absence and presence of  $\text{H}_2\text{O}_2$ .

In the presence of excess trichloroacetic acid (4 equiv.) in acetone ligand **2** was found to convert to a mixture of species within 2 h both in the absence and presence of  $\text{H}_2\text{O}_2$  (Figure 4 and 5, respectively). After 24 h, however, where only trichloroacetic acid was added, the  $^1\text{H}$  NMR spectrum recovered to show only absorptions due to ligand **2**. In the presence of  $\text{H}_2\text{O}_2$  and trichloroacetic acid the absorptions of **2** reappeared partially after 24 h (Figure 5). This recovery of the original spectra with time is indicative of partial hydrolysis under strongly acidic conditions, which reverses as moisture from the air reduces the acidity of the solution.

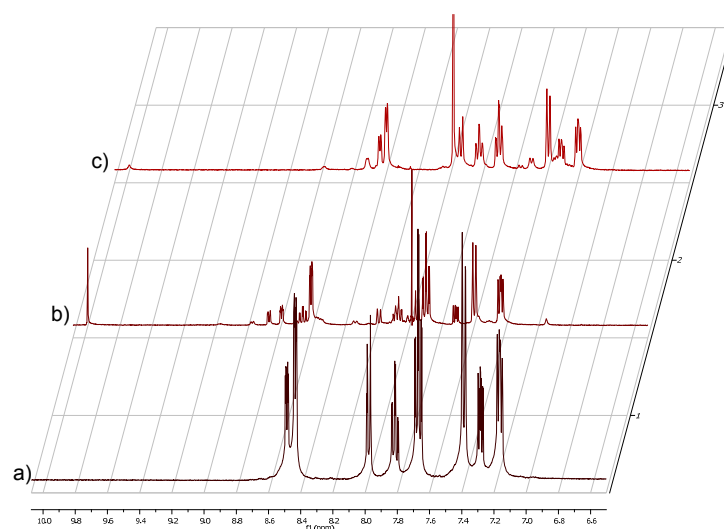


**Figure 4** Ligand **2** a) in acetone, b) in acetone 2 h after addition of trichloroacetic acid (4 equiv.), c) in acetone 24 h after addition of trichloroacetic acid (4 equiv.).

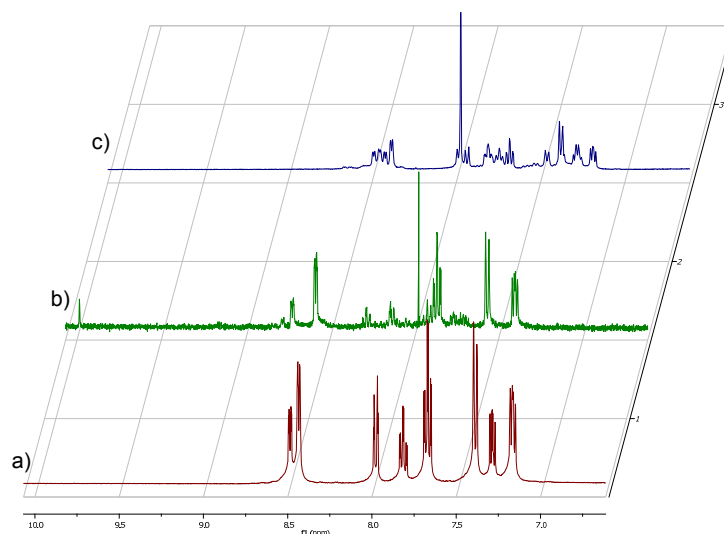


**Figure 5** Ligand **2** a) in acetone, b) in acetone 2 h after addition of trichloroacetic acid (4 equiv.) and H<sub>2</sub>O<sub>2</sub> (7 equiv.), c) in acetone 24 h after addition of trichloroacetic acid (4 equiv.) and H<sub>2</sub>O<sub>2</sub> (7 equiv.).

In the presence of NaOH (4 equiv.) and/or H<sub>2</sub>O<sub>2</sub> (7 equiv.) ligand **2** was found to be stable with no change in the <sup>1</sup>H NMR spectrum over 24 h (Figure 6). This indicates that under the conditions relevant to the catalysed reactions, *i.e.* in acetone/H<sub>2</sub>O with a base and H<sub>2</sub>O<sub>2</sub>, the amina based ligands are in fact stable to ring opening in the absence of metal ions.

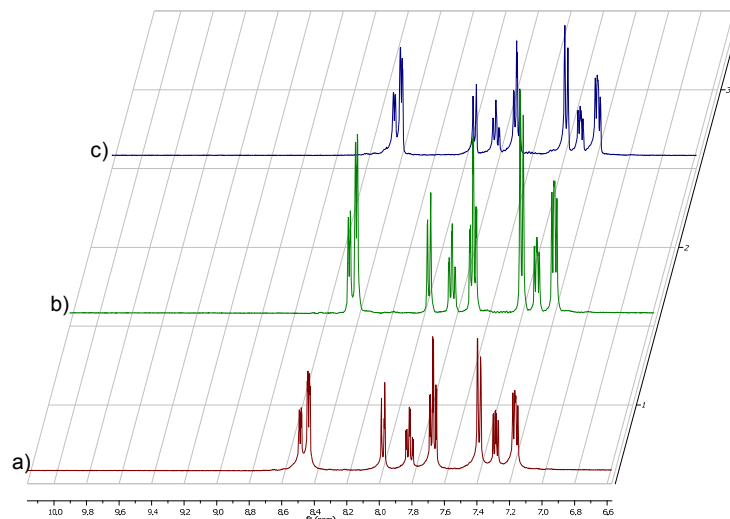


**Figure 6** Ligand **2** a) in acetone, b) in acetone 24 h after addition of NaOH (4 equiv.) c) in acetone 24 h after addition of NaOH (4 equiv.) and H<sub>2</sub>O<sub>2</sub> (7 equiv.).

An indication of the intrinsic instability of the aminal ligands in the presence of metal ions was obtained during attempts to isolate the corresponding Fe<sup>II</sup> complexes. Reaction of ligand **2** or **3** with one equivalent of Fe<sup>II</sup>(ClO<sub>4</sub>)<sub>2</sub> in methanol/acetonitrile lead over 30-60 min to the appearance of an intense purple color. Slow evaporation of solvent provided crystals of a complex obtained from **3** suitable for single crystal structure determination (see the experimental section). From X-ray crystallographic analysis together with elemental analysis it is apparent that the central aminal ring of ligand **3** is opened to release pyridine-2-carboxaldehyde (as a methoxy-hemiacetal) followed by coordination of the ligand fragments to Fe<sup>II</sup>. Attempts to isolate Mn<sup>II</sup> complexes of ligands **2** and **3** were unsuccessful to date, however it should be noted that similar ligands have been employed previously<sup>33</sup> with Mn<sup>II</sup> ions and in these cases the aminal ring was found to be stable.

The stability of TPEN and TPTN with iron<sup>34</sup> contrasts markedly with the instability of their aminal precursors (*e.g.* **2** and **3**). This makes the observation of essentially identical reactivity and selectivity with Mn/H<sub>2</sub>O<sub>2</sub> all the more remarkable. A structure activity study was therefore carried out to identify the key ligand components required to achieve full activity.

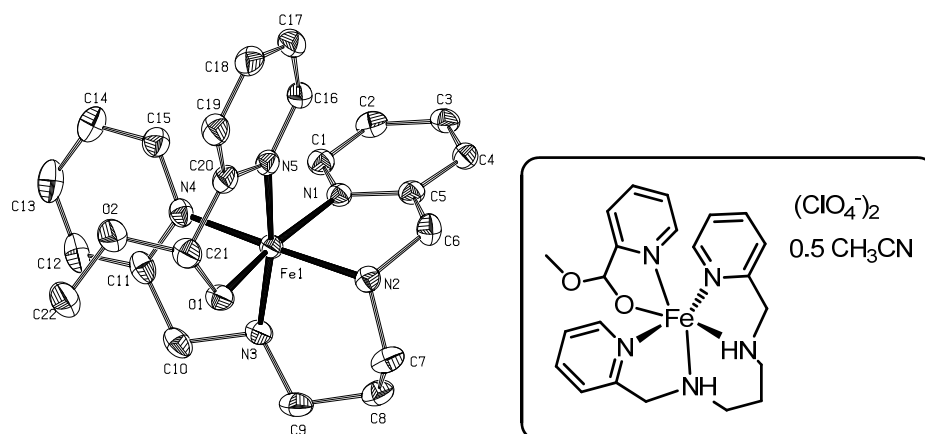


**Figure 7** Ortep representation of the iron complex isolated from the reaction of  $\text{Fe}^{\text{II}}(\text{ClO}_4)_2$  with ligand **3** in acetonitrile/methanol. Counter ions and solvent of crystallisation are omitted for clarity. CCDC 768839 (see details in the experimental section)

### 3.2.3 Catalytic activity of $\text{Mn}^{\text{II}}$ /ligand in relation to ligand structure

The dependence of the observed reactivity and the structure of the amination ligand was investigated using a series of ligands shown in Figure 3. In this series of ligands the pyridyl groups were systematically removed from the amination ring and replaced with other aromatic rings or else methyl groups. Furthermore the non-cyclic ligands **13-16** (Figure 3) were examined including ligands containing the 6-methyl-pyridyl motif.

The catalytic activity of the series of amination based ligands **2-12** in the oxidation of *cis*-cyclooctene was examined. Full conversion with ligands **2-7**, all of which contained at least one pyridin-2-yl moiety, was observed with the *cis*-diol:epoxide ratio being identical in all cases (data not shown). By contrast ligands **8-12**, which do not contain a pyridine-2-yl unit, showed no activity in the oxidation of *cis*-cyclooctene.

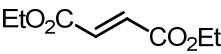
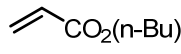
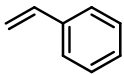
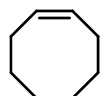
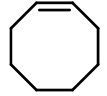
The relative selectivity observed for four substrates with ligands **2-8** was examined (Table 1). The substrates chosen were diethyl fumarate and *n*-butylacrylate, which are converted to the *cis*-diol product exclusively, styrene, which shows an approximately equal mixture of epoxide and *cis*-diol products and *cis*-cyclooctene, which provides the epoxide product primarily but with a minor amount of the *cis*-diol product also.

For ligand **8** no activity was observed for any of the substrates examined. By contrast for ligands **2**, **4** and **7** essential identical conversion and selectivity was observed for all substrates.

From Table 1 it is apparent that a minimum of one pyridine-2-yl group is required in the structure of the ligand in order to obtain substrate conversion, since for ligands **8-12**, which lack a pyridin-2-yl group in their structures, conversion is not observed (data not shown). These observations could be assigned to simply the denticity of the ligand, especially considering that in the presence of iron the amination ring is opened readily yielding ligands analogous to those shown in Figure 1. Furthermore, no significant effect of ligand structure on conversion or product distributions are observed between ligands **2**,

**4** and **7**. The instability of the aminor ring in the case of ligands **2**, **3** and **7**, could indicate that the loss of pyridine-2-carboxaldehyde is the cause of the activity seen. However, for ligands **4-6** the opening of the aminor ring does not lead immediately to free pyridin-2-carboxaldehyde, yet full activity is nevertheless observed for these ligands.

**Table 1** Conversions and product distributions using ligands **2**, **4**, **7** and **8**.

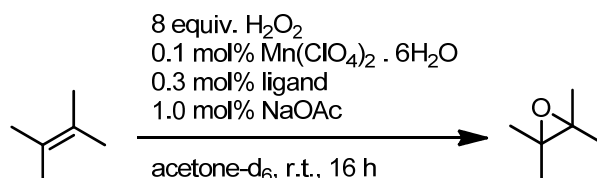
substrate	ligand	conversion (%) <sup>a</sup>	product distribution <sup>b</sup>
	<b>2</b>	full	<i>cis</i> -diol product only ( <i>d/l</i> -diethyl tartrate)
	<b>4</b>	full	
	<b>7</b>	full	
	<b>8</b>	0%	
	<b>2</b>	82%	<i>cis</i> -diol product only
	<b>4</b>	80%	
	<b>7</b>	75%	
	<b>8</b>	0%	
	<b>2</b>	25%	epoxide:diol 1 : 2
	<b>4</b>	20%	
	<b>7</b>	22%	
	<b>8</b>	0%	
	<b>2</b>	full	epoxide:diol 6 : 1
	<b>4</b>	full	
	<b>7</b>	95%	
	<b>8</b>	0%	
	<b>2</b>	full	yield of epoxide
	<b>13</b>		79% <sup>c</sup>
	<b>15</b>		48% <sup>c</sup>
	<b>16</b>		79% <sup>c</sup>
	<b>TPTN</b>		80% <sup>c</sup>
			58% <sup>c</sup>

<sup>a</sup> Reaction conditions: at 0 °C, substrate (1 M), Mn(ClO<sub>4</sub>)<sub>2</sub>·6H<sub>2</sub>O (0.1 mM), ligand (0.1 mM), NaOAc (1.0 mM) in acetone with 8 equiv. of H<sub>2</sub>O<sub>2</sub>. Conversion of substrate was determined by *in situ* Raman spectroscopy by monitoring the decrease of the alkene stretching band at *ca.* 1620 cm<sup>-1</sup> with 1,2-dichlorobenzene as internal standard and confirmed by <sup>1</sup>H NMR spectroscopy. <sup>b</sup> Product yield was determined by <sup>1</sup>H NMR spectroscopy. <sup>c</sup> Reaction conditions: at 0 °C, *cis*-cyclooctene (1 M), Mn(OAc)<sub>3</sub>·2H<sub>2</sub>O (0.1 mM), ligand (0.1 mM) in acetone with 9.6 equiv. of H<sub>2</sub>O<sub>2</sub>. Conversion of substrate and yield of epoxide product was determined by GC (diol not determined).

Notably, the activity observed for ligands such as **13-15** (Figure 3) indicates that opening of the amination ring and/or facile loss of pyridine-2-yl units from the ligand is not required to achieve full activity. What is certain, however, is that in the absence of a pyridin-2-yl unit, activity is not observed. For ligands **13-15**, which do not have the amination structural motif, essentially identical selectivity and activity was observed in the oxidation of *cis*-cyclooctene compared to ligand **2**.

### 3.2.4 Ligand stability under reaction conditions

The stability of the ligands TPTN, **2**, **3** and **4** under reaction conditions was determined by  $^1\text{H}$  NMR spectroscopic analysis of the reaction mixture after catalysed oxidation of 2,3-dimethyl-but-2-ene in acetone- $d_6$ . The  $^1\text{H}$  NMR spectrum of the diluted reaction mixture was recorded 16 h after addition of  $\text{H}_2\text{O}_2$  was complete (Figure 8).



**Scheme 2** Conditions employed for studying ligand decomposition during the oxidation of alkenes with  $\text{H}_2\text{O}_2$  in acetone- $d_6$ .

Due to the relatively low concentration of the ligand, the spectrum is dominated by the absorptions of the substrate, solvent and water. However, the absorptions corresponding to the aromatic protons of the ligand are well-resolved.<sup>35</sup> Figure 8 shows the  $^1\text{H}$  NMR spectrum of pyridine-2-carboxylic acid in acetone- $d_6$ , together with the spectrum of the reaction mixture (Scheme 2, see also the experimental section) after 16 h where the ligand employed is TPTN. The spectrum shows the ligand has decomposed to pyridine-2-carboxylic acid. For ligands **2**, **4** and **5** (Figure 9) essentially the same effect was observed with pyridine-2-carboxylic acid being detected (together with benzoic and thiophene carboxylic acids, respectively) as the principle aromatic component after oxidation reactions.

Confirmation that the degradation products of the ligands, *e.g.* **7**, were responsible for the catalytic activity observed, was obtained from the comparison of the oxidation of cyclooctene and diethylfumarate where 8 and 4 equiv., respectively, of  $\text{H}_2\text{O}_2$  were added in a single addition or batchwise (see the experimental section). For both cyclooctene and diethylfumarate, full conversion was observed overnight when all the  $\text{H}_2\text{O}_2$  was added at once. By contrast addition of half of the  $\text{H}_2\text{O}_2$  achieved only partial conversion (<20%) overnight. Addition of the remaining  $\text{H}_2\text{O}_2$  to these reactions resulted in full conversion.



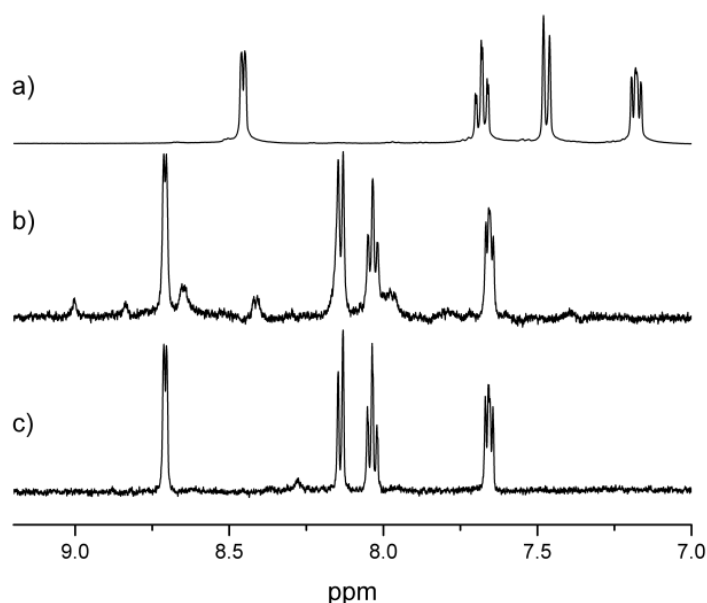


**Figure 8**  $^1\text{H}$  NMR (400 MHz) spectra of the reaction mixture (Scheme 2) with TPTN in acetone- $d_6$  a) before and b) 16 h after addition of  $\text{H}_2\text{O}_2$  and c) pyridine-2-carboxylic acid.

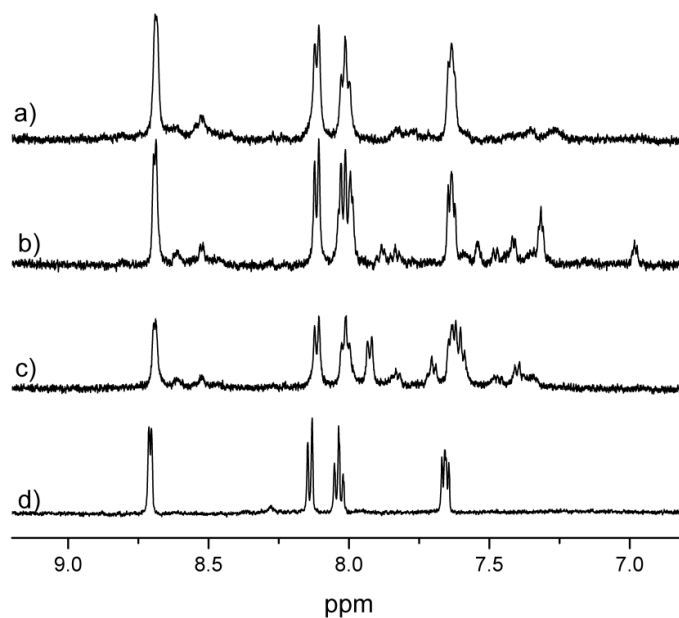


**Figure 9**  $^1\text{H}$  NMR (400 MHz) spectra of reaction mixtures after reaction where ligand is a) **2** b) **4** c) **5** and d) pyridine-2-carboxylic acid.

### 3.2.5 Oxidation catalysis with pyridine-2-carboxylic acid/ $\text{Mn}^{\text{II}}$

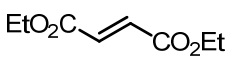
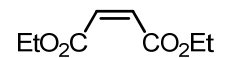
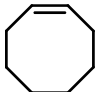
In chapter 4 a remarkably simple system capable of efficient *cis*-dihydroxylation of electron deficient alkenes and epoxidation of electron rich alkenes will be described.<sup>30</sup> This system comprises of pyridine-2-carboxylic acid, a base (*e.g.* NaOH, or NaOAc) and

Mn<sup>II</sup> source (typically at 0.1-0.3 mol%) in combination with acetone and H<sub>2</sub>O<sub>2</sub>. The discovery of this system was as a direct result of the mechanistic studies of the series of Mn/ligand catalysts (Figure 3) systems involving polypyridyl based ligands described in this chapter.

The observation of pyridine-2-carboxylic acid as the principle decomposition product of ligands **1**, **2**, **4**, **5** and TPTN indicates that it may either be a manifestation of catalyst deactivation only or that pyridine-2-carboxylic acid could in fact be responsible for the catalytic activity observed. The observation that a lag period is present after addition of H<sub>2</sub>O<sub>2</sub> to the, *e.g.* **2**/Mn catalysed reactions, during which extensive disproportionation of H<sub>2</sub>O<sub>2</sub> is observed, followed by a second phase in which H<sub>2</sub>O<sub>2</sub> is not disproportionated and oxidation of substrates proceeds provides a strong indication that a decomposition product of the ligands are responsible for catalysis.

The ability of pyridine-2-carboxylic acid together with Mn<sup>II</sup> to catalyse oxidation of alkenes was compared with that of ligand **2** (Table 2). For three substrates used for comparison identical results in terms of conversion and product formation using either the amination ligand or pyridine-2-carboxylic acid were observed (Scheme 1, Table 2). Furthermore, whereas 4-8 equiv. of H<sub>2</sub>O<sub>2</sub> are required to achieve full conversion with the pyridyl ligands, with pyridine-2-carboxylic acid the efficiency in oxidant is substantially higher with only 1.5-2 equiv. of H<sub>2</sub>O<sub>2</sub> required for full conversion. These data provide compelling evidence that under these reaction conditions, it is pyridine-2-carboxylic acid rather than the pyridine-2-yl ligands (including TPTN, ligands **2-7** *etc.*), which together with manganese ions, is responsible for the catalytic activity observed.

**Table 2** Conversions and product distributions using amination ligands **2** or pyridine-2-carboxylic acid (**1**).

substrate	ligand	conversion <sup>a</sup>	product distribution <sup>b</sup>
	<b>2</b>	full	<i>cis</i> -diol product
	<b>1</b>	full	( <i>d/l</i> -diethyl tartrate)
	<b>2</b>	20%	<i>cis</i> -diol product
	<b>1</b>	20%	( <i>meso</i> -diethyl tartrate)
	<b>2</b>	full	epoxide: <i>cis</i> -diol
	<b>1</b>	full	6 : 1

<sup>a</sup>Conditions: 0.1 mol% Mn(ClO<sub>4</sub>)<sub>2</sub>·6H<sub>2</sub>O, 0.1 mol% **2** or 0.3 mol% pyridine-2-carboxylic acid, 1.0 mol% NaOAc and 8 equiv. H<sub>2</sub>O<sub>2</sub> in acetone at 20 °C. Conversion of substrate was determined by Raman spectroscopy after 16 h. <sup>b</sup>Product yield and distribution was determined by <sup>1</sup>H NMR spectroscopy.

### 3.2.6 C-H activation and alcohol oxidation with pyridine-2-carboxylic acid/Mn<sup>II</sup>/NaOAc

The ability of the system pyridine-2-carboxylic acid/Mn<sup>II</sup>/NaOAc to induce in oxidative degradation of the pyridyl ligands investigated in the present study requires that the system can engage in activation of C-H bonds as well as in aryl alcohol and aldehyde oxidation. Although C-H activation<sup>36</sup> is not observed with alkene substrates, when substrates such as cyclooctane and tetraline are employed, good conversion (>70%) and good selectivity to the mono-ketone at (40-50%) is observed using both pyridine-2-carboxylic acid or ligands **2-7**. Furthermore, as for TPTN,<sup>29</sup> toluene and benzyl alcohol can be oxidised to benzaldehyde and eventually benzoic acid with pyridine-2-carboxylic acid/Mn<sup>II</sup>/NaOAc (see the experimental section).

## 3.3 Summary and conclusions

In this chapter the facile decomposition under mildly basic conditions of pyridine-2-yl ligands (**2-16**) in acetone with Mn/H<sub>2</sub>O<sub>2</sub> to yield pyridine-2-carboxylic acids was demonstrated. It is apparent that the pyridine-2-carboxylic acid formed by this ligand decomposition can fully account for the reactivity observed towards oxidation of alkenes, alcohols and for the C-H activation observed for ligands **2-7**, **14**, **15** and TPTN with Mn/H<sub>2</sub>O<sub>2</sub>.

It is important to note that the conditions employed determine the activity observed. For example, under acidic conditions these complexes show relatively little activity and especially those ligands that do not incorporate an aminated ring motif are stable towards decomposition. Furthermore, under mildly acidic conditions (1-20 mol% acetic acid w.r.t. substrate) the reactivity of the pyridine-carboxylic acid system is reduced considerably.<sup>30</sup>

For (chiral) ligand systems, similar to those under consideration in the present study, Stack and co-workers,<sup>37</sup> have reported under acidic conditions with peracetic acid and Costas and co-workers,<sup>25</sup> with acetic acid/H<sub>2</sub>O<sub>2</sub> that with Mn<sup>II</sup> activity is observed, which cannot be ascribed to the formation of pyridine-2-carboxylic acids.

Furthermore, it is important to stress that in acetonitrile or other non-ketone containing solvent systems, the system pyridine-2-carboxylic acid/Mn/NaOAc is essentially inactive (see Chapter 4). The only, and perhaps key, exception to this is that pyridine-2-carboxaldehyde is oxidised readily to pyridine-2-carboxylic acid in CH<sub>3</sub>CN in the presence of Mn and H<sub>2</sub>O<sub>2</sub>. Hence, in these solvent systems oxidative ligand degradation will lead to a suppression of activity, as indeed has been noted by Banse, Girerd and co-workers for TPEN.<sup>19</sup>

Notwithstanding this, it is clear that the methylene C-H's of pyridine-2-yl based ligands are susceptible to oxidation via C-H activation as certainly occurs for the ligands (**2-6**) examined here. In the case of the aminated based ligands the susceptibility to ring opening and hydrolysis with a Lewis acidic metal could be viewed as key to the *in situ* formation of pyridine-2-carboxylic acid. In the case of ligands **4**, **15** and TPTN, however, activity comparable to that observed for an equivalent amount of pyridine-2-carboxylic

acid was observed (*vide supra*) and hence the opening of the amination ring is not the only factor.<sup>38</sup>

In conclusion, for a class of ligands (**2-16** and TPTN) that feature *ortho*-pyridyl functionalities, when combined with manganese salts, an active oxidation catalyst is formed in acetone using H<sub>2</sub>O<sub>2</sub> that actually due to the formation of pyridine-2-carboxylic acid *in situ*, via decomposition of the ligand under the oxidative conditions, which is responsible for the observed catalytic activity. The degradation of the ligand to pyridine-2-carboxylic acid by <sup>1</sup>H NMR spectroscopy was demonstrated, in addition replacement of ligand **2** by equivalent amounts of pyridine-2-carboxylic acid in the oxidation reactions results in identical activity and selectivity for a broad range of substrates. The only notable difference is that with pyridine-2-carboxylic acid much less H<sub>2</sub>O<sub>2</sub> is required to achieve the same levels of substrate conversion.

Ligand degradation is typically considered as a cause of catalyst deactivation. The observation in this case is that *in situ* ligand degradation to relatively simple compounds results in a highly active oxidation system as a whole. This demonstrates the relevance of mechanistic understanding of catalysed reactions, not only in the sense of elucidating catalytic cycles, but crucially in understanding the catalytic system. For example, activity observed with the ligand TPTN in acetonitrile with peracetic acid is due to species distinct to those involved in acetone with H<sub>2</sub>O<sub>2</sub>. This includes the interplay of all of its components, as a whole through speciation analysis. This is especially the case when understanding the effect of variation in ligand structure on reactivity and selectivity is examined. Furthermore, it is an important consideration when understanding how changes in solvent and additives tune the reactivity of a particular system.

### 3.4 Experimental section

All reagents are of commercial grade and used as received unless stated otherwise. Hydrogen peroxide was used as received as a 50 wt. % solution in water; note that the grade of H<sub>2</sub>O<sub>2</sub> employed can affect the reaction negatively when sequestrants are present as stabilizers. Diethyl-2-methylfumarate was prepared by literature procedures.<sup>39</sup> NMR spectra were recorded at <sup>1</sup>H NMR (400.0 MHz) and <sup>13</sup>C NMR (100.59 MHz). Chemical shifts are denoted relative to the residual solvent absorption (<sup>1</sup>H: CDCl<sub>3</sub> 7.26 ppm; <sup>13</sup>C: CDCl<sub>3</sub> 77 ppm, acetone-*d*<sub>6</sub> 2.05 ppm).<sup>40</sup> Raman spectra were recorded using a fibre optic equipped dispersive Raman spectrometer (785 nm, Perkin Elmer Raman Flex). Temperature was controlled using a cuvette holder equipped with a custom made fibre optic probe holder (Quantum Northwest). 1,2-Dichlorobenzene was employed as internal standard for Raman spectroscopy. GC analyses were performed on a Hewlett Packard 6890 Gas Chromatograph equipped with an autosampler, using a HP-1 dimethyl polysiloxane column or a HP-5 5% phenylmethylsiloxane column. Calibration was performed using authentic samples of the alkenes and epoxides. Conversions, yields and turnover numbers are the average of 2-4 experiments (uncertainty ± 10%) and were determined using bromobenzene or 1,2-dichlorobenzene as internal standard. Data for

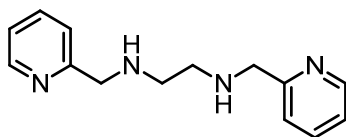
quantification of *cis*-diol products is omitted due to unreliability in their quantification by the GC method used.

**Caution.** The drying or concentration of acetone solutions that potentially contain hydrogen peroxide should be avoided. Prior to drying or concentrating, the presence of  $\text{H}_2\text{O}_2$  should be tested for using peroxide test strips followed by neutralisation on solid  $\text{NaHSO}_3$  or another suitable reducing agent. When working with  $\text{H}_2\text{O}_2$ , especially in acetone, suitable protective safeguards should be in place at all times due to the risk of explosion.<sup>41</sup>

**Caution.** Perchlorate salts are potentially explosive in combination with organic solids and solvents. In the present study  $\text{Mn}(\text{OAc})_2$ ,  $\text{Mn}(\text{OAc})_3$  or  $\text{MnSO}_4$  were found to give essentially identical reactivity and should be used for reactions above 2 gram scale.

### 3.4.1 Ligand syntheses

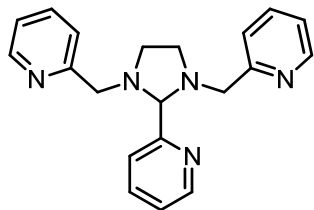
#### *N,N'*-Bis(pyridin-2-ylmethyl)ethane-1,2-diamine (**13**)



Following the procedure described by Mialane *et al.*,<sup>31</sup> to a solution of 1,2-ethanediamine (5.0 g, 80 mmol) in MeOH (80 ml) was added pyridine-2-carboxaldehyde (17.1 g, 160 mmol) and the mixture was heated at reflux overnight.

After cooling to 0 °C,  $\text{NaBH}_4$  (7.6 g, 200 mmol) was added in small portions. After stirring for 3 h at 100 °C, the solvent was removed under reduced pressure. The oily residue was redissolved in water (100 ml) and the aqueous mixture was extracted with  $\text{CH}_2\text{Cl}_2$  (3 × 50 ml). The combined organic layers were dried over  $\text{MgSO}_4$  and concentrated *in vacuo* providing the crude product as a yellow oil (14.5 g, 60 mmol, 75%), which was used in the subsequent step without further purification.  $^1\text{H}$  NMR (400 MHz,  $\text{CDCl}_3$ )  $\delta$  8.49 (d,  $J$  = 4.9 Hz, 2H), 7.58 (td,  $J$  = 7.7 Hz, 1.6 Hz, 2H), 7.27 (d,  $J$  = 7.8 Hz, 2H), 7.09 (t,  $J$  = 6.4 Hz, 2H), 3.87 (s, 4H), 2.77 (s, 4H), 2.31 (b, 2H);  $^{13}\text{C}$  NMR (100 MHz,  $\text{CDCl}_3$ )  $\delta$  160.0, 149.3, 136.5, 122.3, 122.0, 55.3 49.2. HRMS (ESI+,  $m/z$ ) calc. for  $\text{C}_{14}\text{H}_{19}\text{N}_4$   $[\text{M}+\text{H}]^+$  243.1610, found 243.1599.

#### 2,2'-(2-(Pyridin-2-yl)imidazolidine-1,3-diyl)bis(methylene)dipyridine (**2**)

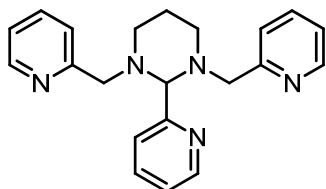


Following the procedure described by Mialane *et al.*,<sup>31</sup> a solution of **13** (3.8 g, 15.9 mmol) and pyridine-2-carboxaldehyde (1.7 g, 15.9 mmol) in  $\text{Et}_2\text{O}$  (15 ml) was stirred at room temperature with  $\text{CaCl}_2$  protection overnight, during which a white precipitate formed. After evaporation of the solvent, the product was purified by column

chromatography ( $\text{SiO}_2$ ,  $\text{CH}_2\text{Cl}_2$ /triethylamine, 8/1, v/v,  $R_f$  = 0.72) and subsequent recrystallisation from  $\text{Et}_2\text{O}$ , providing an off-white crystalline solid (4.5 g, 13.8 mmol, 86%). m.p. 120–121 °C.  $^1\text{H}$  NMR (400 MHz,  $\text{CDCl}_3$ )  $\delta$  8.46 (d,  $J$  = 4.9 Hz, 1H), 8.42 (d,  $J$  = 4.8 Hz, 2H), 7.85 (dd,  $J$  = 7.9 Hz, 1.0 Hz, 1H), 7.66 (td,  $J$  = 7.7 Hz, 1.4 Hz, 1H), 7.52 (td,  $J$  = 7.7 Hz, 1.6 Hz, 2H), 7.30 (d,  $J$  = 7.8 Hz, 2H), 7.18 – 7.10 (m, 1H), 7.08 – 6.97 (m, 2H), 4.24 (s, 1H), 3.91 (d,  $J$  = 14.2 Hz, 2H), 3.62 (d,  $J$  = 14.2 Hz, 2H), 3.37 – 3.20 (m,

2H), 2.78 – 2.62 (m, 2H);  $^{13}\text{C}$  NMR (100 MHz,  $\text{CDCl}_3$ )  $\delta$  160.8, 159.0, 148.8, 148.3, 136.6, 136.2, 123.1, 123.0, 122.7, 121.7, 89.1, 58.8, 51.3. HRMS (ESI+,  $m/z$ ) calc. for  $\text{C}_{20}\text{H}_{22}\text{N}_5$   $[\text{M}+\text{H}]^+$  332.1870, found 332.1867. Elemental analysis (calc. for  $\text{C}_{20}\text{H}_{21}\text{N}_5$ ) C 72.51% (72.48%), H 6.45% (6.39%), N 21.17% (21.13%).

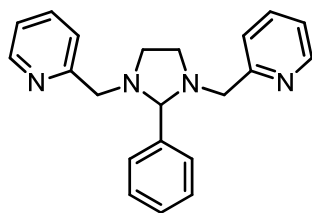
### 2-(Pyridin-2-yl)-1,3-bis(pyridin-2-ylmethyl)hexahydropyrimidine (3)



Pyridine-2-carboxaldehyde (8.7 g, 81.0 mmol) was added to a solution of 1,3-propanediamine (3.0 g, 40.5 mmol) in MeOH (15 ml) and the mixture was heated at reflux for 4 h. After cooling to 0 °C,  $\text{NaBH}_4$  (4.3 g, 113.4 mmol) was added in small portions. The mixture was heated at reflux for 3 h, after which the solvent was removed under reduced

pressure. The oily residue was redissolved in water (100 ml) and the aqueous mixture was extracted with  $\text{CH}_2\text{Cl}_2$  ( $3 \times 50$  ml). The combined organic layers were dried over  $\text{MgSO}_4$  and concentrated *in vacuo* providing the crude diamine product **14** as a yellow oil, which was used in the subsequent step without further purification. A solution of the **14** and pyridine-2-carboxaldehyde (4.3 g, 40.5 mmol) in  $\text{Et}_2\text{O}$  (30 ml) was stirred at room temperature with  $\text{CaCl}_2$  protection overnight, during which a white precipitate formed. After evaporation of the solvent, the product was purified by column chromatography ( $\text{SiO}_2$ ,  $\text{CH}_2\text{Cl}_2$ /triethylamine, 8/1, v/v,  $R_f$  = 0.65) and subsequent recrystallisation from  $\text{Et}_2\text{O}$ , providing a white crystalline solid (1.7 g, 4.9 mmol, 12%). m.p. 129-130 °C.  $^1\text{H}$  NMR (400 MHz,  $\text{CDCl}_3$ )  $\delta$  8.48 (dd,  $J$  = 4.9 Hz, 0.8 Hz, 1H), 8.37 (dd,  $J$  = 4.9 Hz, 0.8 Hz, 2H), 7.86 (d,  $J$  = 7.9 Hz, 1H), 7.61 (td,  $J$  = 7.7 Hz, 1.7 Hz, 1H), 7.52 (td,  $J$  = 7.7 Hz, 1.8 Hz, 2H), 7.36 (d,  $J$  = 7.8 Hz, 2H), 7.10 (ddd,  $J$  = 7.4 Hz, 4.9 Hz, 1.2 Hz, 1H), 7.01 (dd,  $J$  = 6.8 Hz, 5.4 Hz, 2H), 4.02 (s, 1H), 3.54 (d,  $J$  = 14.6 Hz, 2H), 3.29 (d,  $J$  = 14.6 Hz, 2H), 2.99 (dt,  $J$  = 11.7 Hz, 3.6 Hz, 2H), 2.26 (td,  $J$  = 11.7 Hz, 2.7 Hz, 2H), 2.01 – 1.77 (m, 1H), 1.62 – 1.38 (m, 1H);  $^{13}\text{C}$  NMR (100 MHz,  $\text{CDCl}_3$ )  $\delta$  161.8, 159.8 (2 $\times$ ), 148.9 (2 $\times$ ), 148.4, 137.0, 136.4 (2 $\times$ ), 123.7, 123.4, 122.7 (2 $\times$ ), 121.8 (2 $\times$ ), 88.5, 60.0 (2 $\times$ ), 51.9 (2 $\times$ ), 24.6. HRMS (ESI+,  $m/z$ ) calc. for  $\text{C}_{21}\text{H}_{24}\text{N}_5$   $[\text{M}+\text{H}]^+$  346.2026, found 346.2026. Elemental analysis (calc. for  $\text{C}_{21}\text{H}_{23}\text{N}_5$ ) C 72.95% (73.02%), H 6.73% (6.71%), N 20.22% (20.27%).

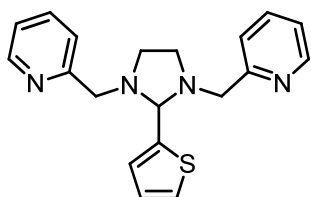
### 2,2'-(2-Phenylimidazolidine-1,3-diyl)bis(methylene)dipyridine (4)



Following the procedure described by Mialane *et al.*,<sup>31</sup> a solution of **13** (9.0 g, 36.9 mmol) and benzaldehyde (3.9 g, 36.9 mmol) in  $\text{Et}_2\text{O}$  (30 ml) was stirred at room temperature with  $\text{CaCl}_2$  protection overnight, during which a white precipitate formed. After evaporation of the solvent, the product was purified by column chromatography ( $\text{SiO}_2$ ,  $\text{EtOAc}$ /heptane/triethylamine, 10/4/1, v/v,  $R_f$  = 0.47) and subsequent recrystallisation from  $\text{Et}_2\text{O}$ , providing a white crystalline solid (6.6 g, 20.0 mmol, 54%). m.p. 151-152 °C.  $^1\text{H}$  NMR (400 MHz,  $\text{CDCl}_3$ )  $\delta$  8.41 (dd,  $J$  = 4.9 Hz, 0.9 Hz, 2H), 7.64 – 7.42 (m, 4H),

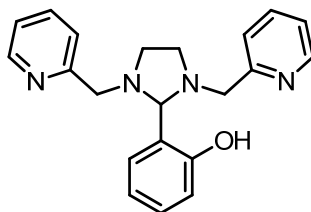
7.39 – 7.23 (m, 5H), 7.04 (t,  $J = 6.3$  Hz, 2H), 3.97 (s, 1H), 3.86 (d,  $J = 14.1$  Hz, 2H), 3.47 (d,  $J = 14.1$  Hz, 2H), 3.39 – 3.14 (m, 2H), 2.73 – 2.50 (m, 2H);  $^{13}\text{C}$  NMR (100 MHz,  $\text{CDCl}_3$ )  $\delta$  159.6 (2 $\times$ ), 148.9 (2 $\times$ ), 140.1, 136.4 (2 $\times$ ), 129.6 (2 $\times$ ), 128.8, 128.4 (2 $\times$ ), 123.0 (2 $\times$ ), 121.9 (2 $\times$ ), 89.1, 58.9 (2 $\times$ ), 51.3 (2 $\times$ ). HRMS (ESI+,  $m/z$ ) calc. for  $\text{C}_{21}\text{H}_{23}\text{N}_4$   $[\text{M}+\text{H}]^+$  331.1917, found 331.1917. Elemental analysis (calc. for  $\text{C}_{21}\text{H}_{22}\text{N}_4$ ) C 76.29% (76.33%), H 6.75% (6.71%), N 16.94% (16.96%).

### 2,2'-(2-(Thiophen-2-yl)imidazolidine-1,3-diyl)bis(methylene)dipyridine (5)



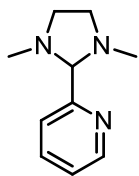
Following the procedure described by Mialane *et al.*,<sup>31</sup> a solution of **13** (1.2 g, 5.0 mmol) and thiophene-2-carbaldehyde (0.56 g, 5.0 mmol) in  $\text{Et}_2\text{O}$  (20 ml) was stirred at room temperature with  $\text{CaCl}_2$  protection overnight, during which a light brown precipitate formed. After evaporation of the solvent, the product was purified by recrystallisation from acetone, providing an off-white crystalline solid (0.5 g, 1.5 mmol, 30%). m.p. 162-163 °C.  $^1\text{H}$  NMR (400 MHz,  $\text{CDCl}_3$ )  $\delta$  8.44 (d,  $J = 4.9$  Hz, 2H), 7.58 (t,  $J = 7.7$  Hz, 2H), 7.43 (d,  $J = 7.9$  Hz, 2H), 7.31 (d,  $J = 5.0$  Hz, 1H), 7.05 – 7.12 (m, 3H), 6.89 (t,  $J = 5.0$  Hz, 1H), 4.40 (s, 1H), 4.01 (d,  $J = 14.0$  Hz, 2H), 3.53 (d,  $J = 14.0$  Hz, 2H), 3.29 – 3.18 (m, 2H), 2.71 – 2.59 (m, 2H);  $^{13}\text{C}$  NMR (100 MHz,  $\text{CDCl}_3$ )  $\delta$  159.4 (2 $\times$ ), 148.9 (2 $\times$ ), 145.8, 136.6 (2 $\times$ ), 128.2, 126.9, 126.1, 123.1 (2 $\times$ ), 122.1 (2 $\times$ ), 109.9, 83.7, 58.8 (2 $\times$ ), 50.9 (2 $\times$ ). HRMS (ESI+,  $m/z$ ) calc. for  $\text{C}_{19}\text{H}_{21}\text{N}_4\text{S}$   $[\text{M}+\text{H}]^+$  337.1487, found 337.1475. Elemental analysis (calc. for  $\text{C}_{19}\text{H}_{20}\text{N}_4\text{S}$ ) C 67.64% (67.83%), H 5.99% (5.99%), N 16.64% (16.65%).

### 2-(1,3-Bis(pyridin-2-ylmethyl)imidazolidin-2-yl)phenol (6)



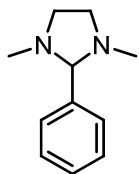
Following the procedure described by Mialane *et al.*,<sup>31</sup> a solution of **13** (1.1 g, 4.5 mmol) and 2-hydroxybenzaldehyde (0.55 g, 4.5 mmol) in  $\text{Et}_2\text{O}$  (30 ml) was stirred at room temperature with  $\text{CaCl}_2$  protection overnight, during which a white precipitate formed. After evaporation of the solvent, the product was purified by column chromatography ( $\text{SiO}_2$ ,  $\text{CH}_2\text{Cl}_2$ /triethylamine, 8/1, v/v,  $R_f = 0.85$ ) and subsequent recrystallisation from  $\text{Et}_2\text{O}$ , providing a white crystalline solid (0.49 g, 1.4 mmol, 31%). m.p. 119-120 °C.  $^1\text{H}$  NMR (400 MHz,  $\text{CDCl}_3$ )  $\delta$  10.96 (s, 1H), 8.45 (d,  $J = 4.9$  Hz, 2H), 7.57 (td,  $J = 7.6$  Hz, 1.5 Hz, 2H), 7.31 (d,  $J = 7.8$  Hz, 2H), 7.20 (ddd,  $J = 10.1$  Hz, 8.5 Hz, 6.3 Hz, 1H), 7.16 – 7.04 (m, 3H), 6.87 (d,  $J = 8.1$  Hz, 1H), 6.76 (t,  $J = 7.4$  Hz, 1H), 4.12 (s, 1H), 4.02 (d,  $J = 13.7$  Hz, 2H), 3.54 (d,  $J = 13.7$  Hz, 2H), 3.29 – 3.04 (m, 2H), 2.77 – 2.50 (m, 2H);  $^{13}\text{C}$  NMR (100 MHz,  $\text{CDCl}_3$ )  $\delta$  158.4, 158.3 (2 $\times$ ), 149.0 (2 $\times$ ), 136.8 (2 $\times$ ), 131.5, 130.4, 123.2 (2 $\times$ ), 122.3 (2 $\times$ ), 120.9, 118.9, 117.0, 88.8, 58.4 (2 $\times$ ), 50.1 (2 $\times$ ). HRMS (ESI+,  $m/z$ ) calc. for  $\text{C}_{21}\text{H}_{23}\text{N}_4\text{O}$   $[\text{M}+\text{H}]^+$  347.1872, found 347.1859. Elemental analysis (calc. for  $\text{C}_{21}\text{H}_{22}\text{N}_4\text{O}$ ) C 72.52% (72.81%), H 6.45% (6.40%), N 16.03% (16.17%).

### 2-(1,3-Dimethylimidazolidin-2-yl)pyridine (7)



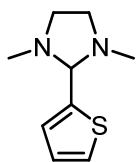
A solution of *N,N*-dimethylethane-1,2-diamine (1.04 g, 10.0 mmol) and pyridine-2-carboxaldehyde (1.07 g, 10.0 mmol) in Et<sub>2</sub>O (20 ml) was stirred at room temperature with CaCl<sub>2</sub> protection overnight. The solvent was removed under reduced pressure, after which purification was performed by column chromatography (SiO<sub>2</sub>, EtOAc/heptane/triethylamine, 10/4/1, v/v, *R<sub>f</sub>* = 0.53) and subsequent vacuum distillation, providing a slightly yellow oil (0.82 g, 4.6 mmol, 46%). <sup>1</sup>H NMR (400 MHz, CDCl<sub>3</sub>) δ 8.48 (dd, *J* = 4.9 Hz, 1.0 Hz, 1H), 7.82 – 7.49 (m, 2H), 7.25 – 7.05 (m, 1H), 3.46 (s, 1H), 3.39 – 3.25 (m, 2H), 2.65 – 2.43 (m, 2H), 2.19 (s, 9H); <sup>13</sup>C NMR (100 MHz, CDCl<sub>3</sub>) δ 160.7, 148.6, 137.0, 123.4, 122.6, 92.8, 53.8 (2×), 39.9 (2×). HRMS (ESI+, *m/z*) calc. for C<sub>10</sub>H<sub>16</sub>N<sub>3</sub> [M+H]<sup>+</sup> 178.1339, found 178.1338.

### 1,3-Dimethyl-2-phenylimidazolidine (8)



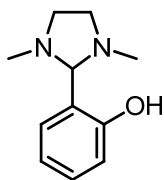
A solution of *N,N*-dimethylethane-1,2-diamine (1.04 g, 10.0 mmol) and pyridine-2-carboxaldehyde (1.07 g, 10.0 mmol) in Et<sub>2</sub>O (20 ml) was stirred at room temperature with CaCl<sub>2</sub> protection overnight. The solvent was removed under reduced pressure, after which purification was performed by column chromatography (SiO<sub>2</sub>, EtOAc/heptane/triethylamine, 10/4/1, v/v, *R<sub>f</sub>* = 0.53) and subsequent vacuum distillation, providing a slightly yellow oil (0.82 g, 4.6 mmol, 46%). <sup>1</sup>H NMR (400 MHz, CDCl<sub>3</sub>) δ 7.44 (d, *J* = 7.5 Hz, 2H), 7.39 – 7.22 (m, 3H), 3.46 – 3.32 (m, 2H), 3.25 (s, 1H), 2.61 – 2.48 (m, 2H), 2.17 (s, 6H); <sup>13</sup>C NMR (100 MHz, CDCl<sub>3</sub>) δ 139.9, 128.9 (2×), 128.6, 128.3 (2×), 92.5, 53.4 (2×), 39.6 (2×). HRMS (ESI+, *m/z*) calc. for C<sub>11</sub>H<sub>17</sub>N<sub>2</sub> [M+H]<sup>+</sup> 177.1392, found 177.1386. Elemental analysis (calc. for C<sub>11</sub>H<sub>16</sub>N<sub>2</sub>) C 74.47% (74.96%), H 9.22% (9.15%), N 15.92% (15.89%).

### 1,3-Dimethyl-2-(thiophen-2-yl)imidazolidine (9)

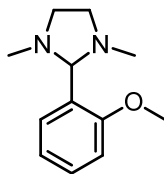


A solution of *N,N*-dimethylethane-1,2-diamine (0.44 g, 5.0 mmol) and thiophene-2-carbaldehyde (0.56 g, 5.0 mmol) in Et<sub>2</sub>O (20 ml) was stirred at room temperature with CaCl<sub>2</sub> protection overnight. The solvent was removed under reduced pressure, after which purification was performed by column chromatography (SiO<sub>2</sub>, pentane/EtOAc/triethylamine, 4/1/0.1, v/v, *R<sub>f</sub>* = 0.43) and subsequent vacuum distillation, providing a colourless oil (0.47 g, 2.6 mmol, 52%). <sup>1</sup>H NMR (400 MHz, CDCl<sub>3</sub>) δ 7.29 (d, *J* = 5.0 Hz, 1H), 7.03 (d, *J* = 3.3 Hz, 1H), 6.94 – 6.84 (m, 1H), 3.61 (s, 1H), 3.40 – 3.26 (m, 2H), 2.64 – 2.42 (m, 2H), 2.23 (s, 6H); <sup>13</sup>C NMR (100 MHz, CDCl<sub>3</sub>) δ 145.3, 127.0, 126.4, 126.0, 87.3, 53.2 (2×), 39.7 (2×). HRMS (ESI+, *m/z*) calc. for C<sub>9</sub>H<sub>14</sub>N<sub>2</sub>SNa [M+Na]<sup>+</sup> 205.0775, found 205.0767. Elemental analysis (calc. for C<sub>9</sub>H<sub>14</sub>N<sub>2</sub>S) C 58.86% (59.30%), H 7.71% (7.74%), N 15.09% (15.37%).

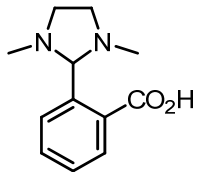


**2-(1,3-Dimethylimidazolidin-2-yl)phenol (10)**

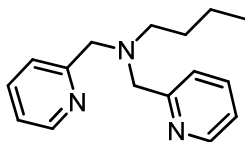
A solution of *N,N*-dimethylethane-1,2-diamine (1.97 g, 19.0 mmol) and 2-hydroxybenzaldehyde (2.32 g, 19.0 mmol) in Et<sub>2</sub>O (20 ml) was stirred at room temperature with CaCl<sub>2</sub> protection overnight. The solvent was removed under reduced pressure, after which purification was performed by column chromatography (SiO<sub>2</sub>, pentane/EtOAc/triethylamine, 4/1/1, v/v, *R<sub>f</sub>* = 0.87) and subsequent vacuum distillation, providing a colourless oil (1.98 g, 10.3 mmol, 54%). <sup>1</sup>H NMR (400 MHz, CDCl<sub>3</sub>) δ 11.46 (b, 1H), 7.18 (ddd, *J* = 8.1 Hz, 7.4 Hz, 1.7 Hz, 1H), 6.93 (dd, *J* = 7.4 Hz, 1.6 Hz, 1H), 6.80 (d, *J* = 8.1 Hz, 1H), 6.74 (td, *J* = 7.4 Hz, 1.2 Hz, 1H), 3.43 – 3.26 (m, 2H), 2.58 – 2.43 (m, 2H), 2.24 (s, 6H); <sup>13</sup>C NMR (100 MHz, CDCl<sub>3</sub>) δ 158.2, 130.2, 129.3, 120.4, 118.2, 116.7, 91.8, 52.1 (2×), 39.0 (2×). HRMS (ESI+, *m/z*) calc. for C<sub>11</sub>H<sub>17</sub>N<sub>2</sub>O [M+H]<sup>+</sup> 193.1341, found 193.1333. Elemental analysis (calc. for C<sub>11</sub>H<sub>16</sub>N<sub>2</sub>O) C 68.85% (68.72%), H 8.46% (8.39%), N 14.51% (14.57%).

**2-(2-Methoxyphenyl)-1,3-dimethylimidazolidine (11)**

A solution of *N,N*-dimethylethane-1,2-diamine (1.97 g, 19.0 mmol) and 2-methoxybenzaldehyde (2.58 g, 19.0 mmol) in Et<sub>2</sub>O (20 ml) was stirred at room temperature with CaCl<sub>2</sub> protection overnight. The solvent was removed under reduced pressure, after which purification was performed by vacuum distillation, providing a colourless oil which solidified to a white solid upon cooling to room temperature (1.36 g, 6.6 mmol, 35%). <sup>1</sup>H NMR (400 MHz, CDCl<sub>3</sub>) δ 7.65 (dd, *J* = 7.6 Hz, 1.6 Hz, 1H), 7.24 (t, *J* = 7.8 Hz, 1H), 6.98 (t, *J* = 7.5 Hz, 1H), 6.86 (d, *J* = 8.2 Hz, 1H), 4.04 (s, 1H), 3.79 (s, 3H), 3.39 – 3.21 (m, 2H), 2.66 – 2.48 (m, 2H), 2.18 (s, 6H); <sup>13</sup>C NMR (100 MHz, CDCl<sub>3</sub>) δ 159.0, 129.4, 129.0, 127.7, 121.2, 110.5, 82.9, 55.6, 53.7 (2×), 39.8 (2×). HRMS (ESI+, *m/z*) calc. for C<sub>12</sub>H<sub>19</sub>N<sub>2</sub>O [M+H]<sup>+</sup> 207.1497, found 207.1485. Elemental analysis (calc. for C<sub>12</sub>H<sub>18</sub>N<sub>2</sub>O) C 69.80% (69.87%), H 8.79% (8.80%), N 13.43% (13.58%).

**2-(1,3-Dimethylimidazolidin-2-yl)-5-methylbenzoic acid (12)**

A solution of *N,N*-dimethylethane-1,2-diamine (1.04 g, 10.0 mmol) and 2-formylbenzoic acid (1.50 g, 10.0 mmol) in MeOH (20 ml) was stirred at room temperature with CaCl<sub>2</sub> protection overnight. The solvent was removed under reduced pressure, after which purification was performed by recrystallisation from Et<sub>2</sub>O, providing a white powder (100 mg, 0.45 mmol, 5%). <sup>1</sup>H NMR (400 MHz, CDCl<sub>3</sub>) δ 7.94 (d, *J* = 7.4 Hz, 1H), 7.41 – 7.28 (m, 2H), 7.24 (b, 1H), 3.70 (b, 1H), 3.37 (b, 2H), 2.72 (b, 2H), 2.17 (s, 3H), 2.16 (s, 3H); <sup>13</sup>C NMR (100 MHz, CDCl<sub>3</sub>) δ 172.1, 137.60, 132.3, 132.2, 131.1, 129.9, 129.8, 90.1, 51.7 (2×), 37.9 (2×). HRMS (ESI+, *m/z*) calc. for C<sub>12</sub>H<sub>17</sub>N<sub>2</sub>O<sub>2</sub> [M+H]<sup>+</sup> 221.1290, found 221.1280. Elemental analysis (calc. for C<sub>11</sub>H<sub>16</sub>N<sub>2</sub>O) C 65.17% (65.14%), H 7.37% (7.74%), N 12.61% (12.66%).

***N,N*-Bis((pyridin-2-yl)methyl)butan-1-amine (15)**

*N*-((pyridin-2-yl)methyl)butan-1-amine (3 g, 18 mmol) was added to a solution of pyridine-2-carboxaldehyde (2.1 g, 20 mmol) in methanol. A  $\text{CaCl}_2$  tube was connected to the reaction flask and the mixture stirred for 16 h at room temperature. 2 equiv.  $\text{NaB}(\text{OAc})_3\text{H}$  (1.0 g, 26.5 mmol) was added in small portions to the mixture. After stirring for an additional 2 h at room temperature, the mixture was acidified to pH 1-2 with 4 M  $\text{HCl}$  (aq.) and stirred 1 h followed by addition of aqueous ammonia (15%) to pH 14. The mixture was extracted with  $\text{CH}_2\text{Cl}_2$  (3 x 50 ml). The combined organic layers were dried over  $\text{Na}_2\text{SO}_4$  and the solvent evaporated *in vacuo*. The product was obtained as a dark brown yellow oil which was purified by column chromatography ( $\text{SiO}_2$ ,  $\text{EtOAc}$ /Hexane/triethylamine, 10/4/1) to provide **15** (3.8 g, 15 mmol, 83%).  $^1\text{H}$  NMR (300 MHz)  $\delta$  0.89 (t,  $J$  = 7.33 Hz, 3H), 1.31 (m, 2H), 1.48 (m, 2H), 2.63 (t,  $J$  = 6.95 Hz, 2H), 3.88 (s, 4H), 7.13 (t,  $J$  = 5.12 Hz, 2H), 7.28 (d,  $J$  = 7.69 Hz, 2H), 7.61 (m, 2H), 8.53 (d,  $J$  = 4.76 Hz, 2H);  $^{13}\text{C}$  NMR (75 MHz,  $\text{CDCl}_3$ )  $\delta$  11.5, 17.9, 29.7, 46.8, 52.7, 119.4, 119.8, 133.9, 146.7, 157.3. HRMS ( $m/z$ ) calc. for  $\text{C}_{16}\text{H}_{21}\text{N}_3$  255.174, found 255.174.

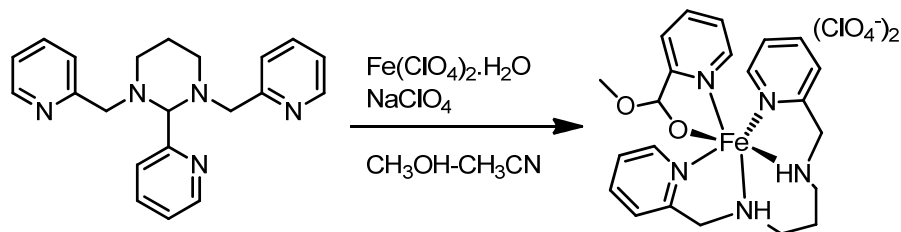
**3.4.2 Procedures used for catalysis experiments****Procedures for analysis of product distribution by  $^1\text{H}$  NMR spectroscopy**

Typical reaction procedure **A**: A stock solution **A** containing both  $\text{Mn}(\text{ClO}_4)_2 \cdot 6\text{H}_2\text{O}$  (3.6 mg, 10  $\mu\text{mol}$ ) and, *e.g.* ligand **2** (3.3 mg, 10  $\mu\text{mol}$ ) in acetone- $d_6$  (20 ml) was prepared. 1.5 ml of this stock solution (0.75  $\mu\text{mol}$   $\text{Mn}(\text{ClO}_4)_2 \cdot 6\text{H}_2\text{O}$ , 0.1 mol%, and 0.75  $\mu\text{mol}$ , *e.g.* ligand **2**, 0.1 mol%) was added to diethyl fumarate (129.1 mg, 0.75 mmol), while stirring the mixture at 0  $^\circ\text{C}$ . After addition of 12.5  $\mu\text{l}$  of a 0.6 M stock (aqueous) of  $\text{NaOAc}$  (7.5  $\mu\text{mol}$ , 1.0 mol%),  $\text{H}_2\text{O}_2$  (50 wt. % in water, 85 or 170  $\mu\text{l}$ , 1.5 or 3.0 mmol, 2 or 4 equiv., respectively) was added in one portion. The mixture was stirred for 16 h, allowing the temperature to rise to room temperature.

After 16 h the reaction mixture was added to saturated aqueous  $\text{NaHCO}_3$  (30 ml) and  $\text{CH}_2\text{Cl}_2$  (30 ml) was added. After separation of the layers, the aqueous layer was extracted with  $\text{CH}_2\text{Cl}_2$  (4 x 30 ml). The combined organic phases were dried over  $\text{Na}_2\text{SO}_4$  and, after filtration, the solvent was evaporated *in vacuo*. The diol and epoxide products were identified by comparison with the  $^1\text{H}$  NMR spectra of authentic samples and their ratio by integration of several of the well-resolved absorptions of the products.

Typical reaction procedure **B**: As for **A** except in the stock solution pyridine-2-carboxylic acid (3.7 mg, 30  $\mu\text{mol}$ ) was used in place of the ligand **2**.

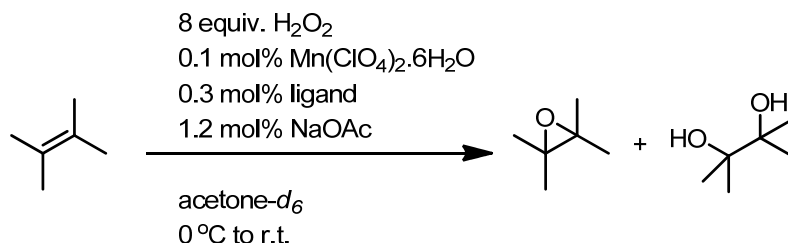
### 3.4.3 Synthesis and characterisation of [Fe(*N,N'*-Bis(pyridin-2-ylmethyl)propane-1,3-diamine)(pyridyl-2-aldehyde-methoxy-hemiacetal)](BF<sub>4</sub>)<sub>2</sub>·CH<sub>3</sub>CN



A solution of  $\text{Fe}(\text{ClO}_4)_2 \cdot \text{H}_2\text{O}$  (0.15 g, 0.58 mmol) in acetonitrile (2 ml) was added to solution of ligand **3** (0.2 g, 0.58 mmol) in methanol (4 ml) (Scheme 3).  $\text{NaClO}_4$  (0.14 g, 1.16 mmol) was added to the mixture and the resulting solution was placed in an EtOAc bath for three days changing colour from yellow to intense purple within 1 h. The solvent was removed *in vacuo* and the residue was washed with  $\text{Et}_2\text{O}$  and pentane to remove free ligand. The residue was redissolved in a minimum of acetonitrile and placed in an EtOAc bath yielding red coloured crystals (0.35 g, 0.52 mmol, 89%). Elemental analysis (calc. for  $\text{C}_{23}\text{H}_{29.5}\text{Cl}_2\text{FeN}_{5.5}\text{O}_{10}$ ) C 41.31%, (41.25%), H 4.51% (4.44%), N 11.53% (11.50%). X-Ray Crystallography [ $\text{C}_{22}\text{H}_{28}\text{FeN}_5\text{O}_2$ ]<sup>2+</sup>·2[ $\text{ClO}_4$ ]<sup>-</sup>·0.5( $\text{C}_2\text{H}_3\text{N}$ ),  $M_r = 669.77$ , monoclinic,  $C2/c$ ,  $a = 37.597(4)$ ,  $b = 9.1237(10)$ ,  $c = 16.3513(18)$  Å,  $\beta = 102.216(1)^\circ$ ,  $V = 5481.9(10)$  Å<sup>3</sup>,  $Z = 8$ ,  $D_x = 1.623$  g cm<sup>-3</sup>,  $F(000) = 2768$ ,  $\mu = 8.12$  cm<sup>-1</sup>,  $\lambda(\text{MoK}\alpha) = 0.71073$  Å,  $T = 100(1)$  K, 21142 reflections measured,  $\text{Goof} = 1.058$ ,  $wR(F^2) = 0.1118$  for 5616 unique reflections and 397 parameters, and  $R(F) = 0.0444$  for 4780 reflections obeying  $F_o \geq 4.0 \sigma(F_o)$  criterion of observability. The asymmetric unit consists of four moieties: a cationic Fe-complex, two perchlorate anions and an half of an acetonitrile solvate molecule. The acetonitrile molecule is located on a twofold axis.

### 3.4.4 Ligand degradation to pyridine-2-carboxylic acid determined by <sup>1</sup>H NMR spectroscopic analysis

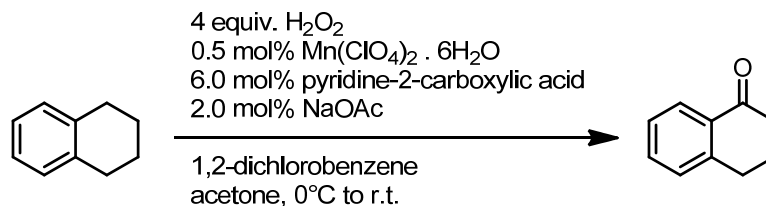
A stock solution containing  $\text{Mn}(\text{ClO}_4)_2 \cdot 6\text{H}_2\text{O}$  (3.6 mg, 10 μmol) and the ligand (*e.g.* ligand **1b**: 9.9 mg, 30 μmol) in acetone-*d*<sub>6</sub> (20 ml) was used. 1.5 ml of the stock solution (0.75 μmol  $\text{Mn}(\text{ClO}_4)_2 \cdot 6\text{H}_2\text{O}$ , 0.1 mol%, and 2.25 μmol ligand, 0.3 mol%) was added to 2,3-dimethyl-butene (63 mg, 0.75 mmol), with stirring at 0 °C. 15 μl of a 0.6 M NaOAc (aqueous) (9.0 μmol),  $\text{H}_2\text{O}_2$  (50 wt. % in water, 340 μl, 6.0 mmol, 8.0 equiv. w.r.t. substrate) was added in one portion. The mixture was stirred for 16 h, with the temperature allowed to rise to room temperature after 3 h. 200 μl of the reaction mixture was diluted with 500 μl of acetone-*d*<sub>6</sub>. The water <sup>1</sup>H NMR signal was suppressed by saturation at 4.8 ppm. The signals corresponding to the aromatic protons of the ligand/pyridine-2-carboxylic acid were readily identifiable in the range 5-10 ppm. The range 0-6 ppm is dominated by the much more intense signals of the substrate and solvent.



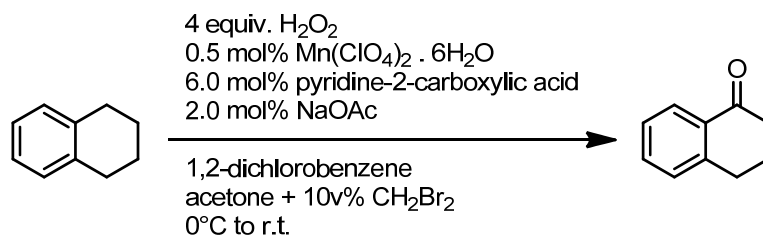
Typical conditions employed in oxidation reactions used to identify ligand decomposition product(s). 2,3-Dimethyl-but-2-ene was employed to avoid overlap of substrate and product  $^1\text{H}$  NMR absorptions with the ligand and for their facile removal from the reaction mixtures by evaporation *in vacuo*.

### 3.4.5 Catalysed oxidation of cyclooctane, tetraline, toluene, benzyl alcohol and benzaldehyde.

#### a. Oxidation of tetraline in the absence and presence of $\text{CH}_2\text{Br}_2$



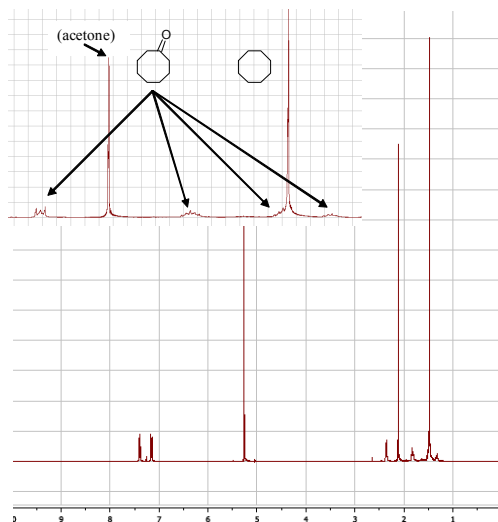
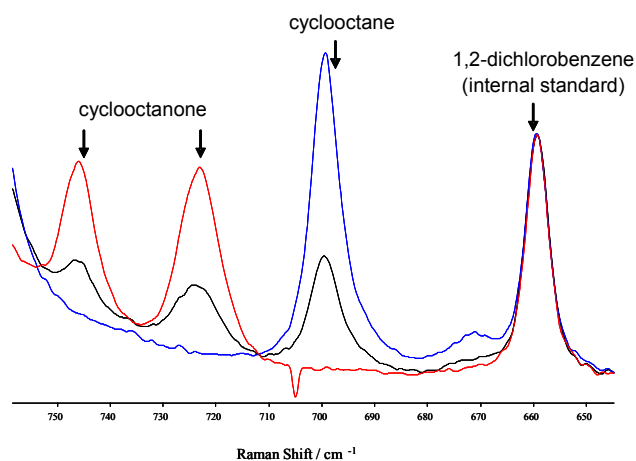
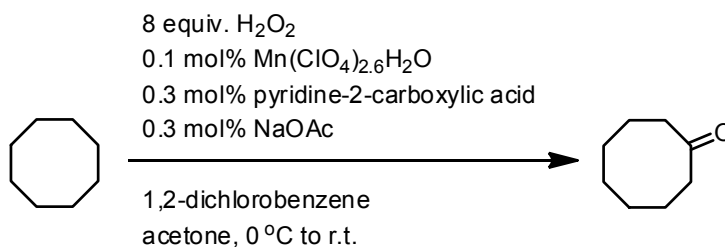
i) A stock solution containing both  $\text{Mn}(\text{ClO}_4)_2 \cdot 6\text{H}_2\text{O}$  (18.1 mg, 50  $\mu\text{mol}$ ) and pyridine-2-carboxylic acid (73.9 mg, 600  $\mu\text{mol}$ ) in acetone (20 ml) was prepared. 6 ml of this stock solution (15  $\mu\text{mol}$   $\text{Mn}(\text{ClO}_4)_2 \cdot 6\text{H}_2\text{O}$ , 0.5 mol%, and 180  $\mu\text{mol}$  pyridine-2-carboxylic acid, 6.0 mol%) was added to tetraline (397 mg, 3.0 mmol) and 1,2-dichlorobenzene (221 mg, 1.5 mmol), while stirring the mixture at room temperature. After addition of 100  $\mu\text{l}$  of a 0.6 M stock (aqueous) of  $\text{NaOAc}$  (60  $\mu\text{mol}$ , 2.0 mol%), the mixture was stirred at 0 °C and  $\text{H}_2\text{O}_2$  (50 wt. % in water, 680  $\mu\text{l}$ , 12 mmol, 4.0 equiv.) was added as a single addition. After 16 h: 92% conversion, 46% tetralone by GC analysis.



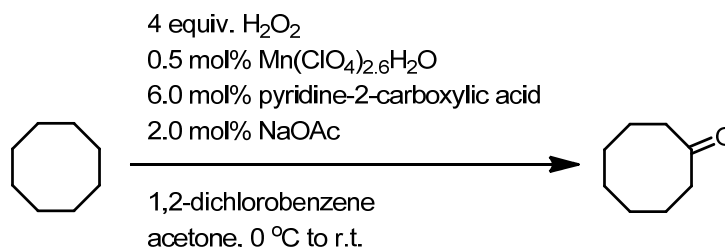
ii) As for i) except 600  $\mu\text{l}$  of  $\text{CH}_2\text{Br}_2$  were added to the reaction mixture After 16 h: 99% conversion, 37% tetralone by GC analysis. Bromoalkyl products were not detected.

### b. Cyclooctane

Cyclooctane was selected to assess the ability of the catalyst system to engage in aliphatic C-H activation due to its low volatility. The conversion achieved in the case of oxidation using 0.1 mol%  $\text{Mn}^{\text{II}}$  was determined by Raman and  $^1\text{H}$  NMR spectroscopies. In contrast to *cis*-cyclooctene where the alkene stretching band at *ca.*  $1600\text{ cm}^{-1}$  allows for conversion to be monitored readily, for cyclooctane bands in the  $650\text{--}750\text{ cm}^{-1}$  region were found to be convenient for estimation of the conversion of cyclooctane and yield of cyclooctanone.



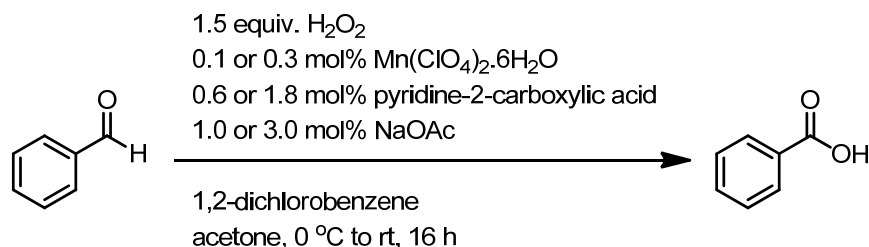
Raman spectra of reaction mixture before (blue) and after (black) reaction. The spectrum in red shows the spectrum containing cyclooctanone in place of cyclooctane. 1,2-Dichlorobenzene was used as internal standard. By comparison with the spectrum before (blue) and with only cyclooctanone (red) a conversion of 63% (370 t.o.n.) was estimated.  $^1\text{H}$  NMR analysis of the reaction mixture shows cyclooctanone as the major product. It should be noted that as conversion of the alkane increases beyond 50%, *i.e.* by using excess  $\text{H}_2\text{O}_2$ , the selectivity decreases due to formation of higher oxidation products. Confirmation that only cyclooctanone was formed was obtained by GC analysis.



A stock solution containing both  $\text{Mn}(\text{ClO}_4)_2 \cdot 6\text{H}_2\text{O}$  (18.1 mg, 50  $\mu\text{mol}$ ) and pyridine-2-carboxylic acid (73.9 mg, 600  $\mu\text{mol}$ ) in acetone (20 ml) was prepared. 6 ml of this stock (15  $\mu\text{mol}$   $\text{Mn}(\text{ClO}_4)_2 \cdot 6\text{H}_2\text{O}$ , 0.5 mol%, and 180  $\mu\text{mol}$  pyridine-2-carboxylic acid, 6.0 mol%) was added to cyclooctane (337 mg, 3.0 mmol) and 1,2-dichlorobenzene (221 mg, 1.5 mmol), while stirring the mixture at room temperature. After addition of 100  $\mu\text{l}$  of a 0.6 M stock (aqueous) of NaOAc (60  $\mu\text{mol}$ , 2.0 mol%), the mixture was cooled in an ice bath and  $\text{H}_2\text{O}_2$  (50 wt. %, 680  $\mu\text{l}$ , 12 mmol, 4.0 equiv.) was added in one addition. After 16 h: 69% conversion, 44% cyclooctanone (selectivity: 64%) analysis by GC.

### c. Oxidation of toluene, benzyl alcohol and benzaldehyde.

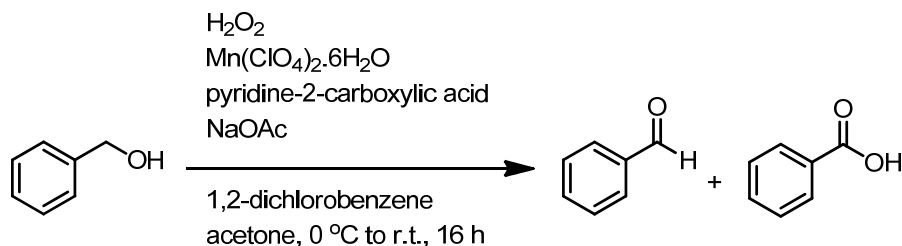
i) The oxidation of benzaldehyde was carried out under two sets of conditions and the yield was determined by  $^1\text{H}$  NMR spectroscopy:



**condition A:** benzaldehyde 2.0 mmol, 0.1 mol%  $\text{Mn}(\text{ClO}_4)_2 \cdot 6\text{H}_2\text{O}$ , 0.6 mol% pyridine-2-carboxylic acid, 1.0 mol% NaOAc,  $\text{H}_2\text{O}_2$  (50 wt. % ) 1.5 equiv. (single addition), total reaction volume 6.0 ml. Yield of benzoic acid: 65%

**condition B:** benzaldehyde 0.67 mmol, 0.3 mol%  $\text{Mn}(\text{ClO}_4)_2 \cdot 6\text{H}_2\text{O}$ , 1.8 mol% pyridine-2-carboxylic acid, 3.0 mol% NaOAc,  $\text{H}_2\text{O}_2$  (50 wt. % ) 1.5 equiv. (single addition), total reaction volume 6.0 ml. Yield of benzoic acid: 68%

ii) The oxidation of benzyl alcohol was carried out under five sets of conditions and the yield was determined by  $^1\text{H}$  NMR spectroscopy. It is clear that the oxidation of benzaldehyde is more efficient than that of benzyl alcohol which precludes selective oxidation to benzaldehyde.



**condition A:** benzyl alcohol 2.0 mmol, 0.1 mol%  $\text{Mn}(\text{ClO}_4)_2 \cdot 6\text{H}_2\text{O}$ , 0.6 mol% pyridine-2-carboxylic acid, 1.0 mol% NaOAc,  $\text{H}_2\text{O}_2$  (50 wt. %) 1.5 equiv. (single addition), reaction volume 6.0 ml. Yield 10%, product is only benzaldehyde

**condition B;** benzyl alcohol 2.0 mmol, 0.1 mol%  $\text{Mn}(\text{ClO}_4)_2 \cdot 6\text{H}_2\text{O}$ , 0.6 mol% pyridine-2-carboxylic acid, 1.0 mol% NaOAc,  $\text{H}_2\text{O}_2$  (50 wt. %) 3.0 equiv. (single addition), reaction volume 6.0 ml. Yield 30%, products were a mixture of benzaldehyde and benzoic acid (ratio of  $\text{PhCHO} : \text{PhCO}_2\text{H} = 1 : 1.1$ )

**condition C:** benzyl alcohol 0.67 mmol, 0.3 mol%  $\text{Mn}(\text{ClO}_4)_2 \cdot 6\text{H}_2\text{O}$ , 1.8 mol% pyridine-2-carboxylic acid, 3.0 mol% NaOAc,  $\text{H}_2\text{O}_2$  (50 wt. %) 1.5 equiv. (single addition), reaction volume 6.0 ml. No conversion observed

**condition D:** benzyl alcohol 0.67 mmol, 0.3 mol%  $\text{Mn}(\text{ClO}_4)_2 \cdot 6\text{H}_2\text{O}$ , 1.8 mol% pyridine-2-carboxylic acid, 3.0 mol% NaOAc,  $\text{H}_2\text{O}_2$  (50 wt. %) 3.0 equiv. (single addition), reaction volume 6.0 ml. Yield 10%, only benzaldehyde obtained.

**condition E:** benzyl alcohol 2.0 mmol, 0.1 mol%  $\text{Mn}(\text{ClO}_4)_2 \cdot 6\text{H}_2\text{O}$ , 0.3 mol% pyridine-2-carboxylic acid, 1.2 mol% NaOAc,  $\text{H}_2\text{O}_2$  (50 wt. %) 8.0 equiv. (single addition), reaction volume 6.0 ml. The reaction mixture was quenched with saturated aqueous  $\text{NaHCO}_3$ , extracted with dichloromethane, dried and solvent removed *in vacuo* yielding a 1:1 mixture of benzyl alcohol and benzaldehyde (by  $^1\text{H}$  NMR spectroscopy). Acidification of the aqueous layer and a subsequent extraction, yielded benzoic acid (70 %).

iii) In contrast to tetraline, the oxidation of toluene did not proceed with clean conversion to benzoic acid (although *ca.* 2% benzoic acid was recovered after work up). The differences in the ease of oxidation of benzaldehyde, benzyl alcohol and toluene are consistent with the formation of acetone/ $\text{H}_2\text{O}_2$  adducts with Mn as the active oxidant.

### 3.5 References and notes

- 1 H. C. Kolb, M. S. VanNieuwenhze and K. B. Sharpless, *Chem. Rev.*, 1994, **94**, 2483.
- 2 (a) B. S. Lane and K. Burgess, *Chem. Rev.*, 2003, **103**, 2457; (b) R. A. Sheldon and J. K. Kochi, *Metal-Catalyzed Oxidations of Organic Compounds*, 1981, Academic Press; (c) W. R. Browne, J. W. de Boer, D. Pijper, J. Brinksma, R. Hage and B. L. Feringa in *Chapter 11, J.-E. Bäckvall, (ed.) Modern Oxidation Methods*, 2010, Wiley-VCH, 371; (d) R. Noyori, M. Aoki and K. Sato, *Chem. Commun.*, 2003, 1977; T. Katsuki, *Chem. Soc. Rev.*, 2004, **33**, 437.
- 3 (a) D. W. Nelson, A. Gypser, P. T. Ho, H. C. Kolb, T. Kondo, H.-L. Kwong, D. V. McGrath, A. E. Rubin, P.-O. Norrby, K. P. Gable and K. B. Sharpless, *J. Am. Chem. Soc.*, 1997, **119**, 1840; (b) T. Katsuki and K. B. Sharpless, *J. Am. Chem. Soc.*, 1980, **102**, 5974; (c) K. Sato, M. Aoki, M. Ogawa, T. Hashimoto and R. Noyori, *J. Org. Chem.*, 1996, **61**, 8310; (d) W. A. Herrmann, R. W. Fischer and D. W. Marz, *Angew. Chem., Int. Ed.*, 1991, **30**, 1638.
- 4 T. J. Collins, *Acc. Chem. Res.*, 1994, **27**, 279.
- 5 T. J. Collins, *Acc. Chem. Res.*, 2002, **35**, 782.
- 6 B. S. Lane, M. Vogt, V. J. DeRose and K. Burgess, *J. Am. Chem. Soc.*, 2002, **124**, 11946.
- 7 K. Chen and L. Que, Jr., *Chem. Commun.*, 1999, 1375.
- 8 (a) J. Kim, R. G. Harrison, C. Kim and L. Que, Jr., *J. Am. Chem. Soc.*, 1996, **118**, 4373; (b) M. H. Lim, J.-U. Rohde, A. Stubna, M. R. Bukowski, M. Costas, R. Y. N. Ho, E. Munck, W. Nam and L. Que, Jr., *Proc. Natl. Acad. Sci. USA*, 2003, **100**, 3665.
- 9 G. Roelfes, M. Lubben, S. W. Leppard, E. P. Schudde, R. M. Hermant, R. Hage, E. C. Wilkinson, L. Que and B. L. Feringa, *J. Mol. Cat. A: Chem.*, 1997, **117**, 223.
- 10 K. Wieghardt, U. Bossek, B. Nuber, J. Weiss, J. Bonvoisin, M. Corbella, S. E. Vitols and J. J. Girerd, *J. Am. Chem. Soc.*, 1988, **110**, 7398.
- 11 (a) R. Hage, J. E. Iburg, J. Kerschner, J. H. Koek, E. L. M. Lempers, R. J. Martens, U. S. Racherla, S. W. Russell, T. Swarthoff, M. R. P. van Vliet, J. B. Warnaar, L. van der Wolf and B. Krijnen, *Nature*, 1994, **369**, 637; (b) D. E. De Vos and T. Bein, *Chem. Commun.*, 1996, 917; (c) C. Zondervan, R. Hage and B. L. Feringa, *Chem. Commun.*, 1997, 419; (d) D. E. De Vos, B. F. Sels, M. Reynaers, Y. V. Subba Rao and P. A. Jacobs, *Tetrahedron Lett.*, 1998, **39**, 3221; (e) A. Berkessel and C. A. Sklorz, *Tetrahedron Lett.*, 1999, **40**, 7965; (f) C. B. Woitiski, Y. N. Kozlov, D. Mandelli, G. V. Nizova, U. Schuchardt and G. B. Shul'pin, *J. Mol. Catal. A*, 2004, **222**, 103; (g) J. Brinksma, L. Schmieder, G. Van Vliet, R. Boaron, R. Hage, D. E. De Vos, P. L. Alsters and B. L. Feringa, *Tetrahedron Lett.*, 2002, **43**, 2619; (h) K. F. Sibbons, K. Shastri and M. Watkinson, *Dalton Trans.*, 2006, 645; (i) D. E. De Vos and T. Bein, *J. Organometal. Chem.*, 1996, **520**, 195.
- 12 L. Gomez, I. Garcia-Bosch, A. Company, J. Benet-Buchholz, A. Polo, X. Sala, X. Ribas and M. Costas, *Angew. Chem. Int. Ed.*, 2009, **48**, 5720.
- 13 (a) A. Murphy, G. Dubois and T. D. P. Stack, *J. Am. Chem. Soc.*, 2003, **125**, 5250; (b) G. Dubois, A. Murphy and T. D. P. Stack, *Org. Lett.*, 2003, **5**, 2469; (c) I. Garcia-Bosch, A. Company, X. Fontrodona, X. Ribas and M. Costas, *Org. Lett.*, 2008, **10**, 2095.
- 14 M. C. White, A. G. Doyle and E. N. Jacobsen, *J. Am. Chem. Soc.*, 2001, **123**, 7194.



- 
- 15 J. W. De Boer, W. R. Browne, S. R. Harutyunyan, L. Bini, T. D. Tiemersma-Wegman, P. L. Alsters, R. Hage and B. L. Feringa, *Chem. Commun.*, 2008, 3747.
- 16 (a) M. Fujita, M. Costas and L. Que, Jr., *J. Am. Chem. Soc.*, 2003, **125**, 9912; (b) K. Chen, M. Costas, J. Kim, A. K. Tipton and L. Que, Jr., *J. Am. Chem. Soc.*, 2002, **124**, 3026; (c) J. Y. Ryu, J. Kim, M. Costas, K. Chen, W. Nam and L. Que, Jr., *Chem. Commun.*, **2002**, 1288.
- 17 J. W. de Boer, J. Brinksma, W. R. Browne, A. Meetsma, P. L. Alsters, R. Hage and B. L. Feringa, *J. Am. Chem. Soc.*, 2005, **127**, 7990.
- 18 J. W. de Boer, W. R. Browne, J. Brinksma, P. L. Alsters, R. Hage and B. L. Feringa, *Inorg. Chem.*, 2007, **46**, 6353.
- 19 M. Martinho, F. Banse, J.-F. Bartoli, T. A. Mattioli, P. Battioni, O. Horner, S. Bourcier and J.-J. Girerd, *Inorg. Chem.*, 2005, **44**, 9592.
- 20 H. Toftlund and S. Yde-Andersen, *Acta Chem. Scand. Ser. A*, 1981, **35**, 575.
- 21 S. Groni, P. Dorlet, G. Blain, S. Bourcier, R. Guillot and E. Anxolabéhère-Mallart, *Inorg. Chem.*, 2008, **47**, 3166.
- 22 A. Thibon, J.-F. Bartoli, S. Bourcier and F. Banse, *Dalton*, 2010, 9587. In this study the authors noted that the sterically encumbered catalyst itself is considerably less capable of C-H abstraction. Hence it could be that electronic rather than steric effects are important in this case.
- 23 J. England, C. R. Davies, M. Banaru, A. J. P. White and G. J. P. Britovsek, *Adv. Synth. Catal.*, 2008, **350**, 883.
- 24 B. C. Gilbert, J. R. Lindsay Smith, A. Mairata I Payeras, J. Oakes, R. Pons I Prats, *J. Mol. Catal. A: Chem.*, 2004, **219**, 265.
- 25 I. Garcia-Bosch, X. Ribas and M. Costas, *Adv. Synth. Catal.*, 2009, **351**, 348.
- 26 (a) A. Company, L. Gomez, M. Guell, X. Ribas, J. M. Luis, L. Que Jr. and M. Costas, *J. Am. Chem. Soc.*, 2007, **129**, 15766; (b) A. Company, Y. Feng, M. Guell, X. Ribas, J. M. Luis, L. Que Jr., M. Costas, *Chem. Eur. J.*, 2009, **15**, 3359.
- 27 (a) M. Wu, B. Wang, S. Wang, C. Xia and W. Sun, *Org. Lett.*, 2009, **11**, 3622; (b) M. C. White, A. G. Doyle and E. N. Jacobsen, *J. Am. Chem. Soc.*, 2001, **123**, 7194; (c) M. Costas, A. K. Tipton, K. Chen, D. H. Jo and L. Que, Jr., *J. Am. Chem. Soc.*, 2001, **123**, 6722; (d) M. S. Chen and M. C. White, *Science*, 2007, **318**, 783; (e) K. Suzuki, P. D. Oldenburg and L. Que, Jr., *Angew. Chem., Int. Ed.*, 2008, **47**, 1887; (f) P. D. Oldenburg and L. Que, Jr., *Catal. Today*, 2006, **117**, 15; (g) A. Murphy, G. Dubois and T. D. P. Stack, *J. Am. Chem. Soc.*, 2003, **125**, 5250; (h) A. Murphy, A. Pace and T. D. P. Stack, *Org. Lett.*, 2004, **6**, 3119; (i) A. Murphy and T. D. P. Stack, *J. Mol. Catal. A: Chem.*, 2006, **251**, 78; (j) L. Gomez, I. Garcia-Bosch, A. Company, X. Sala, X. Fontrodona, X. Ribas and M. Costas, *Dalton Trans.*, 2007, 5539; (k) G. Guillemot, M. Neuburger and A. Pfaltz, *Chem. Eur. J.*, 2007, **13**, 8960.
- 28 J. Brinksma, R. Hage, J. Kerschner and B. L. Feringa, *Chem. Commun.*, 2000, 537.
- 29 J. Brinksma, M. T. Rispens, R. Hage and B. L. Feringa, *Inorg. Chim. Acta*, 2002, **337**, 75.
- 30 P. Saisaha, D. Pijper, J. W. de Boer, R. Hoen, R. P. van Summeren, P. L. Alsters, R. Hage, B. L. Feringa and W. R. Browne, *Org. Biomol. Chem.*, 2010, **8**, 4444.

- 31 P. Mialane, A. Nivorojkine, G. Pratviel, L. Azéma, M. Slany, F.; Godde, A. Simaan, F. Banse, T. Kargar-Grisel, G. Bouchoux, J. Sainton, O. Horner, J. Guilhem, L. Tchertanova, B. Meunier and J.-J. Girerd, *Inorg. Chem.*, 1999, **38**, 1085.
- 32 The formation of aminated structures from structures such as ligand **3** within the mass spectrometer is possible, however, in the present study aminated structures were not detected immediately after addition of H<sub>2</sub>O<sub>2</sub> but rather they appeared and increased in intensity of the course of the lag period observed.
- 33 The X-ray crystal structure of the mononuclear MnII chlorido complex of ligand **2** has been reported by M. Kloskowski, B. Krebs, *Z. Anorg. Allg. Chem.*, 2006, **632**, 771.
- 34 K. B. Jensen, C. J. McKenzie, O. Simonsen, H. Toftlund, A. Hazell, *Inorg. Chim. Acta*, 1997, **257**, 163.
- 35 It should be noted that although complexation to MnII would be expected to broaden the <sup>1</sup>H NMR absorptions of the ligands and ligand degradation products, the ratio of available Mn<sup>II</sup> to pyridine-2-carboxylic acid is lower than 1:3.
- 36 The ability to engage in C-H activation could indicate that alkyl radicals are involved, however, even with 10 vol% of CH<sub>2</sub>Br<sub>2</sub>, the oxidation of diethyl fumarate goes to completion and for tetraline the same conversion and selectivity was observed as in the absence of CH<sub>2</sub>Br<sub>2</sub>.
- 37 A. Murphy, A. Pace and T. D. P. Stack, *Org. Lett.*, 2004, **6**, 3119.
- 38 See Table 1.
- 39 J. C. Tripp, C. H. Schiesser and D. P. Curran, *J. Am. Chem. Soc.*, 2005, **127**, 5518.
- 40 H. E. Gottlieb, V. Kotlyar and A. Nudelman, *J. Org. Chem.*, 1997, **62**, 7512.
- 41 A. D. Brewer, *Chem. Brit.* 1975, **11**, 335; G. M. Bodner, *J. Chem. Educ.*, 1985, **62**, 1105.



## Chapter 4

# Manganese catalysed *cis*-dihydroxylation of electron deficient alkenes with H<sub>2</sub>O<sub>2</sub>

*A practical method for the multigram scale selective cis-dihydroxylation of electron deficient alkenes such as diethyl fumarate and N-alkyl and N-aryl-maleimides using H<sub>2</sub>O<sub>2</sub> is described. High turnover numbers (>1000) can be achieved with this efficient manganese based catalyst system, prepared in situ from a manganese salt, pyridine-2-carboxylic acid, a ketone and a base, under ambient conditions. Under optimized conditions, for diethyl fumarate at least 1000 turnovers could be achieved with only 1.5 equiv. of H<sub>2</sub>O<sub>2</sub> with d/l-diethyl tartrate (cis-diol product) as the sole product. For electron rich alkenes, such as cyclooctene, this catalyst provides for efficient epoxidation.*

*Part of this chapter has been published:*

P. Saisaha, D. Pijper, J. W. de Boer, R. Hoen, R. P. van Summeren, P. L. Alsters, R. Hage, B. L. Feringa and W. R. Browne, *Org. Biomol. Chem.*, 2010, **8**, 4444.

W. R. Browne, P. L. Alsters, R. P. van Summeren, E. Ijpeij, J. W. de Boer, P. Saisaha, D. Pijper and B. L. Feringa, *PCT Int. Appl.*, 2011, WO 2011/04333.

## 4.1 Introduction

The selective and atom efficient *cis*-dihydroxylation of alkenes is a key transformation in synthetic organic chemistry,<sup>1</sup> with contemporary methods relying predominantly on stoichiometric oxidants, such as  $\text{MnO}_4^-$  and  $\text{OsO}_4$ ,<sup>1c,2</sup> or transition metal based oxidation catalysts, in particular, ruthenium,<sup>3,4</sup> and osmium (asymmetric) dihydroxylation methods.<sup>5</sup>

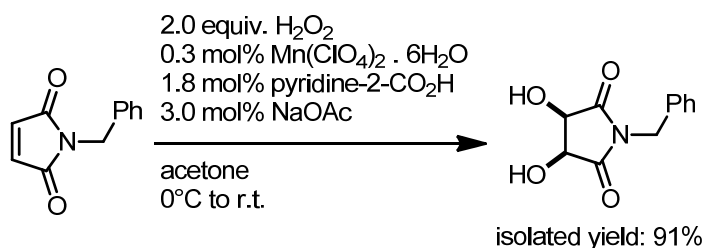
Practical osmium free methods for *cis*-dihydroxylation of alkenes that avoid the need for excess amounts of oxidant are highly desirable, both in synthesis and for the large scale production of important building blocks, not least *N*-aryl and *N*-alkylmaleimides.<sup>6,7</sup> Furthermore, the *cis*-dihydroxylation of electron deficient alkenes such as *N*-alkylpyrrole-2,5-diones remains a major challenge with the more reactive ruthenium based catalysts systems employing  $\text{NaIO}_4$  providing one of the few effective routes available today to prepare the *cis*-diol products. For example 1-benzyl-1*H*-pyrrole-2,5-dione can be converted to (*meso*)-*N*-benzyl-3,4- dihydroxy-2,5-pyrrolidinedione using 1.3 equiv. of  $\text{NaIO}_4$  and 0.8 mol% of  $\text{Ru}^{\text{III}}\text{Cl}_3$  in 73.3% yield.<sup>6</sup>

In recent years, considerable advances have been made in the development of atom-efficient and environmentally friendly catalytic *cis*-dihydroxylation methods employing  $\text{H}_2\text{O}_2$ ,<sup>1</sup> most notably, in the use of iron pyridyl-amine complexes, by Que *et al.*,<sup>8</sup> manganese complexes by De Vos *et al.*<sup>9</sup> and Feringa, Browne *et al.*<sup>10</sup> and others<sup>11</sup> and ruthenium complexes by Che *et al.*<sup>12</sup> With the  $[\text{Mn}^{\text{III,III}}_2\text{O}(\text{RCO}_2)_2(\text{TMTACN})_2]^{2+}$  catalysts<sup>13</sup> we have reported recently,<sup>10b-e</sup> the *cis*-dihydroxylation of electron rich *cis*-alkenes was achieved with over 8000 turnovers to the *cis*-diol product of cyclooctene and near complete atom efficiency in the oxidant  $\text{H}_2\text{O}_2$ . By contrast, this system shows little activity with electron deficient alkenes such as diethyl fumarate.

A key challenge, therefore, is to develop readily accessible methods based on simple catalysts, preferably prepared *in situ*, that are able to achieve similar efficiency in the *cis*-dihydroxylation for electron deficient alkenes.

In this chapter a readily accessible catalytic system based on manganese and  $\text{H}_2\text{O}_2$  that is highly selective in the *cis*-dihydroxylation of electron deficient alkenes such as diethyl fumarate and *N*-alkyl-maleimides on a multigram scale will be described (Scheme 1).

The present system is based on a manganese source in combination with pyridine-2-carboxylic acid, a ketone and a base. With this method electron deficient alkenes can be converted quantitatively to the corresponding *cis*-dihydroxylation products. Furthermore, we show that for electron rich alkenes epoxidation dominates with the ratio between *cis*-diol and epoxide products showing a qualitative correlation between electron deficiency and the product distribution observed.



**Scheme 1** *cis*-Dihydroxylation of 1-benzyl-1*H*-pyrrole-2,5-dione using the present method.

## 4.2 Results and discussion

### 4.2.1 *cis*-Dihydroxylation of electron deficient alkenes

The catalyst is formed *in situ* by addition of a Mn<sup>II</sup> salt and pyridine-2-carboxylic acid to acetone followed by addition of the substrate and then NaOAc (aq.). The reaction mixture is then cooled in ice water and H<sub>2</sub>O<sub>2</sub> is added either as a single batch or by syringe pump. Under optimized conditions, for diethyl fumarate at least 1000 turnovers could be achieved with only 1.5 equiv. of H<sub>2</sub>O<sub>2</sub> with *d/l*-diethyl tartrate (*cis*-dihydroxylation product) as the sole product.<sup>14</sup> Further oxidation of the *cis*-diol formed was not observed, even with excess H<sub>2</sub>O<sub>2</sub>.

A series of electron deficient alkenes together with conversions and isolated yields are shown in Table 1. The reaction conditions were optimized for each of the electron deficient alkenes examined using Raman spectroscopy to monitor conversion of the alkene and <sup>1</sup>H NMR spectroscopy to determine product ratios. Isolation of *cis*-diol products was carried out using standard synthetic procedures (see the experimental section for detailed procedures). The optimum reaction conditions were found to be substrate specific but in general a 1 : 6 : 10 mixture of a Mn<sup>II</sup> salt, pyridine-2-carboxylic acid and NaOAc provided good conversion and yield of the *cis*-diol products.

The present system is equally effective for mono-, di-, tri- and tetra-substituted electron deficient alkenes. For alkenes such as ethyl crotonate (Table 1, entries 10–12) low conversion and selectivity between *cis*-diol and epoxide products was observed. However, overall good to excellent conversion was achieved with electron deficient *trans*-alkenes, such as diethyl fumarate and diethyl-2-methyl-fumarate, and cyclic *cis*-alkenes such as maleimide.

The reduced reactivity towards diethyl maleate and *N,N'*-dibutylmaleamide is surprising considering the fact that, *e.g.* maleimide can be converted to the corresponding *cis*-diol product quantitatively (Table 1). Lowering the substrate concentration provided a modest improvement in conversion for diethyl maleate however a maximum conversion of only 63% was achieved in the present study.

For diethyl fumarate and diethyl maleate a difference in maximum conversion (Table 1) and reaction rate was notable. Diethyl fumarate can be converted quantitatively to the *d/l*-diethyl tartrate within 60 min under optimised reaction conditions. For diethyl maleate, by contrast, only 20–30% conversion over several hours can be achieved using

these conditions. In order to investigate the origin of these differences further a competition experiment in which a 1 : 1 mixture of diethyl fumarate and diethyl maleate was oxidised under conditions optimised for diethyl fumarate was performed (Figure 1 and 2). Under these conditions the conversion of diethyl maleate was 20% as expected. Surprisingly, however, only 90% conversion was achieved for diethyl fumarate (in the absence of diethyl maleate full conversion is achieved under these conditions). The fact that substantial conversion was achieved for both substrates confirms that catalyst inhibition by the substrates does not occur. Hence it is apparent that product inhibition (either from oxidation or hydrolysis products) of the diethyl maleate may be involved.<sup>15</sup> The stability of the substrate and products towards hydrolysis under the reaction conditions employed indicates that it is oxidation products which cause catalyst inhibition.

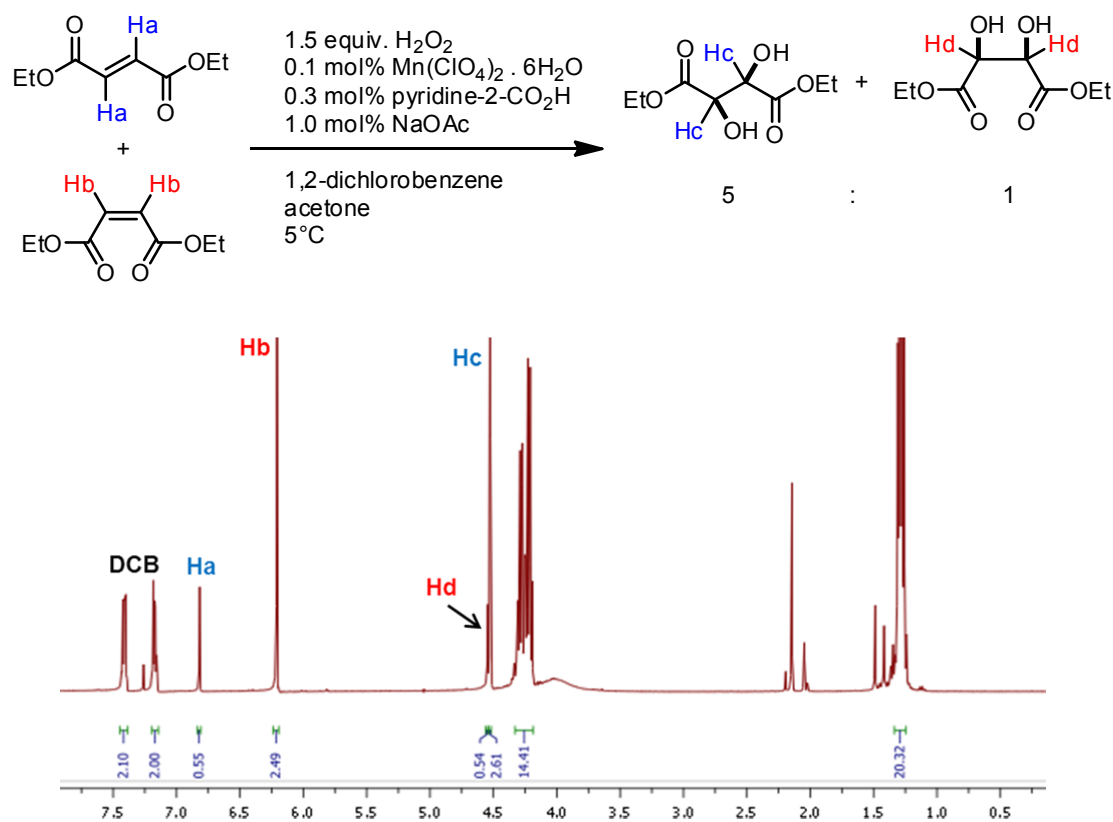


**Figure 1** <sup>1</sup>H NMR spectrum of reaction mixture (diluted in CDCl<sub>3</sub>). Reaction conditions: Mn(ClO<sub>4</sub>)<sub>2</sub>·6H<sub>2</sub>O (1.0 μmol), pyridine-2-carboxylic acid (3.0 μmol), NaOAc (30.0 μmol), 1,2 dichlorobenzene (as internal standard, 0.5 mmol), diethyl fumarate (0.5 mmol) and diethyl maleate (0.5 mmol) in acetone at 5 °C with single addition of H<sub>2</sub>O<sub>2</sub> (1.5 equiv.).

**Table 1** *cis*-Dihydroxylation of alkenes by Mn<sup>II</sup>(ClO<sub>4</sub>)<sub>2</sub>/ pyridine-2-carboxylic acid/ NaOAc/ H<sub>2</sub>O<sub>2</sub> in acetone

entry	substrate	conversion (%) <sup>a</sup>	isolated yield (%)
1		100 (>95) <sup>b</sup>	91 (95) <sup>b</sup>
2		>95	88
3		63	47 <sup>c</sup>
4		100	98
5		100	>95
6		100	91
7		100	75
8		55	32
9		81	55 <sup>a,d</sup>
10		<10	<i>cis</i> -diol:epoxide <sup>a</sup> 2:1
11		<10	<i>cis</i> -diol:epoxide <sup>a</sup> 1:1
12		<10	<i>cis</i> -diol:epoxide <sup>a</sup> 1:1

<sup>a</sup> Determined by Raman spectroscopy using the C=C stretching band at *ca.* 1600 cm<sup>-1</sup> and by <sup>1</sup>H NMR spectroscopy. For detailed conditions and procedures see the experimental section. <sup>b</sup> In 2-butanone. Recovered starting material: <sup>c</sup> 25% and <sup>d</sup> 19%.



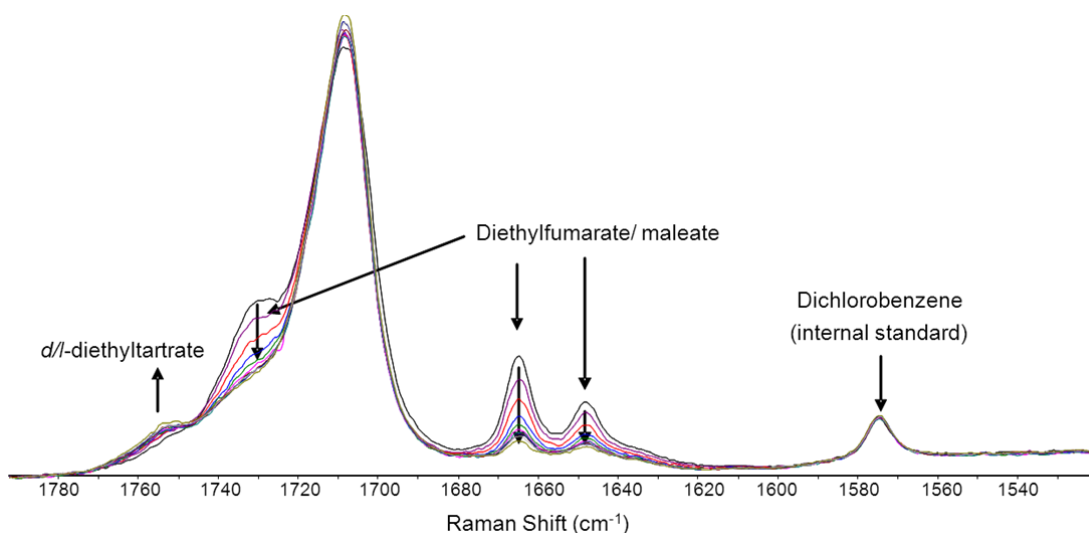


**Figure 2** *In situ* Raman spectra of reaction mixture with 1,2-dichlorobenzene as internal reference. Shown is the decrease of the signals at 1648, 1664 and 1730  $\text{cm}^{-1}$  and the appearance of the products at *ca.* 1753  $\text{cm}^{-1}$  at 40 min intervals between 0 and 7.5 h and after 21 h. The Raman spectrum of diethyl maleate overlaps with that of diethyl fumarate precluding detailed analysis. Nevertheless, the decrease in the intensity of the diethyl fumarate bands is consistent with the conversion determined by  $^1\text{H}$  NMR spectroscopy.

To investigate the possibility of primary oxidation products (*i.e.* *meso*- and *d/l*-diethyltartrate) being responsible for product inhibition, similar experiments were performed using a 1 : 1 mixture of diethyl fumarate and either *meso* or *d/l*-diethyl tartrate. In both cases full conversion of the diethyl fumarate was achieved as shown in Figure 3 and 4. This confirms that the primary oxidation products are not responsible for catalyst inhibition.

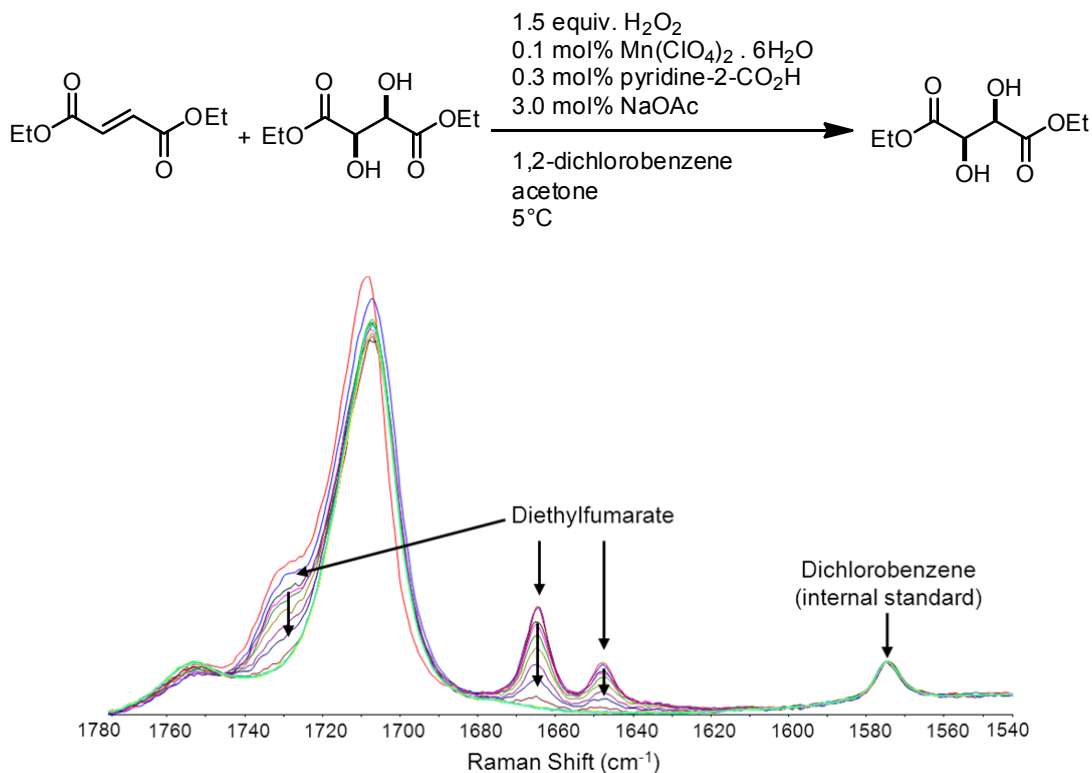


**Figure 3** *In situ* Raman spectra of reaction mixture with 1,2-dichlorobenzene as internal reference. Shown is the decrease of the signals at 1648, 1664 and 1730  $cm^{-1}$  and the appearance of the products at *ca.* 1733  $cm^{-1}$  at 10 min intervals over 2 h 20 min. The bands of the diethyl fumarate are completely gone and the decrease in the intensity of the diethyl fumarate bands is consistent with the conversion determined by  $^1H$  NMR spectroscopy.

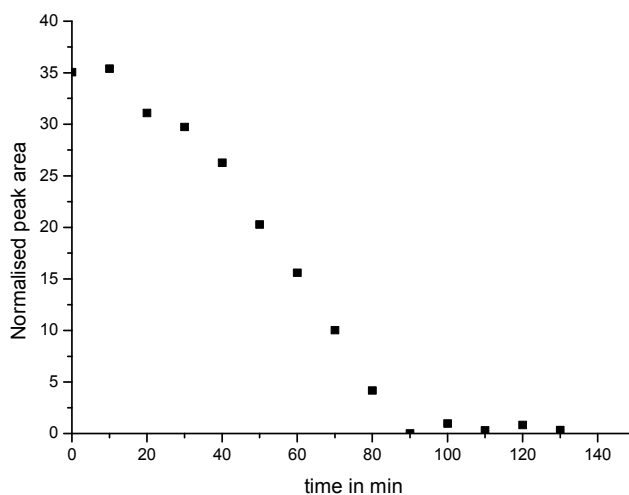


**Figure 4** The time course of the reaction in Figure 3 shows that full conversion is achieved within 90 min.

### 4.2.2 *cis*-Dihydroxylation and epoxidation of electron rich alkenes

The results of oxidation of a series of electron rich alkenes are shown in Table 2. For all substrates examined the main product observed is the epoxide product. However, significant amounts of diol were formed in all cases. As has been noted for the  $\text{RuCl}_3/\text{NaIO}_4$ <sup>6</sup> and  $\text{Ru}^{\text{III}}\text{TMTACN}$ <sup>12</sup> systems, and to a lesser extent the  $\text{Mn-TMTACN}$  systems,<sup>10</sup> the diol produced is readily oxidised further to the  $\alpha$ -hydroxy ketone and ultimately C–C bond cleavage is seen. The propensity for further oxidation of the *cis*-diol products results in reduced selectivity. Nevertheless, the epoxide was observed as the primary product in most cases, especially for electron rich alkenes such as *cis*-cyclooctene and styrene (Table 2, entries 1 and 5). Overall, the substrate scope shows a qualitative correspondence between the *cis*-diol/epoxide ratio with the electron deficiency of the substrate. The extent of epoxidation of alkenes such as *cis*-cyclooctene (1 : 3 diol/epoxide) and ethyl crotonate (2 : 1 diol/epoxide) (see Tables 1 and 2) is comparable to the trends observed by Que and co-workers for  $\text{Fe}^{\text{II}}$  polypyridyl based catalysts.<sup>16</sup> This may indicate that selectivity is substrate, and not catalyst, controlled.

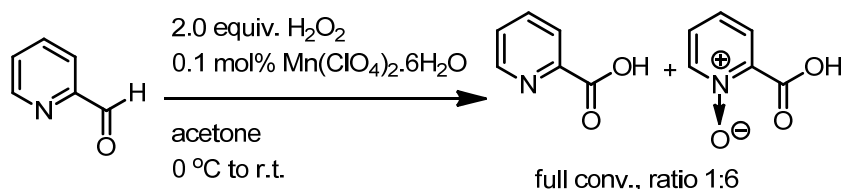
**Table 2** *cis*-Dihydroxylation and epoxidation of electron rich alkenes by  $\text{Mn}^{\text{II}}(\text{ClO}_4)_2/\text{pyridine-2-carboxylic acid}/\text{NaOAc}/\text{H}_2\text{O}_2$  in acetone.

entry	substrate	conversion (%) <sup>a</sup>	yield
1	<i>cis</i> -cyclooctene	97	12% <i>cis</i> -diol (12 %) <sup>b</sup> 72% epoxide (60%) <sup>b</sup> 12% $\alpha$ -hydroxy ketone (10%) <sup>b</sup>
2	cyclohexene	100	2% <i>cis</i> -diol 54% epoxide 14% $\alpha$ -hydroxy ketone 3% cyclohexenone
3	1-methyl-cyclohexene	100	8% <i>cis</i> -diol 64% epoxide
4	1-octene	82	9% <i>cis</i> -diol 35% epoxide 18% $\alpha$ -hydroxy ketone
5	styrene	100	4% <i>cis</i> -diol 75% epoxide 9% other
6	<i>trans</i> - $\beta$ -methylstyrene	100	7% <i>cis</i> -diol 65% epoxide 12% $\alpha$ -hydroxy ketone
7	2-methyl-2-pentene	100	13% <i>cis</i> -diol 62% epoxide

<sup>a</sup> Determined by Raman spectroscopy and by  $^1\text{H}$  NMR spectroscopy. <sup>b</sup> Isolated yields in parentheses.

### 4.2.3 Catalyst composition

The catalyst system is sensitive to changes in catalyst composition. With pyridine-2-carboxaldehyde, which can be oxidized *in situ* (Scheme 2, see also the experimental section), full conversion is observed.



**Scheme 2** Oxidation of pyridine-2-carboxaldehyde.

**Table 3** Effect of molecular structure of the pyridyl ligand on efficiency towards the *cis*-dihydroxylation of diethyl fumarate

ligand	method	conversion (%)	ligand	method	conversion (%)
	A	0		B	0
	A	100		C	100
	A	0		D	100
	B	100		B	0
	D	0		D	0
	D	0		D	80
	D	100			

All reactions carried out in acetone at room temperature. Reaction conditions (Mn/ligand/NaOAc/ H<sub>2</sub>O<sub>2</sub>, mol%): **A** (0.1/ 0.1/ 1.2/ 400), **B** (0.1/ 0.3/ 1.0/ 200). **C**: (0.1/ 0.3/ 1.2/ 800). **D**: (0.1/ 0.3/ 1.0/ 800). The oxidation of diethyl fumarate was monitored by following the intensity of the 1665 and 1648 cm<sup>-1</sup> Raman bands (alkene stretching vibration), relative to the internal standard 1,2-dichlorobenzene (1575 cm<sup>-1</sup>).

With other substituted pyridine carboxylic acids, *e.g.* pyridine-2,5-dicarboxylic acid, full activity was observed (Table 3). By contrast, for picolinic acid *N*-oxide or pyridine-2,6-dicarboxylic acid, activity was not observed (Table 3). This indicates that the co-catalyst is acting as a ligand to the Mn<sup>II</sup> and that the *N*-oxide, although it can be formed under

reaction conditions (Scheme 1), is not involved in the oxidation catalysis. A notable observation is that for quinoline-8-carboxylic acid no conversion was observed in contrast to quinoline-8-carbaldehyde for which 80% was observed. In this case the very limited solubility of the quinoline-8-carboxylic acid in the reaction mixture is almost certainly the reason for the difference in reactivity, emphasizing the point that the conversion achieved is highly dependent on the initial formulation of the reaction mixture.

The system is relatively insensitive to the nature of the base employed with, *e.g.* NaOAc, NaHCO<sub>3</sub> and NaOH or Mn(OAc)<sub>2</sub> providing comparable results (Table 4). The insensitivity in terms of activity or selectivity to variation in the base employed indicates that the catalyst is not dependent on acetate as a ligand. Furthermore, the number of equivalents of base employed does not affect the reaction significantly provided that it is in excess with respect to the pyridine-2-carboxylic acid and Mn<sup>II</sup>.

**Table 4** Conversion of diethyl fumarate in the presence of various bases and acid

<div style="display: flex; align-items: center; justify-content: center;"> <div style="text-align: center;"> </div> </div>		
base or acid	mol%	conversion (%)
none	-	0
NaOAc	1.0	100
KOAc	1.0	100
NaOAc	20.0	100
NaOH	1.0	100
NaHCO <sub>3</sub>	1.0	100
Na <sub>2</sub> CO <sub>3</sub>	1.0	100
NH <sub>4</sub> OAc	1.0	70
AcOH	1.0	0

The oxidation of diethyl fumarate was monitored by following the intensity of the 1665 and 1648 cm<sup>-1</sup> bands (alkene stretching vibration) relative to the internal standard 1,2-dichlorobenzene (1575 cm<sup>-1</sup>).

Notably when a 1 : 1 ratio of pyridine-2-carboxylic acid/Mn<sup>II</sup> is employed (Table 5) the system is highly sensitive to the number of equivalents of base added with a 1 : 1 ratio being optimum. This indicates that the base serves mainly to deprotonate pyridine-2-carboxylic acid and allows the catalyst to form. For the pyridine based ligands (Table 3) that do not bear a carboxylic acid residue, the addition of base is still necessary to ensure the deprotonation of the pyridine in the acetone/water mixture and furthermore is required in order to achieve a significant reaction rate and conversion.

**Table 5** Effect of variation in equivalents of base on reactivity of the present system under conditions where the ratio of  $Mn^{II}$  to pyridine-2-carboxylic acid is 1 : 1.

$  \begin{array}{c}  \text{EtO}-\text{C}(=\text{O})-\text{CH}=\text{CH}-\text{C}(=\text{O})-\text{OEt} \\  \text{O} \qquad \qquad \qquad \text{O}  \end{array}  \xrightarrow[  \begin{array}{c}  \text{1,2-dichlorobenzene} \\  \text{acetone, r.t.}  \end{array}  ]{  \begin{array}{c}  2.0 \text{ equiv. } H_2O_2 \\  0.1 \text{ mol\% } Mn(ClO_4)_2 \cdot 6H_2O \\  0.1 \text{ mol\% pyridine-2-CO}_2H \\  x \text{ mol\% NaOAc}  \end{array}  }  \begin{array}{c}  \text{EtO}-\text{C}(=\text{O})-\text{CH}(\text{OH})-\text{CH}(\text{OH})-\text{C}(=\text{O})-\text{OEt} \\  \text{O} \qquad \qquad \qquad \text{O}  \end{array}  $	
mol% of NaOAc	conversion (%)
0	0
0.1	0
0.2	22
0.3	32
0.5	46
1.0	72
2.0	31

The oxidation of diethylfumarate was monitored by following the intensity of the 1665 and 1648  $cm^{-1}$  bands (alkene stretching vibration) relative to the internal standard 1,2-dichlorobenzene (1575  $cm^{-1}$ ).

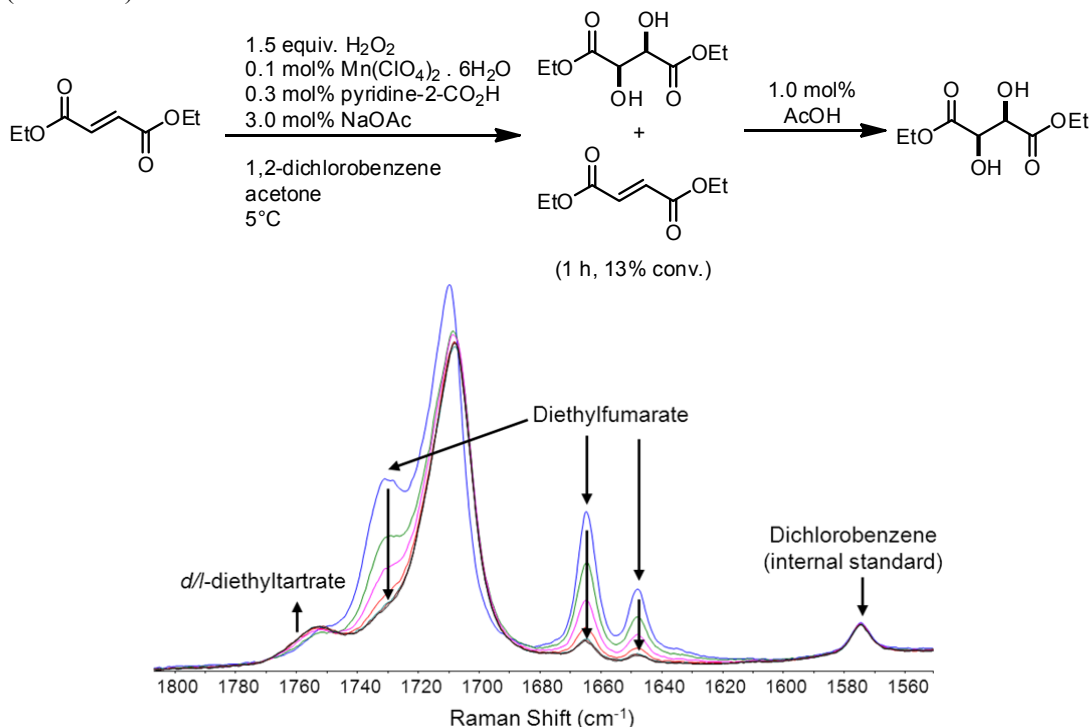


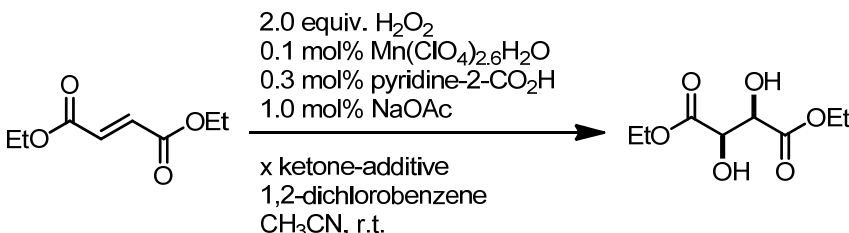
**Figure 5** *In situ* monitoring by Raman spectroscopy before (blue) and after 95 min (green), 195 min (pink), 300 min (red) and at 460, 560 and 620 min. The reaction is retarded by the addition of acetic acid which was added after 60 min. but still proceeds to >85% conversion (confirmed by  $^1H$  NMR spectroscopy). This is in contrast to the situation where acetic acid is added prior to addition of  $H_2O_2$ . See also Table 4.

By contrast, in the absence of added base or where acid, *e.g.* acetic acid, is added prior to addition of  $\text{H}_2\text{O}_2$ , conversion was not observed (Table 4). However, once the reaction had commenced addition of acetic acid resulted in a decrease in reaction rate and conversion but did not inhibit the reaction fully (Figure 5) (see Chapter 5 for further discussion of this effect).

#### 4.2.4 Solvent dependence

Acetone is the solvent of choice in the present study. However, the catalysis proceeded equally well in 2-butanone (Table 1, entry 1). Initial screening of the reaction conditions for solvent tolerance indicated that activity is observed only in ketone based solvents. Notably, the system is tolerant to some co-solvents (Table 6), for example in acetonitrile 20% conversion was obtained with 10 vol% acetone. Furthermore, electron deficient ketones such as 1,1,1-trifluoroacetone can be employed (5 vol%) in acetonitrile providing full conversion (Table 6). This indicates that the ketone may play a role directly in the catalysis over and above its role as a solvent, for example through the intermediacy of ketone/peroxide adducts such as that proposed by Que and coworkers.<sup>17</sup> Notably sub-stoichiometric amounts of  $\text{CF}_3\text{COCH}_3$  provided 90% conversion. In this case  $^{19}\text{F}$  NMR spectroscopy indicated the formation of species other than the ketone. For the hexahaloacetones, however, no conversion was observed (Table 6).

**Table 6** *cis*-Dihydroxylation of diethylfumarate in acetonitrile with various ketones

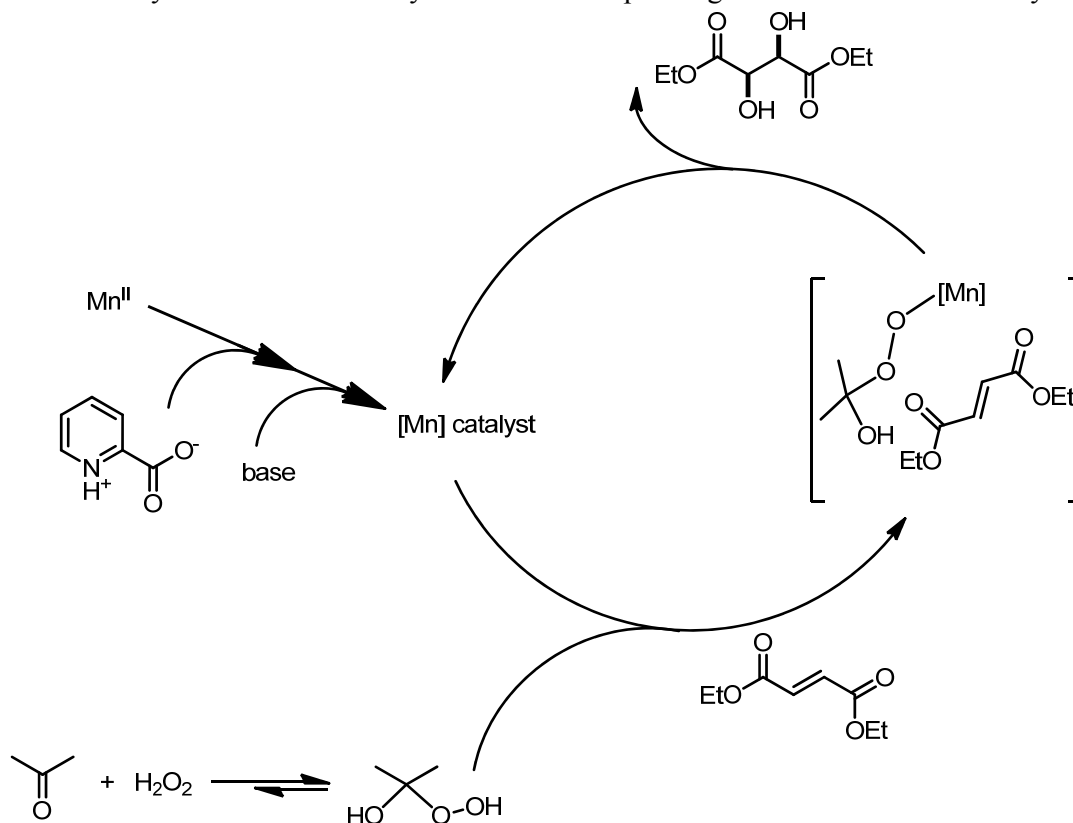
<div style="display: flex; align-items: center; justify-content: center;"> <div style="text-align: center;">  </div> </div>		
ketone	amount	conversion (%)
none	-	0
$\text{CH}_3\text{COCH}_3$	10 vol%	20
$\text{CH}_3\text{COCH}_3$	0.3 equiv.	0
$\text{CF}_3\text{COCH}_3$	30 vol%	full
$\text{CF}_3\text{COCH}_3$	20 vol%	>95
$\text{CF}_3\text{COCH}_3$	10 vol%	>95
$\text{CF}_3\text{COCH}_3$	5 vol %	>95
$\text{CF}_3\text{COCH}_3$	0.3 equiv	90
$\text{CF}_3\text{COCF}_3$	10 vol%	0
$\text{CF}_3\text{COCH}_3$ (in MTBE)	10 vol%	>95

The oxidation of diethylfumarate was monitored by following the intensity of the 1665 and 1648  $\text{cm}^{-1}$  bands (alkene stretching vibration) relative to the internal standard 1,2-dichlorobenzene (1575  $\text{cm}^{-1}$ ). In all cases *d,l*-diethyl-tartrate was the sole product observed.

Overall, however, the use of acetone or 2-butanone is preferred over more electron deficient ketones due to convenience, cost and environmental reasons. The presence of significant amounts of water in the reactions employing acetone as solvent reduces potential hazards associated with the combination of acetone and  $H_2O_2$  significantly. In addition, the activity of this system with 2-butanone allows for oxidation of less hydrophilic substrates.

### 4.3 Mechanistic considerations

The effect of variation in the parameters, *i.e.* solvent, co-catalyst and base on the conversion observed, provides some insight into the reaction mechanism (Scheme 3). The first observation is the importance of the order of addition of the reaction components. Addition of the base, *e.g.* NaOAc, prior to addition of the manganese salt and pyridine-2-carboxylic acid results in formation of a precipitate and reduced or no reactivity. Furthermore, replacement of the pyridine-2-carboxylic acid with pyridine-2-carboxaldehyde shows full activity while the corresponding *N*-oxide shows no activity.



**Scheme 3** Proposed mechanism for *cis*-dihydroxylation of alkenes employing  $Mn^{II}$ /pyridine-2-carboxylic acid/ a base in ketone solvent.

The system is relatively insensitive to the nature of the base employed (Table 4). The presence of a ketone in the reaction is essential as demonstrated in the reactivity observed



in acetonitrile and MTBE (Table 6). The equilibrium between  $\text{H}_2\text{O}_2$  and ketones is well established and essentially all  $\text{H}_2\text{O}_2$  in acetone or 2-butanone solution is present as the hydrogen peroxide/ketone adduct.<sup>17,18</sup> This adduct is likely to be directly involved in the catalytic cycle as no activity (and importantly no decomposition of  $\text{H}_2\text{O}_2$ ) is observed in acetonitrile in the absence of added ketone.

The selectivity observed, *i.e.* electron deficient alkenes undergo predominantly *cis*-hydroxylation, electron rich alkenes undergo epoxidation mainly, indicates that the substrate may determine how the O–O bond is cleaved.

An important question arises as to the nature of the manganese species that engages in activation of the peroxide to oxidise the alkene. One possibility is the formation of a high valent manganese-oxo species through heterolysis of the acetone peroxy O–O bond. The relatively slow reaction rate, even in the presence of excess  $\text{H}_2\text{O}_2$ , could suggest that Lewis acid activation of the coordinated oxygen atom of the acetone- $\text{H}_2\text{O}_2$  adduct by the  $\text{Mn}^{\text{II}}$  centre is important, however. In such a case the oxygen atom of the peroxide that is coordinated to the  $\text{Mn}^{\text{II}}$  ion would be rendered electrophilic in terms of its interaction with the alkene. For electron poor alkenes addition of this oxygen atom may be assisted by nucleophilic attack on the neighbouring carbon atom by the -OH group of the acetone peroxide adduct. Such a mechanism could rationalise the difference in selectivity observed for electron rich and electron deficient alkenes.

With regard to the differences in maximum conversion observed (Table 1) overall the data suggests that it is secondary oxidation products which are responsible for catalyst inhibition. It should be noted that the addition of acids after the reaction has commenced slows, but does not halt, conversion. Hence, in the case of electron rich alkenes (Table 2), secondary oxidation products although formed will not inhibit that catalyst significantly (*vide supra*). For the  $\alpha,\beta$ -unsaturated substrates (Table 1), however, the secondary oxidation products are likely to include oxalate monoester type species, which may sequester the manganese efficiently and thereby reduce or inhibit conversion. The qualitative correlation between the rate of conversion of the substrate and the maximum conversion supports this conclusion. For substrates such as maleimide and diethyl fumarate, further oxidation of the *cis*-diol product is not competitive and hence good conversion and selectivity is observed. For less reactive substrates further oxidation of the *cis*-diol product becomes significant and hence secondary oxidation products form, which can inhibit the reaction, before full conversion.

#### 4.4 Summary and conclusions

Overall, the substrate scope for *cis*-dihydroxylation obtained with  $\text{Mn}^{\text{II}}$ /pyridine-2-carboxylic acid is complimentary to the  $[\text{Mn}^{\text{IV,IV}}_2\text{O}_3(\text{TMTACN})_2]^{2+}$  based systems (see also Chapter 2)<sup>10b,c</sup> (*vide supra*) and extends the scope of alkenes that can be converted with high turnover numbers to *cis*-diols using 1<sup>st</sup> row transition metals and  $\text{H}_2\text{O}_2$ .<sup>19</sup> Importantly, the system presented here is most effective for substrates that, to date, have proven most challenging, even for osmium based reagents. The *in situ* preparation of the

catalyst from readily available reagents together with its ease of application (equally well from milligram to multi-gram scale reactions, see the experimental section) and using H<sub>2</sub>O<sub>2</sub> makes this an excellent alternative to the RuCl<sub>3</sub>/NaIO<sub>4</sub> based *cis*-dihydroxylation method for substrates such as maleimides.<sup>6</sup>

In conclusion, it was demonstrated that the catalyst system Mn<sup>II</sup>/pyridine-2-carboxylic acid/NaOAc in acetone or 2-butanone can achieve high turnover *cis*-dihydroxylation of, in particular, electron deficient *trans*-alkenes. From a broader perspective these results demonstrate, as shown by Burgess and co-workers for epoxidation previously,<sup>20</sup> that relatively simple ligand/metal systems hold remarkable potential in achieving synthetically useful selective oxidative transformations. Importantly, in this chapter it was shown that even at room temperature high turnover numbers and reaction rates can be achieved. Future studies, directed to identifying the catalytically active species involved in the reaction, are described in Chapter 5.

## 4.5 Experimental section

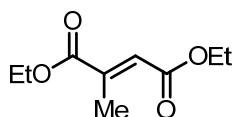
All reagents are of commercial grade and used as received unless stated otherwise. Hydrogen peroxide was used as received as a 50 wt. % solution in water; note that the grade of H<sub>2</sub>O<sub>2</sub> employed can affect the reaction when sequestrants are present as stabilizers. NMR spectra were recorded at <sup>1</sup>H NMR (500 or 400.0 or 200.0 MHz) and <sup>13</sup>C NMR (100.59 or 50.0 MHz). Chemical shifts are denoted relative to the residual solvent absorption (<sup>1</sup>H: CDCl<sub>3</sub> 7.26 ppm, DMSO-*d*<sub>6</sub> 2.50 ppm, CD<sub>3</sub>OD 3.31 ppm, acetone-*d*<sub>6</sub> 2.05 ppm; <sup>13</sup>C: CDCl<sub>3</sub> 77.0 ppm, DMSO-*d*<sub>6</sub> 39.5 ppm, CD<sub>3</sub>OD 49.0 ppm).<sup>21</sup> Raman spectra were recorded using a fibre optic equipped dispersive Raman spectrometer (785 nm, Perkin Elmer Raman Flex). Temperature was controlled using a cuvette holder equipped with a custom made fibre optic probe holder (Quantum Northwest). 1,2-Dichlorobenzene was employed as internal standard for Raman spectroscopy.

**Caution.** The drying or concentration of acetone solutions that potentially contain hydrogen peroxide should be avoided. Prior to drying or concentrating, the presence of H<sub>2</sub>O<sub>2</sub> should be tested for using peroxide test strips followed by neutralisation on solid NaHSO<sub>3</sub> or another suitable reducing agent. When working with H<sub>2</sub>O<sub>2</sub>, especially in acetone, suitable protective safeguards should be in place at all times due to risk of explosion.

**Caution.** Perchlorate salts are potentially explosive in combination with organic solids and solvents. In the present study Mn(OAc)<sub>2</sub> or MnSO<sub>4</sub> were found to give essentially identical reactivity and should be used for reactions above 2 gram scale.

### 4.5.1 Synthesis and characterization of alkene substrates

#### Diethyl-2-methylfumarate<sup>22</sup>



Concentrated H<sub>2</sub>SO<sub>4</sub> (0.6 ml) was added to a stirred mixture of mesaconic acid (5.29 g, 40.3 mmol) in EtOH (40 ml) at room temperature. The reaction mixture was stirred and heated at reflux

for 16 h. After cooling, the reaction mixture was concentrated *in vacuo* and the residue was diluted with H<sub>2</sub>O (20 ml), 2 M NaOH (20 ml), then extracted with EtOAc (3 x 20 ml). The combined organic layers were washed with brine, dried over MgSO<sub>4</sub>, filtered and concentrated *in vacuo*. The crude product was purified by vacuum distillation to afford diethyl-2-methylfumarate as a colourless oil (6.02 g, 32.3 mmol, 80%). <sup>1</sup>H NMR (400 MHz, CDCl<sub>3</sub>) δ 6.74 (m, 1H), 4.24 – 4.14 (m, 4H), 2.25 (d, 3H), 1.31 – 1.24 (m, 6H); <sup>13</sup>C NMR (100 MHz, CDCl<sub>3</sub>) δ 167.0, 165.8, 143.6, 126.5, 61.4, 60.5, 14.12, 14.07, 14.01. HRMS (ESI+, *m/z*) calc. for C<sub>9</sub>H<sub>15</sub>O<sub>4</sub> [M+H]<sup>+</sup> 187.0970, found 187.0965. Elemental analysis (calc. for C<sub>9</sub>H<sub>14</sub>O<sub>4</sub>) C 57.87% (58.05%), H 7.62% (7.58%).

### *N,N*-Dibutylmaleamide

1-[3-(dimethylamino)propyl]-3-ethylcarbodiimide (*n*-Bu)HN-C(=O)-C(=O)-NH(*n*-Bu) hydrochloride (7.50 g, 39.3 mmol) was added to a solution of maleic acid (1.52 g, 13.1 mmol), *n*-butylamine (3.1 ml, 31.4 mmol) and 1-hydroxybenzotriazole (4.20 g, 31.4 mmol) in THF (100 ml) cooled in an ice/water bath. The reaction mixture was stirred for 18 h and allowed to reach room temperature gradually. The reaction mixture was concentrated *in vacuo* and the residue diluted with EtOAc (50 ml) followed by addition of saturated aqueous NaHCO<sub>3</sub> solution (50 ml). The aqueous layer was extracted with EtOAc (3 x 20 ml). The combined organic layers were washed with brine, dried over MgSO<sub>4</sub>, filtered and concentrated *in vacuo*. *N,N*-Dibutylmaleamide (2.86 g, 12.6 mmol, 96%) was obtained as a yellow oil and used directly without further purification. <sup>1</sup>H NMR (400 MHz, CDCl<sub>3</sub>) δ 9.07 (s, 2H), 6.07 (s, 2H), 3.24 (td, *J* = 7.2 Hz, 5.7 Hz, 4H), 1.54 – 1.45 (m, 4H), 1.39 – 1.28 (m, 4H), 0.88 (t, *J* = 7.3 Hz, 6H); <sup>13</sup>C NMR (100 MHz, CDCl<sub>3</sub>) δ 164.9, 132.5, 39.5, 31.1, 20.1, 13.6.

### 4-(Benzylamino)-4-oxobut-2-enoic acid

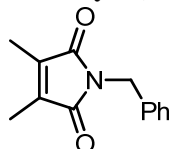
A solution of benzylamine (3.10 g, 28.9 mmol) in dry Et<sub>2</sub>O (100 ml) was added dropwise to a stirred solution of maleic anhydride (2.94 g, 30.0 mmol) in dry Et<sub>2</sub>O (300 ml). The solution was stirred for a further 2 h then filtered, and the filtered solid was washed with Et<sub>2</sub>O and dried *in vacuo* to give the crude 4-(benzylamino)-4-oxobut-2-enoic acid (5.44 g, 26.5 mmol, 92%) which was used without further purification. <sup>1</sup>H NMR (400 MHz, CDCl<sub>3</sub>) δ 7.33 (m, 5H), 6.86 (s, 1H), 6.35 (d, *J* = 12.8 Hz, 1H), 6.17 (d, *J* = 12.8 Hz, 1H), 4.54 (s, 2H), 3.90 (s, 1H). HRMS (APCI+, *m/z*) calc. for C<sub>11</sub>H<sub>12</sub>NO<sub>3</sub> [M+H]<sup>+</sup> 206.0817, found 206.0812.

### 1-Benzyl-1H-pyrrole-2,5-dione

A solution of crude 4-(benzylamino)-4-oxobut-2-enoic acid (3.72 g, 18.13 mmol) in glacial acetic acid (35 ml) was heated under reflux for 16 h then cooled and concentrated under reduced pressure. The residue was diluted with EtOAc (20 ml) and washed with aqueous 10% HCl, aqueous NaHCO<sub>3</sub>, dried and evaporated under reduced pressure. The crude reaction mixture was purified by

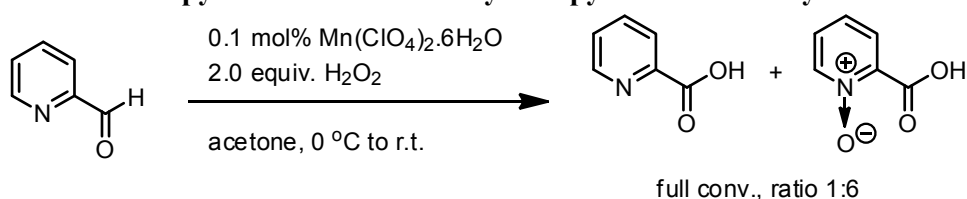
column chromatography (SiO<sub>2</sub>, EtOAc/pentane = 30/70) to provide the product as a white solid (1.13 g, 6.02 mmol, 33%). m.p. 69.9-70.7 °C. <sup>1</sup>H NMR (400 MHz, CDCl<sub>3</sub>) δ 7.37 – 7.27 (m, 5H), 6.71 (s, 2H), 4.68 (s, 2H); <sup>13</sup>C NMR (50 MHz, CDCl<sub>3</sub>) δ 170.3, 136.1, 134.1, 128.6, 128.3, 127.8, 41.3. HRMS (APCI+, *m/z*) calc. for C<sub>11</sub>H<sub>10</sub>NO<sub>2</sub> [M+H]<sup>+</sup> 188.0712, found 188.0706. Elemental analysis (calc. for C<sub>11</sub>H<sub>9</sub>NO<sub>2</sub>) C 70.45% (70.58%), H 4.83% (4.85%), N 7.43% (7.48%).

### 1-Benzyl-3,4-dimethyl-pyrrole-2,5-dione



A solution of benzylamine (1.95 g, 18.2 mmol) in dry Et<sub>2</sub>O (50 ml) was added dropwise to a stirred solution of dimethylmaleic anhydride (2.60 g, 20.0 mmol) in dry Et<sub>2</sub>O (200 ml). The solution was stirred for a further 2 h then filtered, and the filtered solid was washed with Et<sub>2</sub>O and dried *in vacuo* to give the crude 4-(benzylamino)-2,3-dimethyl-4-oxobut-2-enoic acid (2.98 g) which was used without further purification. A solution of crude 4-(benzylamino)-2,3-dimethyl-4-oxobut-2-enoic acid in glacial acetic acid (30 ml) was heated under reflux for 16 h then cooled and concentrated under reduced pressure. The residue was diluted with EtOAc (20 ml) and washed with aqueous 10% HCl, aqueous NaHCO<sub>3</sub>, dried and evaporated under reduced pressure. The crude reaction mixture was purified by column chromatography (SiO<sub>2</sub>, EtOAc/pentane = 30/70) to provide the product as a yellow oil (1.48 g, 6.89 mmol, 38% for 2 steps). <sup>1</sup>H NMR (200 MHz, CDCl<sub>3</sub>) δ 7.38 – 7.23 (m, 5H), 4.64 (s, 2H), 1.95 (s, 6H); <sup>13</sup>C NMR (50 MHz, CDCl<sub>3</sub>) δ 171.8, 137.2, 136.7, 128.5, 128.3, 127.6, 41.4, 8.7. HRMS (APCI+, *m/z*) calc. for C<sub>13</sub>H<sub>14</sub>NO<sub>2</sub> [M+H]<sup>+</sup> 216.1025, found 216.1019. Elemental analysis (calc. for C<sub>13</sub>H<sub>13</sub>NO<sub>2</sub>) C 72.64% (72.54%), H 6.11% (6.09%), N 6.40% (6.51%).

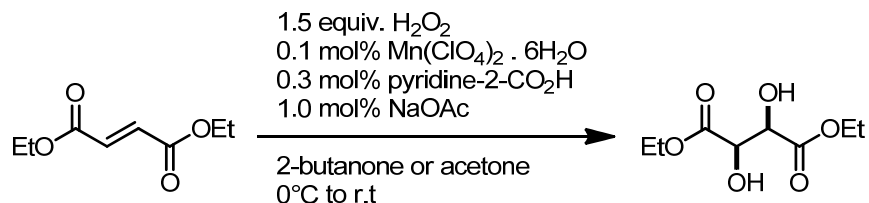
### 4.5.2 Oxidation of pyridine-2-carboxaldehyde to pyridine-2-carboxylic acid



Pyridine-2-carboxaldehyde (3 mmol, 0.32 g) and Mn(ClO<sub>4</sub>)<sub>2</sub>·6H<sub>2</sub>O (3 μmol added as 2 ml of a stock solution in acetone, 10.8 mg in 20 ml) were added to 4 ml of acetone and cooled in an ice/water bath. After addition of 340 μl of H<sub>2</sub>O<sub>2</sub> (50 wt. % in water, 0.34 ml, 6 mmol, 2 equiv.), the mixture was stirred for 16 h, allowing the temperature to rise slowly to room temperature. The reaction mixture was diluted with H<sub>2</sub>O (10 ml) and extracted with CH<sub>2</sub>Cl<sub>2</sub>. The organic extract was dried over MgSO<sub>4</sub> and solvent was removed *in vacuo*.

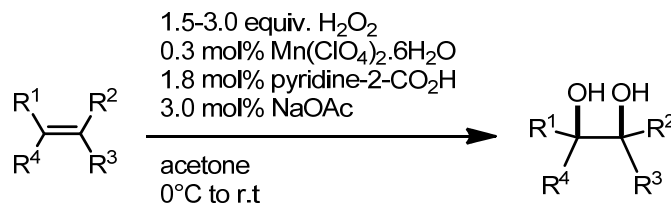
### 4.5.3 Procedures for catalysed *cis*-dihydroxylation of alkenes reported in Table 1

#### 3.1 *cis*-Dihydroxylation of diethyl fumarate using acetone or 2-butanone as solvent (entry 1)



A stock solution containing both  $\text{Mn}(\text{ClO}_4)_2 \cdot 6\text{H}_2\text{O}$  (7.3 mg, 20.0  $\mu\text{mol}$ ) and pyridine-2-carboxylic acid (7.5 mg, 60.0  $\mu\text{mol}$ ) in 2-butanone or acetone (20 ml) was prepared. 1.0 ml of this stock solution (1.0  $\mu\text{mol}$   $\text{Mn}(\text{ClO}_4)_2 \cdot 6\text{H}_2\text{O}$ , 0.1 mol%, and 3.0  $\mu\text{mol}$  pyridine-2-carboxylic acid, 0.3 mol%) was added to the solution of diethyl fumarate (168 mg, 1.00 mmol) in 2-butanone or acetone (0.5 ml), while stirring the mixture at room temperature. After addition of 17.0  $\mu\text{l}$  of a 0.6 M stock (aqueous) of NaOAc (0.1 mmol, 1.0 mol%), the mixture was cooled in ice/water bath and, with stirring,  $\text{H}_2\text{O}_2$  (50 wt. % in water, 85  $\mu\text{l}$ , 1.5 mmol, 1.5 equiv.) was added in one portion. The mixture was stirred for 16 h, allowing temperature to rise to room temperature. Excess solid  $\text{NaHSO}_3$  was added to the reaction mixture, until no peroxides remained (shown by peroxide test-strips). The salts were filtered off, washed several times with acetone, after which the acetone was removed *in vacuo*, giving the product as colourless oil (195 mg, 0.95 mmol, 95%).  $^1\text{H}$  NMR (400 MHz,  $\text{CDCl}_3$ )  $\delta$  4.52 (d,  $J$  = 3.7 Hz, 2H), 4.33 – 4.26 (m, 4H), 3.43 (s, 2H), 1.33 – 1.28 (m, 6H);  $^{13}\text{C}$  NMR (100 MHz,  $\text{CDCl}_3$ )  $\delta$  171.6, 72.0, 62.5, 14.1. HRMS (ESI+,  $m/z$ ) calc. for  $\text{C}_8\text{H}_{14}\text{O}_6$  ( $\text{M}+\text{Na}$ ) $^+$  229.0688, found 229.0683. Elemental analysis (calc. for  $\text{C}_8\text{H}_{14}\text{O}_6$ ) C 45.75% (46.60%), H 6.90% (6.84%).

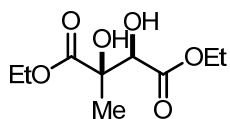
#### 4.5.4 General procedure for *cis*-dihydroxylation of electron deficient alkenes (Table1)



A stock solution containing  $\text{Mn}(\text{ClO}_4)_2 \cdot 6\text{H}_2\text{O}$  (22.0 mg, 0.06 mmol) and pyridine-2-carboxylic acid (45.0 mg, 0.36 mmol) in acetone (20 ml) was prepared. 1.0 ml of this stock solution (3.0  $\mu\text{mol}$   $\text{Mn}(\text{ClO}_4)_2 \cdot 6\text{H}_2\text{O}$ , 0.3 mol%, and 18.0  $\mu\text{mol}$  pyridine-2-carboxylic acid, 1.8 mol%) was added to the solution of substrate (1 mmol) in acetone (2 ml), while stirring the mixture at room temperature. After addition of 50.0  $\mu\text{l}$  of a 0.6 M (aqueous) NaOAc (30.0  $\mu\text{mol}$ , 3.0 mol%), the mixture was cooled in an ice/water bath and  $\text{H}_2\text{O}_2$  (50 wt. % in water, 170  $\mu\text{l}$ , 3.0 mmol, 3.0 equiv. for entry 2, 3, 5 and 8 or 113  $\mu\text{l}$ , 2.0 mmol, 2.0 equiv. for entry 6, 7 and 9 or 85  $\mu\text{l}$ , 1.5 mmol, 1.5 equiv. for entry 4) was added *via* syringe pump (rate between 1-3  $\mu\text{l}/\text{min}$  except for entry 4,  $\text{H}_2\text{O}_2$  is added in

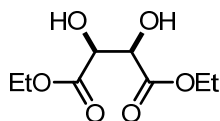
one go). The mixture was stirred for 16 h, allowing temperature to rise to room temperature. After 16 h, excess solid  $NaHSO_3$  was added to the reaction mixture, to remove residual peroxides (verified by peroxide test-strips). The salts were filtered off, washed several times with excess acetone, after which the acetone was removed *in vacuo*, giving product directly or the crude reaction mixture that need to be purified further.

#### Diethyl 2,3-dihydroxy-2-methylsuccinate (entry 2)



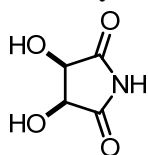
Colourless oil obtained as the product without any purification after work up (207 mg, 0.94 mmol, 91%).  $^1H$  NMR (500 MHz,  $-10^\circ C$ ,  $CDCl_3$ )  $\delta$  4.32 (d,  $J$  = 8.0 Hz, 1H), 4.28 – 4.18 (m, 4H), 4.00 (s, 1H), 3.79 (d,  $J$  = 8.6 Hz, 1H), 1.44 (s, 3H), 1.26 (m, 6H);  $^{13}C$  NMR (100 MHz,  $CDCl_3$ )  $\delta$  174.2, 171.2, 76.7, 75.0, 62.3, 62.0, 21.8, 14.0, 13.9. HRMS (ESI+,  $m/z$ ) calc. for  $C_9H_{16}O_6$  ( $M+Na$ ) $^+$  243.0845, found 243.0839. Elemental analysis (calc. for  $C_9H_{16}O_6$ ) C 49.19% (49.09%), H 7.48% (7.32%).

#### Diethyl 2,3-dihydroxysuccinate (entry 3)



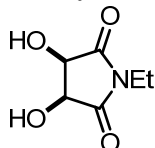
The crude product was purified by column chromatography ( $SiO_2$ , EtOAc/pentane = 40/60 to 100/0) to provide the recovered starting material (213 mg, 1.24 mmol, 25%) and the product as a white solid (489 mg, 2.37 mmol, 47%). m.p.  $57.3-58.1^\circ C$ .  $^1H$  NMR (400 MHz,  $CDCl_3$ )  $\delta$  4.55 (s, 2H), 4.27 (m, 4H), 3.18 (s, 2H), 1.32 – 1.27 (t, 6H);  $^{13}C$  NMR (100 MHz,  $CDCl_3$ )  $\delta$  171.0, 72.9, 62.2, 14.0. HRMS (ESI+,  $m/z$ ) calc. for  $C_8H_{14}O_6$  ( $M+Na$ ) $^+$  229.0688, found 229.0682. Elemental analysis (calc. for  $C_8H_{14}O_6$ ) C 47.99% (46.60%), H 7.07% (6.84%).

#### 3,4-Dihydroxypyrrolidine-2,5-dione (entry 4)

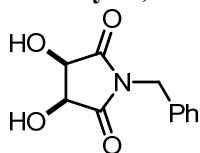


White solid obtained as the product without any purification after work up (640 mg, 4.88 mmol, 98 %). m.p.  $124.7-125.2^\circ C$ .  $^1H$  NMR (400 MHz,  $CD_3OD$ )  $\delta$  4.41 (s, 2H);  $^{13}C$  NMR (100 MHz,  $CD_3OD$ )  $\delta$  179.0, 70.4. HRMS (ESI+,  $m/z$ ) calc. for  $C_4H_6NO_4$  [ $M+H$ ] $^+$  132.0297, found 132.0291. Elemental analysis (calc. for  $C_4H_5NO_4$ ) C 36.60% (36.65%), H 3.76% (3.84%), N 10.71% (10.69%).

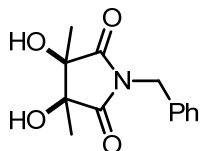
#### 1-Ethyl-3,4-dihydroxypyrrolidine-2,5-dione (entry 5)



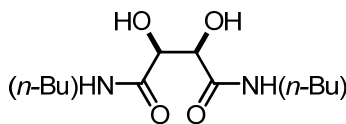
White solid obtained as the product without any purification after work up (150 mg, 0.94 mmol, 98%). m.p.  $122.6-123.9^\circ C$ .  $^1H$  NMR (400 MHz,  $CD_3OD$ )  $\delta$  4.42 (s, 2H), 3.53 (q,  $J$  = 7.2 Hz, 2H), 1.15 (t,  $J$  = 7.2 Hz, 3H);  $^{13}C$  NMR (100 MHz,  $CD_3OD$ )  $\delta$  177.7, 69.3, 34.3, 13.0. Elemental analysis (calc. for  $C_6H_9O_4N$ ) C 44.24% (45.28%), H 5.64% (5.70%), N 8.99% (8.80%).

**1-Benzyl-3,4-dihydroxypyrrolidine-2,5-dione (entry 6)**

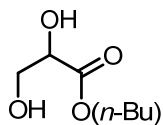
White solid obtained as the product without any purification after work up (403 mg, 1.82 mmol, 91%). m.p. 131.7-132.9 °C.  $^1\text{H}$  NMR (400 MHz,  $\text{DMSO-}d_6$ )  $\delta$  7.35 – 7.22 (m, 5H), 4.55 (s, 2H), 4.42 (s, 2H);  $^{13}\text{C}$  NMR (100 MHz,  $\text{DMSO-}d_6$ )  $\delta$  176.3, 135.9, 128.4, 127.39, 127.37, 68.0, 40.9. HRMS (APCI+,  $m/z$ ) calc. for  $\text{C}_{11}\text{H}_{12}\text{NO}_4$   $[\text{M}+\text{H}]^+$  222.0766, found 222.0761.

**1-Benzyl-3,4-dihydroxy-3,4-dimethylpyrrolidine-2,5-dione (entry 7)**

The crude product was purified by column chromatography ( $\text{SiO}_2$ ,  $\text{EtOAc/pentane} = 30/70$  to  $50/50$ ) to provide the product as an off-white solid (374 mg, 1.50 mmol, 75%). m.p. 96.7-97.1 °C.  $^1\text{H}$  NMR (400 MHz,  $\text{CDCl}_3$ )  $\delta$  7.32 – 7.26 (m, 5H), 4.66 (s, 2H), 3.44 (s, 2H), 1.38 (s, 6H);  $^{13}\text{C}$  NMR (100 MHz,  $\text{CDCl}_3$ )  $\delta$  177.0, 135.0, 128.8, 128.2, 128.1, 75.4, 42.3, 18.9. HRMS (APCI+,  $m/z$ ) calc. for  $\text{C}_{13}\text{H}_{16}\text{NO}_4$   $[\text{M}+\text{H}]^+$  250.1079, found 250.1067.

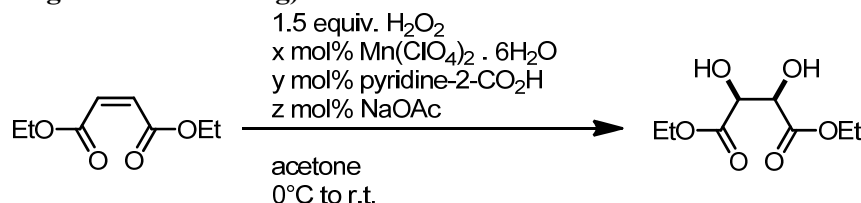
***N,N*-Dibutyl-2,3-dihydroxysuccinamide (entry 8)**

The crude product was purified by recrystallization from hot  $\text{Et}_2\text{O}$  to provide the product as a white solid (175 mg, 0.67 mmol, 32%). m.p. 160.1-160.9 °C.  $^1\text{H}$  NMR (400 MHz,  $\text{CDCl}_3$ )  $\delta$  7.07 (s, 2H), 5.69 (s, 2H), 4.00 (s, 2H), 3.34 – 3.26 (m, 4H), 1.58 – 1.48 (m, 4H), 1.41 – 1.31 (m, 4H), 0.94 (t,  $J = 7.3$  Hz, 6H);  $^{13}\text{C}$  NMR (100 MHz,  $\text{CDCl}_3$ )  $\delta$  172.9, 70.1, 38.8, 31.4, 20.0, 13.7. Elemental analysis (calc. for  $\text{C}_{12}\text{H}_{24}\text{N}_2\text{O}_4$ ) C 55.17% (55.36%), H 9.29% (9.29%), N 10.68% (10.76%).

**Butyl 2,3-dihydroxypropanoate (entry 9)**

1,2-Dichloroethane (44.0 mg, 0.44 mmol) was added to the crude reaction mixture as an external standard, and a sample was diluted with  $\text{CDCl}_3$  to facilitate the measurement by  $^1\text{H}$  NMR spectroscopy.  $^1\text{H}$  NMR analysis of the solution provided a product yield relative to the external standard integration. This reaction showed 19% starting material remaining and 55% of the *cis*-diol product.  $^1\text{H}$  NMR of *n*-butyl acrylate (400 MHz,  $\text{CDCl}_3$ )  $\delta$  6.37 (dd,  $J = 17.3$  Hz, 1.5 Hz, 1H), 6.09 (dd,  $J = 17.3$  Hz, 10.4 Hz, 1H), 5.79 (dd,  $J = 10.4$  Hz, 1.5 Hz, 1H), 4.13 (t,  $J = 6.7$  Hz, 2H), 1.63 (dt,  $J = 14.9$  Hz, 6.8 Hz, 2H), 1.43 – 1.31 (m, 2H), 0.91 (td,  $J = 7.4$  Hz, 2.2 Hz, 3H) and  $^1\text{H}$  NMR of *n*-butyl 2,3-dihydroxypropanoate (400 MHz,  $\text{CDCl}_3$ )  $\delta$  4.26 – 4.22 (m, 1H), 4.20 (td,  $J = 6.7$  Hz, 1.5 Hz, 2H), 3.91 – 3.76 (m, 2H), 3.51 (d,  $J = 4.9$  Hz, 1H), 2.71 (s, 1H), 1.63 (dt,  $J = 14.9$  Hz, 6.8 Hz, 2H), 1.43 – 1.31 (m, 2H), 0.91 (td,  $J = 7.4$  Hz, 2.2 Hz, 3H).

#### 4.5.5 Optimization of conditions for diethyl maleate (improved conversion with lowering substrate loading)



**condition a:** 3.0 mmol diethyl maleate, 0.1 mol%  $\text{Mn}(\text{ClO}_4)_2 \cdot 6\text{H}_2\text{O}$ , 0.6 mol% pyridine-2- $\text{CO}_2\text{H}$ , 1.0 mol%  $\text{NaOAc}$ , 1.5 equiv.  $\text{H}_2\text{O}_2$ , acetone,  $0^\circ\text{C}$  to r.t.

**condition b:** 1.0 mmol diethyl maleate, 0.3 mol%  $\text{Mn}(\text{ClO}_4)_2 \cdot 6\text{H}_2\text{O}$ , 1.8 mol% pyridine-2- $\text{CO}_2\text{H}$ , 3.0 mol%  $\text{NaOAc}$ , 1.5 equiv.  $\text{H}_2\text{O}_2$ , acetone,  $0^\circ\text{C}$  to r.t.

**condition c:** 0.25 mmol diethyl maleate, 1.2 mol%  $\text{Mn}(\text{ClO}_4)_2 \cdot 6\text{H}_2\text{O}$ , 7.2 mol% pyridine-2- $\text{CO}_2\text{H}$ , 12.0 mol%  $\text{NaOAc}$ , 1.5 equiv.  $\text{H}_2\text{O}_2$ , acetone,  $0^\circ\text{C}$  to r.t.

**condition a:** 33% conv. by Raman spectroscopy

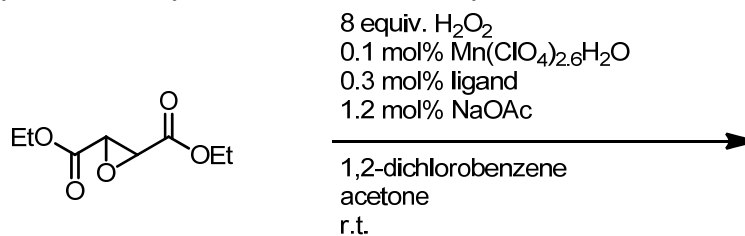
**condition b:** 63% conv., 55% diol product by  $^1\text{H}$  NMR spectroscopy

**condition c:** 63% conv., 55% diol product by  $^1\text{H}$  NMR spectroscopy

#### 4.5.6 General procedure for *cis*-dihydroxylation of electron rich alkenes (Table 2)

A stock solution containing both  $\text{Mn}(\text{ClO}_4)_2 \cdot 6\text{H}_2\text{O}$  (3.6 mg, 0.01 mmol) and pyridine-2-carboxylic acid (62.0 mg, 0.5 mmol) in acetone- $d_6$  (20 ml) was prepared prior to the experiment. 1.5 ml of this stock solution (0.75  $\mu\text{mol}$   $\text{Mn}(\text{ClO}_4)_2 \cdot 6\text{H}_2\text{O}$ , 0.1 mol%, and 37.5  $\mu\text{mol}$  pyridine-2-carboxylic acid, 5.0 mol%) was added to the solution of cyclohexene (54 mg, 0.65 mmol) and 1,2-dichlorobenzene (46 mg, 0.31 mmol) in  $\text{H}_2\text{O}$  (200  $\mu\text{l}$ ), while stirring the mixture at room temperature. After addition of 11.3  $\mu\text{l}$  of a 0.6 M stock (aqueous) of  $\text{NaOAc}$  (6.8  $\mu\text{mol}$ , 0.9 mol%), the mixture was cooled in an ice/water bath and  $\text{H}_2\text{O}_2$  (50 wt. % in water, 64  $\mu\text{l}$ , 1.13 mmol, 1.5 equiv.) was added in one portion. The mixture was stirred for 16 h, allowing temperature to rise to room temperature. After 16 h, the mixture was measured by  $^1\text{H}$  NMR spectroscopy.  $^1\text{H}$  NMR analysis of the solution provided product yield relative to the internal standard (1,2-dichlorobenzene) integration and the products were identified by comparison to the  $^1\text{H}$  NMR spectra of authentic samples.

#### 4.5.7 Stability of *rac*-diethyl oxirane-2,3-dicarboxylate



The epoxide product of diethyl fumarate was subjected to typical reaction conditions to determine the involvement of epoxide ring-opening in the reaction. Under optimised reaction conditions for diethyl fumarate over 24 h no change was noted by Raman



spectroscopy. The reaction was subsequently quenched on saturated aqueous  $\text{NaHCO}_3$ , extracted with  $\text{CH}_2\text{Cl}_2$ , dried and solvent removed *in vacuo*. The  $^1\text{H}$  NMR spectrum obtained for the recovered material showed only the initial epoxide. The stability of the epoxide under reaction conditions confirms that *cis*-diol products are from direct *cis*-dihydroxylation and not from initial epoxidation followed by ring-opening.

## 4.6 References and notes

- 1 (a) B. S. Lane and K. Burgess, *Chem. Rev.*, 2003, **103**, 2457; (b) R. A. Sheldon and J. K. Kochi, *Metal-Catalyzed Oxidations of Organic Compounds*, 1981, Academic Press; (c) W. R. Browne, J. W. de Boer, D. Pijper, J. Brinksma, R. Hage and B. L. Feringa in Chapter 11, J.-E. Bäckvall, (ed.) *Modern Oxidation Methods*, 2010, Wiley-VCH, 371; (d) R. Noyori, M. Aoki and K. Sato, *Chem. Commun.*, 2003, 1977; (e) T. Katsuki, *Chem. Soc. Rev.*, 2004, **33**, 437.
- 2 H. C. Kolb, M. S. van Nieuwenhze and K. B. Sharpless, *Chem. Rev.*, 1994, **94**, 2483.
- 3 (a) B. Plietker and M. Niggemann, *J. Org. Chem.*, 2005, **70**, 2402; (b) V. Piccialli, D. M. A. Smaldone and D. Sica, *Tetrahedron*, 1993, **49**, 4211.
- 4 (a) T. K. M. Shing, E. K. W. Tam, V. W.-F. Tai, I. H. F. Chung and Q. Jiang, *Chem. Eur. J.*, 1996, **2**, 50; (b) T. K. M. Shing, V. W.-F. Tai, E. K. W. Tam, *Angew. Chem., Int. Ed.*, 1994, **33**, 2312.
- 5 (a) D. W. Nelson, A. Gypser, P. T. Ho, H. C. Kolb, T. Kondo, H.-L. Kwong, D. V. McGrath, A. E. Rubin, P.-O. Norrby, K. P. Gable and K. B. Sharpless, *J. Am. Chem. Soc.*, 1997, **119**, 1840; (b) T. Katsuki, K. B. Sharpless, *J. Am. Chem. Soc.*, 1980, **102**, 5974.
- 6 M. Couturier, B. M. Andresen, J. B. Jorgensen, J. L. Tucker, F. R. Busch, S. J. Brenek, P. Dubé, D. J. am Ende and J. T. Negri, *Org. Proc. Res. Dev.*, 2002, **6**, 42.
- 7 T. Kimura, S. Kanagaki, Y. Matsui, M. Imoto, T. Watanabe and M. Shibasaki, *Org. Lett.*, 2012, **14**, 4418.
- 8 (a) M. Fujita, M. Costas and L. Que, Jr., *J. Am. Chem. Soc.*, 2003, **125**, 9912; (b) K. Chen, M. Costas, J. Kim, A. K. Tipton and L. Que, Jr., *J. Am. Chem. Soc.*, 2002, **124**, 3026; (c) J. Y. Ryu, J. Kim, M. Costas, K. Chen, W. Nam and L. Que, Jr., *Chem. Comm.*, 2002, 1288.
- 9 D. E. De Vos, S. De Wildeman, B. F. Sels, P. J. Grobet and P. A. Jacobs, *Angew. Chem. Int. Ed.*, 1999, **38**, 980.
- 10 (a) J. Brinksma, L. Schmieder, G. Van Vliet, R. Boaron, R. Hage, De D. E. Vos, P. L. Alsters and B. L. Feringa, *Tetrahedron Lett.*, 2002, **43**, 2619; (b) J. W. de Boer, J. Brinksma, W. R. Browne, A. Meetsma, P. L. Alsters, R. Hage and B. L. Feringa, *J. Am. Chem. Soc.*, 2005, **127**, 7990; (c) J. W. de Boer, W. R. Browne, J. Brinksma, P. L. Alsters, R. Hage and B. L. Feringa, *Inorg. Chem.*, 2007, 6353; (d) J. W. de Boer, P. L. Alsters, A. Meetsma, R. Hage, W. R. Browne and B. L. Feringa, *Dalton*, 2008, **44**, 6283; (e) J. W. de Boer, W. R. Browne, S. R. Harutyunyan, L. Bini, T. D. Tiemersma-Wegman, P. L. Alsters, R. Hage and B. L. Feringa, *Chem. Commun.*, 2008, 3747.
- 11 The manganese–TMTACN based catalysts have proven versatile in a wide range of oxidative transformations with  $\text{H}_2\text{O}_2$ . (a) K. Wieghardt, U. Bossek, B. Nuber, J. Weiss, J. Bonvoisin, M. Corbella, S. E. Vitols and J. J. Girerd, *J. Am. Chem. Soc.*, 1988, **110**, 7398; (b) R. Hage, J. E. Iburg, J. Kerschner, J. H. Koek, E. L. M. Lempers, R. J. Martens, U. S. Racherla, S.W. Russell, T. Swarthoff, M. R. P. van Vliet, J. B. Warnaar, L. Van Der Wolf and B. Krijnen, *Nature*, 1994, **369**,

- 637; (c) D. E. De, Vos and T. Bein, *Chem. Commun.*, 1996, 917; (d) C. Zondervan, R. Hage and B. L. Feringa, *Chem. Commun.*, 1997, 419; (e) D. E. De Vos, B. F. Sels, M. Reynaers, Y. V. Subba, Rao and P. A. Jacobs, *Tetrahedron Lett.*, 1998, **39**, 3221; (f) A. Berkessel and C. A. Sklorz, *Tetrahedron Lett.*, 1999, **40**, 7965; (g) C. B. Woitiski, Y. N. Kozlov, D. Mandelli, G. V. Nizova, U. Schuchardt and G. B. Shul'pin, *J. Mol. Catal. A.*, 2004, **222**, 103.
- 12 W.-P. Yip, C.-M. Ho, N. Zhu, T.-C. Lau and C.-M. Che, *Chem. Asian J.*, 2008, **3**, 70.
- 13 TMTACN is *N,N',N''*-trimethyl-1,4,7-triazacyclononane.
- 14 Under the reaction conditions employed, the epoxide (diethyl oxirane-2,3-dicarboxylate) was found to be fully stable and did not undergo ring opening, precluding this as being a route to formation of the *cis*-diol products.
- 15 With excess H<sub>2</sub>O<sub>2</sub> (10 equiv.) monomethoxyoxalic acid was formed which could be expected to sequester manganese ions.
- 16 M. Fujita, M. Costas and L. Que, Jr., *J. Am. Chem. Soc.*, 2003, **125**, 9912.
- 17 A. M. I. Payeras, R. Y. N. Ho, M. Fujita and L. Que, Jr., *Chem. Eur. J.*, 2004, **10**, 4944.
- 18 (a) A. D. Brewer, *Chem. Brit.*, 1975, **11**, 335; (b) G. M. Bodner, *J. Chem. Educ.*, 1985, **62**, 1105.
- 19 For the heterogenised Mn-TMTACN catalysts of De Vos and coworkers<sup>9</sup> and Feringa and coworkers<sup>10</sup> using [Mn<sup>IV,IV</sup><sub>2</sub>O<sub>3</sub>(TMTACN)<sub>2</sub>]<sup>2+</sup> with carboxylic acids, in which the active [Mn<sup>III,III</sup><sub>2</sub>O(RCO<sub>2</sub>)<sub>2</sub>(TMTACN)<sub>2</sub>]<sup>2+</sup> catalysts are formed *in situ*, a strong preference for the *cis*-dihydroxylation of electron rich *cis*-alkenes was observed (see also Chapter 2). The latter system is highly active with over 8000 turnovers to the *cis*-diol product of cyclooctene and near complete atom efficiency in the oxidant H<sub>2</sub>O<sub>2</sub>.<sup>9</sup>
- 20 B. S. Lane, M. Vogt, V. J. DeRose and K. Burgess, *J. Am. Chem. Soc.*, 2002, **124**, 11946.
- 21 H. E. Gottlieb, V. Kotlyar and A. Nudelman, *J. Org. Chem.*, 1997, **62**, 7512.
- 22 J. C. Tripp, C. H. Schiesser and D. P. Curran, *J. Am. Chem. Soc.*, 2005, **127**, 5518.



## Chapter 5

# Mechanistic study of an *in situ* prepared $\text{Mn}^{\text{II}}$ /pyridine-2-carboxylic acid catalytic system

*In this chapter a range of spectroscopic techniques were employed to obtain kinetic information regarding the reaction, employing  $\text{Mn}^{\text{II}}$ /pyridine-2-carboxylic acid/butanedione and a base, to elucidate the mechanism. The equilibrium between butanedione and  $\text{H}_2\text{O}_2$  and a competitive reaction to form acetic acid in situ in the reaction mixture are demonstrated as well as the roles played by butanedione and acetic acid.*

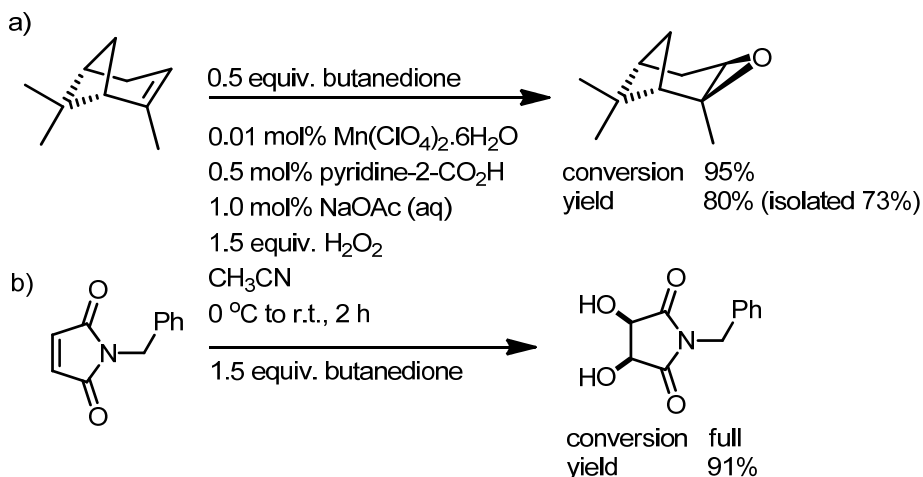
*Part of this chapter has been published:*

J. Dong, P. Saisaha, T. G. Meinds, P. L. Alsters, E. G. Ijpeij, R. P. van Summeren, B. Mao, M. Fañanás-Mastral, J. W. de Boer, R. Hage, B. L. Feringa and W. R. Browne, *ACS catal.*, 2012, **2**, 1087.

## 5.1 Introduction

The decomposition of polypyridyl amine based ligands such as TPTN and their amination precursors under the conditions employed for catalysis was described in Chapter 3. It was also demonstrated that pyridine-2-carboxylic acid and its derivatives formed *in situ* are responsible for the activity observed.<sup>1</sup> The application of an *in situ* formed catalyst system for the epoxidation and *cis*-dihydroxylation of alkenes with H<sub>2</sub>O<sub>2</sub> based on pyridine-2-carboxylic acid, Mn<sup>II</sup>, a base (*e.g.* NaOH or NaOAc) and a ketone either as solvent or co-solvent was described in Chapter 4.<sup>2</sup>

The presence of a ketone either as a solvent or co-solvent was found to be essential to the activity of the catalytic system. Subsequently, butanedione was identified as a ketone that provided a highly active catalytic system and it could be used substoichiometrically.<sup>3</sup> Importantly, the reaction times were dramatically reduced. The system is especially suited for the epoxidation of electron rich alkenes and shows good to excellent selectivity in the epoxidation of dienes and bifunctional substrates. In the case of electron deficient alkenes the method exhibits exceptional selectivity and activity in their *cis*-dihydroxylation (Scheme 1).<sup>3</sup>



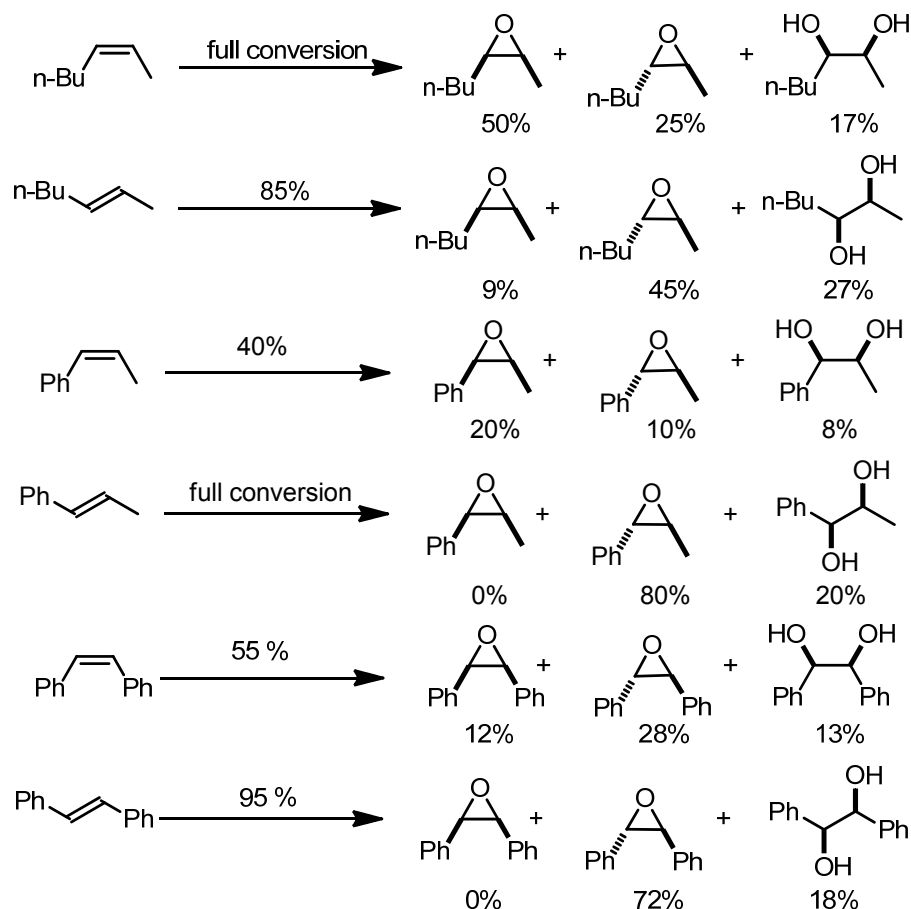
**Scheme 1** Conversions and yields (isolated) obtained for a) the epoxidation of electron rich alkenes and b) *cis*-dihydroxylation of electron deficient alkenes under the standard conditions employing Mn<sup>II</sup>/pyridine-2-carboxylic acid/butanedione/base system.

In this chapter the system employing butanedione in the combination with Mn<sup>II</sup>/pyridine-2-carboxylic acid and a base is investigated in more detail in an attempt to elucidate the reaction mechanism, with particular focus on the role of the ketone and acids in controlling the reaction rate. For details of substrate scope and optimisation of reaction conditions using butanedione please refer to reference.<sup>3</sup>

## 5.2 Mechanistic considerations

### 5.2.1 Information from substrate scope

Several mechanistically relevant observations can be made based on the substrate scope.<sup>3</sup>



**Scheme 2** Oxidation of *cis*-/*trans*-2-heptene, *cis*-/*trans*-1-methyl-styrene and *cis*-/*trans*-stilbene catalysed by  $Mn^{II}$ /pyridine-2-carboxylic acid/butanedione/base.<sup>a</sup>

<sup>a</sup> For conditions see the experimental section. Yields determined by  $^1H$  NMR spectroscopy. Note that the *trans*-dihydroxylation products were not observed in any of the examples and side products were overoxidation products, *i.e.*  $\alpha$ -hydroxyl ketone.

The degree of retention of configuration in the epoxidation of *cis*-/*trans*-2-heptene is relatively low. For *cis*-2-heptene, 75% of the epoxide product was obtained as a mixture of *cis*-2-heptene oxide and *trans*-2-heptene oxide (2 : 1) (Scheme 2). Similarly, *trans*-2-heptene provided 45% *trans*-2-heptene oxide and only 9% *cis*-2-heptene oxide. This indicates that the epoxidation of alkenes is not a concerted reaction but is instead stepwise and favours the *trans*-epoxide product. In strong contrast, the heptane-1,2-diol that was formed as a minor product was in both cases the result of *cis*-dihydroxylation only. This

is remarkable as it suggests that dihydroxylation is a concerted process. Essentially the same trends were observed with both *cis*- and *trans*-1-methylstyrene and *cis*- and *trans*-stilbene. In addition, it is clear that, in contrast to Mn-TMTACN (see Table 4, Chapter 2), *trans*-alkenes are much more reactive under the present conditions.

However, the absence of significant allylic oxidation, for example cyclohexene, indicates that the low retention of configuration observed for 2-heptene is not due to a radical oxidation pathway involving hydroxyl radicals.<sup>4</sup>

### 5.2.2 Kinetic analysis: order of reaction with respect to various components and the rate determining step

The present system is highly active and can achieve up to 300,000 turnovers with respect to Mn<sup>II</sup> with turnover frequencies of up to 40 s<sup>-1</sup> with 1.5 equiv. of H<sub>2</sub>O<sub>2</sub>.<sup>3</sup> However, the high activity and low catalyst loadings required (0.01-0.3 mol%) and the absence of spectroscopic signals assignable to manganese species involved in this system (*e.g.* by EPR or UV/Vis spectroscopy) means that direct identification of the ‘active species’ or even the catalyst in its resting state is essentially impossible. These aspects pose a massive challenge in mechanistic studies for this system. Nevertheless, the techniques and experiments that have been used to understand how individual components are involved in the reaction and, more importantly, why components affect reactions in a negative or positive manner will be described in the following sections.

Kinetic analysis employing Raman spectroscopy was used to obtain mechanistically relevant information for the present system. The conversion of substrate, the formation of products and the changes of butanedione concentration and H<sub>2</sub>O<sub>2</sub> concentration can be monitored by following individual Raman bands relating to each component over time (see Figure 1 for an example). UV/Vis absorption spectroscopy was also used for kinetic analysis in monitoring the butanedione concentration since it has a strong absorption at 417 nm.

Most of the experiments for kinetic analyses by Raman spectroscopy described in this chapter were performed using cyclooctene representing electron rich alkene substrates with 1,2-dichlorobenzene (DCB) as internal standard. The intensity or peak area of Raman bands between 1550-1800 cm<sup>-1</sup> relating to stretching modes of C=C and C=O bonds were used to follow substrate conversion (band at 1650 cm<sup>-1</sup> for cyclooctene) and the change of butanedione concentration (band at 1724 cm<sup>-1</sup>). Moreover Raman bands between 600-900 cm<sup>-1</sup> relating to bending modes of C=C and C=O bonds were used also for reaction monitoring such as following the band at 682 cm<sup>-1</sup> for butanedione, 701 cm<sup>-1</sup> for cyclooctene and at 870 cm<sup>-1</sup> for H<sub>2</sub>O<sub>2</sub>.

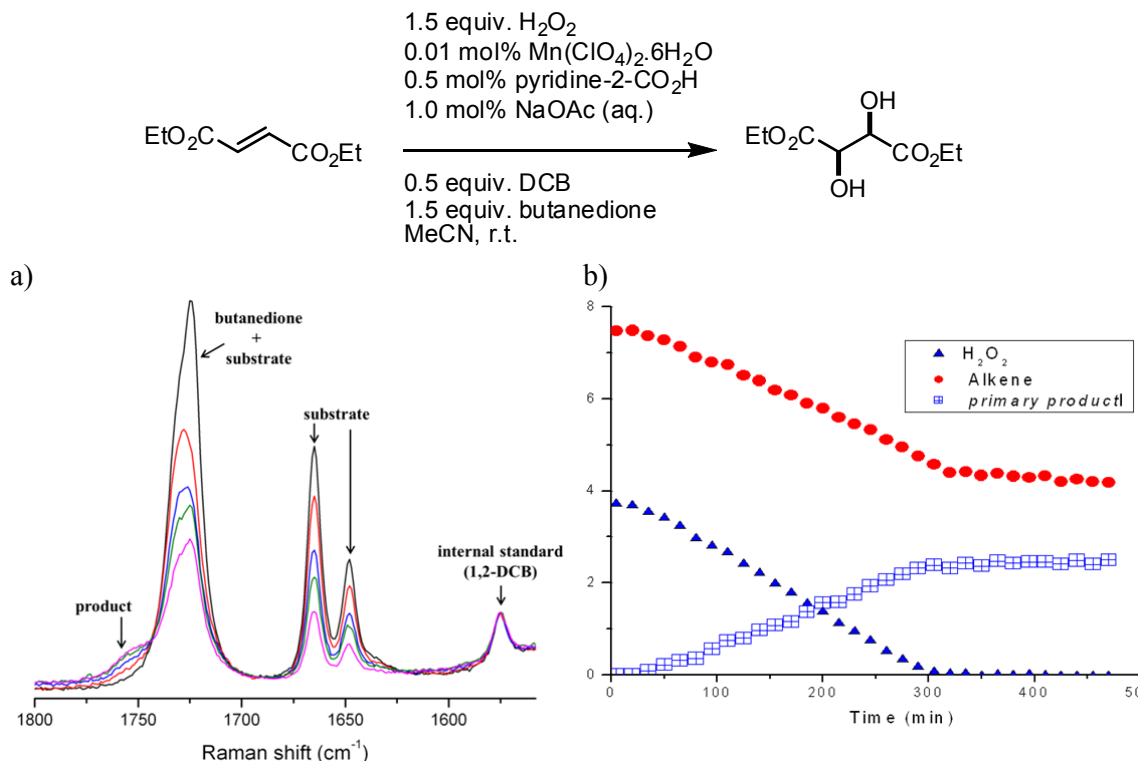


**Figure 1** Online monitoring of a catalytic oxidation reaction using Raman spectroscopy ( $\lambda_{\text{exc}}$  785 nm). Kinetic information is obtained by monitoring individual bands with 1,2-dichlorobenzene as internal standard a) Raman bands of individual components in reaction mixture and b) plot of intensity of bands of individual components in the reaction mixture against time.

#### 5.2.2.1 Order of reaction with respect to manganese

The oxidation of cyclooctene using optimised conditions but varying the concentration of  $Mn^{II}$  was performed and followed in real time by Raman spectroscopy ( $\lambda_{\text{exc}}$  785 nm). A lag time was observed over the first 10 min after the addition of  $H_2O_2$  (Figure 2), which will be discussed in detail in Section 5.2.4.

The rate of reaction, obtained from the slope of the curve, varied depending on the  $Mn^{II}$  concentration. The reaction reaches maximum conversion faster at higher  $Mn^{II}$  concentration. Importantly, however, after the lag period the reaction rate is constant until conversion stops. The change in rate with change in  $Mn^{II}$  concentration confirms that manganese is involved in the rate determining step of the reaction. Again, the shape of the curve is particularly interesting because after the lag phase there is a fast linear part in which the reaction reaches maximum conversion which is unexpected.<sup>5</sup> Normally the rate of a reaction (slope of the curve) changes as the reaction proceeds and the amount of substrate and  $H_2O_2$  changes. However, as this is not observed it would suggest that the substrate (cyclooctene) does not participate in the rate determining step, *i.e.* zero order in substrate. This also applies to  $H_2O_2$  to a certain extent (*vide infra*).



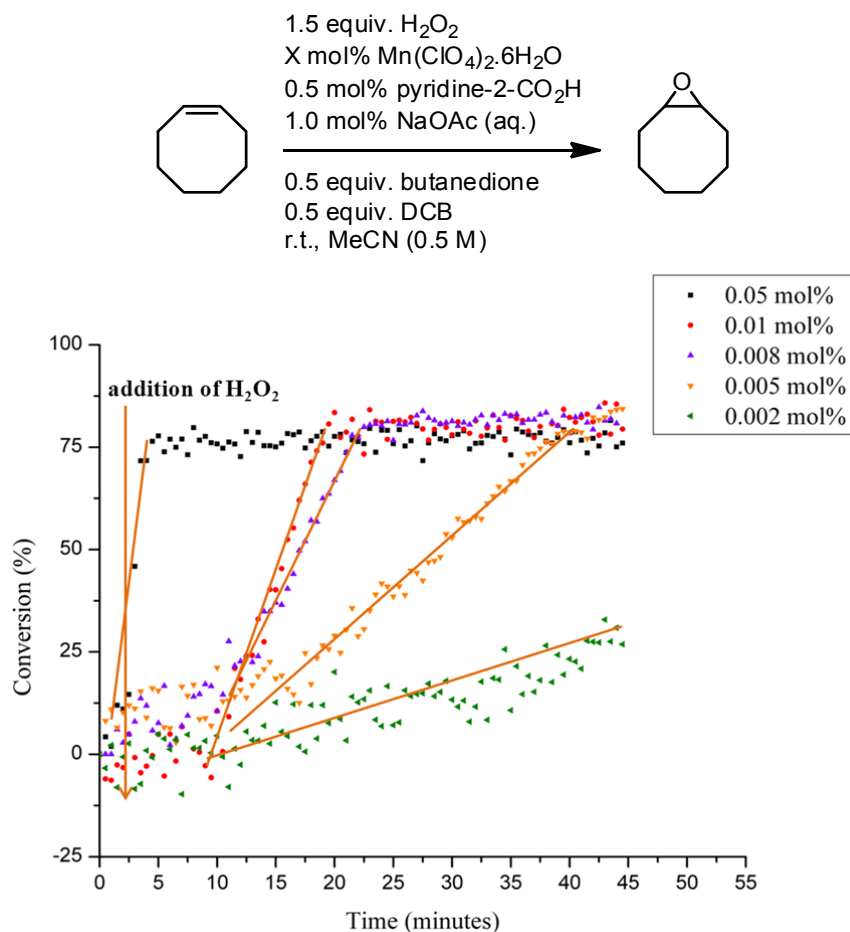


**Figure 2** Conversion of cyclooctene versus time for reactions using various concentrations of  $\text{Mn}^{\text{II}}$  measured by Raman spectroscopy ( $\lambda_{\text{exc}}$  785 nm).

#### 5.2.2.2 Order of reaction with respect to pyridine-2-carboxylic acid

The correlation between the peak area of the substrate and time shows similar behaviour to that observed in Figure 2. A lag time is again observed, however, it is longer when less pyridine-2-carboxylic acid (PCA) is used. Reaction rates varied with the concentration of pyridine-2-carboxylic acid (Figure 3). This indicates that the reaction is non-zero order with respect to pyridine-2-carboxylic acid.

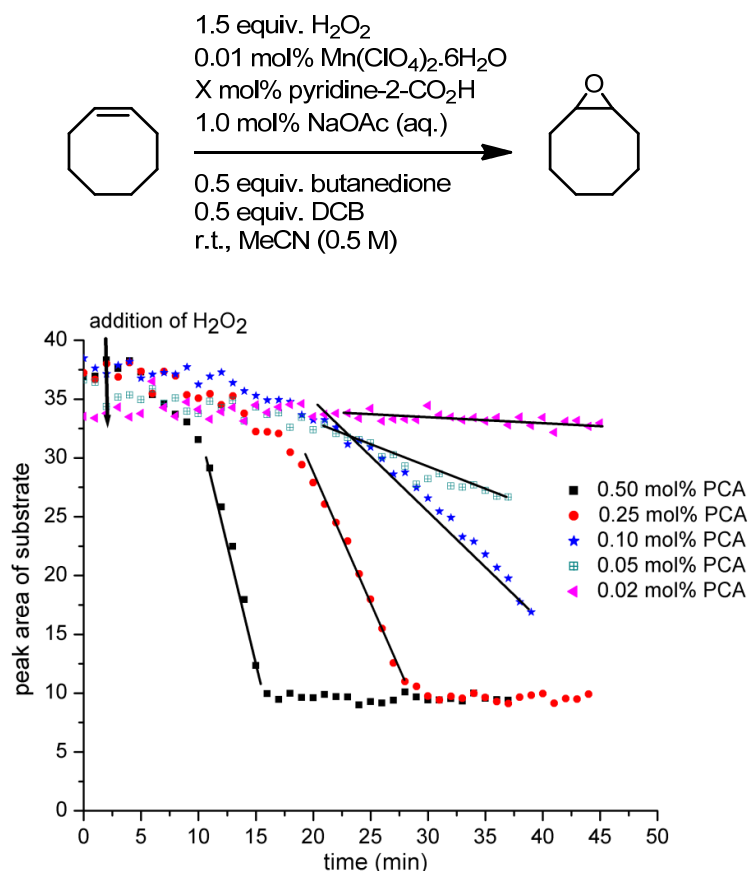


**Figure 3** Peak area of cyclooctene at  $1650\text{ cm}^{-1}$  versus time for reactions using various amounts of pyridine-2-carboxylic acid (PCA) determined by Raman spectroscopy ( $\lambda_{\text{exc}}\ 785\text{ nm}$ ). The concentration of  $Mn^{II}$  is 0.01 mol%.

#### 5.2.2.3 Order of reaction with respect to substrate

As observed and discussed in section 2.2.1, the reaction appeared to show zero order kinetics with respect to substrate. To confirm this observation, reactions with different initial concentrations of cyclooctene were performed (Figure 4). In all cases, a lag time was observed that lasted ca. 10 min. The rate at which the substrate is consumed is almost equal for all three concentrations of substrate for both concentrations of catalyst examined. This confirms that the reaction is zero order with respect to substrate under the conditions employed. Notably the reaction reaches higher conversion when a lower initial concentration of substrate is used (*e.g.* with 0.01 mol% Mn; 80% conversion is obtained with [0.5 M] substrate and with [0.25 M] substrate full conversion is obtained). This is a useful observation for practical applications as it can be applied for substrates that gave low conversion at normal substrate concentration (0.5 M) such as phenanthrene.<sup>3</sup>

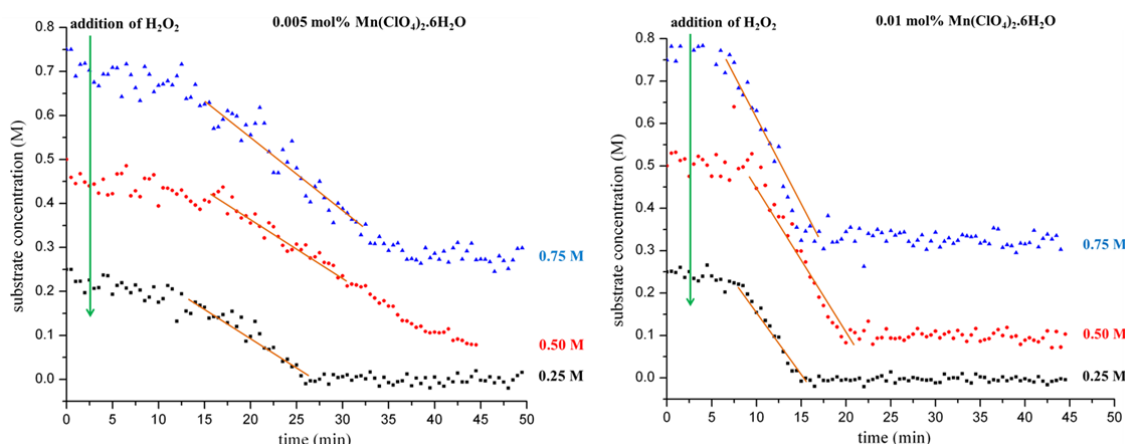
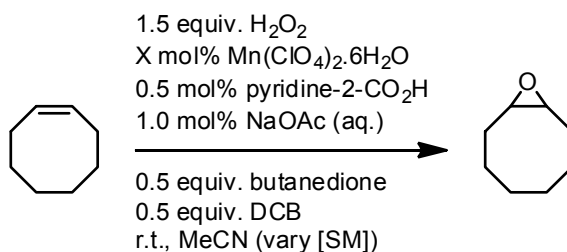


**Figure 4** Conversion of cyclooctene versus time for reactions using various concentrations of cyclooctene monitored by Raman spectroscopy ( $\lambda_{\text{exc}}$  785 nm).

#### 5.2.2.4 Order of reaction with respect to butanedione

From the correlation in Figure 5, it can be concluded that when the amount of butanedione added decreases the rate of the reaction also decreases. This indicates that the order with respect to butanedione is not zero. This implies that butanedione is involved at or before the rate determining step for the reaction. Interestingly, the lag time observed is shorter when a higher concentration of butanedione is used (*vide infra*). The data suggests that butanedione might be involved in the processes occurring during the lag phase of the reaction. In order to obtain more evidence to support this hypothesis, the effect of butanedione concentration in the reaction mixture was studied (see Section 5.2.3).

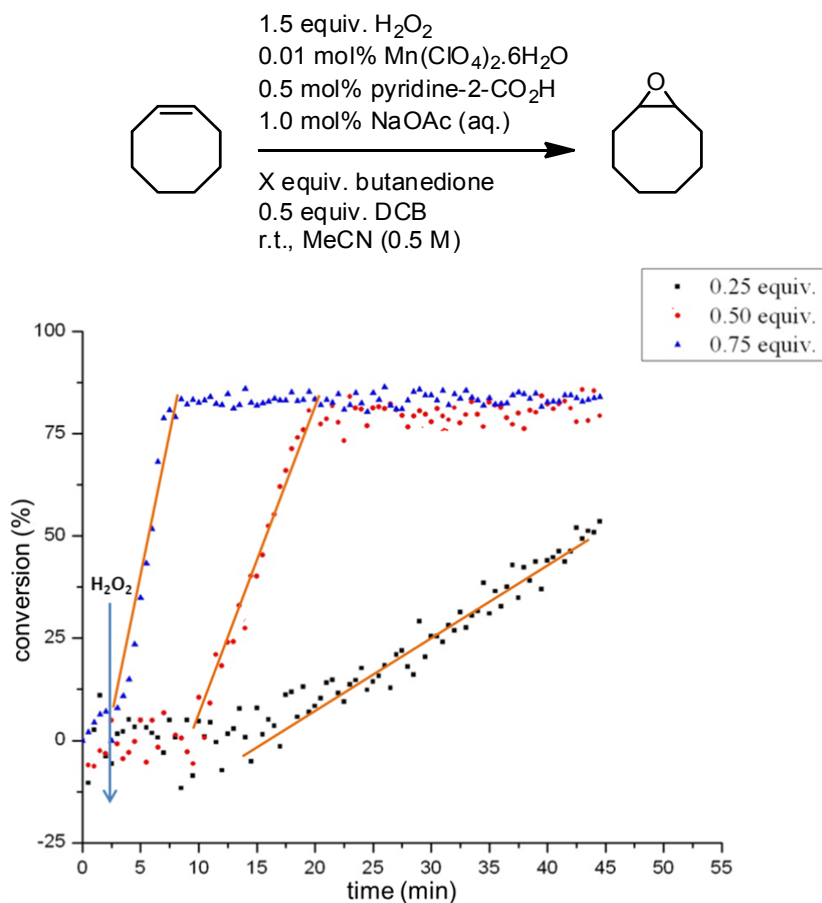


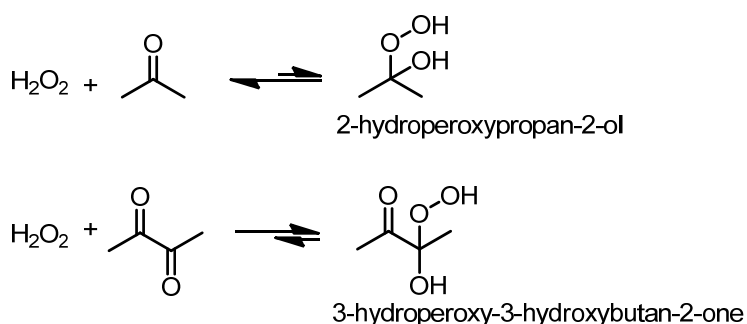
**Figure 5** Conversion of cyclooctene versus time for reactions using various concentrations of butanedione monitored by Raman spectroscopy ( $\lambda_{exc}$  785 nm).

### 5.2.3 Role(s) of ketone in the catalytic reaction

Although the initial objective was to find safer alternatives to acetone as solvent (see Chapter 4), it was discovered that butanedione was a substoichiometrically active ketone for the manganese catalysed oxidation of alkenes.<sup>3</sup> Indeed at low  $Mn^{II}$  loadings the requirement for butanedione to be present, even when acetone was used as solvent, indicated that the ketone was directly involved in the reaction and not simply acting as (co)solvent. Actually, full conversion observed with sub-stoichiometric amounts of butanedione implies that it is involved in the oxidation directly and is catalytic. Furthermore, the broad solvent scope<sup>3</sup> and the absence of activity when butanedione was omitted, together with the increased activity that allows for the use of low  $Mn^{II}$  (<0.01 mol%) and PCA (<0.05 mol%) catalyst loadings, with much shorter reaction times than in acetone alone, hinted that hydrogen peroxide/butanedione adducts (*i.e.* 3-hydroperoxy-3-hydroxybutan-2-one) could be involved. UV/Vis absorption and Raman spectroscopic analysis of the reaction mixture confirmed that the butanedione reacts immediately (<10 s) with  $H_2O_2$  in a 1 : 1 ratio, manifested in a decrease and blue shift in both the carbonyl

stretch ( $1722\text{ cm}^{-1}$ ) in the Raman spectrum (Figure 6) and the absorption band at  $417\text{ nm}$  ( $n\text{-}\pi^*$  absorption of the butanedione) in the UV/Vis absorption spectrum of the reaction mixture (Figure 7).

That the changes observed are due to the formation of a mono-hydroperoxy acetal (Scheme 3) is supported by the 1 : 1 stoichiometry required to see almost loss in the intensity of both the  $1722\text{ cm}^{-1}$  Raman band (Figure 6) and the  $417\text{ nm}$  UV/Vis absorption band (Figure 7). With 1 equiv. of  $\text{H}_2\text{O}_2$  with respect to substrate, the  $1722\text{ cm}^{-1}$  Raman band and the  $417\text{ nm}$  absorption began to recover after approximately 66% of the  $\text{H}_2\text{O}_2$  was consumed (*i.e.*  $<1$  equiv. of  $\text{H}_2\text{O}_2$  with respect to butanedione remained). This is also consistent with the formation of 1 : 1 adduct of  $\text{H}_2\text{O}_2$  and butanedione (Scheme 3).<sup>6</sup>



**Scheme 3** Equilibrium between ketone/ $\text{H}_2\text{O}_2$  and hydroperoxy acetal species.

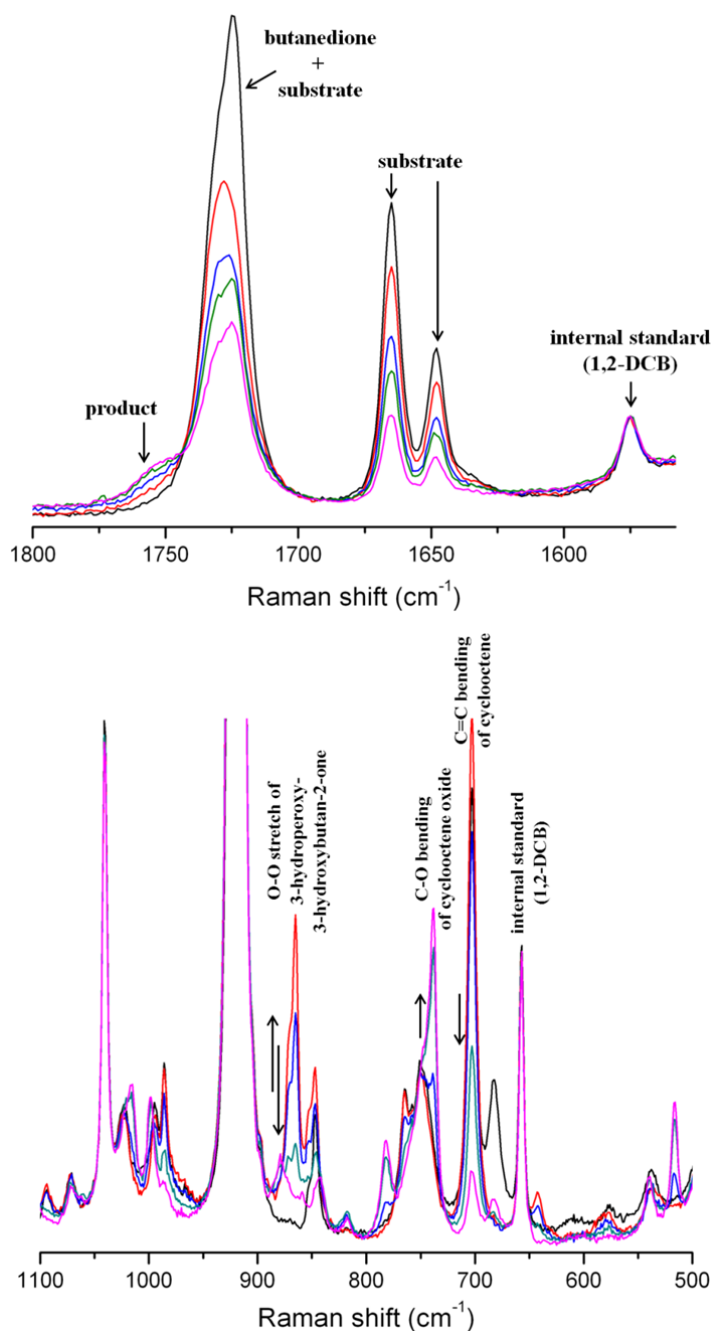


**Figure 6** Changes in the Raman spectrum (upper spectrum 1500-1800  $cm^{-1}$  region, lower spectrum 500-1100  $cm^{-1}$  region),  $\lambda_{exc}$  785 nm, of the reaction mixture during the epoxidation of cyclooctene. Conditions: 0.01 mol%  $Mn^{II}$ , 0.5 mol% pyridine-2-carboxylic acid, 1.0 mol% NaOAc (aq.), 0.5 mol% butanedione, 1.5 equiv.  $H_2O_2$ , MeCN, r.t., substrate concentration = 0.5 M. Spectra prior to (black) and at  $t = 5$  (red), 15 (blue), 20 (green) and 30 (pink) min after addition of  $H_2O_2$ . Directions of change are identical with arrows.

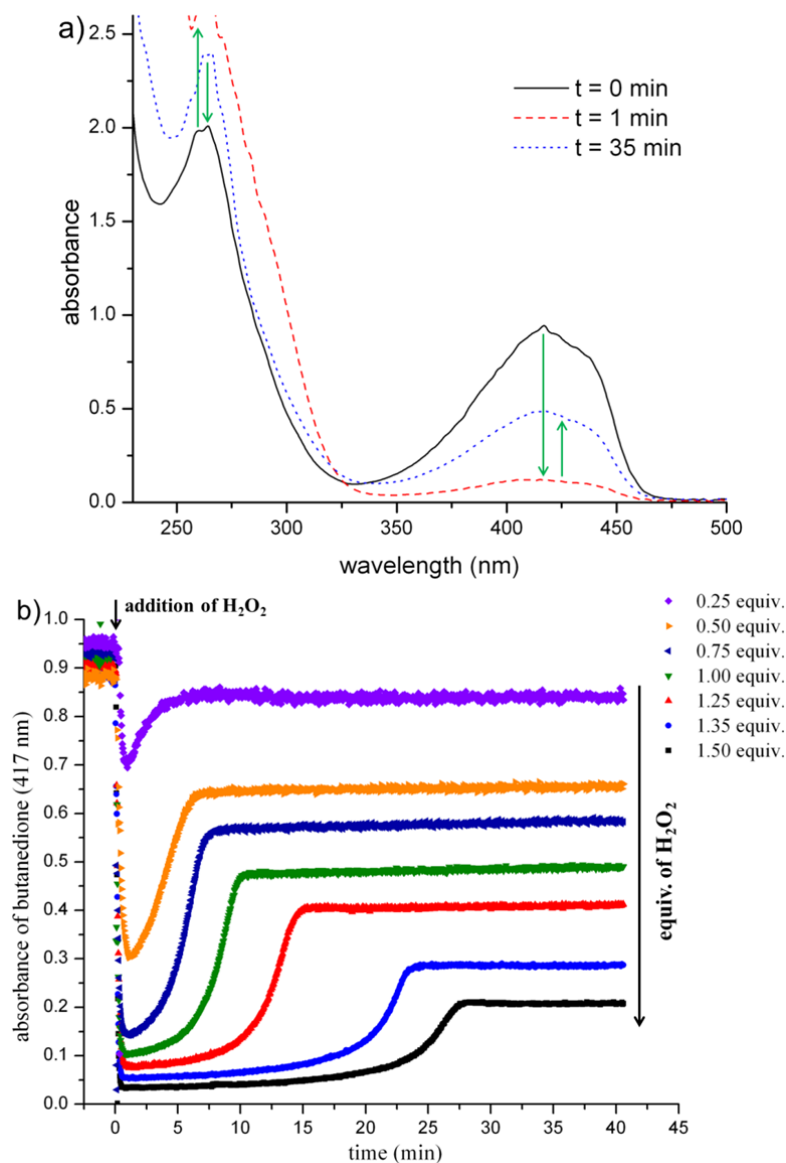


**Figure 7** Changes in a) the UV/Vis absorption spectrum of the reaction mixture 1 min after addition of  $H_2O_2$  and after 35 min b) absorbance of butanedione at 417 nm over time with various equivalents of  $H_2O_2$ . Conditions as stated in Figure 6 with varying equivalents of  $H_2O_2$  (0.25-1.50 equiv.).

The partial recovery of the butanedione is observed to occur concomitantly with the end of the conversion of cyclooctene (*i.e.* after  $t > 25$  min, Figures 8 and 9), as the  $H_2O_2$  concentration decreases below that of the butanedione.

When 1.5 equiv. of  $H_2O_2$  was employed with respect to substrate the recovery of the  $1722\text{ cm}^{-1}$  and 417 nm bands of butanedione was *ca.* 25% indicating that decomposition of butanedione occurs as a competing reaction (Figure 7). The reaction of butanedione with  $H_2O_2$  to form the active hydroperoxy acetal could in principle lead to decomposition to acetic acid (Scheme 4).<sup>7,8,9,10</sup>

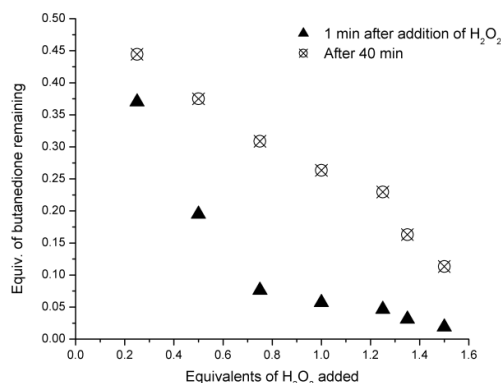


**Figure 8** Equivalents of butanedione remaining (determined by monitoring absorbance at 417 nm) 1 min after the addition of  $H_2O_2$  and after 40 min (*i.e.* after conversion of cyclooctene has stopped) showing partial recovery of butanedione after the reaction.

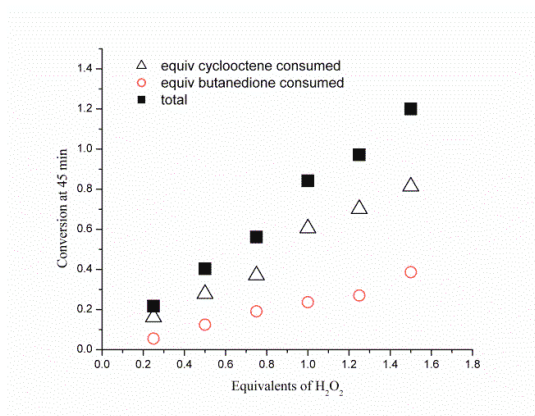
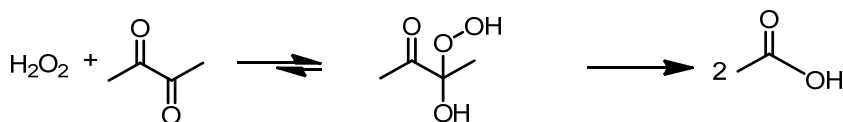


**Figure 9** Conversion of cyclooctene and butanedione (expressed as equivalents with respect to cyclooctene) for various equivalents of  $H_2O_2$  measured by Raman spectroscopy ( $\lambda_{exc}$  785 nm) and UV/Vis absorption spectroscopy, respectively. The total conversion of cyclooctene and butanedione is shown as black squares.



**Scheme 4** Decomposition of butanedione/ $H_2O_2$  adduct to form acetic acid. Although the reaction could proceed uncatalysed, in fact the formation of acetic acid is a catalysed reaction under the reaction conditions employed (*vide infra*).

The formation of hydroperoxy acetal and acetic acid was confirmed by  $^{13}C$  NMR spectroscopy (Figures 10 and 11). In Figure 10, the formation of hydroperoxy acetal (signal at 208 ppm) was observed within 4 min after addition of  $H_2O_2$  and the butanedione signal at 198 ppm disappeared completely as observed earlier by UV/Vis



absorption and Raman spectroscopy (Figures 6 and 7, respectively). After 34 min, the signal of acetic acid at 174 ppm appeared while the butanedione signal at 198 ppm reappeared after 44 min. Moreover products of the reaction which are cyclooctene oxide (major product) and cyclooctane diol (minor product) can also be observed after 4 min at 58 and 76 ppm, respectively. Some of  $^{13}\text{C}$  NMR signals have not been identified yet. Acetic acid might form earlier in the reaction than indicated by  $^{13}\text{C}$  NMR spectroscopy, however, the detection limit of the technique has not been determined for the present case.

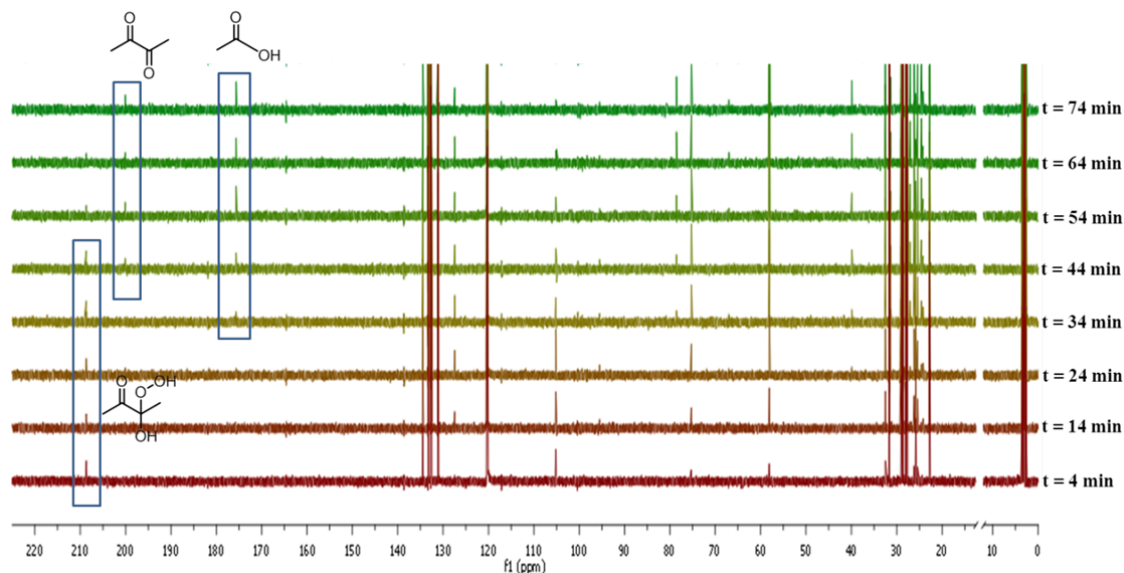


**Figure 10**  $^{13}\text{C}$  NMR spectra of the oxidation of cyclooctene (conditions stated in Figure 6) after addition of  $\text{H}_2\text{O}_2$  showing the presence of hydroperoxy acetal at 208 ppm, butanedione at 198 ppm and acetic acid at 174 ppm (in  $\text{CD}_3\text{CN}$ ).

Furthermore, when the loss of butanedione as well as the conversion of cyclooctene are both taken into account, it is apparent that almost all of the  $\text{H}_2\text{O}_2$  consumed is used in these two processes only (Figure 9). This observation is important as it indicates that the efficiency of the system can be increased by outcompeting the oxidation of the butanedione (*e.g.* by accelerating the catalytic oxidation of the alkene).

It should be noted from reactions in either the absence or presence of acetic acid (*vide supra*) that the breakdown of butanedione or its  $\text{H}_2\text{O}_2$  adduct is observed only when both manganese and pyridine-2-carboxylic acid are present. This strongly indicates that acetic acid is formed by the same species responsible for the oxidation of alkenes (as will be discussed further in Section 5.2.4).

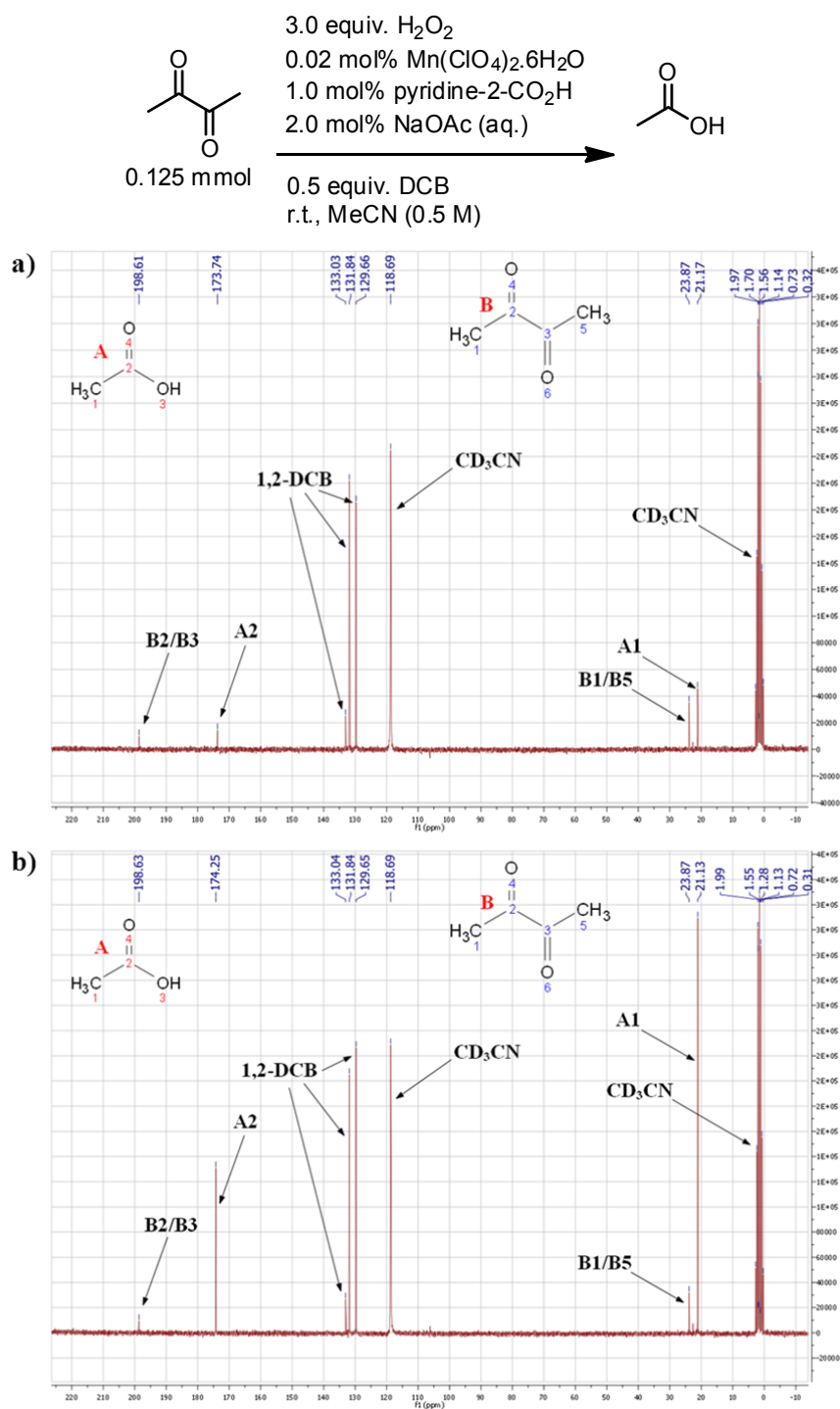


**Figure 11**  $^{13}C$  NMR spectrum of the reaction mixture (in  $CD_3CN$ ) a) after 40 min showing the presence of acetic acid and butanedione and b) reaction mixture from a) spiked with additional acetic acid.

### 5.2.4 Effect of acetic acid on the catalytic oxidation of alkenes

When the reaction was performed in acetone the rate of reaction was dramatically reduced in the presence of acetic acid, albeit with relatively little effect on the overall conversion after 24 h as demonstrated in Chapter 4.<sup>2</sup> The confirmation that acetic acid is formed by decomposition of butanedione in the present system (see Section 2.3) raises a question to its affect on the conversion and reaction rate also. The formation of acetic acid could potentially inhibit the catalytic system in one or more ways including: (i) the loss of butanedione could result in reduced activity since this is required for catalysis, (ii) the acetic acid could affect the equilibrium between butanedione/H<sub>2</sub>O<sub>2</sub> and 3-hydroperoxy-3-hydroxybutan-2-one through reducing the effective nucleophilicity of H<sub>2</sub>O<sub>2</sub>, and (iii) could destabilise a putative Mn<sup>II</sup>/PCA complex.

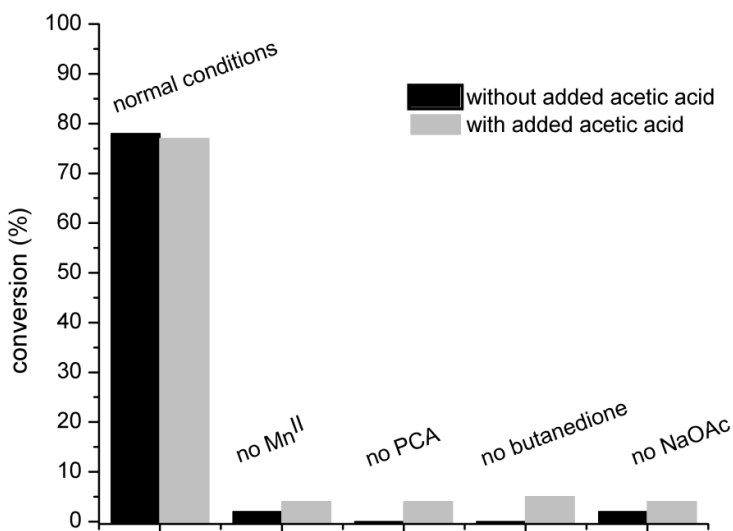
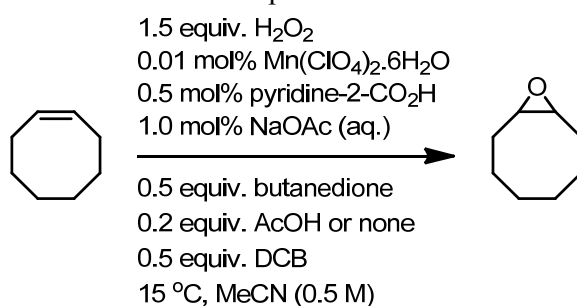


**Chart 1** Effect of added acetic acid on the catalytic oxidation of cyclooctene and the omission of individual components from the catalyst system on conversion. Note that in all cases except when butanedione was omitted, the formation of 3-hydroperoxy-3-hydroxybutan-2-one was observed by Raman spectroscopy. Notably, when manganese or pyridine-2-carboxylic acid were omitted this hydroperoxy species is stable for 24 h. This observation indicates that decomposition to acetic acid is “Mn/pyridine-2-carboxylic acid” catalysed.

Addition of acetic acid to the reaction (0.2 equiv. w.r.t substrate) either before or after addition of  $H_2O_2$  did not affect conversion or yield significantly (Chart 1). The kinetics of the reactions obtained by Raman spectroscopy still showed the same reaction rate for all conditions (Figure 12). Interestingly, both reactions with extra acetic acid start immediately after adding  $H_2O_2$ , *i.e.* a lag time is not observed compared to standard conditions when acetic acid is not added. This confirms that, although acetic acid is formed in significant amounts during the reaction, it does not interfere with the present butanedione based system. Instead, it aids the formation of an active catalyst, manifested in the absence of a lag time.

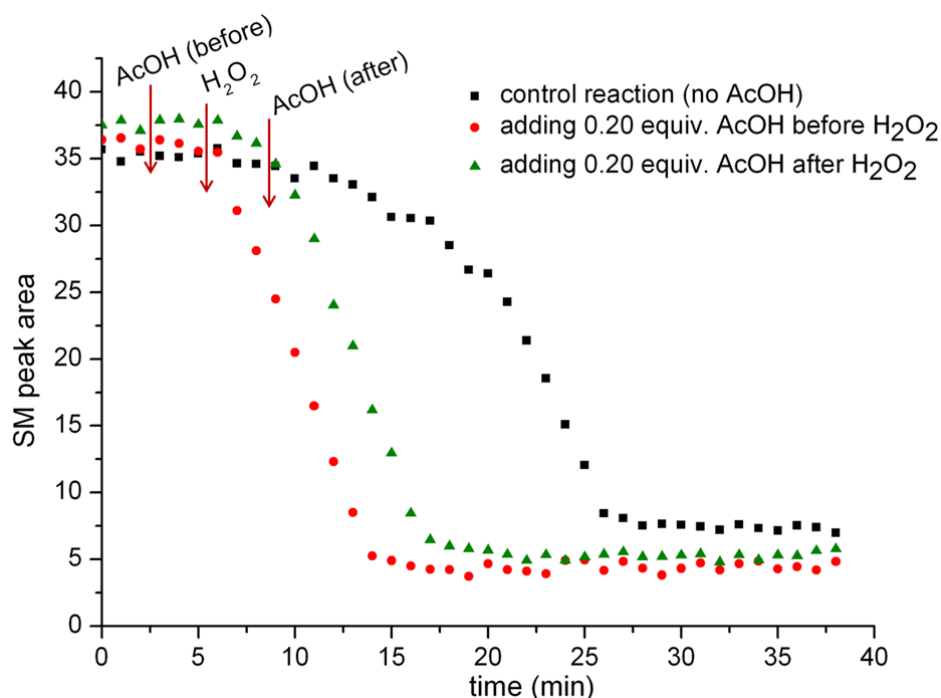


**Figure 12** Correlation between peak areas of substrate and time for the oxidation of cyclooctene using conditions stated in Chart 1 monitored by Raman spectroscopy ( $\lambda_{exc}$  785 nm).

The absence of an effect of acetic acid on reaction rate when butanedione is employed is in stark contrast to reactions carried out in acetone. It is possible that under acidic conditions the formation of the hydroperoxy species (Scheme 3) will be affected more in the presence of acetone (the equilibrium in this case lies to the left) than in the presence of butanedione. Hence, in the latter case the presence of acetic acid does not affect the availability of the proposed oxidant, 3-hydroperoxy-3-hydroxybutan-2-one, sufficiently to retard the reaction. However, an alternative hypothesis for the difference in the effect of acetic acid between acetone and butanedione should also be considered. Specifically potential differences in the ability of acetate to compete with the hydroperoxy acetal of acetone and of butanedione for coordination to the manganese catalyst should be

recognised. Regardless of which effect is most important it is clear that the formation of acetic acid does not lead to catalyst deactivation in the present system.

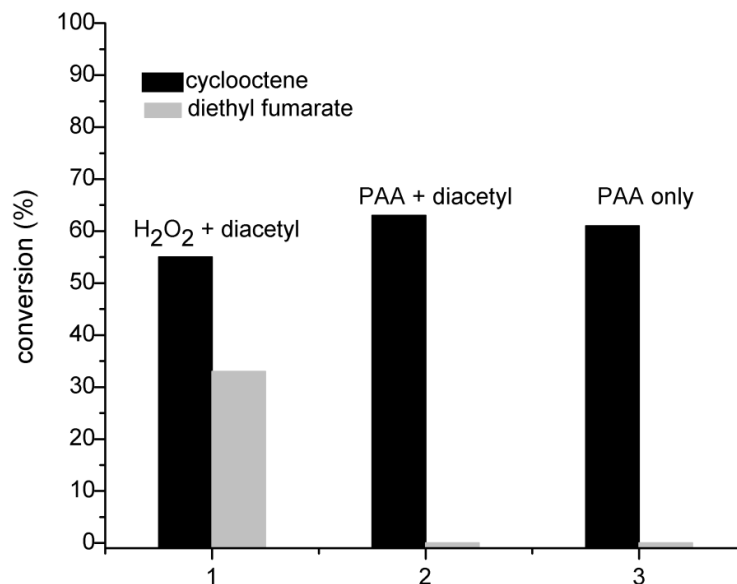


**Chart 2** Oxidation of cyclooctene (red) and diethylfumarate (blue) with peracetic acid in the presence and absence of butanedione under standard reaction conditions (stated in Figure 1).

An additional consideration that must be made with regard to the formation of acetic acid is the possibility of subsequent *in situ* formation of peracetic acid, which is itself capable of oxidizing alkenes.<sup>11</sup> This possibility was investigated in a series of control experiments with cyclooctene and diethylfumarate. Under the present conditions (Figure 1) stoichiometric peracetic acid was found to be effective in the epoxidation of cyclooctene in the absence and presence of butanedione. Importantly, however, no activity in the oxidation of diethylfumarate was observed (Chart 2). Taken together with the absence of activity in the oxidation of cyclooctene with added acetic acid when butanedione is omitted (Chart 1), this confirms that the *in situ* formation of peracetic acid does not occur significantly under these conditions.

To understand more about whether this reaction is a general acid catalysed or specific acid catalysed reaction, the reactions with and without added acetic acid were carried out in both a polar aprotic solvent, acetonitrile, and a polar protic solvent, ethanol (Figure 13).

The rate of reaction is different when using different solvents, however, the same overall result can be seen from reactions in ethanol and acetonitrile, *i.e.* the lag phase is absent upon the addition of acetic acid (as the reaction in the presence of acetic acid shows conversion earlier than without acetic acid). Furthermore, using ethanol allows the determination of solvent kinetic isotope effects (Figure 14). Deuterated ethanol

( $CH_2CH_3OD$ ) and deuterated acetic acid ( $CH_3CO_2D$ ) were used with  $H_2O_2$  or  $D_2O_2$  as terminal oxidant, but a solvent kinetic isotope effect was not observed indicating that proton transfer may not be involved at or before the rate determining step.

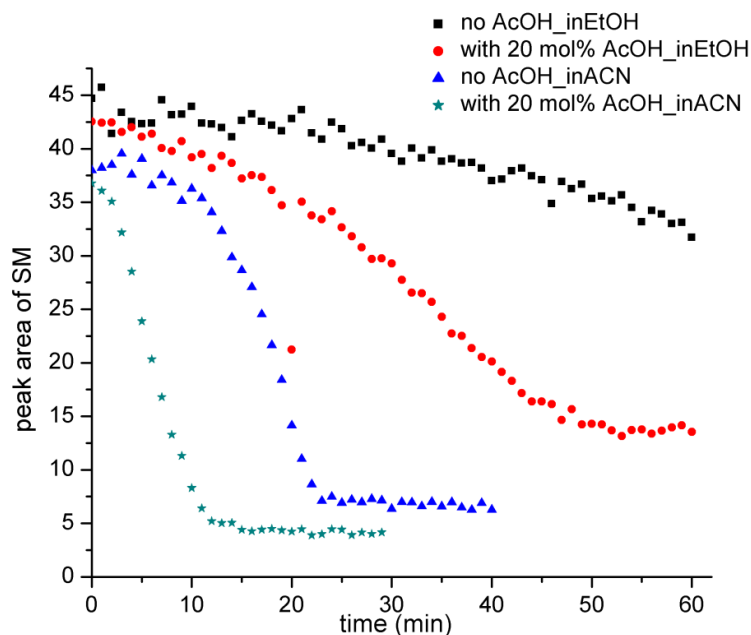


**Figure 13** Correlation between peak areas of substrate and time for the oxidation of cyclooctene using conditions stated in Chart 1 in acetonitrile and in ethanol monitored by Raman spectroscopy ( $\lambda_{exc}$  785 nm).

### 5.2.5 Effect of other acids on catalysis with butanedione

As discussed above acetic acid is formed *in situ* in the reaction mixture by decomposition of the butanedione/ $H_2O_2$  adduct. Acetic acid eliminates the lag time of the reaction but does not affect the rate of reaction. Several other acids with different  $pK_a$ <sup>12,13,14,15</sup> were studied under standard reaction condition both in acetonitrile and in ethanol (Figures 15 and 16, respectively).

All reactions from Figures 15 and 16, except those that contained trichloroacetic acid or perchloric acid, showed conversion under the reaction conditions employed, but gave different conversions. However, there is no clear correlation between  $pK_a$  and conversion. The fact that conversion was not observed with trichloroacetic acid or perchloric acid could be ascribed to the effect of  $pK_a$ . These acids are the only acids employed that have a  $pK_a$  lower than the  $pK_a$  of pyridine-2-carboxylic acid ( $pK_a$  1.07 for  $CO_2H$  and 5.25 for  $PyH^+$ , Scheme 5), and hence will protonate pyridine-2-carboxylic acid inhibiting the formation of the active catalyst.

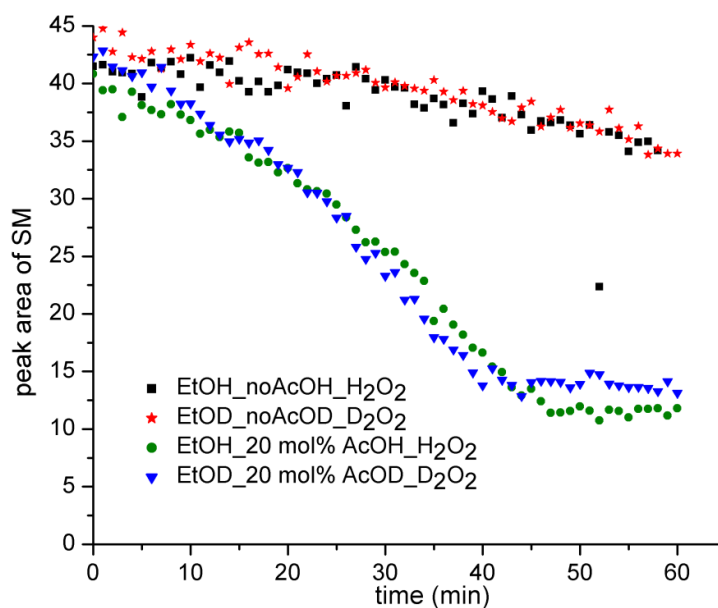


**Figure 14** Correlation between peak areas of substrate and time for the oxidation of cyclooctene using conditions stated in Chart 1 in acetonitrile and in ethanol monitored by Raman spectroscopy ( $\lambda_{\text{exc}}$  785 nm).

The kinetics of the reactions (Figure 17) showed a dependence on the acid added and can be classified into three categories. Type one are those acids that completely inhibit the reaction and consists of acids with  $pK_a$  lower than pyridine-2-carboxylic acid (Table 1, entry 2 and 3). Type two are those that retard the reaction compared to conditions without any added acid. This group consists of acids such as 2,6-dichlorobenzoic acid, 2-nitrobenzoic acid, chloroacetic acid, 2-hydroxybenzoic acid, 3-nitrobenzoic acid ( $pK_a$  range 1.69-3.45) (Table 1, entries 3-8). The third type are those that remove the lag period that follows addition of  $\text{H}_2\text{O}_2$ , but do not affect the rate of reaction significantly (Table 1, entry 9-11).

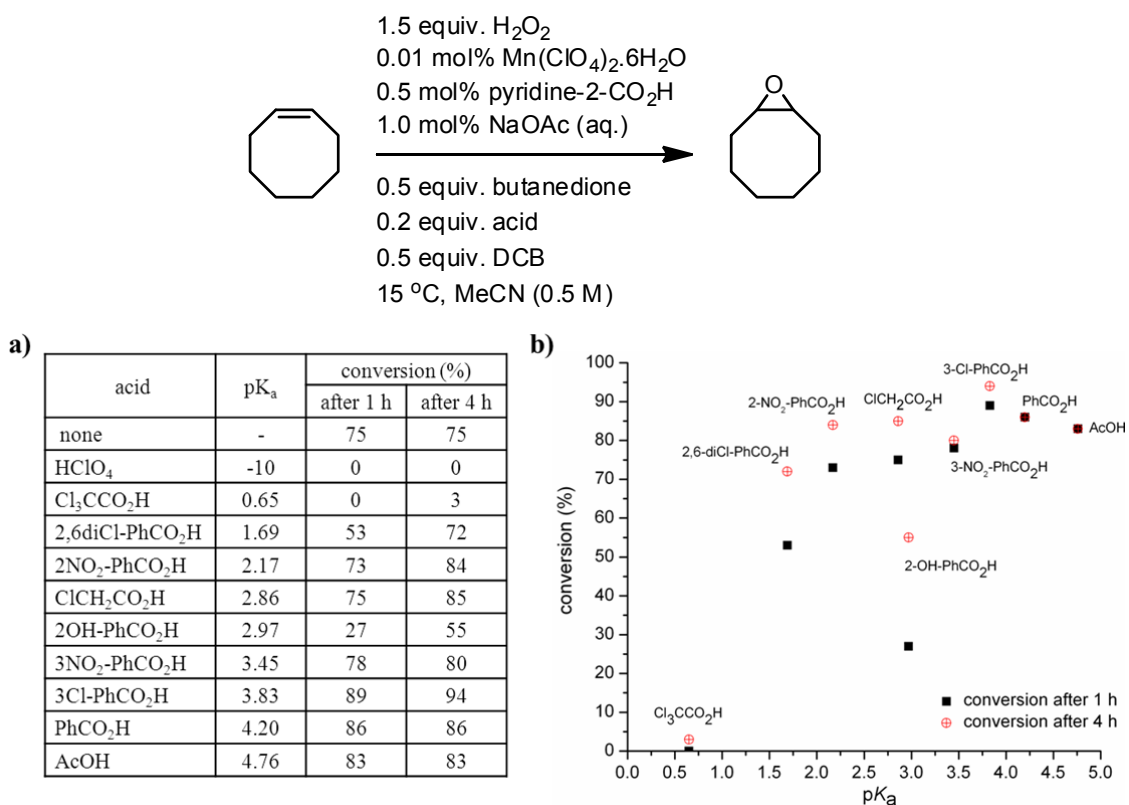


**Figure 15** Conversion of cyclooctene using standard conditions with various acids (different  $pK_a$ ) in acetonitrile monitored by Raman spectroscopy ( $\lambda_{exc}$  785 nm). a) Table shows conversion of reactions after 1 and 4 h with various acids used. b) Correlation between conversion of reactions and  $pK_a$  of acids.



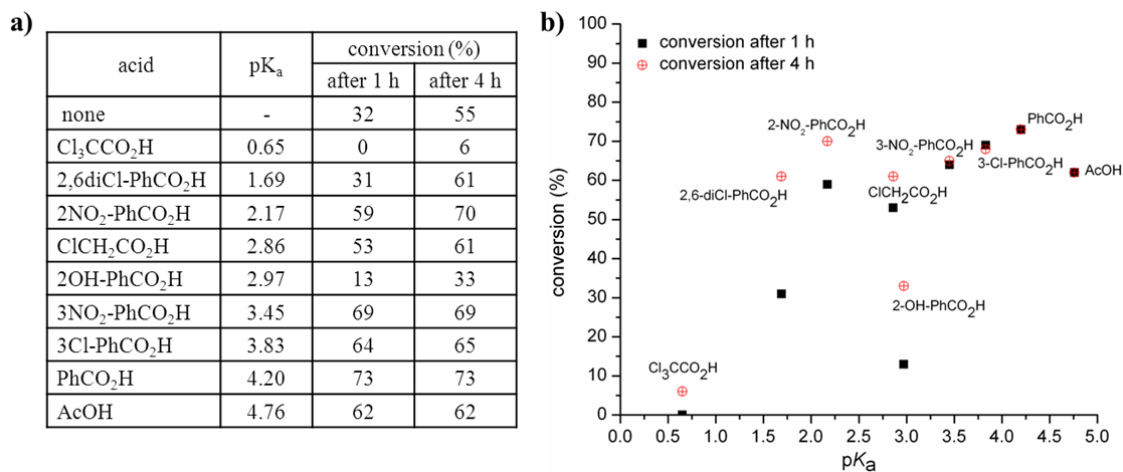
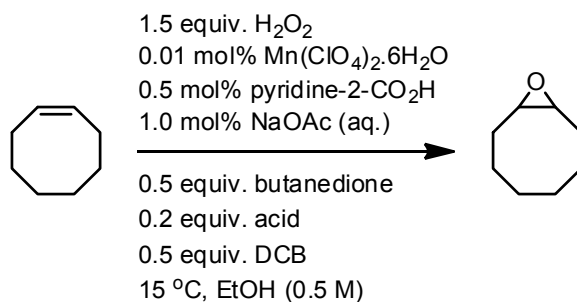
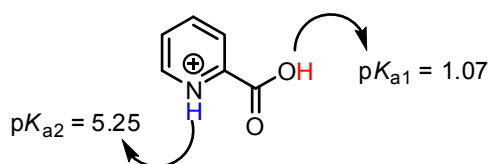


**Figure 16** Conversion of cyclooctene using standard conditions with different acids in ethanol monitored by Raman spectroscopy ( $\lambda_{\text{exc}}$  785 nm) a) Table shows conversion of reactions after 1 and 4 h and b) relation between conversion and  $\text{pK}_a$  of acids.



**Scheme 5**  $\text{pK}_a$  of pyridine-2-carboxylic acid.<sup>16</sup>

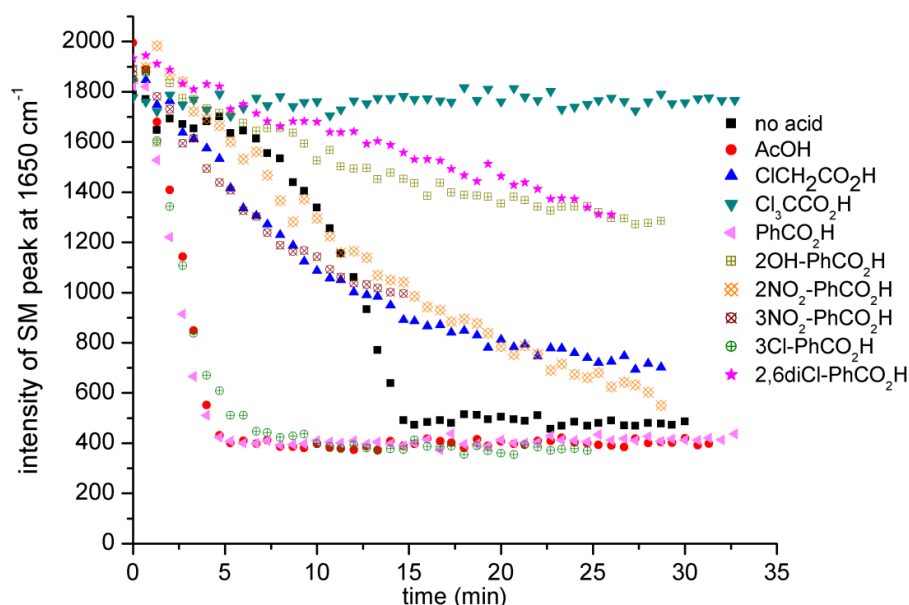


**Figure 17** Intensities of substrate band at  $1650\text{ cm}^{-1}$  against time for the oxidation of cyclooctene using conditions stated in Figure 15 monitored by Raman spectroscopy ( $\lambda_{\text{exc}} 785\text{ nm}$ ).

Thus it can be concluded that acids have different effects on the reaction depending on their  $pK_a$ . Some completely inhibit the reaction, some retard the reaction rate and some only remove the lag period.

The next question that arises is the effect of acid on the equilibrium between butanedione and  $H_2O_2$ . One of the acids in each category (from Table 1) was used to study this. UV/Vis absorption spectroscopy was used to monitor the butanedione concentration in the reaction (Figure 18). From the results, only acetic acid gives similar behaviour compared to the original conditions. Butanedione reacts directly with  $H_2O_2$  manifested in an immediate decrease in absorption at  $417\text{ nm}$  upon addition of  $H_2O_2$ . Since the reaction with acetic acid showed no lag time after addition of  $H_2O_2$  (as discussed above) and reaction reached its maximum conversion sooner than in the absence of acid and the recovery of butanedione occurred earlier here also. So it can be concluded that the equilibrium between butanedione and  $H_2O_2$  and the adduct are unaffected by acetic acid.

**Table 1** Classification of acids and their effects on the oxidation of cyclooctene using conditions stated in Figure 15 (effect on the reaction are based on kinetic analysis in Figure 17)

entry	acid	$pK_a$	type	effect on the reaction
1	none	-	-	-
2	HClO <sub>4</sub>	-10	1	<b>inhibit the reaction completely</b>
3	Cl <sub>3</sub> CCO <sub>2</sub> H	0.65	1	
4	2,6-diCl-PhCO <sub>2</sub> H	1.69	2	<b>retard the reaction</b>
5	2-NO <sub>2</sub> -PhCO <sub>2</sub> H	2.17	2	
6	ClCH <sub>2</sub> CO <sub>2</sub> H	2.86	2	
7	2-OH-PhCO <sub>2</sub> H	2.97	2	
8	3-NO <sub>2</sub> -PhCO <sub>2</sub> H	3.45	2	<b>remove the lag period but do not affect the reaction rate</b>
9	3-Cl-PhCO <sub>2</sub> H	3.83	3	
10	PhCO <sub>2</sub> H	4.20	3	
11	AcOH	4.76	3	

The equilibrium in the presence of chloroacetic acid and trichloroacetic acid was different, however, with a slow decrease in the absorption of butanedione indicating that the equilibrium is shifted to the left (back to butanedione) instead of the butanedione/H<sub>2</sub>O<sub>2</sub> adduct (see the reaction of butanedione and H<sub>2</sub>O<sub>2</sub> in Scheme 3). This supports the kinetic data for conversion obtained with chloroacetic acid, which shows that it retards the oxidation of cyclooctene. The gradual decrease of the absorbance of butanedione with trichloroacetic acid indicates that hydroperoxy acetal is built up slowly in the reaction as was detected by <sup>13</sup>C NMR with a signal at 208 ppm observed (data not shown). Moreover, the exponential decay of butanedione suggests that it decomposed to form other species, albeit, not acetic acid. The <sup>13</sup>C NMR signal at 174 ppm (C=O of acetic acid) cannot be detected even 45 min after addition of H<sub>2</sub>O<sub>2</sub>. Instead an unidentified species at 117 ppm formed in the reaction (data not shown). The fact that the hydroperoxy acetal was formed but no conversion of cyclooctene was observed implied that the formation of the active catalyst did not occur either employing trichloroacetic acid.

The data described above can be rationalised as follows. An acid can have more than one effect on the reaction, for example trichloroacetic acid, inhibits the reaction, possibly because it protonates pyridine-2-carboxylic acid and thus inhibits the formation of the active catalyst and also shifts the equilibrium between butanedione and H<sub>2</sub>O<sub>2</sub> reducing the effective concentration of 3-hydroperoxy-3-hydroxybutan-2-one. Secondly, because of the effect on the equilibrium shown above, some acids retard the reaction. Finally, some acids remove the lag phase because they promote the formation of an active catalyst.

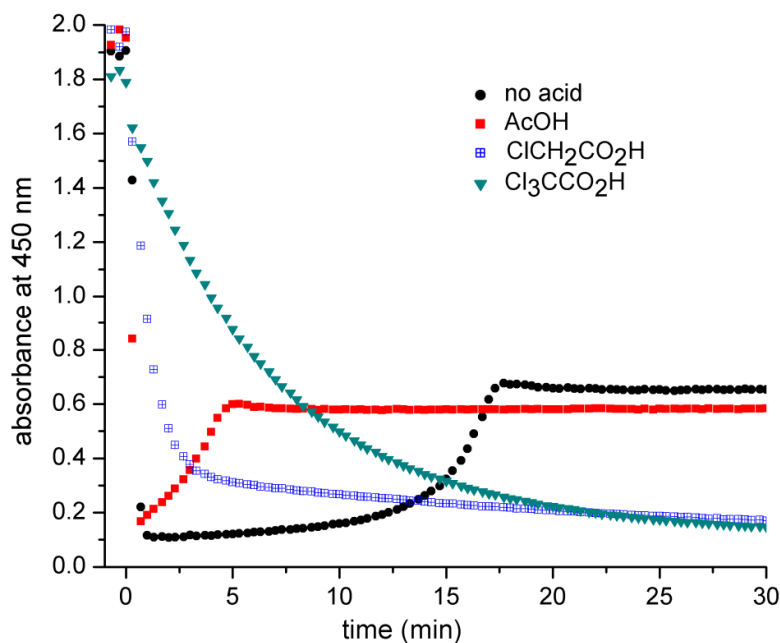
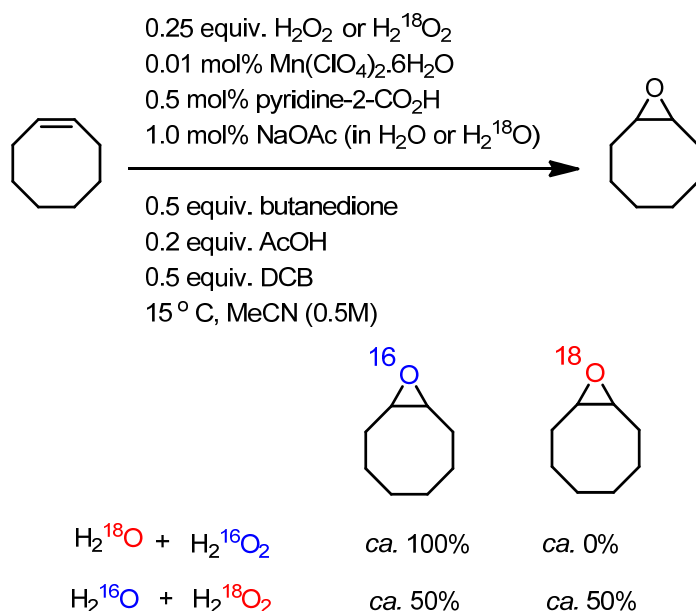


**Figure 18** Changes in the UV/vis absorption spectrum of butanedione at 417 nm in the oxidation reaction of cyclooctene using standard conditions with various acids stated in Figure 15.

#### 5.2.6 $^{18}O$ -labelling studies

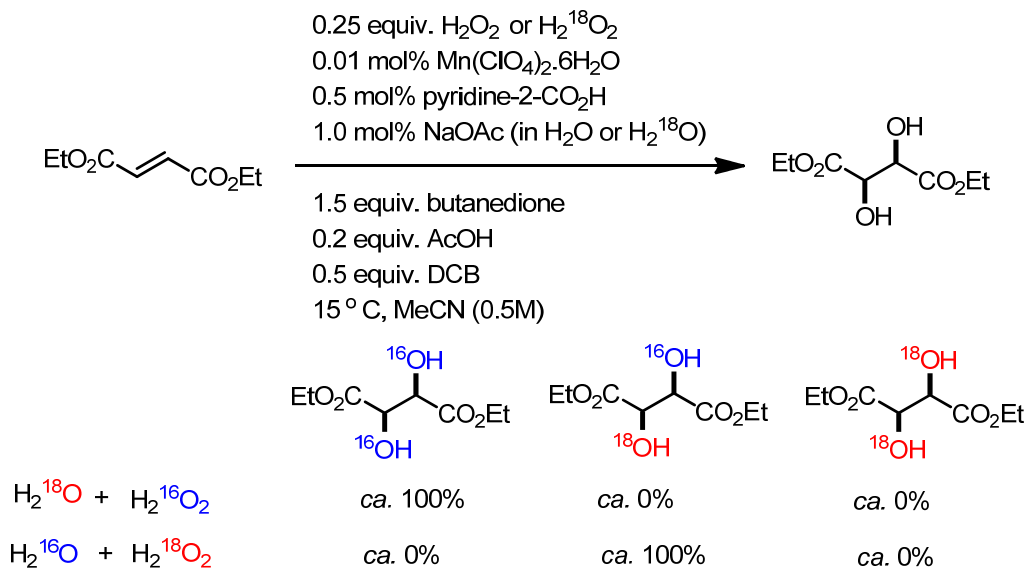
As discussed in Chapter 1, one of the most powerful tools available in studying mechanisms in oxidation catalysis is isotopic labelling, *i.e.* atom tracking of oxygen.<sup>17</sup> Labelled hydrogen peroxide ( $H_2^{18}O_2$ ) and/ or labelled water ( $H_2^{18}O$ ) were used in the reaction in order to identify the origin of oxygen atoms in the products.

The oxidation of cyclooctene employing  $H_2^{18}O$  and  $H_2^{16}O_2$  provided cyclooctene where only  $^{16}O$  was incorporated in the epoxide product (Figure 19). This indicates that the oxygen in the epoxide product is not from water. For the complementary experiment with  $H_2^{16}O$  and  $H_2^{18}O_2$ , surprisingly *ca.* 1 : 1 ratio of epoxide incorporating  $^{16}O$  or  $^{18}O$  was observed. This means only 50% of the oxygen atoms in the product are from  $H_2O_2$ . The other source is possibly from butanedione.  $O_2$  (from air) is excluded as a source since the reaction can be performed under  $N_2$  or Ar atmosphere.



**None from  $\text{H}_2\text{O}$ ; but only half from  $\text{H}_2\text{O}_2$**

**Figure 19**  $^{16}\text{O}$  and  $^{18}\text{O}$  isotopic distribution in the oxidation product of cyclooctene measured by mass spectrometry.



**None from  $\text{H}_2\text{O}$ ; but only half from  $\text{H}_2\text{O}_2$**

**Figure 20**  $^{16}\text{O}$  and  $^{18}\text{O}$  isotopic distribution in the oxidation product of diethylfumarate measured by mass spectrometry.

Diethylfumarate was used also for this study as it provided *cis*-diol as the major product (Figure 20). Similar results were observed with the reaction employing  $H_2^{18}O$  and  $H_2^{16}O_2$ . In agreement, the oxygen atoms in the product are not from water as purely *cis*-diol with both  $^{16}O$  is observed. Interestingly, only *cis*-diol with one atom each of  $^{16}O$  and  $^{18}O$  in the same molecule was observed as the sole product when  $H_2^{16}O$  and  $H_2^{18}O_2$  were used. Again this supports the hypothesis that oxygen atoms in the product are from both  $H_2O_2$  and butanedione.

### 5.3 Proposed mechanism

The goal of this discussion is not to propose a microkinetic description of the catalytic system but instead to rationalise the empirical observation made under the conditions employed in the present system (0.005-0.1 mol%  $Mn^{II}$ /0.02-0.5 mol% pyridine-2-carboxylic acid/1.0 mol% NaOAc (aq.)/1.5 equiv.  $H_2O_2$ /MeCN). The most striking observation for this system is the equilibrium between butanedione and  $H_2O_2$  towards 3-hydroperoxy-3-hydroxybutan-2-one (**A**, Scheme 3). From kinetic analyses, it can be concluded that the reaction is zero order with respect to  $H_2O_2$  when in excess with respect to butanedione. However, the reaction is not-zero order with respect to butanedione (Figure 5). The reason for this difference is that the equilibrium between butanedione and  $H_2O_2$  lies almost completely towards **A**. The concentration of **A** formed in the reaction depends on the primary concentration of butanedione (when  $H_2O_2$  is present in excess). The formation of **A** was confirmed by Raman (Figure 6) and  $^{13}C$  NMR (Figure 10) spectroscopy and the rate of reaction depends on the concentration of **A**.

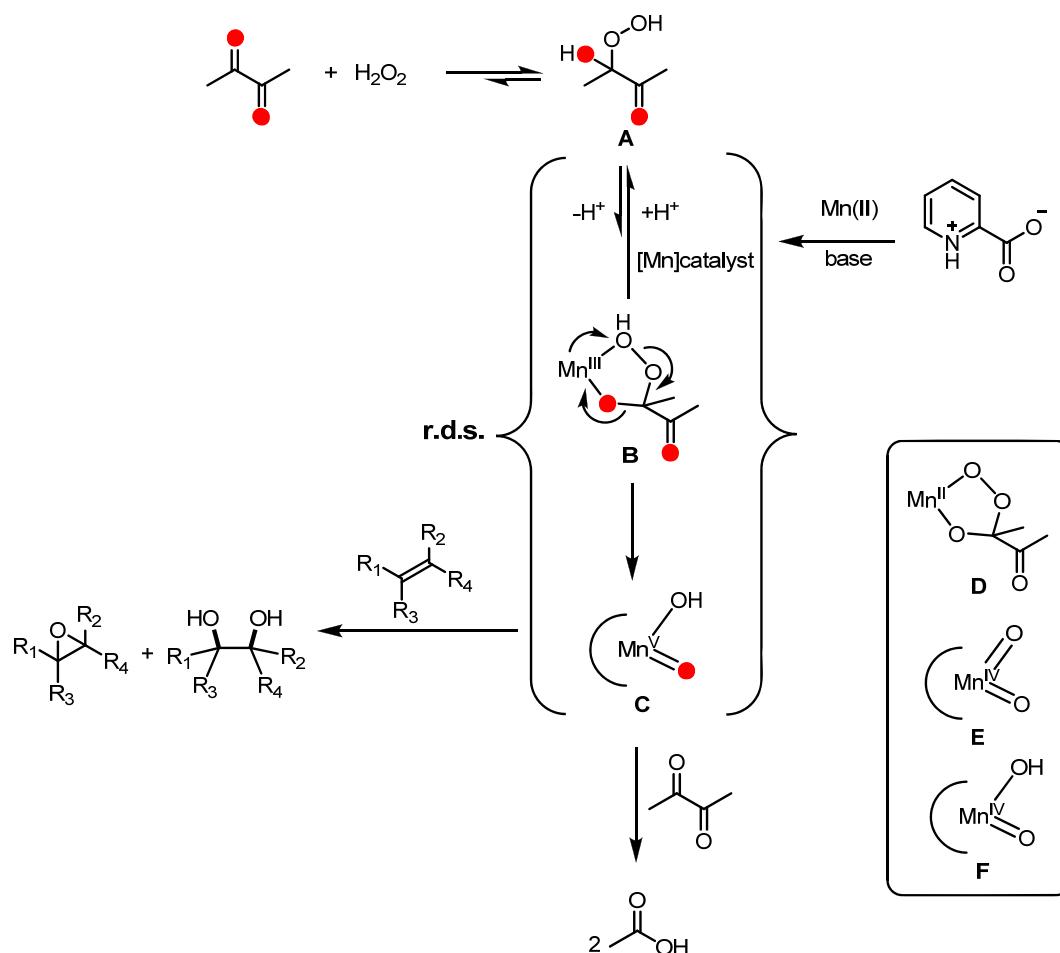
Under the conditions employed, butanedione decomposes to form acetic acid *in situ*, which is catalysed by manganese and pyridine-2-carboxylic acid (Figures 10 and 11 and Chart 1). The formation of acetic acid in the reaction is a competitive process to alkene oxidation. In addition, loss of butanedione reduces the effective concentration of **A**. Acetic acid does not inhibit the present butanedione based system and does not participate in the oxidation through formation of peracetic acid under the conditions employed (Chart 1 and 2). However, it is essential for catalysis, possibly for the formation of the active catalyst as a lag time is eliminated when acetic acid is present. Acids showed several effects on the reaction depending on their  $pK_a$ . Some acids completely inhibit the reaction, some only retard the rate of the reaction and some do not affect the reaction rate but only eliminate the lag time (Table 1).

The reaction shows zero order kinetics with respect to substrate (Figure 4). This means that the formation of the oxygen transferring species is the rate determining step. The product distribution of *cis*- and *trans*-alkenes showed that epoxidation of alkenes is not a concerted reaction, in contrast to *cis*-dihydroxylation, is a concerted reaction (Scheme 2). However, it is still possible that these two transformations go through a common intermediate. Moreover, the present system provides high activity for both epoxidation of electron rich alkenes and *cis*-dihydroxylation of electron deficient alkenes

and low activity for  $\alpha,\beta$ -unsaturated alkenes. This suggests that the catalyst simultaneously has both electrophilic and nucleophilic properties.

As mentioned above the formation of the oxygen transferring species is the rate determining step under the reaction conditions employed. It can also be concluded from kinetic analyses that the reaction is non-zero order with respect to both manganese and pyridine-2-carboxylic acid (Figure 2 and 3). However, varying these two components over a wide range of concentrations showed a concentration dependence, where the concentration of one compound is dependent on the concentration of the other compound, but in general a ratio greater than *ca.* 3 : 1 of pyridine-2-carboxylic acid : manganese provides good activity. A base is also necessary for forming the active catalyst unless sodium pyridine-2-carboxylate is used. This observation is still not fully understood since even addition of the base after addition of acetic acid is sufficient. The characterisation of the active catalyst is challenging and it is not practical to determine its structure due to the low concentration of catalyst used in the reaction. EPR spectroscopy of the reaction mixture showed that no EPR active species were present (perpendicular mode, at 77 K). This indicates that mononuclear  $\text{Mn}^{\text{II}}$  is not present.<sup>18,19</sup> Hence multinuclear  $\text{Mn}^{\text{II}}$  and mononuclear  $\text{Mn}^{\text{III}}$  are possible candidates.

Data obtained from labelling studies provided some insight as to the active species (Figures 19 and 20). Both epoxidation and *cis*-dihydroxylation of alkenes showed that oxygen is not incorporated from water but that half of the oxygen comes from  $\text{H}_2\text{O}_2$  and half, possibly, from butanedione.<sup>20</sup> These data suggest that the active species should contain two equivalent oxygen atoms which are available for transfer to the product. Thus a peracid type or cyclic oxidant, *e.g.* **B** and **D** (Scheme 6), can be excluded. In addition  $\text{Mn}^{\text{IV}}=\text{O}$  or  $\text{HO}-\text{Mn}^{\text{IV}}=\text{O}$  (**E** and **F**, respectively) are unlikely since generally  $\text{Mn}^{\text{IV}}$  oxo complexes are not that reactive for oxidation of alkenes.<sup>21</sup> So a possible active species in this case could be  $\text{Mn}^{\text{V}}=\text{O}$ ,<sup>22</sup> *i.e.* **C** (Scheme 6).



**Scheme 6** Proposed mechanism for the oxidation of alkenes under the present system based on data from kinetic analyses and orders of the reaction.

## 5.4 Summary and conclusions

In this chapter, kinetic analyses using Raman and UV/Vis spectroscopy provided important data in which the relationship between individual components in the reaction and their effects on the reaction can be inferred. It can be concluded that the reaction is zero order with respect to  $H_2O_2$  and substrate and non-zero order with respect to  $Mn^{II}$ , pyridine-2-carboxylic acid and butanedione under the conditions employed.

Both the equilibrium between butanedione and  $H_2O_2$  to form the hydroperoxy acetal and its decomposition to form acetic acid *in situ* were demonstrated using Raman spectroscopy, UV/Vis absorption and NMR spectroscopy. Acetic acid formed in the reaction is not directly responsible for catalysis as no peracetic acid is formed, however, it aids the formation of the active catalyst manifested in a lack of the lag period. Other acids showed different effects on the reaction depending on their  $pK_a$ .

It can be concluded as well that the rate determining step of the reaction is the formation of the oxygen transferring species. In order to identify the structure of active catalyst,



more experiments need to be performed such as  $^{18}\text{O}$ -exchange to butanedione which can provide more evidence for the origin of oxygen atom in the products.

The consequences of the mechanistic understanding for the catalytic system developed here are explored further with regard to future work in Chapter 6.

## 5.5 Experimental section

All reagents are of commercial grade and used as received unless stated otherwise. Hydrogen peroxide was used as received as a 50 wt. % solution in water; note that the grade of  $\text{H}_2\text{O}_2$  employed can affect the outcome of the reaction where sequestrants are present as stabilisers.  $^1\text{H}$  NMR (400.0 MHz) and  $^{13}\text{C}$  NMR (100.59 MHz) spectra were recorded on a Varian Avance 400. Chemical shifts<sup>23</sup> are relative to  $^1\text{H}$  NMR  $\text{CDCl}_3$  (7.26 ppm),  $\text{CD}_3\text{CN}$  (1.94 ppm) and  $^{13}\text{C}$  NMR  $\text{CDCl}_3$  (77 ppm),  $\text{CD}_3\text{CN}$  (118 ppm).

**Caution.** The drying or concentration of solutions that potentially contain  $\text{H}_2\text{O}_2$  should be avoided. Prior to drying or concentrating, the presence of  $\text{H}_2\text{O}_2$  should be tested for using peroxide test strips followed by neutralization on solid  $\text{NaHSO}_3$  or another suitable reducing agent. When working with  $\text{H}_2\text{O}_2$ , suitable protective safeguards should be in place at all times due to the risk of explosion.

**Caution.** Butanedione has been linked with lung disease upon exposure to its vapours. It should be handled in a properly ventilated fumehood and exposure to vapours should be avoided.<sup>24</sup>

### General procedures for catalytic oxidation of alkenes described in Scheme 2

To a solution of  $\text{Mn}(\text{ClO}_4)_2 \cdot 6\text{H}_2\text{O}$  (0.01 mol%, 0.0361 mg) and pyridine-2-carboxylic acid (0.5 mol%, 0.123 mg) in acetonitrile was added the alkene (1 mmol) to give a final concentration of the substrate of 0.5 M,  $\text{NaOAc}$  (aq. 0.6 M, 1 mol%, 16.7  $\mu\text{l}$ ) and 2,3-butanedione (0.5 equiv. 43.5  $\mu\text{l}$ ) to give a final volume of 2 ml. The solution was stirred in an ice/water bath before addition of  $\text{H}_2\text{O}_2$  (50 wt. %, 1.5 equiv., 85  $\mu\text{l}$ ). The reaction mixture was stirred for 1 h. After 1 h, brine (10 ml) was added and the reaction mixture was extracted with dichloromethane. The combined organic layers were washed with brine. The product was dried over  $\text{Na}_2\text{SO}_4$  (anh.), filtered, and the dichloromethane was removed *in vacuo*. 1,2-Dichlorobenzene was employed as internal standard for Raman and  $^1\text{H}$  NMR spectroscopy. The products were isolated by flash column chromatography on silica gel 230-400 or neutral aluminum oxide 70-230.

**Note:** For some reactions  $\text{CD}_3\text{CN}$  was used as solvent with analysis after the reaction carried out by  $^1\text{H}$  NMR spectroscopy directly.

## 5.6 References and notes

- 1 D. Pijper, P. Saisaha, J. W. de Boer, R. Hoen, C. Smit, A. Meetsma, R. Hage, R. van Summeren, P. L. Alsters, B. L. Feringa and W. R. Browne, *Dalton Trans.*, 2010, **39**, 10375.
- 2 (a) P. Saisaha, D. Pijper, J. W. de Boer, R. Hoen, R. P. van Summeren, P. L. Alsters, R. Hage, B. L. Feringa and W. R. Browne, *Org. Biomol. Chem.*, 2010, **8**, 4444; (b) W. R. Browne, P. L. Alsters, R. P. van Summeren, E. Ijpeij, J. W. de Boer, P. Saisaha, D. Pijper and B. L. Feringa, *PCT Int. Appl.*, 2011, WO 2011104333.
- 3 J. Dong, P. Saisaha, T. G. Meinds, P. L. Alsters, E. G. Ijpeij, R. P. van Summeren, B. Mao, M. Fañanás-Mastral, J. W. de Boer, R. Hage, B. L. Feringa and W. R. Browne, *ACS Catal.*, 2012, **2**, 1087.
- 4 W. Zhang, N. H. Lee and E. N. Jacobsen, *J. Am. Chem. Soc.*, 1994, **116**, 425.
- 5 E. V. Anslyn, D. A. Dougherty, in *Chapter 8, Modern Physical Organic Chemistry*, 2004, University Science Books, 421.
- 6 R. P. Barnes and R. E. Lewis, *J. Am. Chem. Soc.*, 1936, **58**, 947.
- 7 The mechanism for the decomposition, e.g. dioxetane, epoxide or Baeyer-Villiger, is not certain. See references: 8-10.
- 8 Y. Sawaki and C. S. Foote, *J. Am. Chem. Soc.*, 1983, **105**, 5035.
- 9 M. Renz and B. Meunier, *Eur. J. Org. Chem.*, 1999, 737.
- 10 W. Frankvoort, *Thermochim. Acta*, 1978, **25**, 35.
- 11 M. Fujita and L. Que, Jr., *Adv. Synth. Catal.*, 2004, **346**, 190.
- 12 These values were measured in water.
- 13 [http://research.chem.psu.edu/brpgroup/pKa\\_compilation.pdf](http://research.chem.psu.edu/brpgroup/pKa_compilation.pdf)
- 14 [http://evans.harvard.edu/pdf/evans\\_pka\\_table.pdf](http://evans.harvard.edu/pdf/evans_pka_table.pdf)
- 15 <http://www.chem.ucla.edu/harding/lecsups/pKatable30.pdf>
- 16 K. A. Connors and J. M. Lipari, *J. Pharm. Sci.*, 1976, **65**, 379.
- 17 (a) M. Costas, K. Chen and L. Que, Jr., *Coord. Chem. Rev.*, 2000, **200-202**, 517; (b) E. M. Simmons and J. F. Hartwig, *Angew. Chem. Int. Ed.*, 2012, **51**, 3066.
- 18 It should be noted, however, that although preliminary EPR spectroscopic studies show that  $Mn^{II}$  at 0.01 mol% shows the expected 6-line signal, under reaction conditions, no EPR signals were observed at room temperature indicating that mononuclear  $Mn^{II}$  is not present in significant amounts.
- 19 The absence of evidence for manganese species in higher oxidation states does not preclude the involvement of such species in a catalytic cycle, however, if such species do form, then the rate at which they react must be significantly faster than their rate of formation. A possibility is that the reaction proceeds via an electron transfer mediated mechanism; see for example J. Piera and J. E. Bäckvall, *Angew. Chem. Int. Ed.*, 2008, **47**, 3506.
- 20 The exchange between oxygen atom of butanedione and  $H_2O$  is possible, however, the exchange rate is relatively slow compared to the reaction time as observed by the new Raman band at  $1690\text{ cm}^{-1}$  which belongs to  $C=^{18}O$  appeared in the reaction mixture after addition of  $H_2O_2$

---

40 min. In order to assign the exact origin of oxygen atom in the products,  $^{18}\text{O}$ -labelled butanedione is required and this will be studied in the near future.

21 G. Yin, A. M. Danby, D. Kitko, J. D. Carter, W. M. Scheper and D. H. Busch, *J. Am. Chem. Soc.*, 2007, **129**, 1512.

22 T. Taguchi, R. Gupta, B. Lassalle-Kaiser, D. W. Boyce, V. K. Yachandra, W. B. Tolman, J. Yano, M. P. Hendrich and A. S. Borovik, *J. Am. Chem. Soc.*, 2012, **134**, 1996.

23 G. R. Fulmer, A. J. M. Miller, N. H. Sherden, H. E. Gottlieb, A. Nudelman, B. M. Stoltz, J. E. Bercaw and K. I. Goldberg, *Organomet.*, 2010, **29**, 2176.

24 S. S. More, A. P. Vartak and R. Vince, *Chem. Res. Toxicol.*, 2012, **25**, 2083.



## Chapter 6

# **General discussion and future perspectives**

One of the challenges in oxidation chemistry is to develop new ‘ideal’ methods that offer easy access (commercially available or straightforward synthesis) and cost-effective ligands, short reaction times, ambient conditions, *i.e.* room temperature in air, as well as, providing high selectivity and high product yield. Another challenge, that might be as important as the former, is to introduce methods to users, *i.e.* synthetic chemists, who usually fall back on efficient and safe methods, that are already at hand. In this thesis, one known catalytic method and one novel method were examined and discussed in terms of substrate scope, functional group and protecting group tolerance and, especially, mechanistic insights for the latter system.

Mn-TMTACN based catalysts are well-known catalyst for oxidative transformations, *i.e.* the oxidation of alkenes to epoxide or *cis*-diol products and oxidation of alcohols to ketones or carboxylic acids, and many research groups have worked on their application.<sup>1</sup> However, only the reports by de Boer *et al.*<sup>2,3</sup> used *bis*-carboxylato bridged complexes, which were found to be the active intermediate formed in many Mn-TMTACN system. Until recently the substrate scope employing *bis*-carboxylato bridged complexes was limited.

The catalytic system based on TMTACN described in this thesis demonstrated broader substrate scope for the oxidation of alkenes to epoxides or *cis*-diols, oxidation of secondary alcohols to ketones, oxidation of primary alcohols to carboxylic acids and C-H activation to mono-ketone product as well as the functional group and protecting group tolerance. Since this catalyst is suitable for many oxidative transformations, sometimes a problem with chemoselectivity of the reaction can be encountered. Even if the system is still limited in terms of selectivity, however, many advantages from this system make it one of the recommended methods for oxidation reactions from laboratory to large scale synthesis. Experimentally, reactions are simple since the reactions can be performed at room temperature and under air. Also the system is more economic than many methods used both in academic and industrial application as Mn, the TMTACN ligand itself and H<sub>2</sub>O<sub>2</sub> are relatively inexpensive reagents compared to others, *e.g.* RuCl<sub>3</sub> and NaIO<sub>4</sub>, and this system requires only low amounts of the catalyst.

The enantioselective transformation based on *bis*-carboxylato bridged complexes is not widely explored yet as only the *cis*-dihydroxylation of one alkene (2,2-dimethylchromene), which is a challenging substrate, was demonstrated employing chiral carboxylic acids as co-catalyst.<sup>3</sup> Many chiral carboxylic acids, mostly amino acids, were tested by de Boer *et al.*<sup>3</sup> Even though, low to moderate *ee*’s were observed in most cases, screening of other types of chiral carboxylic acid and a broaden substrate scope for this transformation should be done in future work. This approach should also be applied for other transformations such as epoxidation of alkenes to obtain a new enantioselective method for epoxidation as well as kinetic resolution of secondary alcohols, for instance. The latter target is more promising as secondary alcohol oxidation is relatively straightforward (see Chapter 3).

The next system described in this thesis is based on pyridine-2-carboxylic acid, which was discovered as a result of the decomposition of more complex ligands, *e.g.* TPTN/TPEN and aminated ligands, under the reaction conditions employed. However, polypyridyl amine based ligands are still a promising ligand if used under other reaction conditions, *e.g.* under acidic condition, as their exceptional efficiency for oxidation of alkenes using acetic acid/H<sub>2</sub>O<sub>2</sub> was demonstrated by Costas and coworkers.<sup>4</sup> Nevertheless, ligand structure modification could provide the solution to avoid the ligand decomposition. Polypyridyl amide based ligands which contain no oxidatively sensitive positions, *i.e.* benzylic positions of pyridine moiety in polypyridyl amine based ligands, could be interesting candidates for pyridyl ligands for oxidation reactions.

A new catalytic system developed with pyridine-2-carboxylic acid ligand meets many requirements to be a new practical method for oxidative transformations. Although the system consists of several components, *i.e.* Mn salt, pyridine-2-carboxylic acid, butanedione and H<sub>2</sub>O<sub>2</sub>, they are inexpensive and all commercially available from most chemical suppliers. The reactions are carried out under air and at room temperature and take short times to reach their highest conversions (from 10 min to a few hours). Moreover, most of the reactions provide good to excellent conversion and product yield for the oxidation of alkenes, except in the case of  $\alpha,\beta$ -unsaturated substrates, *e.g.* cinnamate derivatives.<sup>5</sup> However, the selectivity of the reactions, for example *cis*-dihydroxylation *vs.* epoxidation of alkenes, is limited as the substrates' electronic nature, either electron poor or electron rich, determines selectivity of the product.

There are a few more aspects that should be dealt with to improve this system. Firstly, the functional group and protecting group tolerance need to be broadened to attract the attention of the synthetic chemist. Secondly, the oxidation of substrates containing stereogenic centre(s) needs to be demonstrated further to confirm that it proceeds with retention of configuration under the reaction conditions employed. Furthermore, other oxidative transformations, *i.e.* selective oxidation of primary alcohols to their corresponding aldehydes or oxidation of secondary alcohols to ketones, should be examined in more detail since the few examples of oxidation of primary and benzylic alcohols employing the optimised condition for oxidation of alkenes showed little activity.

As mentioned above mechanistic studies on the newly developed system were reported also in this thesis. Although a mechanism has been proposed in Chapter 5, more information, especially, from <sup>18</sup>O-labelling study is needed in order to support or refute this proposed mechanism. <sup>18</sup>O-labelled butanedione, which can be prepared by reacting butanedione with H<sub>2</sub><sup>18</sup>O (and monitored by Raman spectroscopy), should be used in the reaction in order to establish that one of the oxygen atoms of the product is from butanedione. Moreover, both *cis*-diol and epoxide products from the same substrate should be examined in <sup>18</sup>O-labelling studies to confirm that both transformations proceed by the same mechanism or not.

Mechanistic studies provide useful insights that can improve the performance of the system. For example, the discovery that acetic acid, which is the by-product formed under reaction conditions employed, eliminates the lag-time as the reactions with extra acetic acid start immediately is useful. This should be applied to substrates bearing unstable protecting groups, *i.e.* Si-based protecting group such as TBDPS. If the reaction starts immediately upon addition of H<sub>2</sub>O<sub>2</sub>, the deprotection of protecting group under reaction conditions should be reduced.

## 6.1 References

---

- 1 See references in Chapter 1.
- 2 J. W. de Boer, J. Brinksma, W. R. Browne, A. Meetsma, P. L. Alsters, R. Hage and B. L. Feringa, *J. Am. Chem. Soc.*, 2005, **127**, 7990.
- 3 J. W. de Boer, W. R. Browne, S. R. Harutyunyan, L. Bini, T. D. Tiemersma-Wegman, P. L. Alsters, R. Hage and B. L. Feringa, *Chem. Commun.*, 2008, 3747.
- 4 I. Garcia-Bosch, X. Ribas and M. Costas, *Adv. Synth. Catal.*, 2009, **351**, 348.
- 5 J. Dong, P. Saisaha, T. G. Meinds, P. L. Alsters, E. G. Ijpeij, R. P. van Summeren, B. Mao, M. Fañanás-Mastral, J. W. de Boer, R. Hage, B. L. Feringa and W. R. Browne, *ACS Catal.*, 2012, **2**, 1087.



## Summary



The goal of the research described in this thesis was to develop new methods for oxidative transformations of organic substrates including *cis*-dihydroxylation and epoxidation of alkenes, oxidation of alcohols, aldehydes and C-H activation, that are suitable for both laboratory and industrial scale. The research is based on atom-efficient and environmentally friendly concepts where manganese, a 1<sup>st</sup> row transition metal, and H<sub>2</sub>O<sub>2</sub>, as terminal oxidant, are used. Moreover, the mechanistic insights gained from the systems developed were essential for understanding how the catalysts work, which has proven vital to improve the present systems and develop the new systems.

The first catalytic system described in this thesis employs the combination of [Mn<sup>IV,IV</sup><sub>2</sub>O<sub>3</sub>(TMTACN)<sub>2</sub>]<sup>2+</sup> and carboxylic acids as the catalyst and H<sub>2</sub>O<sub>2</sub> as terminal oxidant. This catalyst has a long history which began in the late 1980s as model systems for the water splitting component of photosystem II (PS II) and dinuclear manganese-based catalase enzymes.<sup>1</sup> Later, several research groups focused on applying this catalyst in oxidative transformations with initial efforts focussing on the use of additives to suppress the H<sub>2</sub>O<sub>2</sub> depleting catalase-type activity of the catalyst and enhance its activity towards the oxidation of alkenes.<sup>2,3,4,5,6,7</sup> Our research group also demonstrated the use of carboxylic acids as an additive, which is responsible for suppressing the catalase-type activity as well as tuning the reactivity and selectivity of the reactions.<sup>6,7</sup>

Studies revealed that *bis*-carboxylato bridged complexes [Mn<sup>III,III</sup><sub>2</sub>O(RCO<sub>2</sub>)<sub>2</sub>(TMTACN)<sub>2</sub>]<sup>2+</sup> were the active intermediate formed in the system.<sup>7</sup> In this thesis, these *bis*-carboxylato bridged complexes obtained from pre-treatment of [Mn<sup>IV,IV</sup><sub>2</sub>O<sub>3</sub>(TMTACN)<sub>2</sub>]<sup>2+</sup> with a carboxylic acid and H<sub>2</sub>O<sub>2</sub> were used as the catalyst for the oxidative transformation of organic substrates. In general, this system showed a broad substrate scope and moderate to excellent conversion and isolated yield for the transformation of secondary alcohols and aldehydes to their corresponding ketones and carboxylic acids, respectively, as well as the oxidation of alkenes to their corresponding epoxides or *cis*-diols. Oxidation of primary alcohols is more challenging. However, varying the carboxylic acid co-catalyst and adding the catalyst batchwise improved conversions. High selectivity for C-H activation to mono-ketone products was also observed.

This method can be viewed as a practical method for small to large scale synthesis since the TMTACN ligand and its manganese complexes are cost-effective catalysts and can be obtained from large scale synthesis. Also, the conditions employed required low catalyst loading (generally 0.1 mol%) and near-stoichiometric amounts of H<sub>2</sub>O<sub>2</sub>. Moreover, the activity and selectivity of the reaction, especially for substrates containing multifunctional groups, can be tuned by varying the carboxylic acid co-catalyst and the amount of H<sub>2</sub>O<sub>2</sub> used.

Polypyridyl amine based ligands such as TPTN or TPEN ligands are a quite attractive class of ligands because their synthetic route allows for the facile introduction of various groups either on the central diamine unit or by replacing one or more of the pyridyl rings. Also, they showed some activity in the epoxidation of alkenes as well as the oxidation of alcohols to their corresponding ketones or aldehydes.<sup>8,9</sup> The intermediate compounds containing the aminal motif in the synthetic route to TPTN/TPEN type ligands were tested as a new ligand class in manganese catalysed reactions. The substrate conversion and product distribution from aminal based ligands were identical to that observed with TPEN based ligand.

Ligand stability is a general issue that needs attention since it can control the reactivity and especially (enantio)selectivity of a reaction. Hence systems containing TPTN and aminal based ligands were studied and both showed that the ligand used decomposed under the reaction conditions employed to form the same species, *i.e.* pyridine-2-carboxylic acid. Furthermore, it was demonstrated that, for example, replacement of the TPTN ligand by an equivalent amount of pyridine-2-carboxylic acid in the oxidation reactions results in identical activity and selectivity for a broad range of substrates. In general, it might be expected that ligand degradation would lead to loss of activity in a catalytic system. This particular case demonstrated clearly that this is not necessarily true.

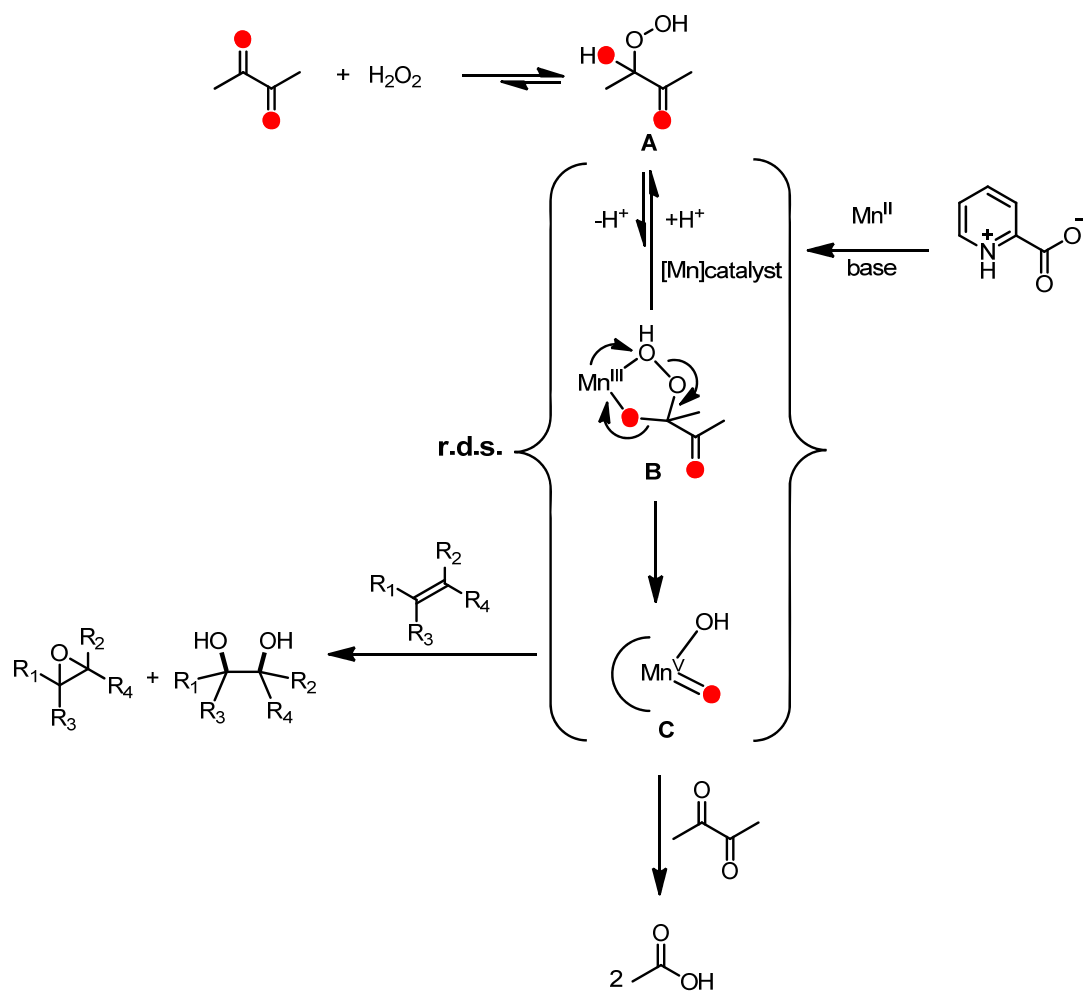
Although ligand degradation to pyridine-2-carboxylic acid is responsible for the conversion observed under slightly basic conditions in the presence of ketones, this does not mean that polypyridyl amine ligands cannot be used with manganese in oxidation catalysis when  $\text{H}_2\text{O}_2$  is used as terminal oxidant. It should be remembered that Costas and coworkers showed the use of this type of ligand for the epoxidation of alkenes under acidic conditions.<sup>10</sup> This demonstrated that the reaction conditions are crucial for the stability of ligand as well as the performance of the catalyst.

The discovery of ligand decomposition leads to a new catalytic system for the oxidation of alkenes based on  $\text{Mn}^{\text{II}}$  salt,  $\text{H}_2\text{O}_2$  and a base in ketone containing solvents. This is a relatively simple ligand/metal system and holds remarkable potential in achieving synthetically useful selective oxidative transformations.

The presence of a ketone either as a solvent or cosolvent was found to be essential to the activity of the catalytic system. However, the use of a combination of acetone and  $\text{H}_2\text{O}_2$  presents a substantial risk of explosion and hence may prove unsuitable for routine use especially on medium and large scale. Subsequently, butanedione was identified as a ketone that provided a highly active catalytic system and could be used substoichiometrically.<sup>11</sup> Importantly, the reaction times were reduced dramatically, which is a key advantage in achieving higher selectivity.

As mentioned before, one of the goals of the research was to understand how the catalyst works and to elucidate the reaction mechanism. The direct identification of an ‘active species’ or even the catalyst in its resting state was essentially impossible for this system because it is highly active and required very low amounts of catalyst.

Kinetic analysis employing Raman spectroscopy was used to obtain mechanistically relevant information about the system. This spectroscopic technique is useful since substantial information can be obtained from one measurement, *e.g.* conversion of substrate, product(s) formation and the presence of  $\text{H}_2\text{O}_2$  and its adduct. The proposed mechanism of this system is shown in Scheme 1 and it is based on the observation of the equilibrium between butanedione and  $\text{H}_2\text{O}_2$  towards 3-hydroperoxy-3-hydroxybutan-2-one, data obtained from the order of the reaction experiments and  $^{18}\text{O}$ -labelling studies.



**Scheme 1** Proposed mechanism for the oxidation of alkenes under the  $\text{Mn}^{\text{II}}$ /pyridine-2-carboxylic acid/butanedione and a base system based on data from kinetic analyses and orders of the reaction.

In summary, the results and discussion presented in this thesis set a solid basis for the development of potentially important oxidation methods. Further work will focus on demonstrating their applicability as a general synthetic tool.

## References

---

- <sup>1</sup> K. Wieghardt, U. Bossek, B. Nuber, J. Weiss, J. Bonvoisin, M. Corbella, S. E. Vitols and J. J. Girerd, *J. Am. Chem. Soc.*, 1988, **110**, 7398.
- <sup>2</sup> D. E. De Vos and T. Bein, *J. Organomet. Chem.*, 1996, **520**, 195.
- <sup>3</sup> A. Berkessel and C. A. Sklorz, *Tetrahedron Lett.*, 1999, **40**, 7965.
- <sup>4</sup> J. Brinksma, L. Schmieder, G. van Vliet, R. Boaron, R. Hage, D. E. De Vos, P. L. Alsters and B. L. Feringa, *Tetrahedron Lett.*, 2002, **43**, 2619.
- <sup>5</sup> (a) G. B. Shul'pin, G. Suss-Fink and J. R. Lindsay Smith, *Tetrahedron*, 1999, **55**, 5345; (b) G. B. Shul'pin, G. Suss-Fink and L. S. Shul'pina, *J. Mol. Cat. A – Chem.*, 2001, **170**, 17.
- <sup>6</sup> J. W. de Boer, J. Brinksma, W. R. Browne, A. Meetsma, P. L. Alsters, R. Hage and B. L. Feringa, *J. Am. Chem. Soc.*, 2005, **127**, 7990.
- <sup>7</sup> J. W. de Boer, W. R. Browne, J. Brinksma, A. Meetsma, P. L. Alsters, R. Hage and B. L. Feringa, *Inorg. Chem.*, 2007, **46**, 6353.
- <sup>8</sup> J. Brinksma, R. Hage, J. Kerschner and B. L. Feringa, *Chem. Commun.*, 2000, 537.
- <sup>9</sup> J. Brinksma, M. T. Rispens, R. Hage and B. L. Feringa, *Inorg. Chim. Acta*, 2002, **337**, 75.
- <sup>10</sup> I. Garcia-Bosch, X. Ribas and M. Costas, *Adv. Synth. Catal.*, 2009, **351**, 348.
- <sup>11</sup> J. Dong, P. Saisaha, T. G. Meinds, P. L. Alsters, E. G. Ijpeij, R. P. van Summeren, B. Mao, M. Fañanás-Mastral, J. W. de Boer, R. Hage, B. L. Feringa and W. R. Browne, *ACS Catal.*, 2012, **2**, 1087.





## **Samenvatting**

Het doel van het onderzoek, dat in dit proefschrift beschreven wordt, was het ontwikkelen van nieuwe methoden voor oxidatieve omzettingen van organische substraten zoals *cis*-dihydroxylering en epoxidatie van alkenen, oxidatie van alcoholen en aldehyden en C-H activatie, die geschikt zijn voor toepassing op zowel lab- als industriële schaal. Het onderzoek is gebaseerd op efficiënte en milieuvriendelijke concepten zoals het gebruik van mangaan en het gebruik van H<sub>2</sub>O<sub>2</sub> als uiteindelijke oxidator. Het mechanistisch inzicht dat verkregen werd met betrekking tot de ontwikkelde systemen was essentieel om te begrijpen hoe deze katalysatoren werken en dit bleek cruciaal om de huidige systemen te verbeteren en om nieuwe systemen te ontwikkelen.

Het eerste katalytische systeem dat in dit proefschrift beschreven wordt maakt gebruik van een combinatie van [Mn<sup>IV,IV</sup><sub>2</sub>O<sub>3</sub>(TMTACN)<sub>2</sub>]<sup>2+</sup> en carbonzuren als katalysator en H<sub>2</sub>O<sub>2</sub> als oxidator. De geschiedenis van deze katalysator begint eind jaren tachtig toen het ontwikkeld werd als model systeem voor het onderdeel dat verantwoordelijk is voor de fotolyse van water in fotosysteem II en voor op mangaan gebaseerde katalase enzymen.<sup>1</sup> Diverse onderzoeksgroepen hebben deze katalysator vervolgens toegepast voor oxidatie reacties en de eerste inspanningen richtten zich op het gebruik van additieven om de nutteloze ontleding van H<sub>2</sub>O<sub>2</sub> (katalase activiteit) door de katalysator te onderdrukken en om de activiteit van de katalysator met betrekking tot de oxidatie van alkenen te bevorderen.<sup>2,3,4,5,6,7</sup> Onze onderzoeksgroep heeft tevens aangetoond dat het gebruik van carbonzuren als additief verantwoordelijk is voor zowel de onderdrukking van deze katalase activiteit als voor het sturen van de reactiviteit en selectiviteit van de reacties.<sup>6,7</sup>

Studies hebben aangetoond dat *bis*-carboxylaat gebrugde [Mn<sup>III,III</sup><sub>2</sub>O<sub>3</sub>(RCO<sub>2</sub>)<sub>2</sub>(TMTACN)<sub>2</sub>]<sup>2+</sup> complexen de actieve intermediären zijn in het systeem.<sup>7</sup> Deze *bis*-carboxylaat gebrugde complexen werden in dit proefschrift verkregen door voorbehandeling van [Mn<sup>IV,IV</sup><sub>2</sub>(O)<sub>3</sub>(TMTACN)<sub>2</sub>]<sup>2+</sup> met een carbonzuur en H<sub>2</sub>O<sub>2</sub> en werden gebruikt als katalysator voor de oxidatieve omzetting van organische substraten. In het algemeen laat dit systeem een grote reikwijdte zien met betrekking tot het type substraat dat geoxideerd kan worden en redelijke tot zeer goede opbrengsten kunnen verkregen worden voor de omzetting van secundaire alcoholen en aldehyden in de corresponderende ketonen en carbonzuren als ook voor de oxidatieve omzetting van alkenen in epoxiden of *cis*-diolen. Oxidatie van primaire alcoholen was meer uitdagend. Maar door de gebruikte carbonzuur co-katalysator te variëren en door gedurende de reactie extra katalysator toe te voegen konden de omzettingen verbeterd worden. Mono-ketonen konden verkregen worden door zeer selectieve C-H activatie van diverse substraten.

Deze methode kan worden gezien als praktisch toepasbare methode voor synthese op kleine en grote schaal aangezien het TMTACN ligand en de mangaan complexen hiervan rendabele katalysatoren zijn en verkregen kunnen worden door synthese op grote schaal. Tevens vereisen de toegepaste condities slechts een kleine hoeveelheid katalysator (in het algemeen 0.1 mol%) en slechts bijna stoichiometrische hoeveelheden  $\text{H}_2\text{O}_2$ . Bovendien kan de activiteit en de selectiviteit van de reactie, in het bijzonder voor substraten met meerdere functionele groepen, gestuurd worden door het carbonzuur dat als co-katalysator gebruikt wordt en de hoeveelheid  $\text{H}_2\text{O}_2$  te variëren.

Polypyridyl amine liganden zoals TPTN of TPEN zijn een aantrekkelijke klasse van liganden aangezien hun synthese route het toestaat dat diverse groepen gemakkelijk geïntroduceerd kunnen worden, zowel op de centrale diamine groep als door één of meerdere pyridyl groepen te vervangen. Tevens lieten ze wat activiteit zien ten aanzien van zowel de epoxidatie van alkenen als de oxidatie van alcoholen waarbij de corresponderende ketonen of aldehydes verkregen werden.<sup>8,9</sup> De tussenproducten in de synthese route van de op TPTN/TPEN gebaseerde liganden bevatten een aminaal motief en deze aminaal verbindingen werden getest als ligand in mangaan gekatalyseerde reacties. De omzettingen van de substraten en de distributie van de producten waren identiek wanneer deze aminaal liganden gebruikt werden in plaats van TPEN gebaseerde liganden.

De stabiliteit van liganden is een algemene kwestie die aandacht verdient aangezien het een cruciale rol kan spelen bij het bepalen van de reactiviteit, met name met betrekking tot de (enantio)selectiviteit van een reactie. Daarom werden de systemen met de TPTN en de aminaal gebaseerde liganden bestudeerd en er werd gevonden dat beide gebruikte liganden kapot gingen tijdens blootstelling aan de toegepaste reactie omstandigheden en in beide gevallen werd dezelfde verbinding gevormd, namelijk pyridine-2-carbonzuur. Tevens werd aangetoond dat wanneer bijvoorbeeld het TPTN ligand werd vervangen met een equivalente hoeveelheid pyridine-2-carbonzuur identieke activiteit en selectiviteit werd verkregen bij de oxidatie van een groot aantal substraten. In het algemeen zou verwacht kunnen worden dat de degradatie van liganden zou leiden tot verlies van de activiteit van een katalysator systeem. Met dit specifieke geval is echter duidelijk aangetoond dit niet noodzakelijkerwijs het geval is.

Hoewel de gedeeltelijke afbraak van de liganden naar pyridine-2-carbonzuur verantwoordelijk is voor de vastgestelde omzettingen onder licht basische condities in aanwezigheid van ketonen, betekent dit niet dat polypyridyl amine liganden niet gebruikt kunnen worden in combinatie met mangaan voor oxidatie katalyse met  $\text{H}_2\text{O}_2$  als oxidator. Het verdient vermeld te worden Costas *et al.* hebben laten zien dat dit type liganden gebruikt kan worden voor de epoxidatie van alkenen onder zure condities.<sup>10</sup> Dit toont aan dat de reactie omstandigheden cruciaal zijn voor zowel de stabiliteit van het ligand als de prestaties van de katalysator.

De ontdekking van de degradatie van de oorspronkelijke liganden heeft geleid tot een nieuw katalytisch systeem voor de oxidatie van alkenen dat gebaseerd is op een  $\text{Mn}^{\text{II}}$  zout,  $\text{H}_2\text{O}_2$  en een base in een oplosmiddel dat een keton functionaliteit bevat. Dit



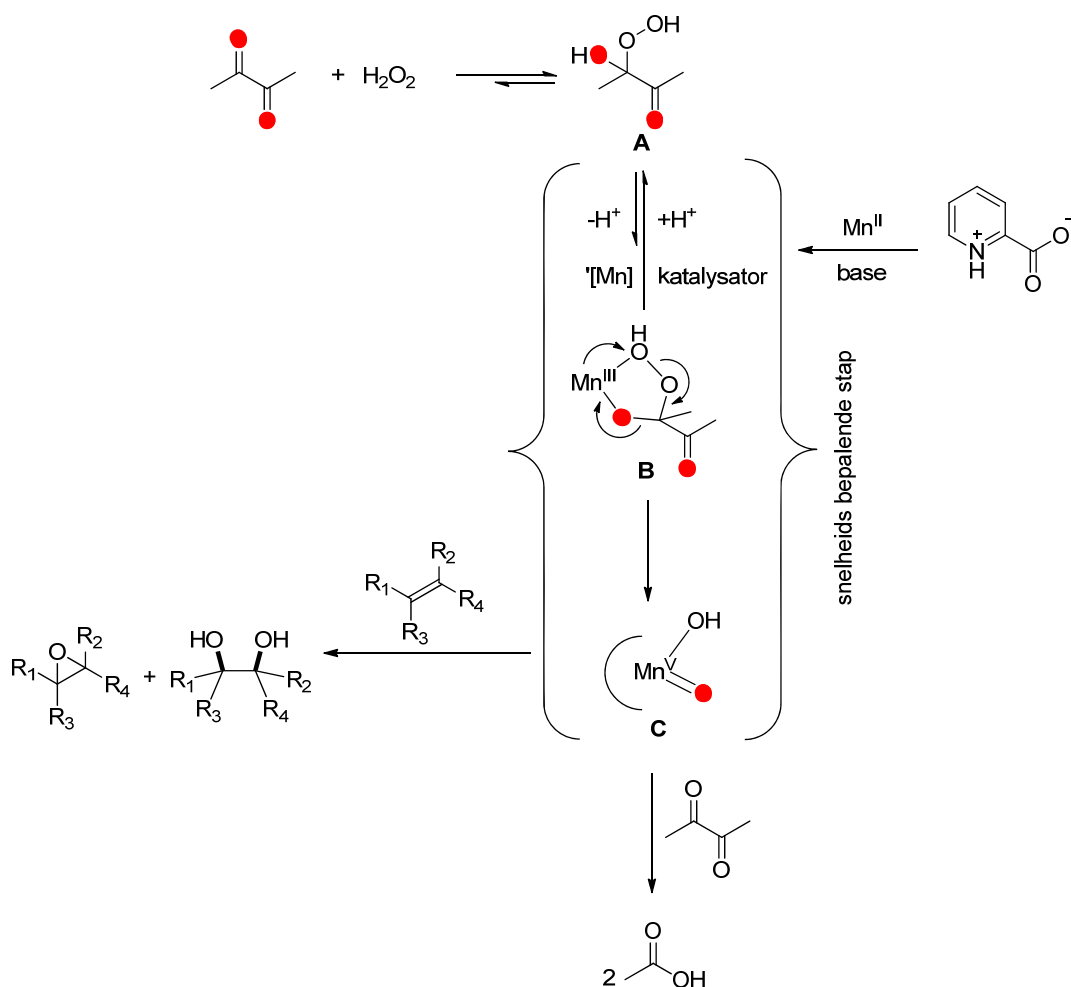
systeem is een relatief simpel ligand/metaal systeem en heeft opmerkelijke potentie voor het bereiken van synthetisch bruikbare selectieve oxidatieve omzettingen.

Er werd gevonden dat de aanwezigheid van een keton, ofwel als enig oplosmiddel ofwel als onderdeel van een mengsel van oplosmiddelen, essentieel is voor het vertonen van activiteit door het katalytische systeem. Echter, het gebruik van een combinatie van aceton en  $\text{H}_2\text{O}_2$  vormt een groot risico met betrekking tot explosiegevaar en mag daarom niet geschikt geacht worden voor routinematige toepassing, met name op middelgrote en grote schaal. Vervolgens werd echter butaandion geïdentificeerd als een keton dat bij gebruik een zeer actief katalytisch systeem opleverde en dat substoichiometrisch gebruikt kon worden.<sup>11</sup> Maar nog belangrijker: het gebruik van butaandion leidde tot dramatisch verkorte reactietijden, wat een essentieel voordeel is voor het bereiken van hogere selectiviteit.

Zoals eerder vermeld, was een van de doelstellingen van het onderzoek dat in dit proefschrift beschreven wordt om te begrijpen hoe de katalysator werkt en om het reactiemechanisme op te helderen. Directe identificatie van het ‘actieve deeltje’ of zelfs van de rusttoestand van de katalysator was voor dit systeem eigenlijk niet mogelijk aangezien dit systeem zeer actief is en slechts een erg lage hoeveelheid katalysator nodig heeft.

Kinetische analyse door middel van Raman spectroscopie werd gebruikt om mechanistisch relevante informatie te verkrijgen betreffende dit systeem. Deze spectroscopische techniek is nuttig aangezien belangrijke informatie verkregen kan worden met één meting, bijvoorbeeld met betrekking tot zowel de omzetting van het substraat, de vorming van producten en de aanwezigheid van  $\text{H}_2\text{O}_2$  en adducten hiervan. Het voorgestelde mechanisme van dit systeem is afgebeeld in Schema 1 en is gebaseerd op de waarnemingen van het evenwicht tussen butaandion en  $\text{H}_2\text{O}_2$  en 3-hydroperoxy-3-hydroxybutan-2-on, gegevens met betrekking tot de orde van de reactie en  $^{18}\text{O}$  labelling experimenten.

Samenvattend, de resultaten en de interpretatie hiervan zoals gepresenteerd in dit proefschrift vormen een solide basis voor de ontwikkeling van potentieel belangrijke oxidatie methoden. Toekomstig werk zal zich toespitsen op het aantonen van het gebruik hiervan als een algemeen toepasbare synthetische methode.



**Schema 1** Voorgesteld mechanisme voor de oxidatie van alkenen met het  $\text{Mn}^{\text{II}}$ /pyridine-2-carbonzuur/butaandion/base systeem, gebaseerd op kinetische analyse van de reactieordes.

## Referenties

- 1 K. Wieghardt, U. Bossek, B. Nuber, J. Weiss, J. Bonvoisin, M. Corbella, S. E. Vitols and J. J. Girerd, *J. Am. Chem. Soc.*, 1988, **110**, 7398.
- 2 D. E. De Vos and T. Bein, *J. Organomet. Chem.*, 1996, **520**, 195.
- 3 A. Berkessel and C. A. Sklorz, *Tetrahedron Lett.*, 1999, **40**, 7965.
- 4 J. Brinksma, L. Schmieder, G. van Vliet, R. Boaron, R. Hage, D. E. De Vos, P. L. Alsters and B. L. Feringa, *Tetrahedron Lett.*, 2002, **43**, 2619.
- 5 (a) G. B. Shul'pin, G. Suss-Fink and J. R. Lindsay Smith, *Tetrahedron*, 1999, **55**, 5345; (b) G. B. Shul'pin, G. Suss-Fink and L. S. Shul'pina, *J. Mol. Cat. A – Chem.*, 2001, **170**, 17.
- 6 J. W. de Boer, J. Brinksma, W. R. Browne, A. Meetsma, P. L. Alsters, R. Hage and B. L. Feringa, *J. Am. Chem. Soc.*, 2005, **127**, 7990.

- 
- 7 J. W. de Boer, W. R. Browne, J. Brinksma, A. Meetsma, P. L. Alsters, R. Hage and B. L. Feringa, *Inorg. Chem.*, 2007, **46**, 6353.
  - 8 J. Brinksma, R. Hage, J. Kerschner and B. L. Feringa, *Chem. Commun.*, 2000, 537.
  - 9 J. Brinksma, M. T. Rispens, R. Hage and B. L. Feringa, *Inorg. Chim. Acta*, 2002, **337**, 75.
  - 10 I. Garcia-Bosch, X. Ribas and M. Costas, *Adv. Synth. Catal.*, 2009, **351**, 348.
  - 11 J. Dong, P. Saisaha, T. G. Meinds, P. L. Alsters, E. G. Ijpeij, R. P. van Summeren, B. Mao, M. Fañanás-Mastral, J. W. de Boer, R. Hage, B. L. Feringa and W. R. Browne, *ACS Catal.*, 2012, **2**, 1087.



## Acknowledgements

All the works described in this thesis would not be possible without the support, suggestions and collaborations from a lot of people. Therefore, I would like to thank them in this moment.

Primarily, and most importantly, I would like to thank my supervisor, Dr. Wesley Browne, for giving me the honour to be the first Ph.D. student to work under his guidance. Wes, thank you very much for everything you have done for me over the past few years. Thank you for giving me the confidence to believe in my own abilities, that I CAN DO IT!!!

I would also like to express my gratitude to my promoter, Prof. Ben Feringa, for his enthusiasm and kind encouragement throughout my study. Ben, thank you very much.

I acknowledge the members of my reading committee, Prof. Costas, Prof. Klein Gebbink and Prof. Roelfes, for their quick corrections and helpful comments and for approving my manuscript.

I would like to thank other people who have contributed to the research described in my thesis. First, thanks Dirk for being a great partner on the aminor project and for cheering me up when the project took an unexpected direction. I acknowledge also the industrial collaborators; Dr. Paul Alster and Dr. Ruben van Summeren from DSM, for the great collaboration and their invaluable advice and help on aminor/picolinic acid project.

Thanks to Dr. Ronald Hage and Dr. Hans de Boer from Catexel for providing me with the Mn-TMTACN catalyst and for their helpful suggestions, especially, for Mn-TMTACN project.

Thank you to all the students whom I have had the chance to supervise during my study. Lea, thanks for all your hard work on Mn-TMTACN project in Chapter 2 and for our friendship. Maggi, thanks you for your contribution that are represented in Chapter 2 and 5. Auke, thanks for all the time in the lab. I wish you all the best for your future.

Tim and Jia Jia, thanks also for your collaborations in the picolinic acid project and mechanistic study. I acknowledge Bin, Martin and Massimo for providing me the substrates for my research.

Thank you all the technicians for their help, especially, Ebe for all problems lab related, Pieter for all NMR related problems, Hans for elemental analysis, Annie and Theodora for mass spectrometry measurements. Thank you also to Hilda and Alphons for helping me with all documents, especially, taxes!

I thank all my labmates who made my everyday life in the lab enjoyable: Dirk (for your nice music in the lab), Hans (for helping me with general problems in the lab and especially for the last minute Dutch translation), Bas, Nikki (for nice chats in front of the fume hood and correcting my chapters), Hella (for all of your help), Appu, Shaghayegh (for tasting products from my cooking/baking experiments ☺), Jia Jia (for being a good partner in food tasting), Peter, Davide, Francesco, Heloise, Rik (for your nice music, dutch lessons in the lab and all your help), Lorina, Jorrit, Pim.

It was a nice experience to work in such a big and international group, I had learnt many things here. Thank you all people from Feringa's, Minnard's, Roelfes's and Otto's group: Nathelie&Tibor, Greg&Angela, Bea, Tati, Natasa, Tony, Nop, Jet, Massimo, Martin K., Jort, Thom, Jochem, Jurica, Erik, Robby, Jiobing, Jiawen, Lili, Xiaoyan, Maria, Kuang Yen, Adi, Ashoka, Celine, Mathieu, Jerome, Miriam, Danny, Felix, Claudia, Tiziana, Wim, Emma, Jos, Nuria, Qian, Jeffrey, Jens, Francesca, Johnny, Antonio, Suresh, Anne, Lachlan, Pieter, Fiora, Vittorio, Giuseppe, Yang, Hugo, Saleh, Bin, Martin F., Amudena, Valentin, Alena, Annick, Wiktor, Jack, Tim, Barbara, Johan, Monolo, Thomas, Derk Jan, Paula, Cati, Santi, Christ, Gabor, Petra, Arjen, Stella, Johannes, Takashi.... The list is endless and I don't think I mentioned everyone but a big thank you to you all in any case.

Thank you to all flatmates in 'Pelsterstraat 42A', Natasa, Jerome, Celine and Mathieu, for having the nice times together ☺

Special thanks to Miriam, Lorina and Nikki, for being my good friends. Thanks for all girlie chats during coffee break, dinner and weekend. It was my great pleasure to share the good moments with you girls ☺

I am very glad to have my best friends as my paranimfs on my graduation day. Miriam, thank you very much for your friendship and the nice weekend chats and coffee sessions. Pim, thanks for your friendship and sharing the good times with me.

ขอบคุณสำหรับพี่น้องคนไทย นักเรียนไทยในโกรนิงเกนเช่นกันค่ะ โดยเฉพาะพี่ พี่กบ พี่เมย์  
แซลลี่ที่ทำให้คิดถึงบ้านและอาหารไทยแบบบางลงไป  
ขอบคุณมากๆเช่นกันสำหรับพี่อ้อที่ช่วยออกแบบปกวิทยานิพนธ์เล่มนี้ค่ะ

ขอบคุณสำหรับเพื่อนๆที่เมืองไทยโดยเฉพาะอย่างยิ่งพี่เก้ง โอ และสวาง ขอบคุณสำหรับมิตรภาพที่มีให้เสมอมา  
ขอบคุณสำหรับกำลังใจที่มีให้นยามที่เราเหงา คิดถึงบ้านและพ่อแม่  
ขอขอบคุณที่ไม่ทิ้งกันแม้ว่าเราจะไม่ได้เจอหรือติดต่อกันตลอดเวลา

ขอบคุณพี่เจตกับพี่นพมาภะคะที่แนะนำโอกาสให้ปีพีมได้มาเรียนที่โกรนิงเกน  
ขอบคุณพี่ๆที่ดูแลเป็นอย่างดีตั้งแต่ก่อนเดินทางจนเดินทางมาถึงที่นี่  
ขอบคุณสำหรับทุกๆคำแนะนำและมิตรภาพที่ดีที่มีให้กันเสมอมาค่ะ

ขอขอบพระคุณอาจารย์เทียนทอง ทองพันธ์่มากๆเช่นกันนะคะ  
ที่ให้โอกาสปัทม์ได้ทำงานวิจัยในแล็บของอาจารย์ในช่วงปริญญาตรีและโท  
ทุกอย่างที่ได้เรียนรู้จากแล็บของอาจารย์เป็นสิ่งที่มีความจำจนถึงปัจจุบัน  
และขอขอบคุณสำหรับแรงบันดาลใจและการสนับสนุนของอาจารย์ที่ทำให้ปัทม์ได้มาเรียนต่อที่เนเธอร์แลนด์

Massimo, thank you very much for all your support and understanding, especially, during  
my thesis stress. Grazie mille per tutto quello che hai fatto per me ☺

สุดท้ายนี้ปัทม์ขอขอบพระคุณป้ากับแม่มากๆนะคะที่ทำให้ลูกประสบความสำเร็จในวันนี้  
ขอบคุณสำหรับความรัก ความเข้าใจ และกำลังใจที่มีให้เสมอมาโดยเฉพาะตลอดสี่ปีที่ผ่านมานะเนเธอร์แลนด์  
สิ่งเหล่านี้เป็นแรงผลักดันที่ดีที่ทำให้ปัทม์ไม่ย่อท้อต่อปัญหาต่างๆที่ผ่านเข้ามา  
ขอขอบคุณพี่ต่ายและพี่ตาเช่นกันนะคะสำหรับกำลังใจที่มีให้เสมอมาและขอขอบคุณพี่ๆที่ดูแลเป็นอย่างดี

*Pat*